Synthesis of Multiple Polybetaine Block Copolymers and Analysis of Their Self-Assembly in Aqueous Media

Jongmin Lim

2020

Synthesis of Multiple Polybetaine Block Copolymers and Analysis of Their Self-Assembly in Aqueous Media

Jongmin Lim

Department of Polymer Chemistry

Kyoto University

March 2020

Table of Contents

Chapter 1. General Introduction

1.1 Polyzwitterions

Polyzwitterions are a distinctive class of polyelectrolytes containing a cationic and an anionic group on their repeating unit. The dual charges in a single repeating unit that accordingly make charge neutrality of a chain, not as polyelectrolytes bearing specific charges. Looking back on the monomers, trimethyl glycin was firstly discovered in sugar beets as a byproduct (so named as betaine) of the processing, then produced as supplements and skin-conditioning agents.[1] The high water-affinity molecule which typically comprises of a positively charged quaternary ammonium and a negatively charged carboxylate or sulfate shows moisturizing effect and anti-irritant property in many formula such as cosmetics, detergent or toothpaste.[2, 3] Betaine-derivative surfactants consist of a betaine headgroup and a tail of alkyl chain on the other side are also widely used instead of anionic surfactants, which disrupt the skin barrier and cause irritation.[4] The most widely known surfactant is cocamidopropyl betaine, in which the alkyl group originates from the fatty acid in coconut oil, is easily spotted in shampoos and hand soaps, etc.

The scientific interest in zwitterion molecules and polymers was slowly grown until several biological molecules (e.g. sphingomyelins and lecithins) were known to have zwitterionic chemical structures. These lipids that consist of long fatty acid chains with zwitterionic phosphocholine headgroup compartmentalise cells and form mesoscopic structures in nature, hence brought a perception about the role of the zwitterions in biological systems.[5] Widespread usage of zwitterionic materials in designing bioinspired materials discovered this chemical structure is highly biocompatible.[6-9] Stimulated by the characteristics, polyzwitterions were under the main investigation, meanwhile they actually do not present in nature unlike proteins and polynucleotides hence are rather classified as biomimicking materials.[5] Reported since 1950s,[10, 11] the research of synthetic polyzwitterions went toward obtaining hydrophilic and neutral film on the surface for biomedical purposes over the past decades.[12-19]

The strategy of biocompatible surface is creating a strong hydrophilic layer on surface to preclude protein adsorption, which is promoted by hydrophobic interactions[20] or electrostatic attractions between an electrical double layer of the interface and charged proteins.[21] Additional adhesion of microbes or subsequent cell growth by consuming nutrients follows on the protein layer.[22] Hence, preventing the initial biofilm formation is quintessential method to keep materials inert in physiological condition. Polyethylene glycol (PEG)-based non-

ionic hydrophilic polymers have been utilised for surface protection prior to polyzwitterions by providing a hydration layer, and demonstrated inhibition of living organism attachment to surfaces.[23-25] Poly(hydroxyfunctional acrylates) such as poly(2-hydroxethyl methacrylate) (PHEMA) and poly(hydroxypropyl methacrylate) (PHPMA), and poly(*N*-vinylpyrrolidone) (PVP) also have long history as a biocompatible polymer for good hydrophilicity and electric neutrality.[26] Compared to the non-ionic hydrophilic polymers, polyzwitterions showed superior antifouling property[27-30] also in a free chain state,[31] whereas water molecules are bound to a non-ionic polymer surface by hydrogen bonding, electrostatically induced attractions to polyzwitterions play in hydration.[32] Since hydrogen bond is relatively weak and breaking and reforming within very short time, disruption of the water molecule structure could happen in non-ionic polymers then it eventually leads to fouling, which is caused by structural issues[33] or temperature changes.[34] On the other hand, the hydration layer of polyzwitterions was not disturbed as revealed by sum frequency generation vibrational (SFG) spectroscopy, which is a surface-sensitive method of tracking what types of molecules exist at the interface.[31] Under several protein solutions, no disruption of H-bonding structure near polysulfobetaine surfaces was represented while the disordered water molecule structure by inhibition of proteins happened at PEG and poly(oligo(ethylene glycol) methacrylate) (POEGMA) surfaces.[31] The unperturbed hydration layer of polyzwitterions is discussed that water around polyzwitterions seems to have no more or less strong structure than in bulk water and it fortifies antifouling behaviour.[35] No noticeable surface activity of polyzwitterions,[36] in other words no existence of nonpolar parts moving to the air-water surface could be an evidence to this idea.

In aqueous solution, polyzwitterions can have electrostatic attractions/repulsions between adjacent charged motifs or other chains, which induce clear differences from general polyelectrolytes and non-ionic hydrophilic polymers on the solution behaviour. These interactions are often classified as three modes: intra-mer, inter-mer, and inter-chain modes (see **Figure 1.1**). For intra-mer interaction, the spacer alkyl chains must bend to meet the inner charged group with the outer charged group. Energy calculation results of molecular mechanics on zwitterionic surfactants suggested this configuration does not occur in aqueous media due to more favourable interaction with water molecules.[37] But nonlinearly increased critical salt concentrations against the spacer length upon disassociating polycarboxybetaine-polymethacrylic acid complex hypothesised the intra-mer attraction.[38] "Soliton-like" waving model of consecutive pairings with nearest neighbours in polysulfobetaines was proposed based on the light scattering study.[39] All kinds of the electrostatic interactions are thought to occur chain collapse and phase separation in salt-free water if the attraction is more favoured than the solvation. Consequently, the collapsed chains can be swollen into water again by salt addition which diminishes short- and long range

electrostatic attraction. The phenomenon is generally explained by screening effect, considering Debye length $\lambda_D = \kappa^{-1} \equiv 1/[8\pi l_B N_A I]^{-0.5}$, where l_B is Bjerrum length (the length where the Coulombic energy is equal to the thermal energy), N_A is Avogadro number, and I is the ionic strength. The scale describes the distance from a particle in which the electrostatic force is significantly reduced. As a consequence, all attraction/repulsion forces between polyzwitterions are diminished by additional salts which reduce the Debye length of the solution, and chain expansion occurs.[40] This behaviour is opposite to that of ordinary polyelectrolytes that become less soluble in salt addition by charge screening of the polymer surface, hence discussed as anti-polyelectrolyte effect[40-43] with study of hydrodynamic radii,[39, 44, 45] viscosity,[46] or theoretical analysis.[47]

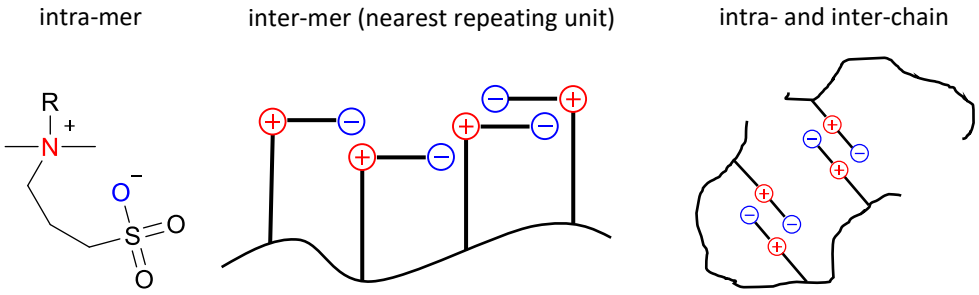

Figure 1.1. Three interaction modes in polyzwitterions[35]

Most researches on polyzwitterions have been carried out against three species: Polysulfobetaines, polycarboxybetaines and polyphosphobetaines. (**Figure 1.2**) Each has individual characteristics originating from different combinations of positive and negative charged groups. Firstly, polysulfobetaines (**Figure 1.2(a)(b)**) containing a strong acidic sulfonate end explicitly show the solution behaviour affected by dipole–dipole pairing. Due to strong interactions, polysulfobetaines are hard to dissolve in pure water nor organic solvent, and increasing temperature or salt concentration promotes the bad solubility. The upper critical solution temperature (UCST) is dependent on the chain length,[48] hydrophobicity of the monomers,[49, 50] and presence of ions.[40, 48] Basically hydrophilic, their surfaces show hydrophilic-hydrophobic transition as the investigation result of wetting property change under varying temperature.[51] However, they seem not be in a completely segregated state from water molecules because of slightly visible ^{1}H NMR signals in the collapsed state.[52, 53]

Besides, polycarboxybetaines (**Figure 1.2(c)**) show no thermoresponsive behaviour presumably higher pK_a (~3) that stems from the weakly acidic carboxylate group disabling fully ionised state. Under pK_a, the protonated carboxylate ends shift the entire charge from neutral to positive, therefore the dynamics in solution also change to more polyelectrolyte-like in acidic solution. The alteration is reflected in zeta potential variations from positives

to even negatives.[45, 54] Although the partially zwitterionic state in moderate pHs, polycarboxybetaine chains can form pairings which appear as multiple diffusive modes[45] similar to polysulfobetaines. However, pH change does not critically affect on the hydrophilicity as opposed to other pH-responsive polymers that experience globule-to-coil transition by ionisation like poly(acrylic acid). Thus, it is thought that this type of polyzwitterions was less covered on the attempt of designing stimuli-responsive polymers than polysulfobetaines.

Polyphosphobetaines (**Figure 1.2(d)(e)**) have got interests in biomedical field because of similarities with phospholipids consisting cell membrane. Commercialised monomer 2-(methacryloyloxy)ethylphosphatidyl-choline (MPC), the polymer (PMPC, **Figure 1.2(d)**), and polymerisable phospholipids[55, 56] have been mainly used for designing materials requiring high biocompatibility. PMPC could be found elsewhere more frequently than bioinspired phospholipid-derivatives, presumably it is easy to be synthesised by conventional or living radical polymerisation. Coupled with controlled radical polymerisation such as atom-transfer radical polymerisation (ATRP) or reversible addition-fragmentation chain transfer polymerisation (RAFT) technique, PMPC chains of narrow molecular weight distribution are able to be obtained in bulk or on the surface of substrates. (Of course, it is also available for other type of betaines) Due to the pK_a of phosphate group (~2), the zwitterionic state could be presenting in wider pH than polycarboxybetaines. However, the chains do not respond to temperature variations and maintain strong hydrophilicity even in cold environment. This difference could make us raise an assumption that the strength of the pairing is weaker than the case of polysulfobetaines, so solvation is always predominant over the binding force. In recent studies, new phosphobetaines having inverted zwitterionic structure[57-60] in comparison to MPC were synthesised (**Figure 1.2(e)**), and showed slight differences. Multiple diffusive modes of PMPC-*block*-inverted PMPC aqueous solutions revealed there are certain types of zwitterionic attraction between phosphobetaine chains and it might be modulated by increased chain hydrophobicity.[61]

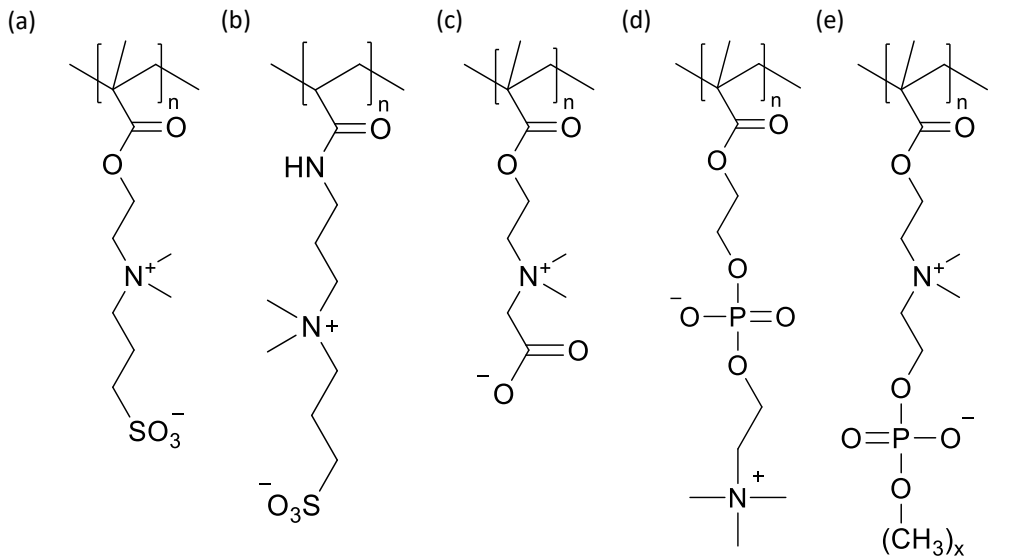

Figure 1.2. Chemical structures of Representatives of polysulfobetaine(a)(b), polycarboxybetaine(c), and polyphosphobetaine(d)(e)

When it comes to applications of polybetaines, utilising stimuli-responsive characters of polyzwitterions diverged from the initial research scope, building non-fouling materials. By combining other non-ionic polymers, polysulfobetaine motifs demonstrated thermoresponsive characters in the form of block copolymers with relatively hydrophobic moieties,[52, 62, 63] crosslinked hydrogels,[64, 65] or as ligand of inorganic nanoparticles.[66, 67] Incorporation with lower critical solution temperature (LCST)-type non-ionic polymers[68-72] resulted in intriguing "schizophrenic" micelles, which can switch the core and the shell at a lower and upper registers of temperature respectively. pH-responsive behaviour of polycarboxybetaines was exploited to build active surface. For example, surfaces repelling protein in neutral and basic condition and kill and release bacterias in acidic condition,[28, 30, 73] and changing flux of polycarboxybetaine-coated membranes upon various eluents having different pH- and salt species were demonstrated.[74]

1.2. Stimuli-responsive polymers

Demands for "smart" materials that can change their properties under the alteration of the outer environment or specific external stimuli have been growing since several decades for development of highly functional applications in various fields. Stimuli-responsive polymers, which are in this category, exhibit physical or chemical property change in response to heat, pH, light, electrical and magnetic fields, redox potential and mechanical force.[75] As feedback-control living organisms, the synthetic polymers can amplify relatively minor

changes in the media to apparent macroscopic differences.[76] In this section, the principles and recent progress of temperature and pH responsive water-soluble polymers are reviewed.

1.2.1 Temperature-responsive polymers

Changing temperature is presumably the most direct way to achieve transformation of aqueous solutions as solubility change of solutions of small molecular weight solutes. Temperature-responsive behaviour of polymers are classified by two kinds: LCST, and UCST polymers. Perhaps LCST-type non-ionic polymers are the most extensively explored stimuli-responsive materials on their behaviours and applications. Actually, the phenomenon is pervasive for us when cooking eggs or meat: Heating up temperature breaks the initial folding of proteins contained in food and turns them from liquid into a solid state. In the synthetic polymer field, the earliest example, poly(*N*-isopropylacrylamide) (PNIPAM), was reported by Scarpa et al. in 1967.[77] PNIPAM is undoubtedly the most widely studied LCST polymer since decades due to sharp phase change around ~31 °C. Many scientific works about tuning the transition point by copolymerisation,[78, 79] and tracking the coil-to-globule transition process in microsecond scale,[80, 81] effect of Hofmester series ions on solvation for comparison with proteins[82-84] still have been published. Commonly, LCST-type non-ionic polymers can dissolve into water below their critical temperature (T_c), and the transparent solutions go to a turbid state above the T_c due to segregated chains from water molecules. UCST-type polymers act opposite to them: soluble at high temperature and insoluble at low temperature. In other words, applying heat promotes phase separation in LCST system and homogeneous mixing in UCST system. A well-known phase diagram (**Figure 1.3**) summarises the two behaviours, and the shape of curves depends on parameters. (a polymer could show both LCST and UCST or single behaviour in certain solvents) Phase diagrams of thermoresponsive polymers are able to be constructed by considering the Gibbs free energy of mixing ΔG_m:

$$\Delta G_m = \Delta H_m - T\Delta S_m \tag{1.1}$$

Where ΔG_m goes to minus, the mixing is favoured and the polymer is miscible. ΔH_m, the enthalpy of mixing, is related to internal attraction force of polymers. The entropy of mixing ΔS_m, the probability of exchanging positions between different molecules, is related to molecular weight. Both terms are influenced by the affinity of a polymer to a solvent; unfavourable interactions generally lead ΔH_m to positive and ΔS_m to negative. ΔG_m is expressed as eq(1.2) by Flory-Huggins theory:

$$\frac{\Delta G_{\mathrm{m}}}{k_{\mathrm{B}}T} = \phi_1 \ln\phi_1 + \frac{\phi_2}{N}\ln\phi_2 + \phi_1\phi_2\chi \qquad (1.2)$$

Where ϕ_1 and ϕ_2 is the volume fraction of the component 1 (solvent) and 2 (polymer), N is the ratio of the molar volume of the polymer to that of the solvent, χ is the interaction parameter, and k_{B} is Boltzmann constant. The big difference from regular solution theory is N on the denominator of the entropy term of polymer, therefore the contribution of entropy $\phi_1 \ln\phi_1 + \frac{\phi_2}{N}\ln\phi_2$ decreases more for higher molecular weight polymers. χ is determined by the difference of attractive forces between the components 1-1, 2-2, and 1-2. However, Flory-Huggins theory can only predict UCST correctly because the approach is premised on the assumptions which ignore volume changes of mixing and simplify the interactions to just one enthalpic term.[85] In practice, most water-soluble polymers exhibit LCST behaviour in water, and the hydration mechanism of non-ionic polymers is proposed that H-bonding of water molecules to available sites of the polymers solvate the chain. (e.g. C=O or N-H group in PNIPAM) In this view, ΔH_{m} is negative (H-bonding is favoured) and ΔS_{m} is negative (decreased probability by fixed position of water molecules), then ΔG_{m} eventually goes to positive under a temperature increase. For UCST behaviour, it is discussed that ΔH_{m} is positive due to internal cohesive forces competing with hydration force and ΔS_{m} is positive.

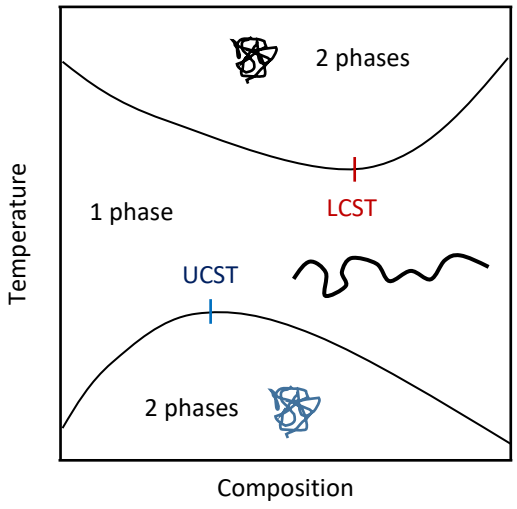

Figure 1.3. An example of phase diagram depicting UCST and LCST

The free energy of mixing can be divided by two parts, an ideal and an excess terms. The ideal entropy is same as the entropic term of eq.(1.2) since the system only deals the combinatorial entropy of mixing, therefore the excess entropy is zero. The ideal enthalpy of mixing is zero then the excess enthalpy term is directly related to χ. Now the effective interaction parameter χ_{eff} can be defined as follows:

$$\chi_{\text{eff}} \equiv \frac{\Delta G_{\text{m}}^{\text{ex}}}{\phi_1 \phi_2 kT} = A + \frac{B}{T} \quad or \quad A + \frac{B}{T} + \frac{C}{T^2} \tag{1.3}$$

The arbitrary parameters A, B and C obtained by fitting data with experimental results may be positive or negative, respectively. A is called the noncombinatorial entropic contribution and might reflect molecular packing state.[86] B involves in specific interaction between the components, negative B means attraction such as H-bonding. C is introduced when heat capacities of the components show nonlinear temperature dependence.[87] For LCST-type polymers, the two parameters are often regarded as $A > 0$ and $B < 0$. For UCST-type polymer, A is zero or < 0 and $B > 0$. These parameters we reviewed define the phase separation behaviour of polymers: sole LCST/UCST or both (LCST at higher temperature and UCST at lower temperature), and extraordinary x-shaped (the left and right section are two phase) or loop-shaped (LCST at lower and UCST at higher temperature, the inner loop is two phase) diagrams are plotted on composition versus temperature graphs.

Publications of LCST polymers were 7.5 times more than UCSTs (~330 vs. 44) during 2005–2010 as Seuring et al. pointed out.[88] Also, most researches were concentrated on PNIPAM alongside few other examples such as POEGMA amongst those articles.[88] In addition, it should be noted that although a variety of examples of LCST polymers were reported, quite a lot of examples are analogous to PNIPAM, having slight difference of chemical structure with H-bonding sites C=O or NH group in their repeating unit. Some polymers having different structures (e.g. poly(*N*-acryloylpiperdine), poly(*N*-acryloylpyrrolidine), and poly(*N*-vinyl caprolactam), or PEG derivatives) also fall into the range of PNIPAM upon the phase separation mechanism. So, specific examples of LCST polymers are not introduced in this section. (The detailed information of LCST polymers are nicely listed in the article of Aseyev et al.[89]) On the aspect of practical usage, biocompatibility of the non-ionic LCST polymers would be issues for biomedical applications due to hydrophobic interaction with proteins onto the hydrophobic site of the polymer surface. Particularly, acrylamide-based polymers such as PNIPAM are considered not suitable for implantation due to possible cell toxicity and non-degradability, therefore most of drug delivery systems are exploiting PEG and poly(propylene glycol) copolymers (PEG-PPG-PEG).[90] To compensate the drawback, the thermoresponsive polymers were copolymerized with other biocompatible or biodegradable polymers,[91, 92] otherwise biopolymers.[93]

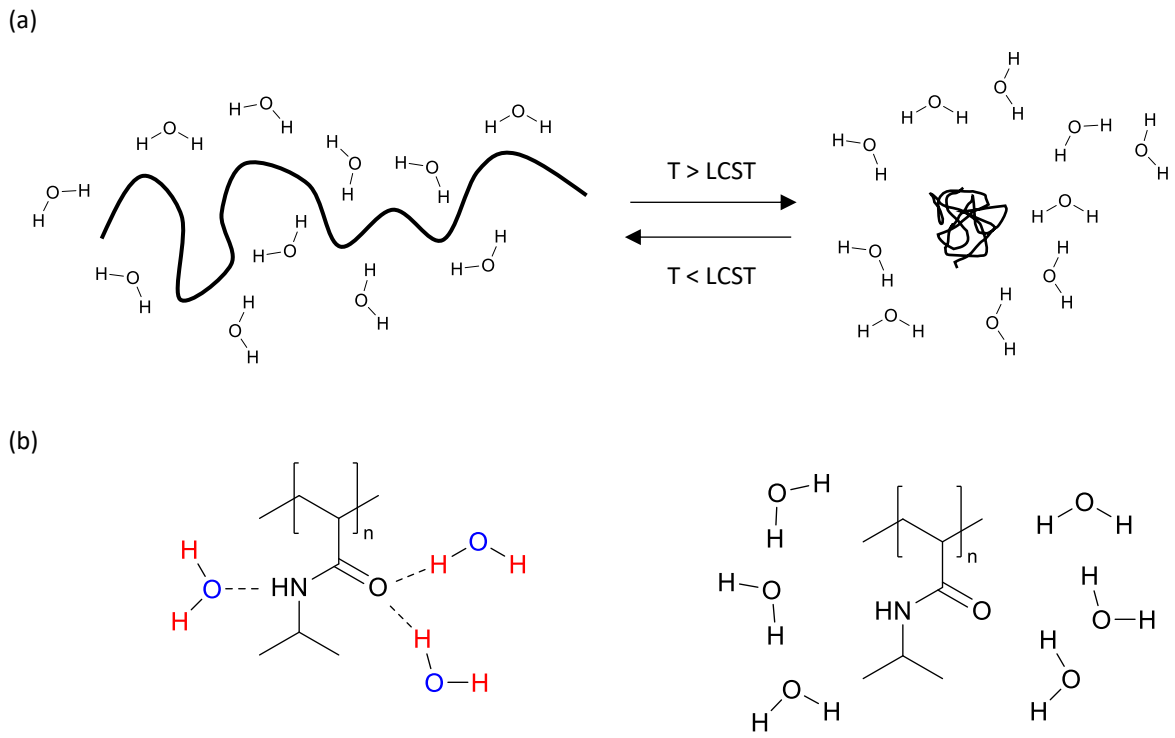

Figure 1.4. (a) Schematic view of phase separation of LCST polymer (coil-to-globule transition) (b) proposed model of hydration and dehydration of PNIPAM (Left: ordered water molecules by H-bonding Right: disordered water molecules around the polymer chains leading to phase separation)

Since UCST behaviour of polymers scarcely appears around the practical temperature range in aqueous solution, the polymers of this class likely have got less interest and been infrequently reported. Amongst well-known polymers having simple structures, PEGs exhibit UCST as well as LCST and the shape of phase diagram is closed-loop, but the both transitions happen above 100 ºC.[87] PHEMA, which possesses a H-bonding site with some extent of hydrophobicity in the pendent group, showed LCST and UCST which depended on the polymer concentration. PHEMA-4K (DP ~25; MW ~4 KDa) was revealed to show a LCST at ~23 ºC, and an UCST over 90 ºC, and the immiscible regime between two points became narrower on more diluted solutions.[94] And, PHEMAs copolymerized with *N,N*-dimethylaminoethyl methacrylate (DMAEMA) or [2-(methacryloyloxy)ethyl]trimethyl-amonium chloride (MOETAC) exhibited the same soluble-insoluble-soluble behaviour in acidic condition (HCl solution) and NaCl presence, respectively. The UCSTs on the higher temperature side appeared more clearly under salt presence in many cases, which may be attributed to the charge screening effect and breakage of H-bonds between polymers.[94]

A non-ionic polymer poly(*N*-acryloyl glycinamide) (PNAGA) and the derivatives have been extensively studied for their UCST behaviour in water since recent years. PNAGA was known long ago in 1964, the synthesis of the

homopolymer and copolymers, and the aggregation at low temperature as thermoresponsive gels were reported.[95, 96] A patent[97] mentioned UCSTs of PNAGA as well as their derivatives and copolymers, then synthesis and the transition behaviour of the polymers were rigorously elucidated by Glatzel et al.[98, 99] and Seuring et al.[100, 101] with the aid of controlled radical polymerisation technique. The UCST behaviour of those polymers is based on H-bonding between amide groups which acts interchain binding force (**Figure 1.5**), and the critical point was able to be controlled to get the response near room temperature by tuning the degree of polymerisation and increasing the concentration. Interestingly, the phase transition of Poly(*N*-acryloylasparaginamide) (PNAAAm) was observed similarly in phosphate buffered saline (PBS) solutions[99] as the case of PNAGA in human blood serum.[101] Poly(*N*-methacyloylasparagineamide) (PMNAAAm) was reported to have both UCST and LCST at 13 °C and 33 °C in pure water, respectively,[97] presumably due to higher hydrophobicity than PNAGA. However, the stability of the polymers would be doubted for consistent demonstrations of the feature. Especially for PNAGA, the UCST was heavily relied on the monomer purity (acrylates in monomer), ionic groups at the end of the chain (radical initiator- or CTA-originated), and the percentage of unwanted acrylic acid motifs accidentally derived by hydrolysis of the repeating unit during polymerisation in water or thermoresponse tests of the final product.[101] According to the authors, these several factors lower or supress the UCST, consequently the polymer had not been popularised for those reasons.[101] Thus, it is thought that much attention has to be paid for exploiting the PNAGA family in all steps from monomer preparation to synthesis and characterisation of the polymers.

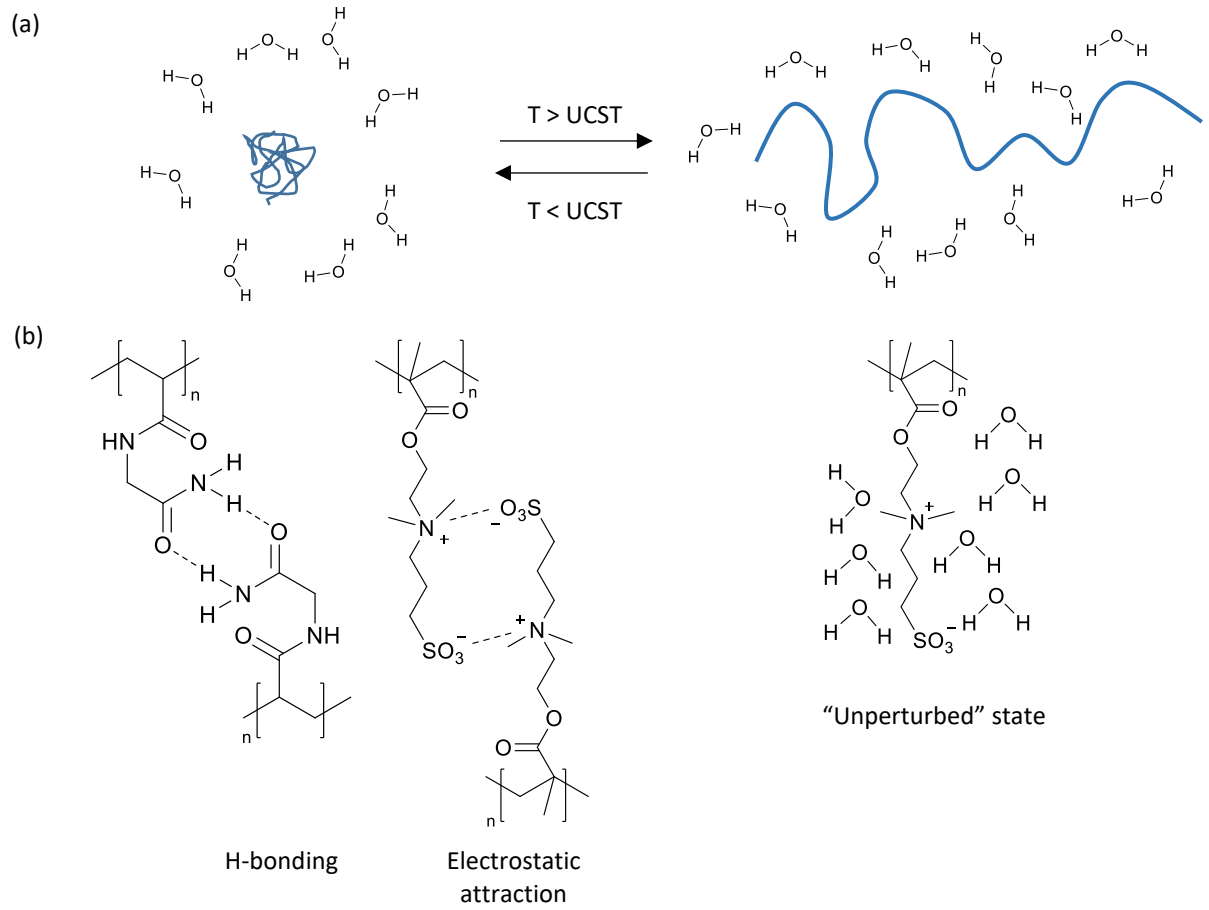

Figure 1.5. (a) Schematic view of phase behaviour of UCST polymers (b) Chemical structures representations of UCST polymers in a phase separated and dissolved state (Left: the cohesive force is H-bonding for PNAGA and electrostatic attraction for PSPE Right: the original ordering of water molecules are not disturbed by dissolution of polysulfobetaines)

UCST behaviour in aqueous solution was also found on some random copolymers composed of simpler chemical structured motifs. Poly(allylamine-*co*-allylurea) exhibited variable UCSTs in buffer or salt solutions.[102] Similar to the formal cases, intermolecular H-bonding between the ureido groups triggered phase separation, and the critical temperature became higher by increasing the ureido content. Poly(acrylamide-*co*-acrylonitrile), whose repeating units are produced on large scales in industries, showed UCST behaviour in pure water and PBS.[100, 103] The author added acrylonitrile as comonomer for modifying the hydrophilic-lyphophilic balance of the copolymer, and higher percentages of acrylonitrile increased the cloud point from ~5 to ~55 °C.[100] In this case, hydrophobic acrylonitrile moieties affected the decrease of ΔS_m because more structured water molecules around the hydrophobic motif were required for solvation than the case of homo-polyacrylamide, which can make H-bonding each other but cannot exhibit UCST solely. Besides, few polyelectrolyte copolymers revealed this behaviour by electrostatic attraction. A polyampholyte poly(vinylbenzyl trimethylammonium chloride-*co*-sodium styrenesulfonate) (PVBTC-*co*-PSSNa) where the ratio of each component was almost identical revealed insoluble-soluble transition

under heating.[104] The critical temperature was affected by the degree of polymerisation, and the concentration of added electrolytes (NaCl) due to screening effect of cations and anions. It is known that only polysulfobetaines show UCST transition, however a polyphosphobetaine-based block copolymer unexpectedly manifested the transition by introducing pendent ureido groups.[105] The poly(2-ureidoethyl methacrylate-*block*-MPC) (PUEM-*b*-PMPC) chains in water showed unimer-to-micelle transition (~5 nm to ~20 nm) under temperature decreases when the PUEM moiety was quite enough compared to the MPC units, which was inert in the system. In consequence, it should be noted that the transition mechanism of the block copolymer is not classified as that of polyzwitterions but other non-ionic UCST polymers driven by H-bonding.

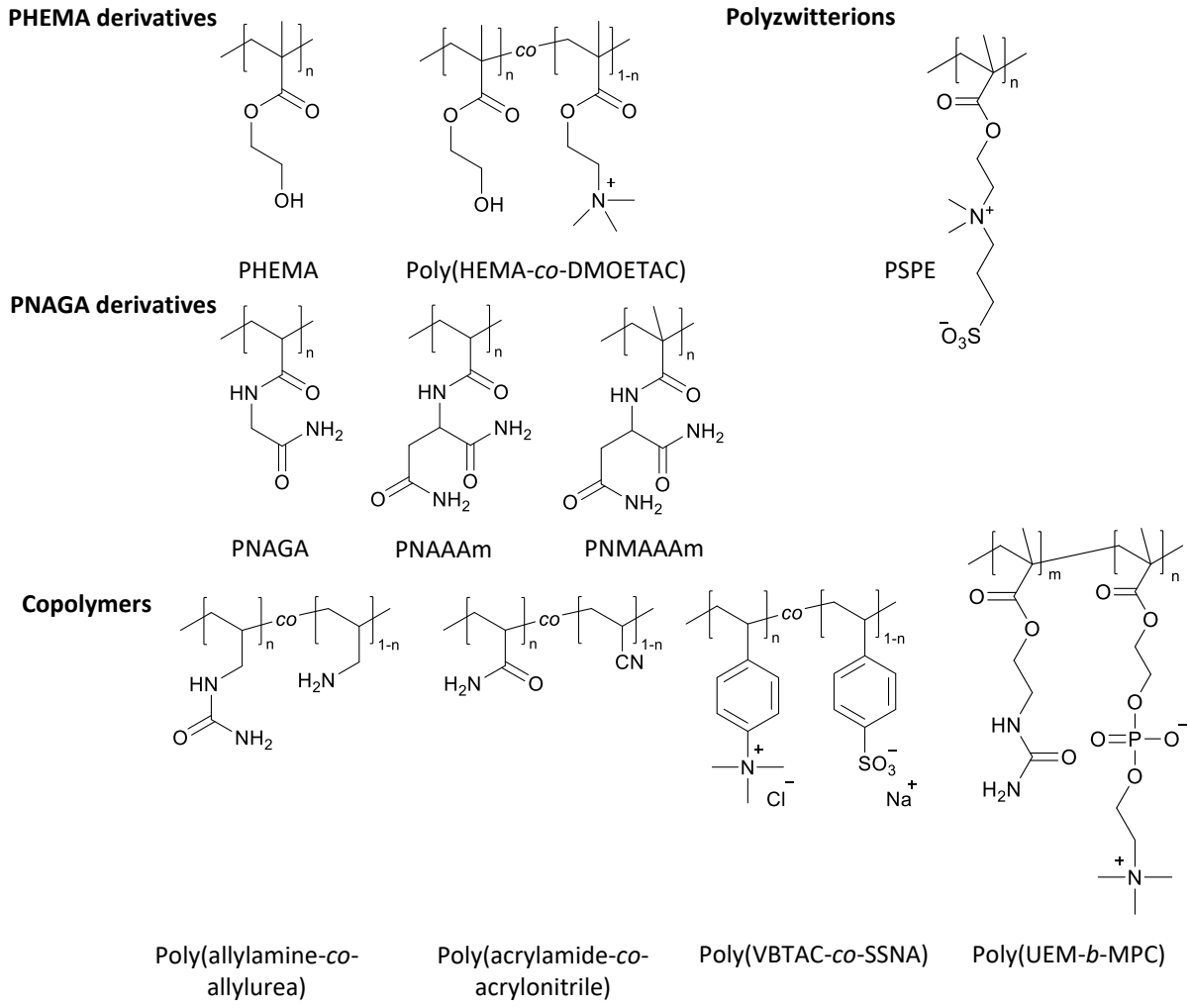

Figure 1.6. Examples of UCST polymers (homopolymers and copolymers)

1.2.2. pH-responsive polymers

Polymers having weak acidic or basic functional groups are able to respond against pH. As general weak acids or bases, the pendent groups are in a protonated/ionized state when the pH is under/over the pK_a, and it affects the hydrophilicity and the swelling behaviour of the chain. One of the most frequently mentioned polymer is poly(acrylic acid) (PAA), also known as carbomer, which is utilised as rheology modifier and suspending agent in water-based products. In pure water, some extent of carboxylic acid provides excess proton and makes the initial pH to 2.5–3.5, which is lower than the pK_a of PAA = 4.2–4.5, hence most of pendent groups remain in the protonated form. In the state, the polymer chains do not fully dissolved and exist as dispersion of globules in water due to insufficient hydrophilicity, and hydrogen bondings among other sites of polymers may involve the chain collapse.[106] Above pH ~5, deprotonation of carboxylates starts and promotes the solubility, hence the globules go into a swollen chain state seen as clear viscous solution. (**Figure 1.7**) The straightforward mechanism has been still exploited to realise pH-responsive colloidal objects.[107, 108] Other polymers having carboxylates in the repeating unit are also able to respond to pH variation and show different hydrophilicity. For example, poly(4-vinylbenzoic acid) (PVBA) exhibited insoluble-soluble transition along acidic to neutral and basic conditions in copolymerised forms with another ionic or hydrophobic block,[109, 110] which resulted in PVBA-centred polymer micelles. Phosphonic acid polymers might have the potential, although their pK_a is lower than carboxylic acid. Poly(vinylphosphonic acid) showed pK_a ~3 whereas the monomer had two pK_a at 2.74 and 7.34,[111] however the pH effect was minor on the swelling behaviour of the crosslinked hydrogel.[112] Poly(ethylene glycol methacrylate phosphate) (PEGMP) embedded PHEMA hydrogel showed increase of water uptake at pH 2–3 due to the pH-responsive PEGMP,[113] however there are only few studies of phosphonic acid polymers focused on their pH sensitivity compared to carboxylic acid type polymers. A biodegradable synthetic peptide poly(L-glutamic acid) (PLGA) which has been applied for providing negative charges on the surface as well as attachment point for polymer-drug conjugates could be used for pH-responsive application. Thanks to the carboxylate end, PLGA nanogels were revealed surface charge variations against pH and different release behaviours of loaded molecules.[114, 115]

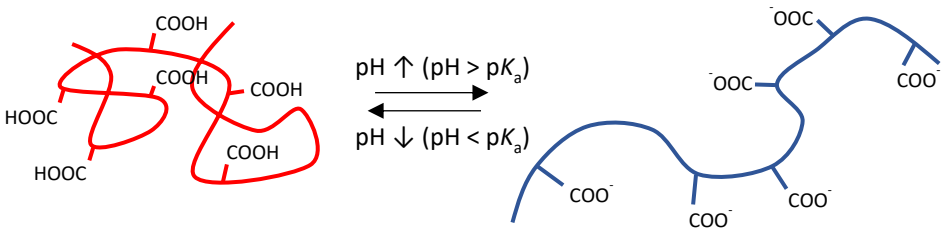

Figure 1.7. Schematic view of PAA in water and globule-to-coil transition against pH variation

Besides, weak polybases undergo a swollen state below pK_a and a hydrophobic state over pK_a in contrast to weak polyacids, owing to positive charged groups by accepting protons. Poly(2-vinylpyridine) (P2VP) or poly(4-vinylpyridine) (P4VP) is presumably the most well-known example for the property and stark difference to poly(styrene) (PS) as well. Having substituted a carbon in the phenyl group with a nitrogen, P2VP shows clear phase separation behaviour in PS/P2VP blends and a block copolymer PS-*b*-P2VP, and can dissolve in acidic water (pK_a = 4.98) by protonation of the pyridine group. A variety of (meth)acrylate polymers and (meth)acrylamide polymers are also known for pH-responsive property approximately over pH = 7. Poly(2-(dimethylamino)ethyl methacrylate) (PDMAEMA), poly(2-(diethylamino) ethyl methacrylate) (PDEAEMA), and poly(2-(diisopropylamino)ethyl methacrylate) (PDPA) are showing soluble-insoluble transition in water promoted by protonation of tertiary amine group in common. Since the moderate hydrophilic/hydrophobic balance, PDMAEMA can dissolve in water and precipitate at 32–53 °C, which depends on the molecular weight,[116] hence has been dealt as PNIPAM.[117] However, PDEMAEMA and PDPA are insoluble to water at neutral or alkaline pH, only the protonated forms are soluble. The pH-responsivity of those three polymers have been utilised for designing nanocarriers that could release drugs at acidic-neutral environment by disassociation of polymer micelles. The block copolymers incorporated with inert motifs form PDPA-core micelles in PBS (pH = 7.4) demonstrated release of inner molecules at slightly acidic tumoral extracellular environments (pH ~5) by disassociation of micelles.[118, 119] Incorporation with other temperature-responsive motifs[78, 120, 121] (e.g. PNIPAM or PSPE) showed dual stimuli-responsive property against pH and temperature both that originated from respective blocks. The block copolymer chains formed core-shell structured micelles in the given temperature and pH, which preferentially dissolved one side, and phase inversion occurred by heating or pH change. In addition, compared to the methacrylate type polymers, acrylate types having tertiary amine revealed irreproducible stimuli-responsive behaviour under high temperatures due to self-catalysed hydrolysis in water, which eventually yields PAA.[122] Therefore, it is not recommended to use acrylate type tertiary amine polymers as stimuli-responsive block in terms of stability.

Other polymers containing pyrrolidine,[123] morpholino,[124] and imidazole[125] functional groups are also available for pH-responsivity. Notably, poly(2-(N-morpholino)ethyl methacrylate) (PMEMA) is a multiple stimuli-responsive polymer against not only pH (pK_a = 4.9)[126] but also temperature (LCST at ~44 ^oC)[126, 127] and salt[128, 129] in a homopolymer and block copolymer form. Moreover, the biocompatibility of PMEMA was evaluated in transfection test of an oligonucleotide,[130] expecting potential for nanomedical applications. Polymers having imidazole-ends in the repeating unit are expected to have a tunable pH response range by modifying the carbon spacer length between the ester group to the imidazole. Poly(6-(1H-imidazol-1-yl)hexyl methacrylate) (PImHeMA) with PEG and poly(glycerol methacrylate) (PGMA) blocks recorded pK_a = 5.7, consequently the triblock copolymer was able to create polymersomes in alkaline solutions then release encapsulated substances in acidic conditions (pH < 5).[125]

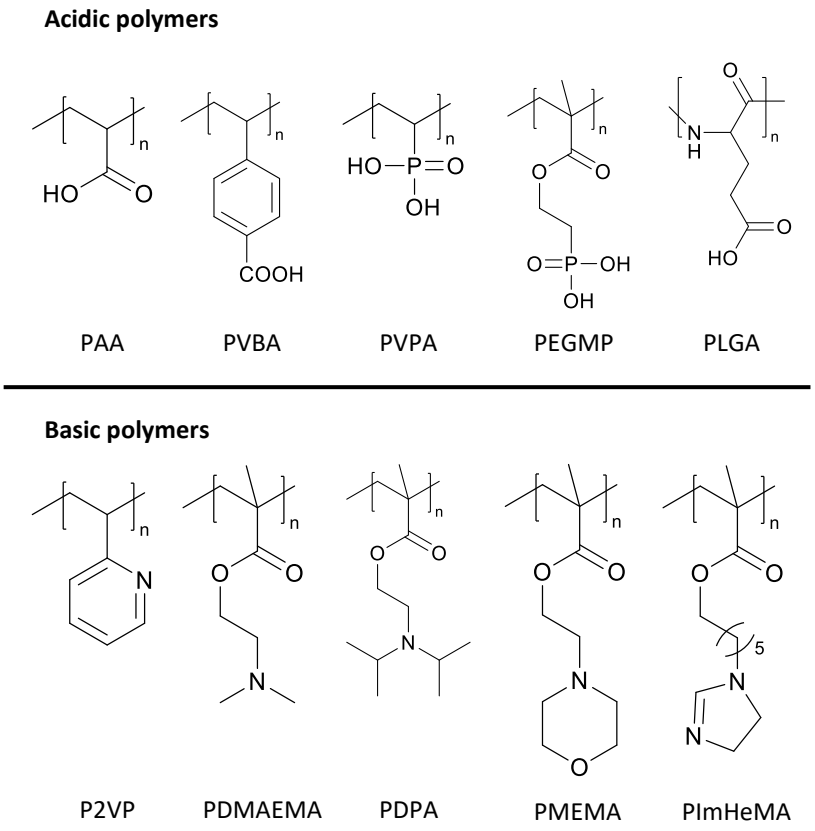

Figure 1.8. Examples of pH-responsive polymers

1.3 Double hydrophilic block copolymers

1.3.1 Brief overview: self-assembly of polymers

Setting up nanostructures by synthetic polymers has been received considerable attention for fabricating highly functional materials in nanoscales. Also, that is a biomimetic attempt with synthetic polymers to build self-assembled complex small-scale structures as natural polymers (e.g. proteins, cellulose, etc.) create bilayers and specific chain foldings. In the industrial field, spontaneous structure formation of synthetic polymers has been systematically studied since several decades to achieve nanoscale patterns which could be applied to build semiconductor circuit ("bottom-up" approach) instead of optical lithography ("top-down" approach). With the progress of polymerisation technique, chain length and molecular weight distribution of block copolymers became able to be controlled so that well-defined nanostructures by adjusting compositions of blocks and molecular weights have been demonstrated. In principle, the difference of the chemical affinity of respective motifs against outer environment is the key factor upon alignment of polymers in a confined area. PS-*b*-P2VP or PS-*b*-PMMA is the classical example of demonstrating lamellar, cylindrical, spherical or gyroid structures on a substrate. To produce the self-assembled nanostructures, thermal or solvent annealing process is necessary to equilibrate the thermodynamics of block copolymer thin films. The self-assembled structure on a substrate could be modified further by selective removal of one block then used as mask layer in etching process (e.g. reactive ion etching).[131]

If a block copolymer has one hydrophilic part and one hydrophobic part on the other side, it becomes compatible to both water/oil phase. This clear contrast of chemical affinities between the two blocks lets the chains get the label "amphiphilic" block copolymer. In aqueous system, amphiphilic block copolymers can create self-assembled structures as surfactants that consist of an alkyl chain and an ionised group. The polymer chains go to water/air interface then eventually form micelles to reduce the high interfacial tension of hydrophobic parts when the concentration of the polymer exceeds the critical micelle concentration, which is much lower than that of small-molecule surfactants because of the larger molecular weight of polymers. The self-assembled structures are explained and able to be predicted by introducing the concept of molecular packing parameter[132] $p = v_o/a_o l_c$, where v_o and l_c are the volume and the length of the hydrophobic motif, and a_o is the surface area of the core part. Considering the geometrical relations and constraints of aggregates, the parameter is divided by specific ranges for each shape: $0 \leq v_o/a_o l_c \leq 1/3$ for spherical micelles, $1/3 \leq v_o/a_o l_c \leq 1/2$ for cylinders, $1/2 \leq v_o/a_o l_c \leq 1$ for vesicles or bilayers.[133]

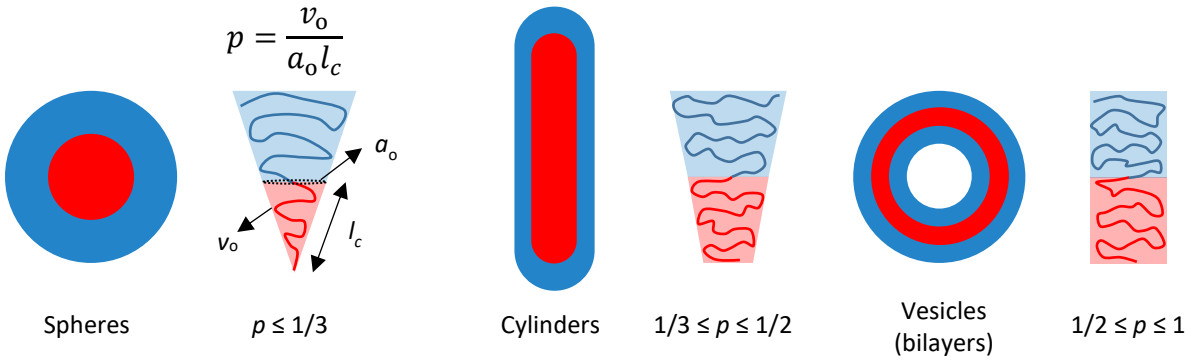

Figure 1.9. Morphologies of amphiphilic block copolymers and the effect of packing parameter *p* to the final structure

Thanks to progress of polymerisation technique, various kinds of hydrophilic-hydrophobic block copolymers, and the control of DP, molecular weight distribution, and structure became available. Notably, polymerisation-induced self-assembly (PISA) technique has been established as a powerful and convenient approach to get various structures in aqueous media. In short, a hydrophilic homopolymer A is obtained in advance by living radical polymerisation (typically RAFT polymerisation[134-136]), which can commence further chain extension after termination, then a hydrophobic monomer B is added in water or alcoholic media. The B block gradually becomes more insoluble in the media by the chain growth, finally *in-situ* self-assembly of AB diblock copolymer occurs.[137] The final structure of the amphiphilic block copolymers obtained by this method is determined by the ratio of chain length, consequently the self-assembly behaviour directly shows the varying morphology of sphere, worm-like, or vesicle that depends on the monomer B content against the homopolymer A in the second step. More complex structures such as framboidal vesicles,[138, 139] yolk-shell particles,[140-142] or morphology transition triggered by a stimulus-responsive functional group have been reported.[143-145]

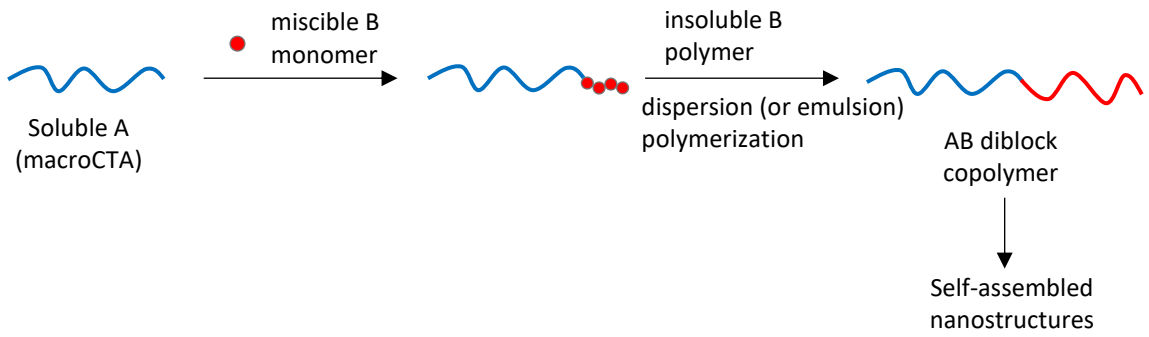

Figure 1.10. Preparation of amphiphilic block copolymers through polymerisation-induced self assembly (PISA)

1.3.2 Double Hydrophilic block copolymers

Double hydrophilic block copolymers (DHBC) seem to be an unfamiliar concept since the "hydrophilic" expression are likely to shade the gap of the chemical affinity between two components. As other block copolymers, they also have the different affinities against water molecules, therefore the chains are also able to form self-assembled structures in specific conditions. Perhaps the often-argued case is stimuli-responsive double hydrophilic block copolymers that bear the functionality of changing hydrophilic to hydrophobic in specific conditions, or vice versa. Hence, strictly speaking, their self-assembly is technically based on the mechanism of amphiphilic block copolymers. Microphase separation similarly occurs like amphiphilic block copolymes when the one side lose hydrophilicity and tend to merge together. Temperature-responsive polymers are easily applied for this system. For instance, the system of a LCST/UCST-type moiety plus a permanent hydrophilic moiety can demonstrate a swollen chain state and core/shell polymer micelles at respective sides of the transition temperature. PEG or POEGMA is typically incorporated as hydrophilic stabiliser to form hydrophilic layers of the micelles with another hydrophilic functional group.[146-151] In addition, combinations of LCST-UCST type block copolymers or temperature- and pH-double responsive block copolymers can result "schizophrenic" micelles at each extreme condition (e.g. hot/cold or acidic/basic) and free chains in the moderate condition.[69, 70, 79, 121, 128] Specific ion effect can drive the phase change by inducing solubility deviations of the two components. For example, PMEMA-*b*-PSBMA which fully dissolved in $NaBr_{(aq)}$ showed selective dehydration of PMEMA block under Na_2SO_4 addition and eventual phase inversion, whereas the PSBMA block created the core at low salt concentrations then became more soluble by introducing both salts.[128, 129]

Upon the design of the stimuli-responsive DHBC, the original behaviour of a stimuli-responsive moiety would be modified due to the hydrophilic stabiliser on the opposite side. For some cases of DHBCs having a temperature-responsive block, increased LCST/decreased UCST has been found, indicating broadened one-phase region. It is thought that a block which remain hydrophilic may moderate the hydrophilic-hydrophobic balance of the other block affected by outer stimuli.[121, 152] Therefore, additional characterisation must be followed on each case of the obtained DHBCs to confirm the modified transition point in order to optimising the feature to desired properties.

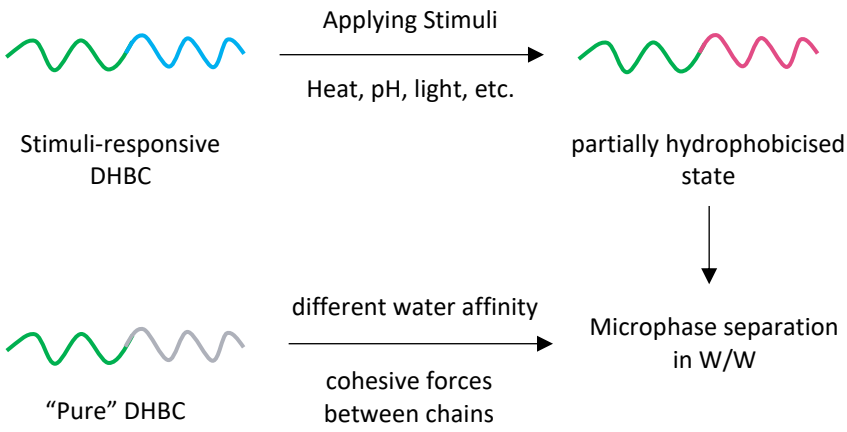

Figure 1.11. Two DHBCs: stimuli-responsive and non-responsive ("pure") DHBC

Non-responsive DHBCs, which were less discovered but have been explored recently, correspond more exactly to the definition of DHBC. The both motifs have no responsive functional groups so the original hydrophilicity of both motifs is kept in any circumstances. Accordingly, the process of self-assembly can be figured out in a different viewpoint, as two-phase coacervation of two hydrophilic homopolymers.[153] The water/water (W/W) phase separation has been demonstrated by bulky hydrophilic substances, such as glycopolymers[154-158] (pullulan, dextran, etc.) and their derivatives, and poly(2-methyl-2-oxazoline) (PMOXA)-contained systems.[159-161] Two approaches are applied to obtain glycopolymer-based DHBCs: coupling of glycopolymers with other synthetic hydrophilic polymers, and free radical polymerisation of glucosyl methacrylates with other moieties. In the first method, an alkyne end-functionalised glycopolymer and an azide end-functionalized hydrophilic polymer is prepared separately, then linked by 1,3-dipolar cycloaddition (famously known as "click" chemistry). The block copolymers with PEG and poly(sarcosine), where the hydroxyl group is substituted with amine, were revealed mesophase separation in water and the structure was identified as vesicle-like aggregates (R_h = 250 nm), not solid particles or gels.[154] The other hydrophilic blocks can be incorporated through living radical polymerisation technique: coupling of a CTA (RAFT agent) or ATRP-mediating functional group to glycopolymers then subsequent polymerisation of the second block. By this approach, easily obtainable hydrophilic polymers such as PVP, PHEMA, PMEMA, or poly(betaine methacrylates) are able to be added as the second block. The self-assembly of glycopolymer-based DHBC is thought to be attributed by H-bonding between hydroxyl groups and chain entanglement between glycopolymer chains.[156] Disassociation to unimers at high temperatures implies the driving force is H-bonding rather than hydrophobic interaction.[157] Or, the other motif would render phase separation and become the core part of the object if the water affinity is weaker than that of glycopolymers in the opposite side.[158] Besides, the solution behaviour of oxazoline-based DHBCs (PEG-*b*-PMOXA) was reported that

they started to create nanostructures (roughly spheres, R_h = ~100 nm) where the concentration was above 1 wt%, even PMOXA took up almost 10 folds more water than PEG in water uptake experiment.[160] Hence, the authors concluded that the entropic contribution to aggregation formation is subtle unlike typical amphiphilic block copolymers, and the phenomenon could be understood by "graded hydrophilicity".[160]

What DHBCs are better than amphiphilic copolymers is easy control of the spontaneous state without usage of cosolvents and selective drying process for assembly. Because of higher molecular weights, the final structure of amphiphilic copolymers is not always corresponded with theoretically predicted models unlike surfactant molecules, particularly for direct dissolution of the chains into a solvent which preferentially solvates one side. Additional treatment is required for releasing kinetically frozen structures and obtaining thermodynamically equilibrated structures, which is similar to the preparation of block copolymer morphologies in a thin film. Meanwhile, adjusting properties of water is the only prerequisite for getting the thermodynamically equilibrated state in DHBCs, hence incorporation and disassociation of other functional materials (e.g. drugs or nanoparticles) with copolymer chains would be also more accessible as well. Moreover, they are expected to have high biocompatibility and degradability due to uniformly hydrophilic behaviour[153] that may prevent adsorption of outer molecules by hydrophobic attraction, of course the non-fouling feature has to be confirmed in respective cases. Superior permeability than that of self-assembled structure of amphiphilic copolymer having stiff hydrophobic cores, which showed insufficient permeability for drug delivery application,[162, 163] is another powerful potential. The compartmentalised inner volume in the self-aseembly of DHBCs is thought to be surrounded by a soft and flexible layer where some extent of water molecules can go through, suggested by visible ^{1}H NMR spectra indicating the inner motif.[53, 164]

Characterisation of DHBC is more difficult than typical amphiphilic copolymers, since the self-assembled structures are generally not fixed and hard to maintain the original form outside of water. It makes TEM analysis much harder; merging or disruption of objects is unavoidable under drying. Hence, cryogenic technique (cryo-TEM or cryo scanning electron microscopy (cryo-SEM)) is forced to displaying the direct image of DHBC particles.[154, 156, 160] For the same reason, atomic force microscopy (AFM) is inappropriate for correct imaging since the water content varies on drying so that it alters the equilibrium point, and the original structure on a substrate gets the influence. In-situ AFM measurement (wet AFM) may compensate the issue.[165, 166] Non-invasive method (light, x-ray and neutron scattering) is relatively free from the problem, but the data analysis should be carefully performed not to include errors.

1.4 Aims of the thesis

The study is focused on a double zwitterionic block copolymer, PGLBT-*b*-PSPE. Composed of a polycarboxybetaine and a polysulfobetaine, the polymer is basically holding double hydrophilic motifs, and two stimuli-responsive functions against temperature and pH, respectively. Surprisingly, any other studies have not been yet investigated this block copolymer, only few betaine random copolymer studies were reported.[46, 167] To my best knowledge, this is the first in-depth study of multiple zwitterionic block copolymers. In this dissertation, synthesis of whole betaine block copolymers, the temperature- and pH-responsive behaviour and the self-assembly in aqueous solutions are systematically studied.

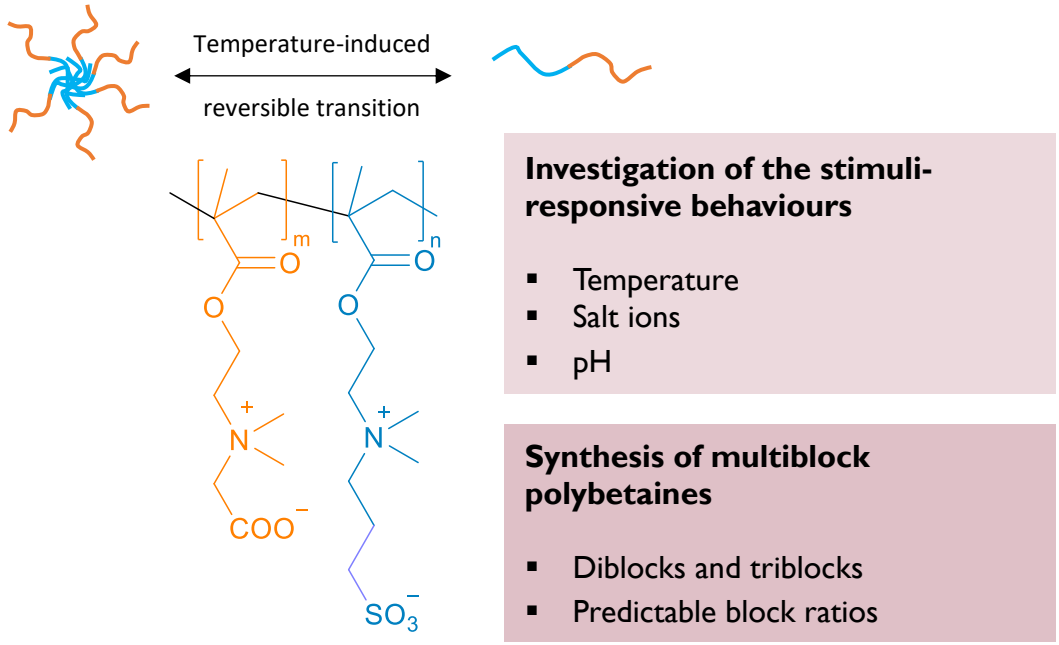

Figure 1.12. A schematic view of the investigation objectives in the thesis

In Chapter 2, the synthesis and general characteristics of PGLBT-*b*-PSPE are presented. It was the first attempt to obtain carboxybetaine-*block*-sulfobetaine block copolymers. The second block PSPE was extended from PGLBT macroCTAs by RAFT polymerisation performed in water. Obtained PGLBT-*b*-PSPE repeatedly showed unimer-to-micelle transition: monodisperse polymer micelles (R_h = 40–60 nm) under the UCST, and back to unimers at higher temperatures. However, most of PGLBT chains did not participate in the second polymerisation step, therefore excess purification of residual PGLBTs from the product was necessary. For that reason, the precise control of the block ratio was not available, to the extent that the influence of the block ratio on the thermoresponsive behaviour is not dealt meticulously.

In Chapter 3, specific ion effect of halide anions on PGLBT-*b*-PSPE is studied. The difference of degree of promoting solvation or precipitation of ions in polymer aqueous solutions is known as "Hofmeister series", which classifies ions into chaotropes and kosmotropes. Since it could not be explained the difference of ions by continuum electrostatic theories and depends on so many factors,[168] arguments and experimental results continuously have been proposed to define the phenomenon. The salt effect in aqueous solutions of proteins and non-ionic synthetic polymers was extensively studied, while just several polyzwitterions have been yet under investigation. In the section, the effect of four halide ions on the solution behaviour of PGLBT-*b*-PSPE is compared by observing the formation-deformation of polymer micelles.

In Chapter 4, pH effect on the thermo-induced self-assembly behaviour of PGLBT-*b*-PSPE is delivered. Since PGLBT is protonated under acidic conditions, the charge neutrality is disrupted and goes to a partly positive state. To prove the pH influence, the solution behaviour of the chains and the charge variations in acidic, neutral, and basic conditions are investigated.

In Chapter 5, one-pot synthesis of PGLBT-*b*-PSPE is presented. As described in chapter 2, block extensions from polybetaine macroCTAs was poorly controlled due to unstable RAFT functional groups in water. Accepting the methodology of one-pot multiblock acrylamide polymer synthesis,[169] di- and triblock betaine methacrylate copolymers were successfully obtained without any purification during the interval. The degree of polymerisation of each block was able to be predicted theoretically, since full consumption of betaine monomers was accomplished.

In Chapter 6, the effect of the block ratio [PGLBT]:[PSPE] is carefully scrutinised. The precise control of the block ratio finally became available by the result of chapter 5, and several diblocks having similar total DP with different block ratios were prepared. The observation results suggest that the ratio strongly governs the sensitivity against temperature, however the effect of DP is not critical on the behaviour. Triblocks having the same ratio and DP with diblocks rendered more significant phase behaviour at higher temperatures.

References

1. L. Rigano, G. Dell'Acqua and R. Leporatti, *Cosmetics & Toiletries*, 2000, **115**, 47-54.
2. A. M. Le Bell, E. Soderling and J. Tenovuo, *Journal of Dental Research*, 1998, **77**, 974-974.
3. I. Nicander, I. Rantanen, B. L. Rozell, E. Soderling and S. Ollmar, *Skin Research and Technology*, 2003, **9**, 50-58.
4. S. Ghosh and D. Blankschtein, *Journal of Cosmetic Science*, 2007, **58**, 109-133.
5. A. Laschewsky and A. Rosenhahn, *Langmuir*, 2019, **35**, 1056-1071.
6. D. Chapman, *Langmuir*, 1993, **9**, 39-45.
7. E. F. Murphy, J. R. Lu, J. Brewer, J. Russell and J. Penfold, *Langmuir*, 1999, **15**, 1313-1322.
8. K. Glasmastar, C. Larsson, F. Hook and B. Kasemo, *Journal of Colloid and Interface Science*, 2002, **246**,

40-47.
9. J. Sun, F. Zeng, H. L. Jian and S. Z. Wu, *Biomacromolecules*, 2013, **14**, 728-736.
10. H. Ladenheim and H. Morawetz, *Journal of Polymer Science*, 1957, **26**, 251-254.
11. R. Hart and D. Timmerman, *Journal of Polymer Science*, 1958, **28**, 638-640.
12. E. Wischerhoff, N. Badi, A. Laschewsky and J. F. Lutz, *Bioactive Surfaces*, 2011, **240**, 1-33.
13. Y. Chang, S. C. Liao, A. Higuchi, R. C. Ruaan, C. W. Chu and W. Y. Chen, *Langmuir*, 2008, **24**, 5453-5458.
14. W. Yang, S. F. Chen, G. Cheng, H. Vaisocherova, H. Xue, W. Li, J. L. Zhang and S. Y. Jiang, *Langmuir*, 2008, **24**, 9211-9214.
15. C. R. Emmenegger, E. Brynda, T. Riedel, Z. Sedlakova, M. Houska and A. B. Alles, *Langmuir*, 2009, **25**, 6328-6333.
16. S. Abraham, M. S. Bahniuk and L. D. Unsworth, *Biointerphases*, 2012, **7**.
17. C. Blaszykowski, S. Sheikh and M. Thompson, *Chemical Society Reviews*, 2012, **41**, 5599-5612.
18. L. Tauhardt, D. Pretzel, K. Kempe, M. Gottschaldt, D. Pohlers and U. S. Schubert, *Polymer Chemistry*, 2014, **5**, 5751-5764.
19. S. C. Lange, E. van Andel, M. M. J. Smulders and H. Zuilhof, *Langmuir*, 2016, **32**, 10199-10205.
20. B. Bendinger, H. H. M. Rijnaarts, K. Altendorf and A. J. B. Zehnder, *Applied and Environmental Microbiology*, 1993, **59**, 3973-3977.
21. L. D. Blackman, P. A. Gunatillake, P. Cass and K. E. S. Locock, *Chemical Society Reviews*, 2019, **48**, 757-770.
22. J. W. Costerton, Z. Lewandowski, D. E. Caldwell, D. R. Korber and H. M. Lappinscott, *Annual Review of Microbiology*, 1995, **49**, 711-745.
23. H. W. Ma, J. H. Hyun, P. Stiller and A. Chilkoti, *Advanced Materials*, 2004, **16**, 338-+.
24. C. S. Gudipati, J. A. Finlay, J. A. Callow, M. E. Callow and K. L. Wooley, *Langmuir*, 2005, **21**, 3044-3053.
25. J. L. Dalsin, B. H. Hu, B. P. Lee and P. B. Messersmith, *Journal of the American Chemical Society*, 2003, **125**, 4253-4258.
26. S. Lowe, N. M. O'Brien-Simpson and L. A. Connal, *Polymer Chemistry*, 2015, **6**, 198-212.
27. J. Ladd, Z. Zhang, S. Chen, J. C. Hower and S. Jiang, *Biomacromolecules*, 2008, **9**, 1357-1361.
28. Z. Zhang, H. Vaisocherova, G. Cheng, W. Yang, H. Xue and S. Y. Jiang, *Biomacromolecules*, 2008, **9**, 2686-2692.
29. S. Y. Jiang and Z. Q. Cao, *Advanced Materials*, 2010, **22**, 920-932.
30. L. Mi and S. Y. Jiang, *Angewandte Chemie-International Edition*, 2014, **53**, 1746-1754.
31. C. Leng, H. C. Hung, S. W. Sun, D. Y. Wang, Y. T. Li, S. Y. Jiang and Z. Chen, *Acs Applied Materials & Interfaces*, 2015, **7**, 16881-16888.
32. S. F. Chen, L. Y. Li, C. Zhao and J. Zheng, *Polymer*, 2010, **51**, 5283-5293.
33. D. J. Vanderah, H. L. La, J. Naff, V. Silin and K. A. Rubinson, *Journal of the American Chemical Society*, 2004, **126**, 13639-13641.
34. J. F. Lutz, O. Akdemir and A. Hoth, *Journal of the American Chemical Society*, 2006, **128**, 13046-13047.
35. J. B. Schlenoff, *Langmuir*, 2014, **30**, 9625-9636.
36. A. B. Lowe, N. C. Billingham and S. P. Armes, *Macromolecules*, 1999, **32**, 2141-2148.
37. J. G. Weers, J. F. Rathman, F. U. Axe, C. A. Crichlow, L. D. Foland, D. R. Scheuing, R. J. Wiersema and A. G. Zielske, *Langmuir*, 1991, **7**, 854-867.
38. V. A. Izumrudov, N. I. Domashenko, M. V. Zhiryakova and O. V. Davydova, *Journal of Physical Chemistry B*, 2005, **109**, 17391-17399.
39. J. D. Delgado and J. B. Schlenoff, *Macromolecules*, 2017, **50**, 4454-4464.
40. P. Mary, D. D. Bendejacq, M. P. Labeau and P. Dupuis, *Journal of Physical Chemistry B*, 2007, **111**, 7767-7777.
41. A. B. Lowe and C. L. McCormick, *Chemical Reviews*, 2002, **102**, 4177-4189.
42. F. Wang, J. F. Yang and J. Zhao, *Polymer International*, 2015, **64**, 999-1005.
43. H. Matsuoka, Y. Yamakawa, A. Ghosh and Y. Saruwatari, *Langmuir*, 2015, **31**, 4827-4836.
44. Z. L. Cao and G. Z. Zhang, *Physical Chemistry Chemical Physics*, 2015, **17**, 27045-27051.
45. A. Z. Niu, D. J. Liaw, H. C. Sang and C. Wu, *Macromolecules*, 2000, **33**, 3492-3494.
46. E. E. L. Kathmann, L. A. White and C. L. McCormick, *Macromolecules*, 1997, **30**, 5297-5304.
47. R. Kumar and G. H. Fredrickson, *Journal of Chemical Physics*, 2009, **131**.
48. V. Hildebrand, A. Laschewsky and D. Zehm, *Journal of Biomaterials Science-Polymer Edition*, 2014, **25**, 1602-1618.
49. Y. C. Zhu, J. M. Noy, A. B. Lowe and P. J. Roth, *Polymer Chemistry*, 2015, **6**, 5705-5718.
50. H. Willcock, A. Lu, C. F. Hansell, E. Chapman, I. R. Collins and R. K. O'Reilly, *Polymer Chemistry*, 2014, **5**, 1023-1030.

51. O. Azzaroni, A. A. Brown and W. T. S. Huck, *Angewandte Chemie-International Edition*, 2006, **45**, 1770-1774.
52. K. E. B. Doncom, A. Pitto-Barry, H. Willcock, A. Lu, B. E. McKenzie, N. Kirby and R. K. O'Reilly, *Soft Matter*, 2015, **11**, 3666-3676.
53. J. Lim, H. Matsuoka, S. Yusa and Y. Saruwatari, *Langmuir*, 2019, **35**, 1571-1582.
54. S. Abraham, A. So and L. D. Unsworth, *Biomacromolecules*, 2011, **12**, 3567-3580.
55. M. P. Cashion and T. E. Long, *Accounts of Chemical Research*, 2009, **42**, 1016-1025.
56. A. Puri and R. Blumenthal, *Accounts of Chemical Research*, 2011, **44**, 1071-1079.
57. E. K. Perttu, A. G. Kohli and F. C. Szoka, *Journal of the American Chemical Society*, 2012, **134**, 4485-4488.
58. X. F. Yu, Z. H. Liu, J. Janzen, I. Chafeeva, S. Horte, W. Chen, R. K. Kainthan, J. N. Kizhakkedathu and D. E. Brooks, *Nature Materials*, 2012, **11**, 468-476.
59. X. F. Yu, Y. Q. Zou, S. Horte, J. Janzen, J. N. Kizhakkedathu and D. E. Brooks, *Biomacromolecules*, 2013, **14**, 2611-2621.
60. G. J. Hu, S. S. Parelkar and T. Emrick, *Polymer Chemistry*, 2015, **6**, 525-530.
61. S. Morozova, G. Hu, T. Emrick and M. Muthukumar, *Acs Macro Letters*, 2016, **5**, 118-122.
62. K. E. B. Doncom, N. J. Warren and S. P. Armes, *Polymer Chemistry*, 2015, **6**, 7264-7273.
63. K. E. B. Doncom, H. Willcock and R. K. O'Reilly, *European Polymer Journal*, 2017, **87**, 497-507.
64. Y. Chang, W. Yandi, W. Y. Chen, Y. J. Shih, C. C. Yang, Q. D. Ling and A. Higuchi, *Biomacromolecules*, 2010, **11**, 1101-1110.
65. B. G. Yang, C. Y. Wang, Y. B. Zhang, L. Ye, Y. F. Qian, Y. Shu, J. M. Wang, J. J. Li and F. L. Yao, *Polymer Chemistry*, 2015, **6**, 3431-3442.
66. Z. X. Dong, J. Mao, M. Q. Yang, D. P. Wang, S. Q. Bo and X. L. Ji, *Langmuir*, 2011, **27**, 15282-15291.
67. C. Durand-Gasselin, R. Koerin, J. Rieger, N. Lequeux and N. Sanson, *Journal of Colloid and Interface Science*, 2014, **434**, 188-194.
68. J. Virtanen, M. Arotcarena, B. Heise, S. Ishaya, A. Laschewsky and H. Tenhu, *Langmuir*, 2002, **18**, 5360-5365.
69. N. S. Vishnevetskaya, V. Hildebrand, B. J. Niebuur, I. Grillo, S. K. Filippov, A. Laschewsky, P. Muller-Buschbaum and C. M. Papadakis, *Macromolecules*, 2016, **49**, 6655-6668.
70. N. S. Vishnevetskaya, V. Hildebrand, B. J. Niebuur, I. Grillo, S. K. Filippov, A. Laschewsky, P. Muller-Buschbaum and C. M. Papadakis, *Macromolecules*, 2017, **50**, 3985-3999.
71. M. Ranka, H. Katepalli, D. Blankschtein and T. A. Hatton, *Langmuir*, 2017, **33**, 13326-13331.
72. Y. Zhao, T. Bai, Q. Shao, S. Y. Jiang and A. Q. Shen, *Polymer Chemistry*, 2015, **6**, 1066-1077.
73. Z. Q. Cao, L. Mi, J. Mendiola, J. R. Ella-Menye, L. Zhang, H. Xue and S. Y. Jiang, *Angewandte Chemie-International Edition*, 2012, **51**, 2602-2605.
74. M. Birkner and M. Ulbricht, *Journal of Membrane Science*, 2015, **494**, 57-67.
75. R. T. Shafranek, S. C. Millik, P. T. Smith, C. U. Lee, A. J. Boydston and A. Nelson, *Progress in Polymer Science*, 2019, **93**, 36-67.
76. D. Roy, W. L. A. Brooks and B. S. Sumerlin, *Chemical Society Reviews*, 2013, **42**, 7214-7243.
77. J. S. Scarpa, D. D. Mueller and I. M. Klotz, *Journal of the American Chemical Society*, 1967, **89**, 6024-&.
78. A. Skandalis and S. Pispas, *Polymer*, 2018, **157**, 9-18.
79. N. S. Vishnevetskaya, V. Hildebrand, M. A. Dyakonova, B. J. Niebuur, K. Kyriakos, K. N. Raftopoulos, Z. Y. Di, P. Muller-Buschbaum, A. Laschewsky and C. M. Papadakis, *Macromolecules*, 2018, **51**, 2604-2614.
80. T. Tada, Y. Katsumoto, K. Goossens, H. Uji-i, J. Hofkens, T. Shoji, N. Kitamura and Y. Tsuboi, *Journal of Physical Chemistry C*, 2013, **117**, 10818-10824.
81. Y. Tsuboi, Y. Yoshida, K. Okada and N. Kitamura, *Journal of Physical Chemistry B*, 2008, **112**, 2562-2565.
82. Y. J. Zhang, S. Furyk, D. E. Bergbreiter and P. S. Cremer, *Journal of the American Chemical Society*, 2005, **127**, 14505-14510.
83. Y. Zhang, S. Furyk, L. B. Sagle, Y. Cho, D. E. Bergbreiter and P. S. Cremer, *Journal of Physical Chemistry C*, 2007, **111**, 8916-8924.
84. S. Z. Moghaddam and E. Thormann, *Langmuir*, 2017, **33**, 4806-4815.
85. J. S. Higgins, J. E. G. Lipson and R. P. White, *Philosophical Transactions of the Royal Society a-Mathematical Physical and Engineering Sciences*, 2010, **368**, 1009-1025.
86. P. C. Hiemenz and T. P. Lodge, *Polymer Chemistry, second edition*, CRC Press, 2007.
87. P. Knychala, K. Timachova, M. Banaszak and N. P. Balsara, *Macromolecules*, 2017, **50**, 3051-3065.
88. J. Seuring and S. Agarwal, *Macromolecular Rapid Communications*, 2012, **33**, 1898-1920.
89. V. Aseyev, H. Tenhu and F. M. Winnik, *Self Organized Nanostructures of Amphiphilic Block Copolymers*

Ii, 2011, **242**, 29-89.
90. A. Hatefi and B. Amsden, *Journal of Controlled Release*, 2002, **80**, 9-28.
91. R. Z. Li, N. Liu, B. Q. Li, Y. O. Wang, G. L. Wu and J. B. Ma, *Polymer Chemistry*, 2015, **6**, 3671-3684.
92. L. F. Sun, R. X. Zhuo and Z. L. Liu, *Macromolecular Bioscience*, 2003, **3**, 725-728.
93. D. Das, P. Ghosh, A. Ghosh, C. Haldar, S. Dhara, A. B. Panda and S. Pal, *Acs Applied Materials & Interfaces*, 2015, **7**, 14338-14351.
94. R. Longenecker, T. T. Mu, M. Hanna, N. A. D. Burke and H. D. H. Stover, *Macromolecules*, 2011, **44**, 8962-8971.
95. H. C. Haas and N. W. Schuler, *Journal of Polymer Science Part B-Polymer Letters*, 1964, **2**, 1095-&.
96. H. C. Haas, R. D. Moreau and N. W. Schuler, *Journal of Polymer Science Part a-2-Polymer Physics*, 1967, **5**, 915-&.
97. H. Nagaoka, N. Ohnishi, M. Eguchi (Chisso Corporation), US2007203313, A1, 2007.
98. S. Glatzel, N. Badi, M. Pach, A. Laschewsky and J. F. Lutz, *Chemical Communications*, 2010, **46**, 4517-4519.
99. S. Glatzel, A. Laschewsky and J. F. Lutz, *Macromolecules*, 2011, **44**, 413-415.
100. J. Seuring and S. Agarwal, *Macromolecules*, 2012, **45**, 3910-3918.
101. J. Seuring, F. M. Bayer, K. Huber and S. Agarwal, *Macromolecules*, 2012, **45**, 374-384.
102. N. Shimada, H. Ino, K. Maie, M. Nakayama, A. Kano and A. Maruyama, *Biomacromolecules*, 2011, **12**, 3418-3422.
103. A. Asadujjaman, B. Kent and A. Bertin, *Soft Matter*, 2017, **13**, 658-669.
104. K. K. Sharker, Y. Ohara, Y. Shigeta, S. Ozoe and S. Yusa, *Polymers*, 2019, **11**.
105. A. Fujihara, N. Shimada, A. Maruyama, K. Ishihara, K. Nakai and S. I. Yusa, *Soft Matter*, 2015, **11**, 5204-5213.
106. T. Swift, L. Swanson, M. Geoghegan and S. Rimmer, *Soft Matter*, 2016, **12**, 2542-2549.
107. R. T. Woodward, C. Hight, U. Yildiz, N. Schaeffer, E. M. Valliant, J. R. Jones, M. M. Stevens and J. V. M. Weaver, *Soft Matter*, 2011, **7**, 7560-7566.
108. S. H. R. Shin, P. T. McAninch, I. M. Henderson, A. Gomez, A. C. Greene, E. C. Carnes and W. F. Paxton, *Chemical Communications*, 2018, **54**, 9043-9046.
109. A. B. Lowe, M. Torres and R. Wang, *Journal of Polymer Science Part a-Polymer Chemistry*, 2007, **45**, 5864-5871.
110. R. Wang and A. B. Lowe, *Journal of Polymer Science Part a-Polymer Chemistry*, 2007, **45**, 2468-2483.
111. B. Bingol, W. H. Meyer, M. Wagner and G. Wegner, *Macromolecular Rapid Communications*, 2006, **27**, 1719-1724.
112. B. Bingol, C. Strandberg, A. Szabo and G. Wegner, *Macromolecules*, 2008, **41**, 2785-2790.
113. E. Kemal, K. O. Adesanya and S. Deb, *Journal of Materials Chemistry*, 2011, **21**, 2237-2245.
114. M. Q. Li, W. T. Song, Z. H. Tang, S. X. Lv, L. Lin, H. Sun, Q. S. Li, Y. Yang, H. Hong and X. S. Chen, *Acs Applied Materials & Interfaces*, 2013, **5**, 1781-1792.
115. S. Yan, Y. Sun, A. Chen, L. Liu, K. X. Zhang, G. F. Li, Y. R. Duan and J. B. Yin, *Rsc Advances*, 2017, **7**, 14888-14901.
116. S. Y. Liu, J. V. M. Weaver, Y. Q. Tang, N. C. Billingham, S. P. Armes and K. Tribe, *Macromolecules*, 2002, **35**, 6121-6131.
117. C. Pietsch, U. Mansfeld, C. Guerrero-Sanchez, S. Hoeppener, A. Vollrath, M. Wagner, R. Hoogenboom, S. Saubern, S. H. Thang, C. R. Becer, J. Chiefari and U. S. Schubert, *Macromolecules*, 2012, **45**, 9292-9302.
118. F. C. Giacomelli, P. Stepanek, C. Giacomelli, V. Schmidt, E. Jager, A. Jager and K. Ulbrich, *Soft Matter*, 2011, **7**, 9316-9325.
119. A. Jager, E. Jager, F. Surman, A. Hocherl, B. Angelov, K. Ulbrich, M. Drechsler, V. M. Garamus, C. Rodriguez-Emmenegger, F. Nallet and P. Stepanek, *Polymer Chemistry*, 2015, **6**, 4946-4954.
120. A. E. Smith, X. W. Xu, S. E. Kirkland-York, D. A. Savin and C. L. McCormick, *Macromolecules*, 2010, **43**, 1210-1217.
121. H. Sun, X. L. Chen, X. Han and H. L. Liu, *Langmuir*, 2017, **33**, 2646-2654.
122. P. Cotanda, D. B. Wright, M. Tyler and R. K. O'Reilly, *Journal of Polymer Science Part a-Polymer Chemistry*, 2013, **51**, 3333-3338.
123. N. Gonzalez, C. Elvira and J. S. Roman, *Macromolecules*, 2005, **38**, 9298-9303.
124. V. Butun, S. P. Armes and N. C. Billingham, *Polymer*, 2001, **42**, 5993-6008.
125. T. Matini, N. Francini, A. Battocchio, S. G. Spain, G. Mantovani, M. J. Vicent, J. Sanchis, E. Gallon, F. Mastrotto, S. Salmaso, P. Caliceti and C. Alexander, *Polymer Chemistry*, 2014, **5**, 1626-1636.
126. S. Eggers, B. Fischer and V. Abetz, *Macromolecular Chemistry and Physics*, 2016, **217**, 735-747.
127. S. Eggers, F. Lauterbach and V. Abetz, *Polymer*, 2016, **107**, 357-367.
128. D. Wang, T. Wu, X. J. Wan, X. F. Wang and S. Y. Liu, *Langmuir*, 2007, **23**, 11866-11874.

129. M. D. Rodriguez-Hidalgo, C. Soto-Figueroa and L. Vicente, *Soft Matter*, 2013, **9**, 5762-5770.
130. N. Van Overstraeten-Schlogel, Y. H. Shim, V. Tevel, G. Piel, J. Piette, P. Dubois and M. Raes, *Drug Delivery*, 2012, **19**, 112-122.
131. M. Dialameh, F. F. Lupi, D. Imbraguglio, F. Zanenga, A. Lamperti, D. Martella, G. Seguini, M. Perego, A. M. Rossi, N. De Leo and L. Boarino, *Nanotechnology*, 2017, **28**.
132. J. N. Israelachvili, D. J. Mitchell and B. W. Ninham, *Journal of the Chemical Society-Faraday Transactions Ii*, 1976, **72**, 1525-1568.
133. R. Nagarajan, *Langmuir*, 2002, **18**, 31-38.
134. C. J. Ferguson, R. J. Hughes, D. Nguyen, B. T. T. Pham, R. G. Gilbert, A. K. Serelis, C. H. Such and B. S. Hawkett, *Macromolecules*, 2005, **38**, 2191-2204.
135. Y. T. Li and S. P. Armes, *Angewandte Chemie-International Edition*, 2010, **49**, 4042-4046.
136. B. Charleux, G. Delaittre, J. Rieger and F. D'Agosto, *Macromolecules*, 2012, **45**, 6753-6765.
137. S. L. Canning, G. N. Smith and S. P. Armes, *Macromolecules*, 2016, **49**, 1985-2001.
138. C. J. Mable, N. J. Warren, K. L. Thompson, O. O. Mykhaylyk and S. P. Armes, *Chemical Science*, 2015, **6**, 6179-6188.
139. C. J. Mable, L. A. Fielding, M. J. Derry, O. O. Mykhaylyk, P. Chambon and S. P. Armes, *Chemical Science*, 2018, **9**, 1454-1463.
140. W. M. Wan and C. Y. Pan, *Macromolecules*, 2010, **43**, 2672-2675.
141. L. P. D. Ratcliffe, A. Blanazs, C. N. Williams, S. L. Brown and S. P. Armes, *Polymer Chemistry*, 2014, **5**, 3643-3655.
142. M. Semsarilar, V. Ladmiral, A. Blanazs and S. P. Armes, *Polymer Chemistry*, 2014, **5**, 3466-3475.
143. E. R. Jones, M. Semsarilar, A. Blanazs and S. P. Armes, *Macromolecules*, 2012, **45**, 5091-5098.
144. J. R. Lovett, N. J. Warren, L. P. D. Ratcliffe, M. K. Kocik and S. P. Armes, *Angewandte Chemie-International Edition*, 2015, **54**, 1279-1283.
145. N. J. W. Penfold, J. R. Lovett, N. J. Warren, P. Verstraete, J. Smets and S. P. Armes, *Polymer Chemistry*, 2016, **7**, 79-88.
146. V. Butun, M. Vamvakaki, N. C. Billingham and S. P. Armes, *Polymer*, 2000, **41**, 3173-3182.
147. K. H. Markiewicz, L. Seiler, I. Misztalewska, K. Winkler, S. Harrisson, A. Z. Wilczewska, M. Destarac and J. D. Marty, *Polymer Chemistry*, 2016, **7**, 6391-6399.
148. L. Makinen, D. Varadharajan, H. Tenhu and S. Hietala, *Macromolecules*, 2016, **49**, 986-993.
149. J. S. Chen, B. Yan, X. G. Wang, Q. X. Huang, T. Thundat and H. B. Zeng, *Polymer Chemistry*, 2017, **8**, 3066-3073.
150. N. M. Nizardo, D. Schanzenbach, E. Schonemann and A. Laschewsky, *Polymers*, 2018, **10**.
151. D. Giaouzi and S. Pispas, *Journal of Polymer Science Part a-Polymer Chemistry*, 2019, **57**, 1467-1477.
152. H. Yang, R. J. Ma, J. Yue, C. Li, Y. Liu, Y. L. An and L. Q. Shi, *Polymer Chemistry*, 2015, **6**, 3837-3846.
153. B. Schmidt, *Macromolecular Chemistry and Physics*, 2018, **219**.
154. S. M. Brosnan, H. Schlaad and M. Antonietti, *Angewandte Chemie-International Edition*, 2015, **54**, 9715-9718.
155. N. Al Nakeeb, J. Willersinn and B. Schmidt, *Biomacromolecules*, 2017, **18**, 3695-3705.
156. J. Willersinn and B. Schmidt, *Polymer Chemistry*, 2018, **9**, 1626-1637.
157. T. Oh, M. Nagao, Y. Hoshino and Y. Miura, *Langmuir*, 2018, **34**, 8591-8598.
158. A. Adharis, T. Ketelaar, A. G. Komarudin and K. Loos, *Biomacromolecules*, 2019, **20**, 1325-1333.
159. A. Taubert, E. Furrer and W. Meier, *Chemical Communications*, 2004, 2170-2171.
160. O. Casse, A. Shkilnyy, J. Linders, C. Mayer, D. Haussinger, A. Volkel, A. F. Thunemann, R. Dimova, H. Colfen, W. Meier, H. Schlaad and A. Taubert, *Macromolecules*, 2012, **45**, 4772-4777.
161. J. Willersinn and B. Schmidt, *Polymers*, 2017, **9**.
162. M. W. Tibbitt, J. E. Dahlman and R. Langer, *Journal of the American Chemical Society*, 2016, **138**, 704-717.
163. A. Peyret, E. Ibarboure, A. Tron, L. Beaute, R. Rust, O. Sandre, N. D. McClenaghan and S. Lecommandoux, *Angewandte Chemie-International Edition*, 2017, **56**, 1566-1570.
164. F. Pooch, M. Sliepen, K. D. Knudsen, B. Nystrom, H. Tenhu and F. M. Winnik, *Macromolecules*, 2019, **52**, 1317-1326.
165. I. W. Hamley, S. D. Connell and S. Collins, *Macromolecules*, 2004, **37**, 5337-5351.
166. Y. Pei, K. Jarrett, L. G. Garces, M. Saunders, J. P. Croue, P. J. Roth, C. E. Buckley and A. B. Lowe, *Rsc Advances*, 2016, **6**, 28130-28139.
167. M. Danko, Z. Kronekova, M. Mrlik, J. Osicka, A. bin Yousaf, A. Mihalova, J. Tkac and P. Kasak, *Langmuir*, 2019, **35**, 1391-1403.
168. K. D. Collins, *Biophysical Chemistry*, 2012, **167**, 43-59.
169. G. Gody, T. Maschmeyer, P. B. Zetterlund and S. Perrier, *Nature Communications*, 2013, **4**.

Chapter 2. Temperature-Responsive Behaviour of Double Hydrophilic Carboxy-Sulfobetaine Block Copolymers and Their Self-Assemblies in Water

ABSTRACT: The block copolymer poly(2-((2-(methacryloyloxy)ethyl)dimethylammonio)acetate)-*b*-poly(3-(*N*-(2-metharyloylethyl)-*N*,*N*-dimethylammonio)propanesulfonate) (PGLBT-*b*-PSPE) was synthesised by reversible addition-fragmentation chain transfer (RAFT) technique under precise control. The PGLBT-*b*-PSPE block copolymers showed upper critical solution temperature (UCST) behaviour originating from PSPE moieties. Unlike PSPE homopolymers, the transmittance change with temperature was gradual and unexpected retardation or slight changes in a reverse direction were found at the intermediate stage. Light scattering and ^{1}H NMR studies proved that the block copolymers formed spherical micelles that were composed of a PSPE core and PGLBT shell around room temperature and lower temperatures, and slowly disassociated with temperature increase. During the transition, fast (small particle) and slow (large particle) diffusive modes were detected by dynamic light scattering (DLS), which implied that the unimers were escaping from the self-assembled structure and swollen micelles, respectively. At sufficiently high temperatures where the solutions became almost transparent, the slow mode eventually disappeared and only the fast mode remained. In addition, once the polymeric particles are formed, the size did not vary much with additional cooling. The transition point and the pattern of transmittance alteration were dependent on the degree of polymerisation and the [PGLBT]:[PSPE] ratios; more PGLBT made the block copolymer less responsive to temperature and led the cloud point to lower degrees. However, random copolymers PGLBT-*r*-PSPE did not show any temperature-responsivity, and even small amount of GLBTs (10%) distributed in a PSPE chain significantly suppressed the transition.

Introduction

Polyzwitterions are a kind of polyelectrolyte that have equal numbers of both positive and negative charges in one repeating unit. Several kinds of zwitterions (betaines) are often used in detergents, cosmetics, and body washes as surfactants and emulsifiers or skin conditioning agents because they cause less irritation on skin than other cationic/anionic agents.[1] These types of polymers have been growing academic attention for decades for their unique properties in bulk and in solution. With similarity to some lipids, polybetaines show good biocompatibility, antifouling property, and immobilization of biomolecules because of their low surface activity on proteins.[2-4] It is proposed that the unperturbed hydrated state would protect the polymer surface from protein adsorption.[5] This

property has been utilised for designing polymeric materials that require high biocompatibility such as blood-contacting[6] or wound-dressing[7] applications. Moreover, responses to outer stimuli which appear from some kinds of polyzwitterions make them more attractive than other conventional stimulus-responsive polymers relatively vulnerable to adsorption of outer molecules by hydrophobic interactions and possible cell toxicity.[8] Different from other nonionic or cationic/anionic water-soluble polymers, inter- or intrachain attraction/repulsion between charged groups of polyzwitterions intricately cause their solvation and give them sensitivity against temperature, pH, and salt ions. Among the three generally studied polybetaines (polysulfobetaine, polycarboxybetaine and polyphosphobetaine), polysulfobetaines have been widely researched during the past couple of decades because of their upper critical solution temperature (UCST) behaviour, which only a few known polymers show particularly at 0–100°C.[9, 10] Not only on homopolymers (salt effect on dissolved state,[11-13] effect of alkyl spacer between cationic and anionic groups[14] and ligand materials for inorganic nanoparticles[15]), but also block copolymers (polymeric micelles obtained by polysulfobetaine-hydrophobic block copolymers,[16-18] sphere- or wormlike structures obtained by polymerisation-induced self- assembly (PISA),[19, 20] and blocks with non-ionic branching polymers[21]) have been studied thanks to their hydrophobic-to-hydrophilic transition.[22] The "schizophrenic" type was enabled by incorporating nonionic LCST polymers (poly(*N*-isopropylacrylamide) (PNIPAM)[23-25] or poly(2-dimethylaminoethyl methacrylate) (PDMAEMA)).[26] These UCST-LCST type block copolymers responded to both low and high temperatures, and micelle formation was observed in both ranges where the hydrophobically altered segments became cores. In addition, polycarboxybetaines have been receiving less attention than polysulfobetaines for obtaining self-assembled polymer objects because of their relatively elusive stimulus-responsivity. Although there are both cationic and anionic parts in their repeating units, they do not show responses against temperature but to pH and salts. Some aspects of their behaviours have been revealed by a couple of studies, such as by capillary electrophoresis[27] or stability evaluation of polyelectrolyte complexes formed with other polyanions[28, 29] with several kinds of polycarboxybetaines having different spacer lengths. Permeability variations of polycarboxybetaine-grafted membranes gave clues to the responsivity to pH, salt species, and concentration.[30] For applications, polymer gels copolymerised with 2-hydroxyethyl methacrylate (HEMA)[31] were obtained because of their superior resistance of protein adsorption compared with nonionic or even polysulfobetaines. In our previous research, several kinds of polycarboxybetaine (PGLBT) derivative amphiphilic block copolymers were synthesised, and we investigated their responses to pH or added salts when they formed micelles in aqueous solution or monolayers on the air-water surface.[32, 33] The surface activity and micelle formation of carboxybetaine-based amphiphilic copolymers were observed by light scattering and X-ray

reflectivity. Both showed chain stretching of the polycarboxybetaine chains by salt addition, unlike cationic or anionic polyelectrolytes. However, synthesising different kinds of polybetaines has been scarcely tested to the best of our knowledge; only random copolymers of polycarboxybetaine with polysulfobetaine obtained by free radical polymerisation[34] were examined for their temperature, pH, and salt dependence. In addition, a double polyphosphobetaine block copolymer composed of 2-methacryloyloxyethyl phosphorylcholine (MPC) and an analogous phosphobetaine that had inverse arrangement of zwitterions was synthesised, and the aqueous solution was examined.[35, 36] This block copolymer chain existed as unimers and multiple-sized aggregates simultaneously due to dipole-dipole associations between the two units at room temperature, but the responsivity against salt or other stimuli was not systematically investigated yet.

Recently, many research reports of polybetaines in various aspects have been published about stimulus-responsivity, chain conformation, biocompatibility, etc. However, most of those involved in polybetaines with other nonionic or hydrophobic substances. This report investigating double betaine, and double hydrophilic block copolymer is a rare case study in the field of not only stimulus-responsive soft materials but also polyzwitterions since our block copolymer is composed of two different kinds of betaines which show different properties, particularly temperature-responsivity. Moreover, the block copolymers are able to form self-assembled particles spontaneously and their sizes were able to be controlled by tuning each block length. In this study, the double polybetaine block copolymer poly(2-((2-(methacryloyloxy)ethyl)dimethylammonio)acetate)-*b*-poly(3-(*N*-(2-metharyloylethyl)-*N*,*N*-dimethylammonio)propanesulfonate) PGLBT-*b*-PSPE was synthesised by reversible addition-fragmentation chain transfer (RAFT) polymerisation, and its sensitivity against temperature change was determined. Both parts of the block copolymer are hydrophilic inherently, and the UCST-type PSPE moiety can become less soluble in water under critical temperature points. Hence, this arrangement enables the acquisition of a self-assembled structure in water more conveniently among double hydrophilic block copolymers (DHBC) which requires high concentrations or additional cross-linking.[37, 38] The obtained PGLBT-*b*-PSPE formed micelles having narrow size distributions below certain temperature, and slowly turned into unimers with heating. The temperature-responsive behaviour of the PSPE moiety affected by PGLBT counterparts and their self-assembly is discussed.

Experimental Section

Materials The 2-((2-(methacryloyloxy)ethyl)dimethylammonio)acetate (carboxybetaine methacrylate, GLBT) and 3-((2-(methacryloyloxy)ethyl)dimethylammonio)propane-1-sulfonate (sulfobetaine methacrylate, SPE) were a kind donation from Osaka Organic Chemical Industry LTD (Osaka, Japan) and used without further purification. The chain transfer agent (CTA), 4-cyano-4-(phenylcarbonothioylthio)pentanoic acid, was synthesised by the method previously reported.[39] Radical initiators 2,2′-azobis[2-(2-imidazolin-2-yl)propane]dihydrochloride (VA-044) and 4,4′-azobis(4-cyanovaleric acid) (ACVA) were purchased from Wako Chemicals (Osaka, Japan) and used as received. Deuterated water (D_2O) was purchased from Cambridge Isotope Laboratories. Ultrapure water with a minimum resistivity of 18.2 MΩ cm obtained by Milli-Q system was used for preparing solutions and dialysis. Regenerated cellulose membranes (MWCO 3500 and 15000) were used for dialysis to remove residual monomers and salt ions.

Synthesis of PGLBT Macro-CTA The PGLBT homopolymer was synthesised by reversible addition-fragmentation chain transfer (RAFT) polymerisation as shown in **Scheme 2.1**. GLBT monomer (100–300 mol equiv.), CTA (1 equiv.), and VA-044 (0.1 equiv.) were dissolved in water with vigorous stirring and sonication. The solution was transferred to a Schlenk flask with a stirrer bar and degassed through three cycles of freeze-pump-thaw. After being filled with argon gas, the vessel was immersed in an oil bath set to 45 °C to conduct polymerisation for 20 h. The reaction was terminated by rapid cooling in an ice bath and exposure to air. The product was purified by dialysis against water. After the reservoir was discarded two times a day until the conductivity showed no significant change, the product was recovered as a pink powder by freeze-drying. The yield of the product was 85–87%.

Synthesis of Block Copolymer PGLBT-*b*-PSPE The block copolymer was synthesised by RAFT polymerisation as shown in **Scheme 2.1**. SPE monomer (100–300 mol equiv.), PGLBT macro-CTA (1 equiv.) and VA-044 (0.5 equiv.) were dissolved in water with vigorous stirring and sonication. The solution was transferred to a Schlenk flask with a stirrer bar and degassed by three cycles of freeze-pump-thaw. After being filled with argon gas, the vessel was immersed in an oil bath set at 45°C to conduct polymerisation for 20 h. The reaction was terminated by rapid cooling in an ice bath and exposure to air. The crude product was precipitated into excess methanol to remove residual monomers and PGLBT homopolymers. The precipitated solid was washed 2 times with methanol and once with ethanol by centrifugation. The sediments were redissolved in water and dialyzed against water overnight followed by 3 days of water changed twice a day. After freeze-drying, the pure block copolymer was

obtained as a white powder, and characterised by ^{1}H NMR spectroscopy and aqueous size-exclusion chromatography (SEC) to calculate the block ratios. The product yield was 40 %.

Synthesis of PGLBT-*r*-PSPE Random Copolymer GLBT and SPE monomers (50–200 mol equiv), CTA (1 equiv.) and ACVA (0.1 equiv.) were dissolved in water with vigorous stirring and sonication. The solution was transferred to a schlenk flask with a stirrer bar and degassed by three cycles of freeze-pump-thaw. After filled with argon gas, the vessel was immersed in an oil bath set to 70ºC for 2 h to conduct polymerisation. The reaction was terminated by rapid cooling in an ice bath and exposure to air. Unreacted monomers and other impurities were eliminated by dialysis against water for more than 3 days with a change of water twice a day. Freeze-drying yielded pure polymer as a pink powder (yield: 87%).

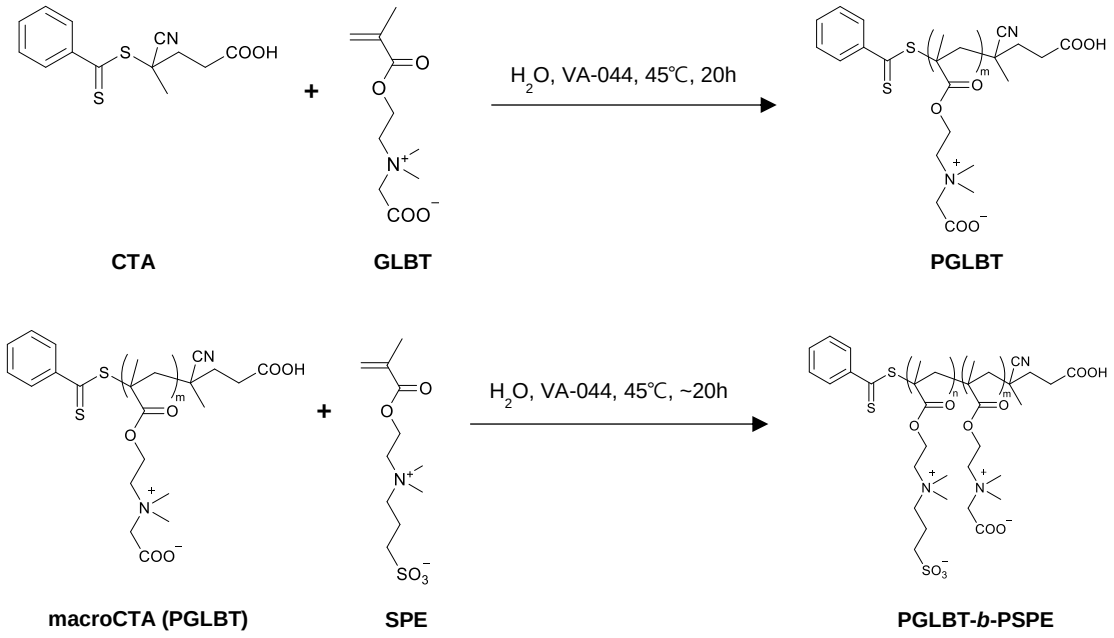

Scheme 2.1. Synthesis of PGLBT-*b*-PSPE

Copolymer Characterisation

^{1}H NMR Spectroscopy Signals of obtained polymers were recorded using a 400 MHz JEOL JNM-AL 400 spectrometer (JEOL, Tokyo, Japan) using deuterated water (D_2O) as a solvent.

Size-Exclusion Chromatography (SEC) The molecular weight and polydispersities of homo- and block or random copolymers were determined by SEC with an aqueous eluent (0.5 M CH_3COOH and 0.3 M of Na_2SO_4). The instrument consisted of a column (SB-804 HQ, Shodex) and a refractive index detector (RI-830, JASCO,

Japan). The flow rate of the eluent was 0.5 mL/min. The calibration was carried out with a set of poly(2-vinylpyridine) standards (M_n range: 5500–142000 g/mol, Sigma-Aldrich). The data was analysed by the software provided by JASCO.

Turbidimetry The transmittance of the aqueous solutions of the block copolymers (concentration: 10 mg/mL) at various temperatures was measured at 400 nm with a UV-vis spectrometer (Hitachi U-3310 spectrophotometer) equipped with a water circulator for temperature control. A quartz cell with a light path of 10 mm was used. The solutions were filtered with a syringe filter unit (pore size: 0.2 μm, mdi) prior to measurement. The transmittance was recorded after stabilisation for 5 min at each temperature. The cloud points (CPs) were determined at the temperatures where the transmittance is 50% by interpolation between each point.

Light Scattering Dynamic light scattering (DLS) was conducted to measure hydrodynamic radii of the polymers in water. A 15 mW He-Ne laser (wavelength λ = 632.8 nm) illuminated the polymer solutions. The sample was loaded in a goniometer (BI-200SM, Brookhaven Instruments, New York), and the scattered light at 60°, 75°, 90°, and 105° was detected with a BI-DS2 photomultiplier tube. The temperature of the cell was controlled by a water circulator appended to the goniometer. The normalised intensity autocorrelation function $g^{(2)}(q,t)$ was obtained by a correlator (TurboCorr, Brookhaven Instruments), and by the Siegert relation (2.1):

$$g^{(2)}(q,t) = 1 + \beta\left|g^{(1)}(q,t)\right|^2 \tag{2.1}$$

where β is a coherence factor, and $g^{(1)}(q,t)$ is normalised electric field autocorrelation function to be evaluated. For a polydisperse particle system, the $g^{(1)}(q,t)$ can be written as

$$g^{(1)}(q,t) = \int_0^\infty G(\Gamma)\exp(-\Gamma\tau)d\Gamma \tag{2.2}$$

where G(Γ) is the normalised distribution of decay rates $\int G(\Gamma)\mathrm{d}\Gamma = 1$. Each autocorrelation function was analysed by the data analysis software provided by the manufacturer: CONTIN[40] and cumulant functions[41] for monodisperse particles, CONTIN and double exponential functions for polydisperse systems. The translational diffusion coefficients D (= Γ/q^2) were calculated from the slope of the decay rate Γ versus q^2. The scattering vector q is

$$q = \frac{4\pi n}{\lambda}\sin\left(\frac{\theta}{2}\right) \tag{2.3}$$

where n is the refractive index of the water, λ is the wavelength of the incident laser (632.8 nm), and θ is the scattering angle. The hydrodynamic radius R_h was then calculated by the Stokes-Einstein equation

$$R_h = \frac{k_B T}{6\pi\eta D} \tag{2.4}$$

Where k_B is the Boltzmann constant, T is the absolute temperature, and η is the viscosity of solvent (water), respectively.

In the static light scattering (SLS) studies, the measurements were performed over an angular range between 40° and 150° at 10° intervals. A partial Zimm equation (eq. 2.5) of the inverse scattering intensity ($1/I_{ex}$) versus the square of the scattering vector q^2 at a single concentration was used to determine the radius of gyration (R_g), as follows:

$$\frac{1}{I_{ex}(q)} = C(1 + \frac{R_g^2 q^2}{3}) \tag{2.5}$$

where C is the arbitrary constant, and $I_{ex}(q)$ is the intensity of scattered light. Several points that were markedly discrepant from the overall results were exempted from the linear fitting. Some highly turbid solution samples were diluted from 10 mg/mL to lower concentrations to prevent multiple scattering.

Transmission electron microscopy (TEM) Images of the self-assembled structure of polymer solutions were taken by using a JEOL TEM-2100 electron microscope operated at a 200 kV accelerated voltage. TEM samples were prepared by placing one drop of aqueous solution on a Formvar-coated copper grid, and the excess water was blotted with filter paper. Each sample was stained by sodium phosphotungstate and dried under vacuum for 1 day.

Results and Discussion

Synthesis of PGLBT-*b*-PSPE Copolymers

The betaine diblock copolymers, PGLBT-*b*-PSPE was synthesised by RAFT polymerisation with different monomer ratios. Synthesis conditions of polymers and specifications are summarised in **Table 2.1**. The polymerisation was performed at a reduced temperature (45 °C) with VA-044 to minimise possible hydrolysis of the CTA in aqueous condition, which deactivates controlled polymerisation.[42, 43] The homo-PGLBT synthesis gave

similar results to previous examples carried out at 70 °C.[32, 33] At the second step, SPEs were not polymerised under the same reaction condition and feed ratio, while the polymerisations of homo-SPEs and random copolymer PGLBT-*r*-PSPEs were carried out well under the identical operation condition. In our experiment, a larger amount of the initiator was required to start the second polymerisation with PGLBT macroCTAs. Five times more initiator was fed to the second polymerisation: eventually the reaction solution became opalescent and thick which indicates further polymerisation. The crude product of the block copolymerisation was required to separate unreacted homo-PGLBTs by precipitation into methanol, which selectively dissolves PGLBT. After subsequent dialysis, the polymers showed both characteristic peaks of PGLBT and PSPE blocks in ^{1}H NMR spectra (see **Figure 2.1**) and gave unimodal peaks in SEC measurement with narrow polydispersities (polydispersity index (PDI) ~1.2, **Figure 2.2**) indicating effective controlled copolymerisation of SPEs. The DPs determined by SEC are described in the **Table 2.1**. By end group analysis of ^{1}H NMR spectra, the ratio of PGLBT:PSPE was also determined by comparing the area of the peak at δ = 3.97 ppm (PGLBT, 4H) to δ = 2.99 ppm (PSPE, 2H), and also the height of the peak at δ = 3.32 ppm (PGLBT, 6H) to δ = 3.24 ppm (PSPE, 6H). However, the molecular weights and ratios of each block obtained by SEC and ^{1}H NMR sometimes showed a discrepancy. For example, the degree of polymerisation of $GLBT_{86}$-*b*-SPE_{164} based on NMR ratio was 86-*b*-230, and $GLBT_{86}$-b-SPE_{144} was 86-*b*-172. All of the PSPE moieties in other block copolymers showed larger values than the SEC results. The difference was also observed in previous studies of polyzwitterions;[14] usually the apparent molecular weights of SEC were smaller than the absolute molecular weights obtained by end group analysis.

Table 2.1. Conditions of synthesis and characterisation of polybetaines: homopolymers (PGLBT) and double betaine block copolymers (PGLBT-*b*-PSPE)

Sample name[a]	Feed Ratio [M]:[I]:[CTA][b]	M_n^{SEC} (g/mol)	$Đ$ (M_w/M_n)	$M_n^{1H\ NMR}$ (g/mol)[c]	M_n^{EA} (g/mol)	yield (%)	Cloud Point (°C)
$GLBT_{86}$	100:0.1:1	18700	1.07			87	
$GLBT_{86}$-*b*-SPE_{164}	100:0.5:1	64600	1.13	83000	77700	43	27.6
$GLBT_{86}$-*b*-SPE_{144}	50:0.5:1	59000	1.08	66800		46	20
$GLBT_{182}$	300:0.1:1	39500	1.10			80	
$GLBT_{182}$-*b*-SPE_{204}	300:0.5:1	96500	1.21	101000	137000	53	48.7
$GLBT_{182}$-*b*-SPE_{166}	150:0.5:1	85800	1.18	92000	115000	70	31.6
$GLBT_{182}$-*b*-SPE_{237}	450:0.5:1	99200	1.1	120000	188000	29	>60
$GLBT_{131}$	200:0.1:1	28400	1.06			90	
$GLBT_{131}$-*b*-SPE_{193}	200:0.5:1	82300	1.14	103000		32	51.2
$GLBT_{131}$-*b*-SPE_{167}	100:0.5:1	75000	1.08	68400		67	15.8

[a] Each degree of polymerisation was determined from the result of SEC. [b] The concentration of the monomer [M], the initiator [I], and the chain transfer agent [CTA]. [c] determined at room temperature. [EA] determined by elemental analysis

It should be noted that the ^{1}H NMR samples were not transparent and appeared blue or nearly white translucent solution which indicates small particles are formed and scattering the incident light, probably due to association of temperature-responsive PSPE units. To minimise the possible self-assembly, NMR measurement was performed again at the elevated temperatures (up to 60 °C) where the solutions become almost transparent. As compared with the initial spectrum taken at 25 °C, several vague peaks of PSPE became more clearly visible (particularly between 3.5 to 4.5 ppm) as well as the other two peaks (δ = 3.24 and 3.00) increasing their intensities during heating, (**Figure 2.3**) consequently the PSPE ratios were determined higher than those of 25 °C. For example, $PGLBT_{86}$-*b*-$PSPE_{164}$ which indicated [PGLBT]:[PSPE] = 1:2.46 (DP: 86-*b*-230) at room temperature then altered to 1:4.8 (DP: 86-*b*-413) at 60 °C. Another transparent sample was prepared by salt addition, which was reported to hinder collapse of PSPE by screening the attraction between zwitterions themselves.[11] A transparent $GLBT_{86}$-*b*-SPE_{164} sample that dissolved in 0.5M $NaCl_{(aq)}$ D_2O gave 1:4.2 (86-*b*-361) at any temperature, which is similar to the result at 60 °C without additional ions. Thus, it is obvious that the PSPE segments of the copolymer which have UCST behaviour do not fully dissolve in deuterated water but are in a shrunken state assembled with other PSPE chains to form a core-like structure, and it prevents correct determination through end group analysis. Not to take account of the solvation state of polymers, we used elemental analysis to judge DPs by counting the percentage of the sulfur in PSPE against other elements (carbon and nitrogen). By the measurement, $GLBT_{182}$ series block copolymers were found as 182-*b*-350, 182-*b*-272, 182-*b*-532, respectively. In spite of the discrepancy, the tendency of the DPs was in agreement with each SPE feed

ratio and results of SEC and NMR. Taking the variances into account, we would explain each sample using the SEC results as a standard since it is a consistent way of determining the molecular weights of the block copolymer excluding particle formation due to large extent of salt ions which promote solvation of sulfobetaines.[11, 13] In any cases of the results, the degree of polymerisation of the second blocks was always greater than that of homo-polymerisation of PSPEs, which showed similar kinetics and degree of polymerisation to those of PGLBTs. It might be thought that some extent of PGLBTs lost their livingness during polymerisation because hydrolysis of DCTA was inevitable in water even using a small amount of initiator at a reduced temperature. Consequently, it led to imbalance of the ratio of PGLBT:PSPE which was polymerised under the same feed ratio.

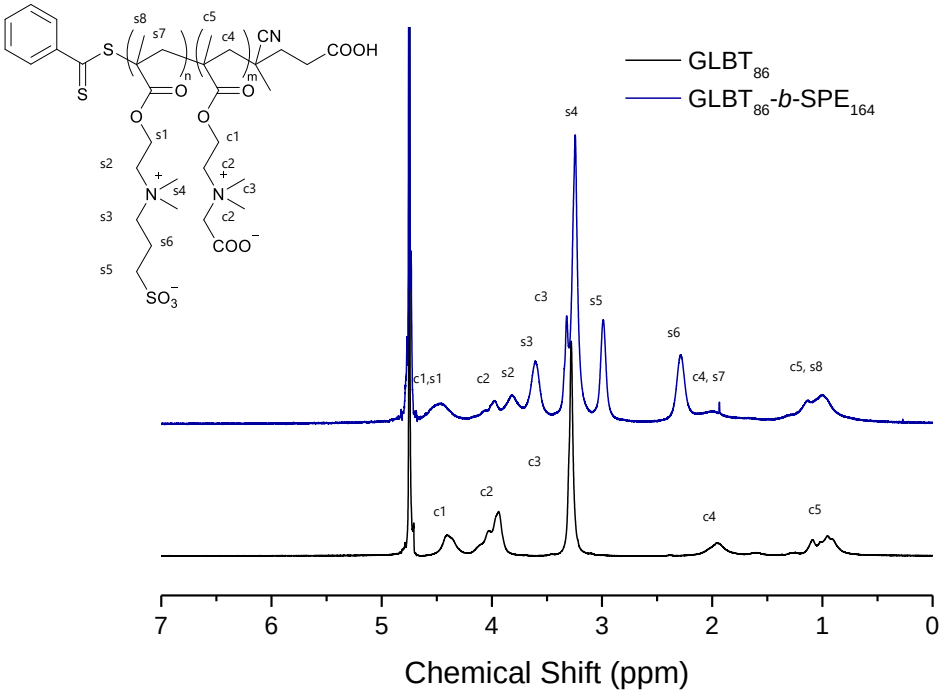

Figure 2.1. ^{1}H NMR spectra of $GLBT_{86}$ (black) and $GLBT_{86}$-*b*-SPE_{164} (blue)

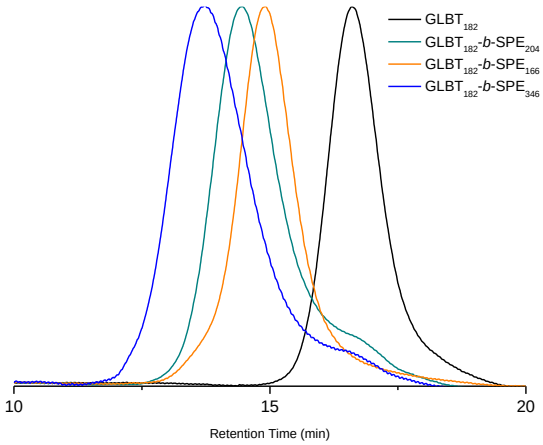

Figure 2.2. SEC Chromatograms of $GLBT_{182}$ and their derivative block copolymers

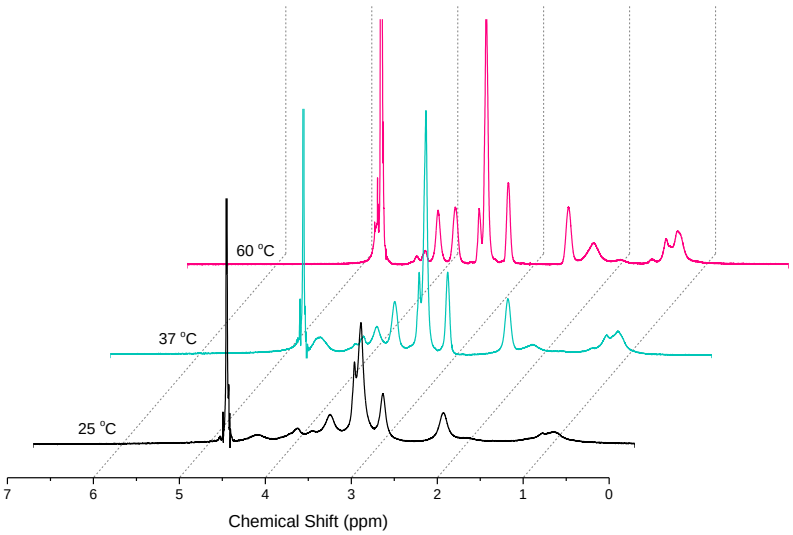

Figure 2.3. ^{1}H NMR spectra of $GLBT_{86}$-*b*-SPE_{164} (in D_2O) at different temperatures.

Turbidity of PGLBT-*b*-PSPE in Water

PGLBT-*b*-PSPEs are expected to reveal temperature-responsivity due to the PSPE moieties, and it might be under the influence of PGLBT moieties. The transmittance of PGLBT-*b*-PSPE solutions at 400 nm showed a gradual increase/decrease in a wide temperature range as shown in **Figure 2.4** in contrast to homo-PSPE polymers, which show abrupt changes within only a few degrees around cloud points. As shown in **Figure 2.4(a)**, the transmittance alteration of 2 block copolymers synthesised from $GLBT_{86}$ continuously varied within 20 °C. $GLBT_{86}$-*b*-SPE_{144} showed a lower cloud point (CP = 20 °C) than $GLBT_{86}$-*b*-SPE_{164} (CP = 27.6 °C) and always recorded higher

transmittances as presumed to be due to the smaller portion of PSPE. In the cases of others that have higher overall DPs, $GLBT_{182}$-*b*-SPE_{204} and $GLBT_{131}$-*b*-SPE_{193} become transparent at higher temperatures as compared to those synthesised with half SPE ratios, and some differences were observed depending on the chain length. As shown in **Figure 2.4(b)**, $GLBT_{182}$-*b*-SPE_{204} suddenly became transparent from a translucent state much similar to the response of PSPE homopolymers rather than the other block copolymers, while $GLBT_{182}$-*b*-SPE_{166} showed a broad transmittance curve as $GLBT_{86}$-*b*-SPE_{144}. $GLBT_{182}$-*b*-SPE_{346} remained in a highly opaque state until 50 ℃, and then became slightly translucent at 60 ℃ but did not reach a fully transparent state in the experimental range. For $GLBT_{131}$-*b*-SPE_{193}, an abrupt shift like $GLBT_{182}$-*b*-SPE_{204} was shown also, but a small peak was observed before the main transition appeared at 35–45 ℃ (**Figure 2.4(c)**). Upon cooling, the transmittance dropped from 90% to almost 0% and then increased to 10% at 40 ℃ followed by a decrease to nearly 0%. This unexpected behaviour was observed under repeated heating/cooling, which suggested not a temporary event but an additional step of shrinking/swelling of chains that occurs. A similar result was found in a hysteresis study on $GLBT_{86}$-*b*-SPE_{164} which resembled $GLBT_{131}$-*b*-SPE_{193} in an extra run (**Figure 2.10**); the transmittance fell to 66% (42 ℃) from 90% on cooling, then rose to 72% (37 ℃) followed by a constant drop down to 13% (6.5 ℃). The trend of transmittance change with heating and cooling was similar at 6.5–25 ℃, but at 25–50 ℃ where the reversed shift occurred, the transmittance values of the heating step rapidly increased and were higher than those of the cooling step. It is notable that the hysteresis only appeared in the middle range while the transition below 25 ℃ did not suffer such hysteresis as homopolymer PSPEs: therefore, two distinctive phases during the process might be postulated. Upon consideration of the data with the NMR study at several temperatures that anticipate PSPE core and PGLBT shell structure, it could be summarise that a gradual association/dissociation of the core−shell-like structure happens under temperature change. At room temperature or lower temperatures, the PSPE moieties gather each other and form PSPE-centred particles, making the solution more translucent. With elevating temperature, the PSPE segments start disassembling and then may eventually turn into free chains which results in a transparent solution.

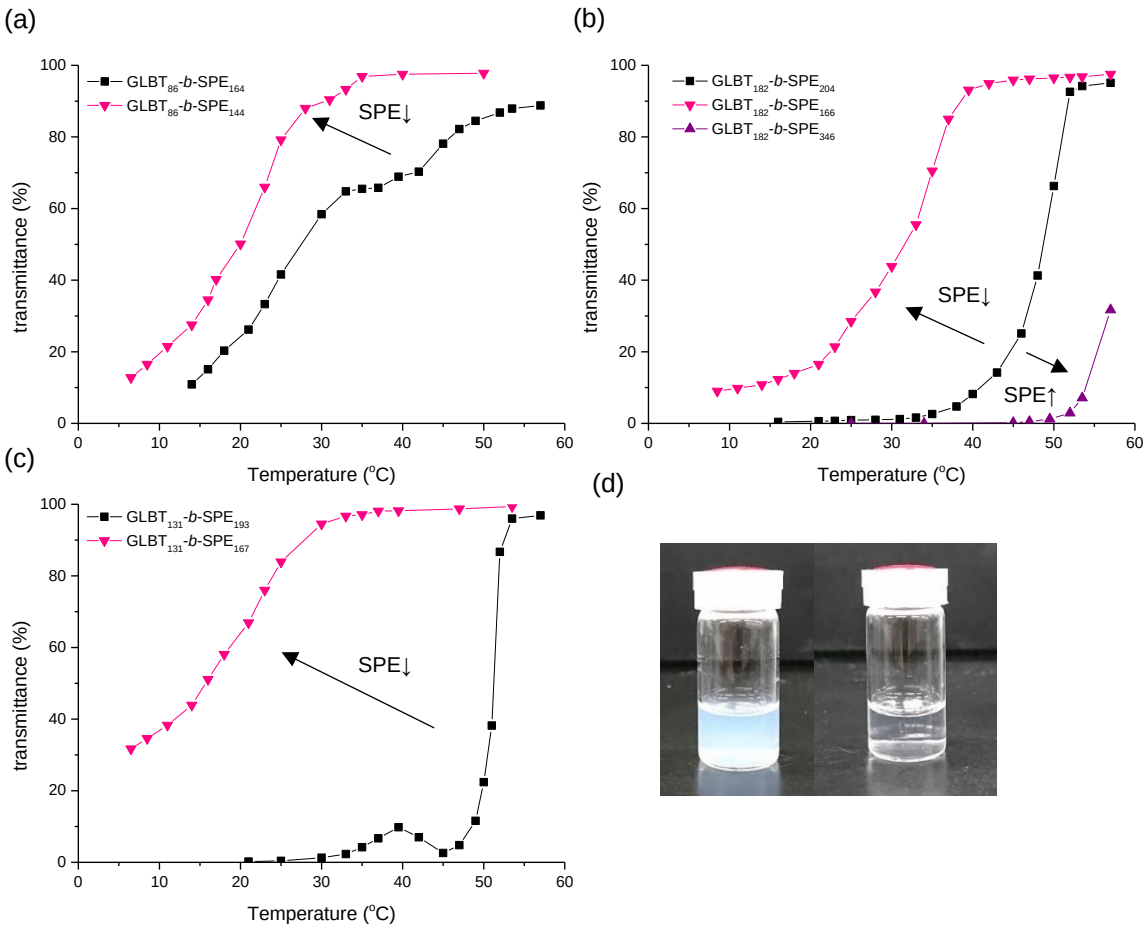

Figure 2.4. Transmittance change of PGLBT-*b*-PSPEs. (a) $GLBT_{86}$-*b*-SPE_{164} and $GLBT_{86}$-*b*-SPE_{144} (b) $GLBT_{182}$-*b*-SPE_{204}, $GLBT_{182}$-*b*-SPE_{166} and $GLBT_{182}$-*b*-SPE_{346} (c) $GLBT_{131}$-*b*-SPE_{193} and $GLBT_{131}$-*b*-SPE_{167} (d) photos of $GLBT_{86}$-*b*-SPE_{164} aqueous solutions of translucent state (left, room temperature) and transparent state (right, ~45 °C). (concentration = 10 mg/mL)

Scattering Results of Polymer Solutions

The size and distributions of the block copolymers and their assembly in water were investigated by DLS as a function of temperatures. Three types of autocorrelation functions were obtained through lower and higher temperatures as depicted in **Figure 2.5(a)**: unimodal fast decay, slow decay functions, and bimodal functions, which represent free chains (small R_h), homogeneous nanoparticles (large R_h) and coexistence of small and large particles, respectively. $GLBT_{86}$-*b*-SPE_{164} existed as monodisperse nanoparticles (R_h = 41 nm, the polydispersity obtained by cumulant analysis μ_2/Γ^2 = 0.120) at 25 °C, and the associations were split by two small and large particles at 37 °C; finally, the larger particles disappeared, and only unimers (R_h = 6.8 nm) were left at 60 °C. The bimodal function at 37 °C is thought to be an intermediate state, where the transmittance changed only a few percent around the point. The hydrodynamic radii recorded as R_h = 9.8 nm in the fast mode and R_h = 417.9 nm in the slow mode while the transmittance recorded as 65.8%. The two modes of the autocorrelation function were

maintained unless heated further, and the function for the slow mode became less pronounced at higher temperatures and then eventually disappeared at 60 ℃.

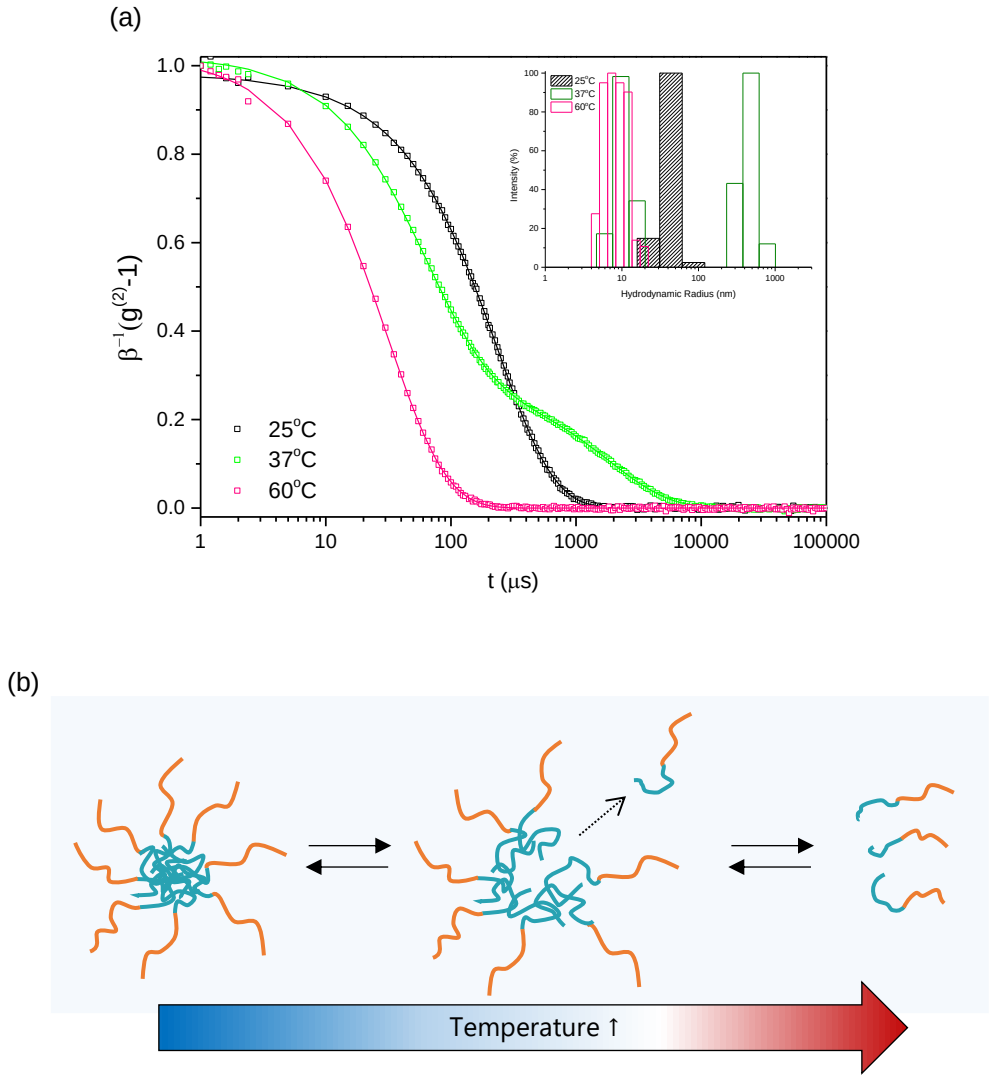

Figure 5. (a) Autocorrelation functions of $GLBT_{86}$-*b*-SPE_{164} of at 25 ℃, 37 ℃, and 60 ℃. Inset shows the distribution of R_h evaluated by CONTIN at 90° (b) Schematic model of core-shell particle formation and dissociation. (orange: PGLBT, blue-green: PSPE)

Upon consideration that the scattered light intensity is proportional to the sixth power of the scatterer's size ($I_s \sim cR^6$, c: constant), these large particles occupying 73% on the intensity-based distribution can be estimated to be 1% in the volume fraction, which means that there are very few actual fractions in the solution. Upon review of the ^1H NMR study at different temperatures, the particle was considered to have a temperature-responsive PSPE core and inert PGLBT shell structure. However, partly distinguishable peaks of PSPE at the particle state suggested a slightly hydrated PSPE surface, which means that the core could not be a perfect hard sphere segregated from

water molecules such as hydrophilic-hydrophobic block copolymer micelles or polyion complex micelles. Thus, the transition process can be summarised into three steps as shown in **Figure 2.5(b)**. Micelles are composed of shrunken PSPE chains and flexible PGLBT brushes formed; the PSPE cores are expanded by swelling while single block copolymer chains start escaping from the centre under heating, and finally no self-assembled structure remains above 50 ℃.

The size variation of the other copolymers obtained by DLS measurement also showed micellar formation and disassociation as shown in **Figure 2.6**, and hydrodynamic radii of nanoparticles and unimers met an agreement with their DP and synthesis feed ratios. $GLBT_{182}$-*b*-SPE_{204} was 63.9 and 13.8 nm when they are in the particle and unimer state, respectively, while $GLBT_{131}$-*b*-SPE_{193} was 51.1 and 10.2 nm, respectively. (see **Table 2.2**). Other block copolymers with less DP of PSPEs also formed uniform ($\mu_2/\Gamma^2 = 0.1–0.13$) smaller micelles and turned into unimers at relatively low temperatures. It should be noted that the correct sizes of the $GLBT_{131}$-*b*-SPE_{193} which showed a small up-and-down transmittance at 40–45℃ could not be determined by multiangle DLS since the sample solution became an extraordinary fuzzy state, and harsh multiple scattering was inevitable, which indicates immense coalescence. Mie scattering by enlarged particles made the autocorrelation functions very dependent to each angle (**Figure 2.11**), but soon turned transparent under subsequent heating or became translucent under subsequent cooling.

Commonly, the block copolymers attempted to have identical ratios of each monomer (black squares in **Figure 2.6** (a)–(c)) showed an increase in size of the micelles shortly before splitting into slow and fast modes, which implies the core expansion before transition. However, other block copolymers synthesised with half SPE monomer ratios (red triangle) did not show the behaviour and disassociated more quickly. The size increase before complete transition in the former case can be regarded that the shrunken and interlocked PSPE segments located at the particle core become swollen then expand, but the dissociation is still hindered by other adjacent PSPE chains which are sufficiently long to hold the core structure sustained by Coulombic attraction. Under subsequent heating, the entropic term of Gibbs free energy of mixing becomes more dominant and some polymer chains start leaving from the core while the structure is not completely disassembled but expands more. Finally, at the temperature where the transmittance reaches almost 100% no self-assembled structures exist and PGLBT-*b*-PSPEs exist as only individual chains. On the other hand, in the latter case the block copolymers whose PSPE segments are short disassociate at a lower temperature without having a recognizable swelling stage. The smaller

ratio of PSPE may not be enough to build a firmly interlocked core so the each block copolymer chain easily detaches from the polymeric micelle.

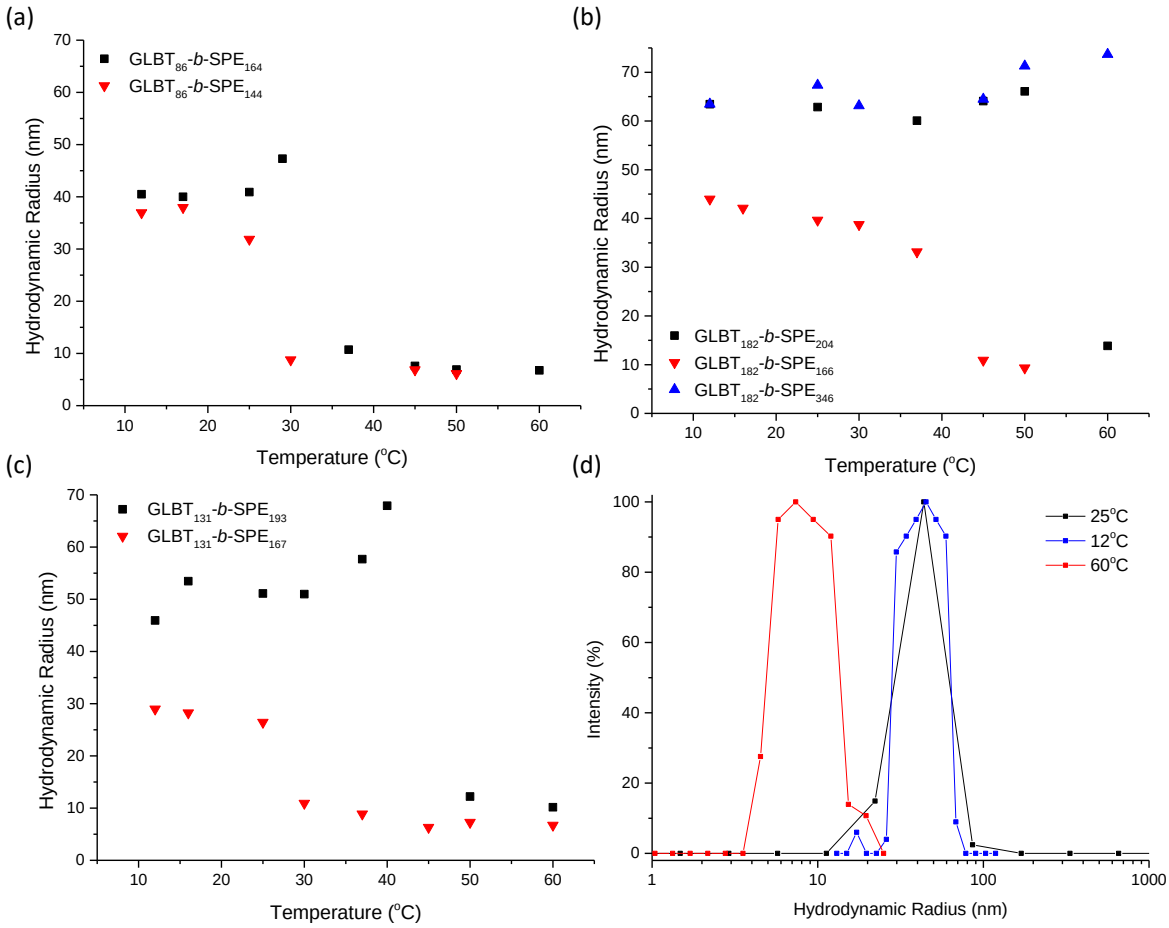

Figure 2.6. Alterations of the R_h of PGLBT-*b*-PSPEs with temperature (a) $GLBT_{86}$ (b) $GLBT_{182}$, and (c) $GLBT_{131}$ derivatives. (d) Size distributions of $GLBT_{86}$-*b*-SPE_{164} at 25, 12, and 60 °C, (intensity based %, obtained at 90°)

Table 2.2. Particle sizes of PGLBT-*b*-PSPEs obtained by light scattering (DLS and SLS) at 25 °C

Sample	R_h (nm) (10 mg/mL)	PDI (μ_2/Γ^2)	R_g (nm) (10 mg/ml)	R_g/R_h	R_h (nm) (diluted)	R_g (nm) (diluted)	R_g/R_h
$GLBT_{86}$	2.6	0.21	-	-	-		
$GLBT_{86}$-*b*-SPE_{164}	40.9 6.8 (unimer)	0.12	-	-	75.6 [a]	60.6 [a]	0.80 [a]
$GLBT_{86}$-*b*-SPE_{144}	31.9 6.1 (unimer)	0.13	30.3	0.95	45.4 [b]	43.4 [b]	0.96 [b]
$GLBT_{182}$	4.2	0.17	-	-	-	-	-
$GLBT_{182}$-*b*-SPE_{204}	62.9 13.8 (unimer)	0.14	-	-	63.9 [a]	37.1 [a]	0.68 [a]
$GLBT_{182}$-*b*-SPE_{166}	39.7 9.3 (unimer)	0.05	-	-	46.5 [a]	30.8 [a]	0.66 [a]
$GLBT_{182}$-*b*-SPE_{346}	54.6	0.23	-	-	-	-	-
$GLBT_{131}$	3.5	0.24	-	-	-	-	-
$GLBT_{131}$-*b*-SPE_{193}	51.1 10.2 (unimer)	0.15	-	-	54.9 [a]	35.6 [a]	0.65 [a]
$GLBT_{131}$-*b*-SPE_{167}	26.4 6.7 (unimer)	0.21	24.5	0.93	27.7 [b]	32.1 [b]	1.16 [b]

[a]: conc. = 2.5 mg/mL, [b]: conc. = 5 mg/mL, R_h of unimers were determined at 60°C

For clarification of the nature of the structures more precisely, an SLS study was carried out to obtain the radius of gyration (R_g) and the shape factor R_g/R_h. Samples were diluted for proper measurement of SLS followed by reexamination through DLS. In the case of diluted $GLBT_{86}$-*b*-SPE_{164} solution, the R_g was 60.6 nm, and the ratio of R_g/R_h was 0.80, which is close to that of hard-sphere particles ($R_g/R_h = \sqrt{3/5} \sim 0.775$) while the other derivative $GLBT_{86}$-*b*-SPE_{144} had R_g = 43.4 nm and R_g/R_h = 0.96 as shown in **Figure 2.7**. In addition, the R_g/R_h of $GLBT_{182}$-*b*-SPE_{204} and $GLBT_{131}$-*b*-SPE_{193} was 0.68 and 0.65, respectively, while R_g/R_h of $GLBT_{182}$-*b*-SPE_{166} and $GLBT_{131}$-*b*-SPE_{167} was 0.65 and 1.16. A shape factor less than 0.77 may reflect that there is a brush layer on the core contributing small masses usually observed for polymeric micelles, and most of the weight is concentrated at the centre of the micelles. In addition, there might be small stressed loops on shrunken chains of the core section which could increase the hydrodynamic radii.[44] On the other hand, values over 1 suggest that the weight of the chains is more likely to be distributed at the particle surface such as a vesicle (R_g/R_h = 1) or anisotropic shape. Some polymers increased in size after dilution, particularly $GLBT_{86}$-*b*-SPE_{164} and $GLBT_{86}$-*b*-SPE_{144}. These results are similar to the increase in size of undiluted samples before their monodisperse particles split up fast and slow modes; hence, it is thought that the UCST of the polymer was shifted to lower temperature because of the reduced fractions of the PSPE in water. This diluted sample of $GLBT_{86}$-*b*-SPE_{164} recorded R_h = 41.3 nm at 12 °C, which is close to the size of original sample (10 mg/mL) at 25 °C and lower temperatures.

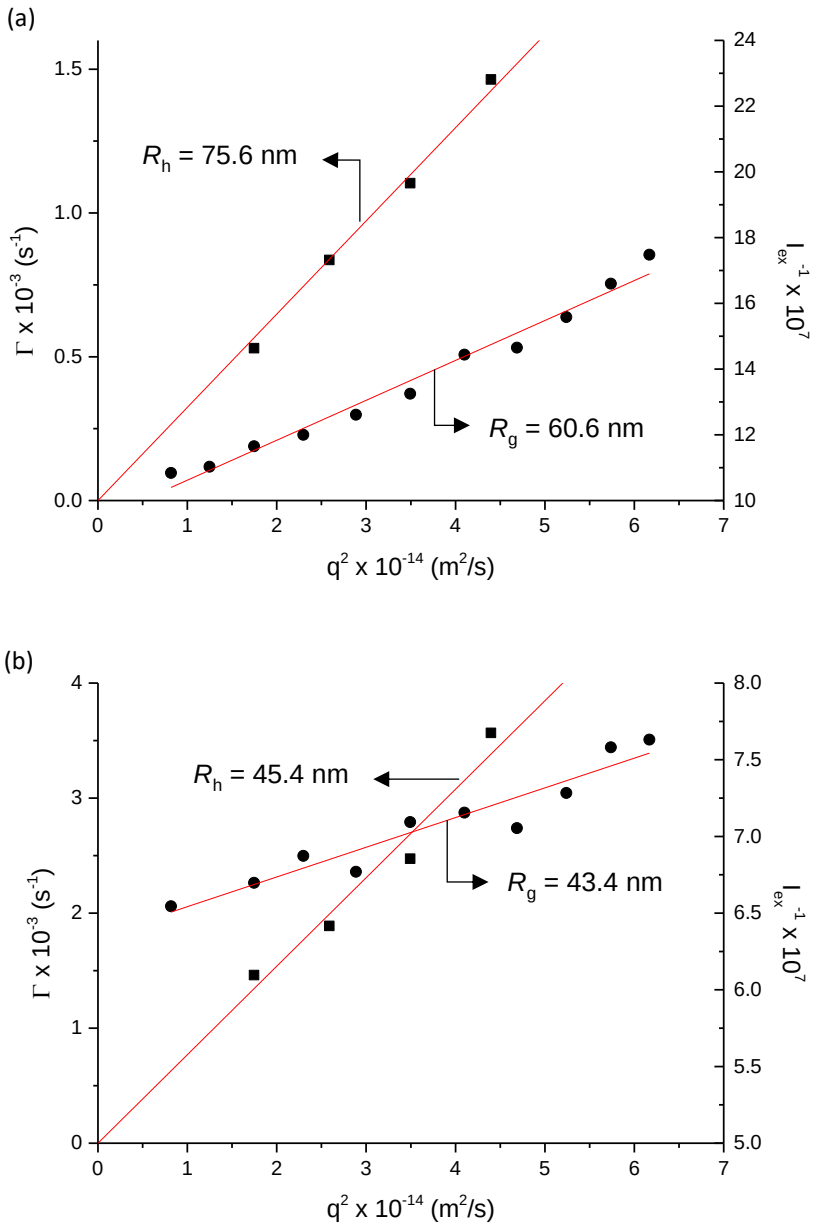

Figure 2.7. Multiangle measurements DLS (■) and SLS (●) performed on (a) $GLBT_{86}$-*b*-SPE_{164} and (b) $GLBT_{86}$-*b*-SPE_{144} at 25 ℃

TEM studies supported the result of light scattering. Since the self-assembly was very sensitive to temperature and concentration, the dried polymer sample on the grid is not in the exactly same state as that in the solution. Nevertheless, regularly distributed spherical particles were observed from the block copolymer samples prepared at room temperature, and the morphology varied by sample preparation temperature. For $GLBT_{86}$-*b*-SPE_{164}, there are no particular aggregations from the sample prepared at room temperature; however, another sample prepared at 37 ºC showed large anisotropic aggregates with small particles as **Figure 2.8**, which is anticipated by the DLS

and transmittance study. The particle sizes obtained by TEM image (average radius = 49 nm) were correlated with the result analysed by light scattering (R_h = 40.9 nm).

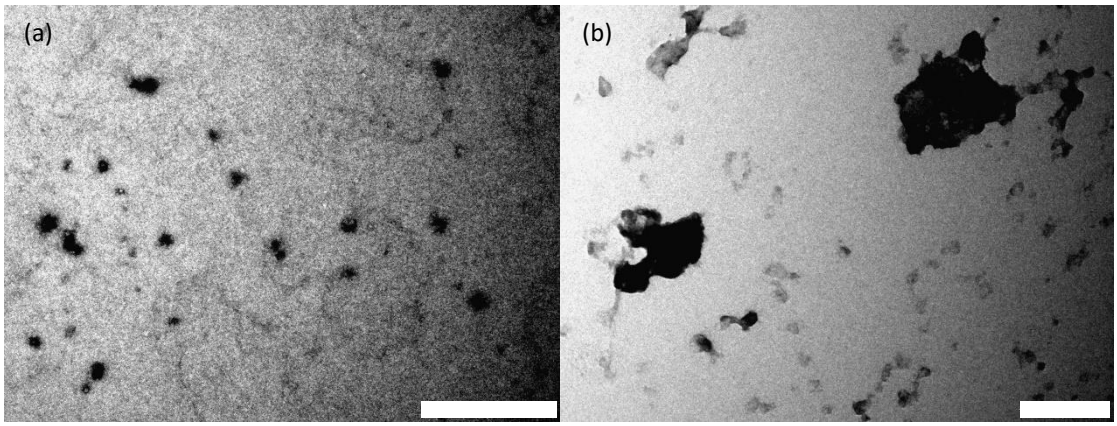

Figure 2.8. TEM images of $GLBT_{86}$-*b*-SPE_{164} prepared at (a) 25 ºC, (b) 37 ºC (scale bar: 1μm)

Additional Discussion

According to previous reports,[32, 33] PGLBT does not respond to temperature unlike UCST-type PSPE and other sulfobetaine species; it remains in a dissolved state in spite of having zwitterions. Comparing the transmittance change with that of homo-PSPE having a similar extent of repeating unit (**Figure 2.8**), it is evident that the PGLBT segment affects the hydrophobic collapse of PSPE segments. The block copolymers form monodisperse polymeric nanoparticles instead of phase separation as PSPE does (coil-to-globule transition followed by size growth to a few thousand nanometers and then becomes sediment) revealed by light scattering studies. The behaviour of forming polymeric micelles suggests that the hydrophilic PGLBT segment of the block copolymers provides additional affinity to water thereby preventing phase separation and sedimentation of PSPE. In addition, a continuous decrease of transmittance after a certain temperature at which the size of polymeric micelles settled seems to be the number increase of nanoparticles. To elucidate the role of GLBT units on thermo-responsivity, we synthesised PGLBT-*r*-PSPE random copolymers and compared them to block copolymers for viewing the influence of monomer sequence. The feed ratio of [GLBT]:[SPE] = 1:1, 1:3, and 1:9. Neither of them showed noticeable turbidity changes but only one random copolymer whose ratio of [PGLBT]:[PSPE] = 1:9 showed a few % of change despite the large extents of PSPE as shown in **Figure 2.9**. Those results suggest that not only the chemical composition but also the sequence and locations of each unit dominate the temperature-responsivity of polysulfobetaines; in particular, just a few percent of GLBTs randomly incorporated around SPEs significantly alter the property of a whole chain. It is thought that hydrophobic collapse of homopolymer PSPEs at low

temperatures starts shrinking by itself because of intrachain/interchain attractions between adjacent cationic and anionic groups, and then the folded individual chains would become closer and merge together to minimise the surface energy penalty caused by the increased hydrophobic surface. Similar to this manner, PSPE segments of block copolymers would collapse and aggregate with adjacent PSPE blocks while PGLBT units on the opposite side still remain flexible chains below critical temperatures; eventually polymeric micelles are generated. On the other hand, the random copolymers became independent of temperature variation just with a small amount of incorporated GLBT units. Why do the random copolymers show no response although there is a presence of zwitterion pairs in PGLBT? It is apparent that randomly distributed GLBT units tend not to have zwitterionic interactions and rather screen the inter- and intrachain approaches between PSPEs. According to a molecular dynamics simulation study of a polycarboxybetaine having 1 more carbon on the spacer than PGLBT and PSPE, it is proposed that the different stimulus-responsive behaviour of two polybetaines originates from the charge density difference of cationic/anionic functional groups.[45] The charge density imbalance between dimethylammonium (3.0 e/nm^3) and acetate (-5.3 e/nm^3) was calculated and proposed as the reason for non-temperature-responsivity while PSPE was revealed to have less imbalance (3.0 e/nm^3 for dimethylammonium and -4.5 e/nm^3 for sulfonate). The authors thought that the difference of charge densities may dominate associations among zwitterions: when the difference is less, the association strengthens among zwitterions, and when the difference is greater, it leads to fewer associations and strong hydration. Therefore, polycarboxybetaines are likely to be inert in water, and meanwhile it is not easy for sulfobetaines to dissolve in water without interaction-breaking sources (heat, additional salt ions, etc.). When the carboxybetaines are incorporated with other nonionic units, they tend to be independent of their counterpart's own behaviour rather than active as found in other examples. For copolymers obtained with other temperature-responsive nonionic substances, zwitterion units scarcely affect their nonionic counterparts. First, random copolymers, which consisted of PNIPAM and a carboxybetaine having 1 more carbon as spacer unit between the cationic and anionic group than GLBT, kept the intrinsic LCST behaviour of PNIPAM with only slight alterations. This random copolymer chain formed a blob-coil structure at high temperatures while PSPE-*r*-PNIPAM showed higher LCSTs and formed weaker elastic networks with increasing the SPE amounts, which anticipates enhanced hydration.[46] Similarly, for the "schizophrenic" type block copolymers such as PSPE-*b*-PNIPAM[24, 47] or PSPE-*b*-PDMAEMA[26] which form micelles at low (PSPE core) and high (PNIPAM or PDMAEMA core) temperature, the one side weakly affected the property of the opposite side as is the case of random copolymers. Although the LCSTs and UCSTs were shifted to upper or lower register, the transition usually occurred in a very short time as their homopolymers occur within less than 10 °C. On the

contrary, our experiment results showed that the carboxybetaine significantly influenced the temperature-responsivity of the sulfobetaine on the other side or their vicinity. In addition, it is intriguing that the polymeric micelles of PGLBT-*b*-PSPE did not coalesce and grow over few microns such as PSPE-*b*-PDMAEMA which showed an immense size increase thanks to zwitterions of PGLBT on the particle surface. Hence, the carboxybetaine units of the block copolymer seem to not remain in the inert state but have some extent of interactions with adjacent ionic pairs.

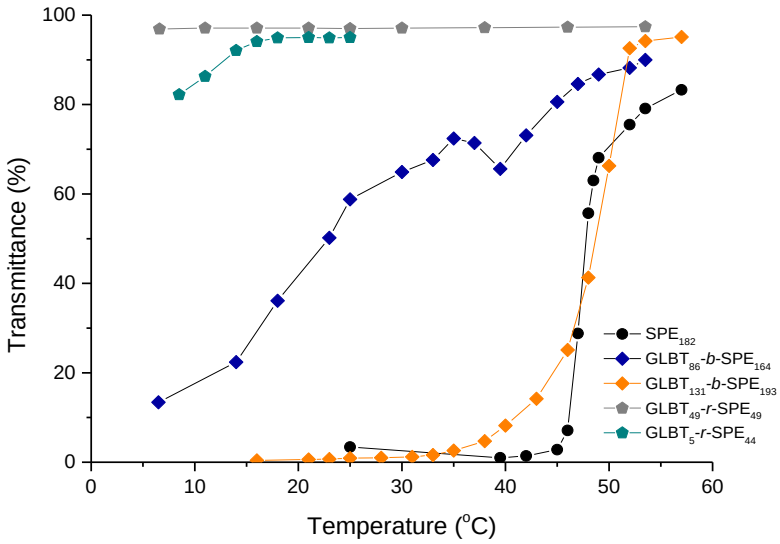

Figure. 2.9 Comparison of transmittance change among (circle) homo-PSPE, (diamond) PGLBT-*b*-PSPE block copolymers, and (pentagon) random copolymers

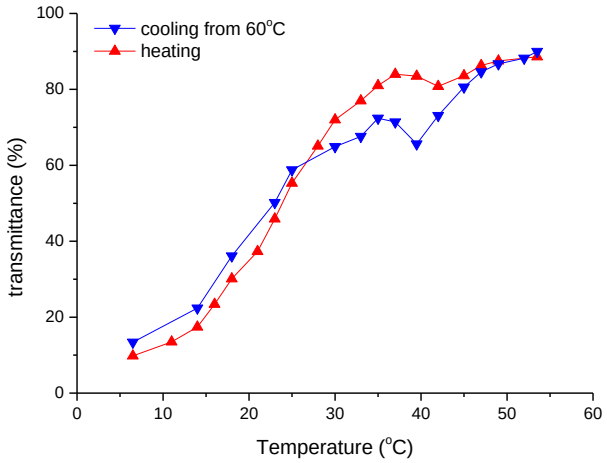

Figure 2.10. Transmittance variation of PGLBT-*b*-PSPE on cooling and heating cycle. First, each transmittance of the sample solution heated up to 60℃ was recorded in cooling step (blue), then the sample was heated again up to 60℃.

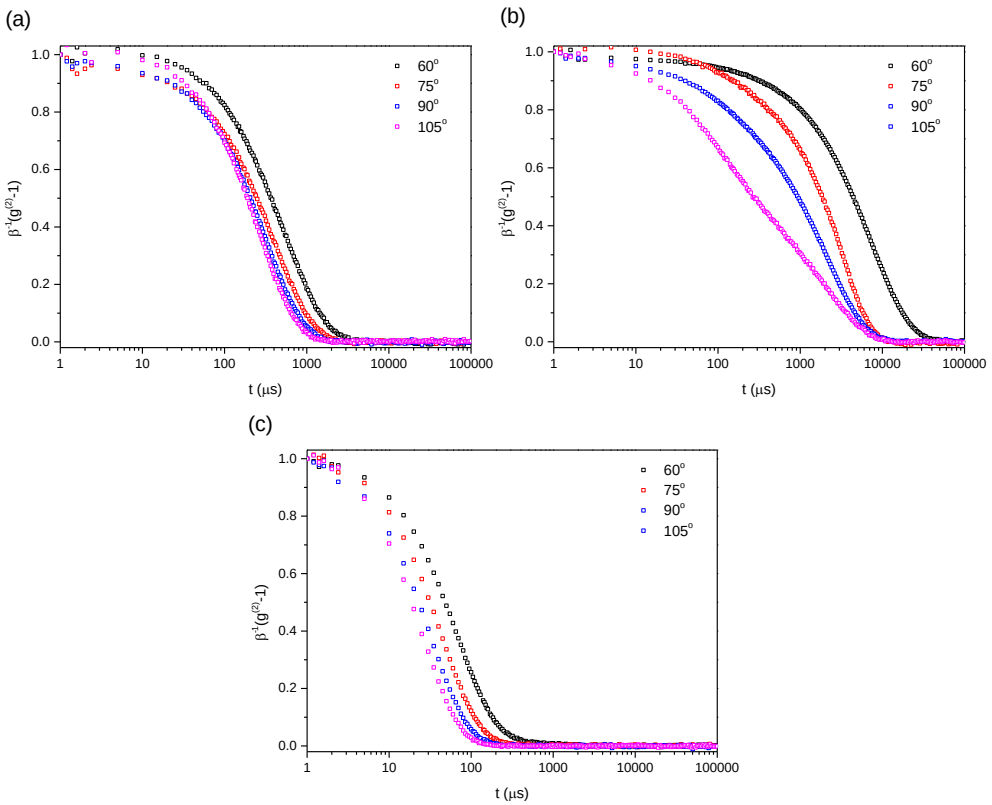

Figure 2.11. DLS autocorrelation functions of $GLBT_{131}$-*b*-SPE_{193} at 60, 75, 90, 105° (a) obtained at 25 °C (b) at 45°C (c) at 60 °C

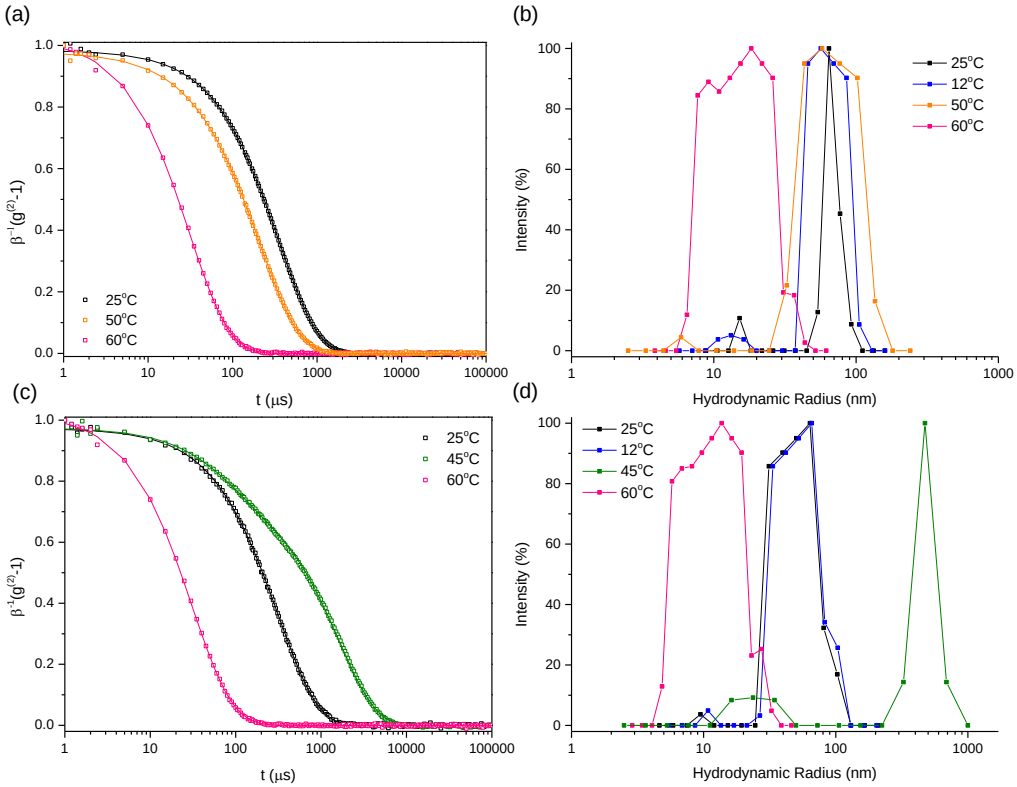

Figure 2.12. Autocorrelation functions(ACF) of PGLBT-*b*-PSPEs and hydrodynamic radius distribution of PGLBT-*b*-PSPEs obtained by CONTIN analysis at 90°. (a) $PGLBT_{182}$-*b*-$PSPE_{204}$, ACF (b) $PGLBT_{182}$-*b*-$PSPE_{204}$, CONTIN analysis (c) $PGLBT_{131}$-*b*-$PSPE_{193}$, ACF (d) $PGLBT_{131}$-*b*-$PSPE_{193}$, CONTIN analysis

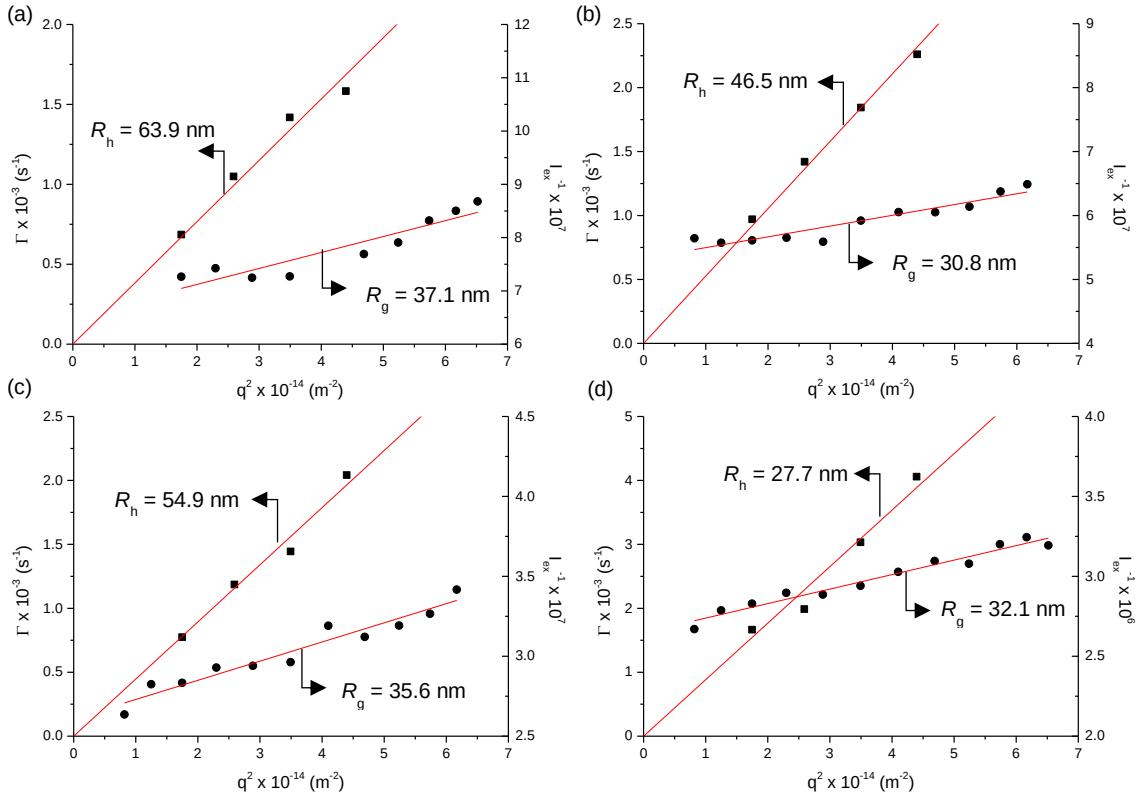

Figure 2.13. multiangle measurements DLS (■) and SLS (●) performed on (a) $GLBT_{182}$-*b*-SPE_{204} and (b) $GLBT_{182}$-*b*-SPE_{166} (c) $GLBT_{131}$-*b*-SPE_{193} (d) $GLBT_{131}$-*b*-SPE_{167} at 25°C

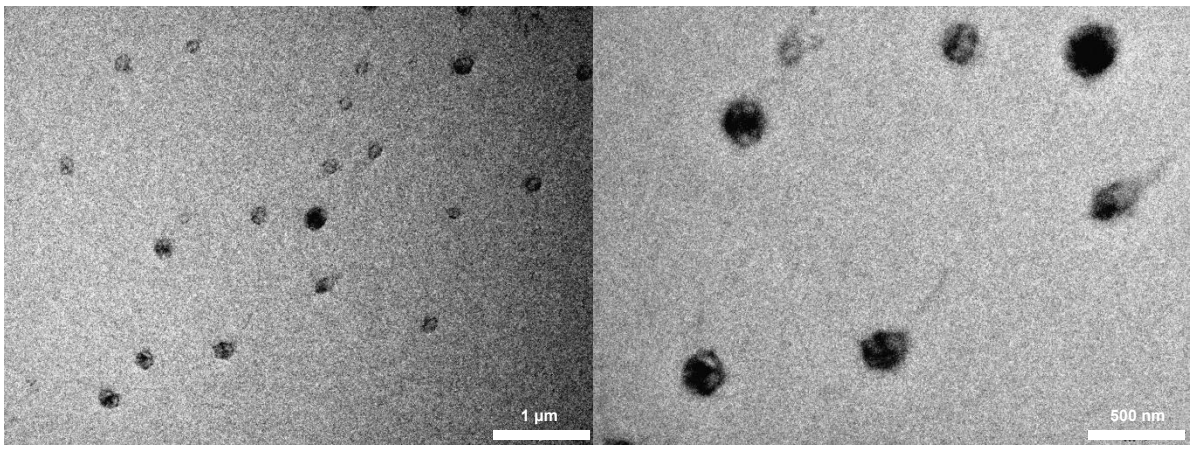

Figure 2.14. TEM image of $GLBT_{182}$-*b*-SPE_{204} prepared at 25 ºC. (The average particle radius = 84.3 nm, calculated by image analysis)

Conclusion

We successfully obtained a double zwitterion block copolymer PGLBT-*b*-PSPE with narrow molecular weight distribution by RAFT polymerisation using the betaine monomers directly. Unlike what was initially expected

from this double hydrophilic copolymer, it formed homogeneous particles in water at room temperature because of the UCST behaviour of the PSPE segment, in spite of the absence of any hydrophobic block. ^{1}H NMR spectra and light scattering data at low and high temperatures revealed that the block copolymers formed polymeric micelles having a PSPE core and PGLBT shell. The polymers existed in three regimes: polymeric micelles, intermediate stage of coexisting unimers and highly swollen associations, and unimer-only. Under repeated heating-cooling cycles, the transmittance curve and light scattering results always showed the same tendency, which means that the self-assembly is a thermodynamically spontaneous process, and the particle sizes and temperature-responsive features were governed by the ratio of [PGLBT]:[PSPE] and the whole molecular weight. Different from conventional temperature-responsive polymers and their copolymers, the phase transition of those double zwitterionic block copolymers appeared as very gradual trends through wide temperature range accompanied by unexpected perturbations. To reveal the properties of the new polyzwitterions in more detail, we need to investigate other stimulants further: pH and salt, which affect ionisation of the carboxylate end group of the PGLBTs and Coulombic forces between ion pairs of zwitterions on the polymer surface. Also, it is expected that this double zwitterionic block copolymer enables the carrying of active materials at the inside of the core and their release[48] during extended periods against temperature variation, if highly prolonged release is necessary.

References

1. I. Nicander, I. Rantanen, B. L. Rozell, E. Soderling and S. Ollmar, *Skin Research and Technology*, 2003, **9**, 50-58.
2. S. Y. Jiang and Z. Q. Cao, *Advanced Materials*, 2010, **22**, 920-932.
3. C. Blaszykowski, S. Sheikh and M. Thompson, *Chemical Society Reviews*, 2012, **41**, 5599-5612.
4. K. H. A. Lau, T. S. Sileika, S. H. Park, A. M. L. Sousa, P. Burch, I. Szleifer and P. B. Messersmith, *Advanced Materials Interfaces*, 2015, **2**.
5. J. B. Schlenoff, *Langmuir*, 2014, **30**, 9625-9636.
6. L. Tauhardt, D. Pretzel, K. Kempe, M. Gottschaldt, D. Pohlers and U. S. Schubert, *Polymer Chemistry*, 2014, **5**, 5751-5764.
7. R. Lalani and L. Y. Liu, *Biomacromolecules*, 2012, **13**, 1853-1863.
8. A. Hatefi and B. Amsden, *Journal of Controlled Release*, 2002, **80**, 9-28.
9. J. Niskanen and H. Tenhu, *Polymer Chemistry*, 2017, **8**, 220-232.
10. J. Seuring and S. Agarwal, *Macromolecular Rapid Communications*, 2012, **33**, 1898-1920.
11. P. Mary, D. D. Bendejacq, M. P. Labeau and P. Dupuis, *Journal of Physical Chemistry B*, 2007, **111**, 7767-7777.
12. P. Mary and D. D. Bendejacq, *Journal of Physical Chemistry B*, 2008, **112**, 2299-2310.
13. J. D. Delgado and J. B. Schlenoff, *Macromolecules*, 2017, **50**, 4454-4464.
14. Y. C. Zhu, J. M. Noy, A. B. Lowe and P. J. Roth, *Polymer Chemistry*, 2015, **6**, 5705-5718.
15. C. Durand-Gasselin, R. Koerin, J. Rieger, N. Lequeux and N. Sanson, *Journal of Colloid and Interface Science*, 2014, **434**, 188-194.
16. K. E. B. Doncom, H. Willcock and R. K. O'Reilly, *European Polymer Journal*, 2017, **87**, 497-507.
17. P. A. Woodfield, Y. C. Zhu, Y. W. Pei and P. J. Roth, *Macromolecules*, 2014, **47**, 750-762.
18. M. T. Cai, M. T. Leng, A. J. Lu, L. He, X. X. Xie, L. Huang, Y. H. Ma, J. Cao, Y. W. Chen and X. L. Luo, *Colloids and Surfaces B-Biointerfaces*, 2015, **126**, 1-9.

19. K. E. B. Doncom, N. J. Warren and S. P. Armes, *Polymer Chemistry*, 2015, **6**, 7264-7273.
20. Y. W. Pei and A. B. Lowe, *Polymer Chemistry*, 2014, **5**, 2342-2351.
21. H. Willcock, A. Lu, C. F. Hansell, E. Chapman, I. R. Collins and R. K. O'Reilly, *Polymer Chemistry*, 2014, **5**, 1023-1030.
22. O. Azzaroni, A. A. Brown and W. T. S. Huck, *Angewandte Chemie-International Edition*, 2006, **45**, 1770-1774.
23. J. Virtanen, M. Arotcarena, B. Heise, S. Ishaya, A. Laschewsky and H. Tenhu, *Langmuir*, 2002, **18**, 5360-5365.
24. N. S. Vishnevetskaya, V. Hildebrand, B. J. Niebuur, I. Grillo, S. K. Filippov, A. Laschewsky, P. Muller-Buschbaum and C. M. Papadakis, *Macromolecules*, 2016, **49**, 6655-6668.
25. N. S. Vishnevetskaya, V. Hildebrand, B. J. Niebuur, I. Grillo, S. K. Filippov, A. Laschewsky, P. Muller-Buschbaum and C. M. Papadakis, *Macromolecules*, 2017, **50**, 3985-3999.
26. H. Sun, X. L. Chen, X. Han and H. L. Liu, *Langmuir*, 2017, **33**, 2646-2654.
27. J. Bohrisch, T. Schimmel, H. Engelhardt and W. Jaeger, *Macromolecules*, 2002, **35**, 4143-4149.
28. V. A. Izumrudov, N. I. Domashenko, M. V. Zhiryakova and O. V. Davydova, *Journal of Physical Chemistry B*, 2005, **109**, 17391-17399.
29. V. A. Izumrudov, A. N. Zelikin, M. V. Zhiryakova, W. Jaeger and J. Bohrisch, *Journal of Physical Chemistry B*, 2003, **107**, 7982-7986.
30. M. Birkner and M. Ulbricht, *Journal of Membrane Science*, 2015, **494**, 57-67.
31. N. Y. Kostina, S. Sharifi, A. D. Pereira, J. Michalek, D. W. Grijpma and C. Rodriguez-Emmenegger, *Journal of Materials Chemistry B*, 2013, **1**, 5644-5650.
32. H. Matsuoka, Y. Yamakawa, A. Ghosh and Y. Saruwatari, *Langmuir*, 2015, **31**, 4827-4836.
33. S. Murugaboopathy and H. Matsuoka, *Colloid and Polymer Science*, 2015, **293**, 1317-1328.
34. E. E. L. Kathmann, L. A. White and C. L. McCormick, *Macromolecules*, 1997, **30**, 5297-5304.
35. G. J. Hu, S. S. Parelkar and T. Emrick, *Polymer Chemistry*, 2015, **6**, 525-530.
36. S. Morozova, G. Hu, T. Emrick and M. Muthukumar, *Acs Macro Letters*, 2016, **5**, 118-122.
37. B. Schmidt, *Macromolecular Chemistry and Physics*, 2018, **219**.
38. N. Al Nakeeb, J. Willersinn and B. Schmidt, *Biomacromolecules*, 2017, **18**, 3695-3705.
39. Y. Mitsukami, M. S. Donovan, A. B. Lowe and C. L. McCormick, *Macromolecules*, 2001, **34**, 2248-2256.
40. S. W. Provencher, *Biophysical Journal*, 1976, **16**, 27-41.
41. D. E. Koppel, *Journal of Chemical Physics*, 1972, **57**, 4814-&.
42. J. F. Baussard, J. L. Habib-Jiwan, A. Laschewsky, M. Mertoglu and J. Storsberg, *Polymer*, 2004, **45**, 3615-3626.
43. B. A. Abel and C. L. McCormick, *Macromolecules*, 2016, **49**, 465-474.
44. X. H. Wang, X. P. Qiu and C. Wu, *Macromolecules*, 1998, **31**, 2972-2976.
45. Q. Shao, L. Mi, X. Han, T. Bai, S. J. Liu, Y. T. Li and S. Y. Jiang, *Journal of Physical Chemistry B*, 2014, **118**, 6956-6962.
46. Y. Zhao, T. Bai, Q. Shao, S. Y. Jiang and A. Q. Shen, *Polymer Chemistry*, 2015, **6**, 1066-1077.
47. Y. J. Shih, Y. Chang, A. Deratani and D. Quemener, *Biomacromolecules*, 2012, **13**, 2849-2858.
48. Z. Ahmad, A. Shah, M. Siddiq and H. B. Kraatz, *Rsc Advances*, 2014, **4**, 17028-17038.

Chapter 3. Effects of Halide Anions on the Solution Behaviour of Double Hydrophilic Carboxy-Sulfobetaine Block Copolymers

ABSTRACT: The solution behaviour of the double polybetaine block copolymer poly(2-((2-(methacryloyloxy)ethyl)dimethylammonio)acetate)-*block*-poly(3-((2-(methacryloyloxy)ethyl)dimethyl-ammonio)propane-1-sulfonate (PGLBT-*b*-PSPE) in sodium halide aqueous solutions was investigated. In the presence of salt ions, the unimer-to-micelle transition of PGLBT-*b*-PSPE that originated by Coulombic attraction between PSPE motifs was suppressed and shifted to much lower temperatures. The transition was more hindered by increases in the salt concentration due to additional counterion binding on the ionized site of PGLBT-*b*-PSPE chains which screens the dipole-dipole attractions. The specific ion effect was investigated on four different halides, Cl^-, Br^-, I^- and F^-. Cl^- and two chaotropes (Br^- and I^-) apparently prevented micelle formation, and the hindering effectiveness on the PSPE pairing followed the general Hofmeister series of anions: $I^- > Br^- > Cl^-$. More chaotropic anions strongly maintained the polymer chains in a fully hydrated state when the same amount of salts was incorporated. However, F^-, which is classified as kosmotrope, only did small contribution on lowering the transition point and led to abrupt transition without showing a gradual phase change prior to the transition. The variations of hydrodynamic radius zeta potentials of unimers and micelles gave hints of the solvation state of salt-incorporated PGLBT-*b*-PSPEs in each state. These results suggest that chaotropes tend to exist in the vicinity of the diblock polybetaine chain surface thus prominently influenced the thermoresponsive solution behaviour, whereas kosmotropes prefer water molecules and cause minor changes in the PGLBT-*b*-PSPE aqueous solution.

Introduction

Polyzwitterions are a unique type of polyelectrolytes having dipoles permanently in their repeating units. Their whole charge is neutral[1, 2] unlike ordinary polyelectrolytes having cations or anions solely. The charged surface of polyzwitterions that can effectively prevent adsorption of proteins or other impurities are getting attention for utilizing the polymers as functional materials which require high biocompatibility. Various kinds of polyzwitterionic coatings have been showing reduced adhesion of bacteria,[3-5] high resistance against protein adsorption,[6-8] or simultaneous resistance against microbial and protein.[9] These nonfouling behaviours of polyzwitterions are discussed on the point of hydration mechanisms; the water molecules around polyzwitterions are supposed to be no more or less structured in contrast to other polyelectrolytes.[10]

Three types of polybetaine have been mainly investigated. Polyphosphobetaines have been widely studied because of their superior biocompatibility, and the modified surfaces have been revealed improved resistance to nonspecific protein adsorption.[11, 12] They are regarded as a class of biomimetic materials due to the phosphorylcholine headgroup, which is the component of phosphatidylcholine most abundant in eukaryotic cell membranes.[13] However, only rare characteristics that occurred by dipole interactions were found.[14] Polysulfobetaines and polycarboxybetaines show not only high biocompatibility[15-17] but also stimuli-responsive behaviour[18, 19] depending on their cationic/anionic functional groups. Polysulfobetaines which usually consist of a quaternary ammonium with a sulfonate in their repeating unit exhibit upper critical solution temperature (UCST) behaviour in water, whereas polycarboxybetaines that have a carboxylate instead of a sulfonate are independent to temperature variation but altered to polycations under acidic conditions due to protonation of the carboxylates. Therefore, these two polybetaines may be feasible for designing "smart" polymer materials which can respond to surrounding changes by exploiting the characteristics as other non-ionic stimuli-responsive polymers, but which are more susceptible to fouling by deposition.[20]

"Anti-polyelectrolyte" behaviour of polyzwitterions are often discussed to understand the characteristic of the chains in water. In general, polyelectrolyte chains in aqueous solutions shrink by ion addition because of screening of electrostatic repulsion between charged units. However, polyzwitterions swell more by added ions and their solubility increases as does viscosity.[21, 22] The Debye length, which means the range of electrostatic interactions, decreases by increasing ionic strength and attenuation of electrostatic attractions between adjacent pendent groups or chains happens, which leads to eventual chain expansion. The behaviour also occurs on amphiphilic betaine-hydrophobic diblock copolymers which were spread on an water/air interface and formed a carpet-brush layer[23] or which showed micellar formation in aqueous medium.[24] Since the stimuli-responsive characters of polybetaines come from the zwitterionic interactions, understanding the interplay of anions and cations with polyzwitterions in water is crucial for designing and operating polyzwitterion-based applications under optimum conditions. Upon non-ionic polymers including proteins and synthetic polymers both, specific ion effects affecting chain folding and colloidal stability have been extensively studied on a certain trend of ion species, which is known as the Hofmeister series. The influence by anions is more pronounced than that of cations.[25] The generally considered order is as follows:

$$CO_3^{2-} > SO_4^{2-} > F^- > Cl^- > Br^- > NO_3^- > I^- > ClO_4^{2-} > SCN^-$$

where the left side of the ions are classified as kosmotropes, which tend to precipitate proteins and non-ionic polymers, and the right side of the ions are chaotropes, which promote the solvation of solutes. Chloride is often considered the centre point of dividing the two types of ions. The classification was named according to the concept of ion behaviour in water structure. Kosmotropic ions are referred to have high affinity to water molecules and can be included around water molecules forming hydrogen bonding, whereas chaotropic ions are likely to be excluded from the H-bonding structure of water and are more placed to the vicinity of polymer chains, but recently the notion has been doubted.[26-28] The Law of Matching Water Affinity is proposed to understand the behaviour more systematically by arguing the energetic cost of dehydrating a strongly hydrated small monovalent ions and a weakly hydrated large monovalent ions.[29] According to the viewpoint, the pair between solely weakly hydrated ions or strongly hydrated ions (chaotropes-chaotropes / kosmotropes-kosmotropes) is only energetically favoured so that the ions can stay together, whereas weak-strong pairs are not stable and tend to be placed in water molecules.[30] The series has been verified by investigating thermoresponsive polymers[25, 31-33] (e.g. poly(*N*-isopropylacrylamide) and their derivatives,[34, 35] or latex particles[36] and proteins[37] in salt solutions, and inversed behaviour appeared at specific conditions.[38, 39] Several studies on polyzwitterions based on the idea of Hofmeister series were reported, but only a few examples of homopolymers were tested.[40-44]

In our previous work,[45] the double zwitterionic and double hydrophilic block copolymer PGLBT-*b*-PSPE showed self-assembly in water thanks to PSPE segments bearing UCST-type temperature responsivity. (**Scheme 3.1**) Spherical micelles composed of shrunken PSPE cores and PGLBT coronas were observed under their critical temperatures when the solution became translucent or opaque, and unimers were observed in the high temperature region from the solution which turned into a transparent state. In the present work, the specific ion effect of four halide ions (Cl^-, Br^-, I^-, and F^-) on PGLBT-*b*-PSPE is studied by examining the altered temperature-responsive solution behaviour.

Experimental Section

Materials

2-((2-(Methacryloyloxy)ethyl)dimethylammonio)acetate (carboxybetaine methacrylate, GLBT) and 3-((2-(methacryloyloxy)ethyl)dimethylammonio)propane-1-sulfonate (sulfobetaine methacrylate, SPE) were kindly donated from Osaka Organic Chemical Industry LTD (Osaka, Japan) and used as received. The chain transfer

agent (CTA), 4-cyano-4-(phenylcarbonothioylthio)pentanoic acid, was synthesized by the literature.[46] A radical initiator 2,2'-azobis[2-(2-imidazolin-2-yl)propane]dihydrochloride (VA-044) was purchased from Wako Chemicals (Osaka, Japan) and used as received. Deuterated water (D_2O) was purchased from Cambridge Isotope Laboratories. Ultrapure water (minimum resistivity ~ 18.2 MΩ cm) obtained by Milli-Q system was used for preparing aqueous solutions and dialysis. Regenerated cellulose membranes (MWCO 3500 and 15000) were used for dialysis to remove residual monomers, salt ions and other impurities. Inorganic salts NaCl, NaBr, and NaI were purchased from Wako Chemicals. NaF was purchased from Nacalai Tesque.

Synthesis of double polybetaine block copolymer PGLBT-*b*-PSPE

The polybetaine homo- and block copolymers were obtained as previously reported.[45] First, PGLBT homopolymers were synthesized by reversible addition-fragmentation chain transfer (RAFT) polymerization. Unreacted GLBT monomers were removed through dialysis prior to the next step. PGLBT-*b*-PSPEs were synthesized with the PGLBT macroCTAs and SPE monomers, and residual PGLBTs were removed by precipitation into ethanol. The product was recovered as a white powder by lyophilization.

Polymer characterisation

^{1}H NMR spectra of synthesized polymers were acquired using a 400 MHz JEOL JNM-AL 400 spectrometer (JEOL, Tokyo, Japan) in deuterated water (D_2O).

The molecular weight distributions of homo- and block copolymers were determined by aqueous size exclusion chromatography (SEC) operated with a column (SB-804 HQ, Shodex) and a refractive index detector (RI-830, JASCO, Japan), using a buffer eluent (0.5 M CH_3COOH and 0.3 M of Na_2SO_4) at a flow rate of 0.5 mL/min. The calibration was carried out with a set of poly(2-vinylpyridine) standards (Mn range: 5500 to 142000 g/mol, Sigma-Aldrich). The data was analyzed by the software provided by JASCO.

The transmittance of the aqueous solutions of the block copolymers (concentration: 10 mg/mL) was measured at 400 nm with a UV-VIS spectrometer (Hitachi U-3310 spectrophotometer) equipped with a water circulator for temperature control. A quartz cell with a light path of 10 mm was used. The solutions were filtered by a syringe filter unit (pore size: 0.2 μm, mdi) prior to measurement. The transmittance was recorded after stabilization for 5 min at each temperature. The cloud point (CP) was determined at the temperatures where the transmittance is 50%

by interpolation between each point. In general, each solution was heated up to 60 ºC then cooled down (to ~5 ºC) with regular intervals.

Dynamic light scattering (DLS) and static light scattering (SLS) were performed to measure hydrodynamic radius and radius of gyration of the polymer objects in aqueous soluton. The sample solutions were loaded in a goniometer (BI-200SM, Brookhaven Instruments, New York, USA) filled with decahydronaphtalene (decaline) used as index matching fluid. A 15 mW He-Ne laser (wavelength λ = 632.8 nm) illuminated the polymer solutions and the scattered light at 60º, 75º, 90º, and 105º was detected by a BI-DS2 photomultiplier tube. The measurement temperature was controlled by a water circulator connected to the goniometer. The scattering intensity of toluene was used to obtain the calibration ratio. The field autocorrelation functions were obtained by a correlator (TurboCorr, Brookhaven Instruments) and analysed by CONTIN regularization. The analysis results were crosschecked by cumulant (for unimodal ACFs) or double exponential fits (for multimodal ACFs), and both were similar. Multimodal decay rates were divided by more than two averaged values, represented as "fast" and "slow" diffusive modes that depend on the estimated diffusion coefficient. The refractive index of polymer solutions was measured by DRM-3000 (Otsuka, Japan). Details of DLS study are following the description in **Chapter 2.**

In the SLS study, the scattered intensities were collected over an angular range between 40º and 150º at 10º intervals at several concentrations (2–10 mg/mL). Zimm equation (Eq. 3.5) was used to determine the radius of gyration, R_g and the weight average molecular weight, M_w in the limit of concentration and angle→0:

$$\frac{Kc}{\Delta R_\theta} = \frac{1}{M_w}\left[1 + \frac{q^2}{3}R_g^2\right] + 2A_c c \tag{3.1}$$

where ΔR_θ is the excess Rayleigh ratio of the solute which is calibrated scattered intensity, c is the concentration of the solute, A_2 is the second virial coefficient. K is the optical constant written as:

$$K = \frac{4\pi^2 {n_0}^2 \left(\frac{dn}{dc}\right)^2}{N_0 \lambda^4} \tag{3.2}$$

n_0 is the refractive index of water, dn/dc is the specific refractive index increment of the solution which was measured with known concentrations of PGLBT-*b*-PSPE solutions, λ is the wavelength of the laser (632.8 nm), and N_0 is Avogadro's number, 6.022 x 10^{23} mol^{-1}. R_g at individual concentration was determined by partial Zimm equation written as:

$$\frac{1}{I_{ex}(q)} = C\left(1 + \frac{q^2}{3}R_g^2\right) \tag{3.3}$$

where C is the arbitrary constant, and $I_{ex}(q)$ is the intensity of scattered light. R_g was calculated from the slope of the inverse scattering intensity ($1/I_{ex}$) versus q^2.

Electrophoretic light scattering was performed to obtain zeta potential with ELSZ-2000 (Otsuka, Japan) using the Smoluchowski approximation.

Results and Discussions

PGLBT-*b*-PSPE in NaCl solutions

The double polybetaine block copolymer PGLBT-*b*-PSPE was prepared through the previously reported procedure,[45] and two block copolymers having different chain lengths and block ratios were selected for this study. The specification of **#1** and **#2** are described in **Table 3.1**. The temperature-responsive behaviour of the double zwitterionic block copolymer chains in pure water was elucidated as represented by the black lines and symbols in **Figure 3.1(a)–(d)**. According to the result, the polymer chains existed as unimers (R_h < 10 nm) at high temperatures (~60 ºC) while the solution showed high transparency. Upon decreasing temperature, the transmittance gradually reduced then monodisperse polymer micelles (R_h = 40–50 nm) emerged where the transmittance was typically under 50 %. The boarder of unimer-to-micelle transition depended on the molecular weight and the ratio of PGLBT:PSPE. On the interval of the transition, over hundreds of nanometer-sized large aggregates coexisted with unimers simultaneously while the transmittance drop temporarily stopped or slightly increased at the middle temperature range (35–45 ºC for **#1** and 40–50 ºC for **#2**, the slow modes (larger objects) were plotted separately in **Figure 3.9)**.

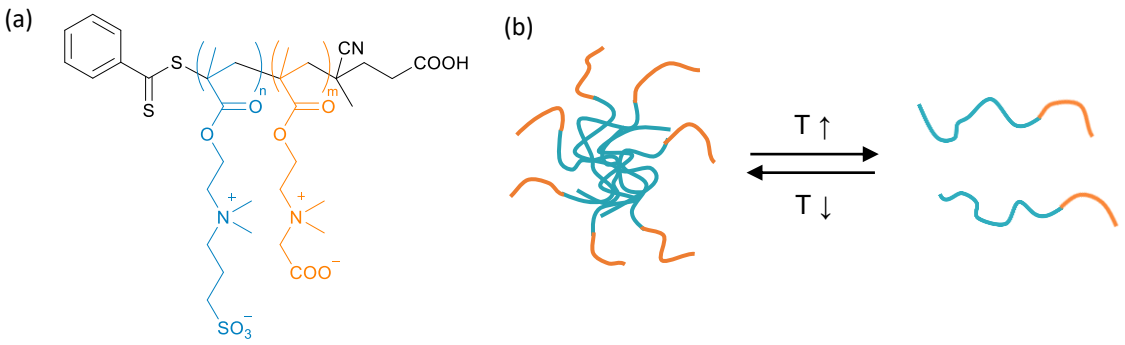

Scheme 3.1. (a) The chemical structure of PGLBT-*b*-PSPE (b) Representation of temperature-responsive self-assembly of PGLBT-*b*-PSPE (orange: PGLBT, blue: PSPE)

Table 3.1. Information of double polybetaine block copolymer PGLBT-*b*-PSPE used in the study (the DPs were determined by SEC results)

ID	M_n^{SEC} (g/mol)	DP^{SEC} (GLBT:SPE)	$Đ$ (M_w/M_n)	$^*M_n^{NMR}$ (g/mol)	$^*DP^{NMR}$ (GLBT:SPE)	Cloud Point (℃)
#1	64600	86:164	1.13	143400	86:446	27.6
#2	82300	131:193	1.14	240000	131:758	51.2

* The determined values are based on the ^{1}H NMR spectra taken at 60 ºC

Since electrostatic attractions between the cationic and anionic part of PSPE segments are the main driving force of the polymeric particle formation, this temperature-responsive behaviour of the block copolymer would be influenced by introduced salt ions which could diminish the inter-chain/intra-chain dipole-dipole attractions. To investigate the salt effect, PGLBT-*b*-PSPEs were dissolved in several concentrations of $NaCl_{(aq)}$ (up to 20 mM), and the transmittance and R_h were monitored along 10–60 ºC. **Figure 3.1(a)–(d)** show the influence of NaCl in the transmittance shift and size variations upon several salt concentration. For **#1**, the CP decreased from 27.6 ºC (salt-free water) to below 12 ºC (20 mM), and polymer micelles (R_h = 41 nm, no salt) which originally appeared from 30 ºC were observed under 20 ºC in 5 mM and 15 ºC in 20 mM. For **#2**, which had more PSPE units, the CP substantially decreased from 51.2 ºC (no salt) to 27.6 ºC (20 mM). The polymer in micellar form (R_h = 55 nm, no salt) that originally generated under 40 ºC started to emerge below 30 ºC in 5 mM and 16 ºC in 20 mM $NaCl_{(aq)}$. **Figure 3.1(e)** taken at room temperature directly shows the relationship of salt concentration; more added salt made the solution more transparent and effectively hindered nanoparticle formation. Besides, some **#1** solutions of low NaCl concentrations (less than 10 mM) showed an earlier transmittance drop and increased CPs compared to the salt-free sample. This behaviour could be related to the emergence of slow modes (R_h of slow modes of **#1** is plotted on **Figure 3.9(a)**) at higher temperatures. Typically, the slow diffusive modes appeared clearly just prior to micelle formation in salt-free solutions. However, the slow modes persistently appeared to some extent at higher

temperatures in low concentrations (up to 5 mM) of NaCl solutions whereas these intermediates were not observed at more than 20 mM.

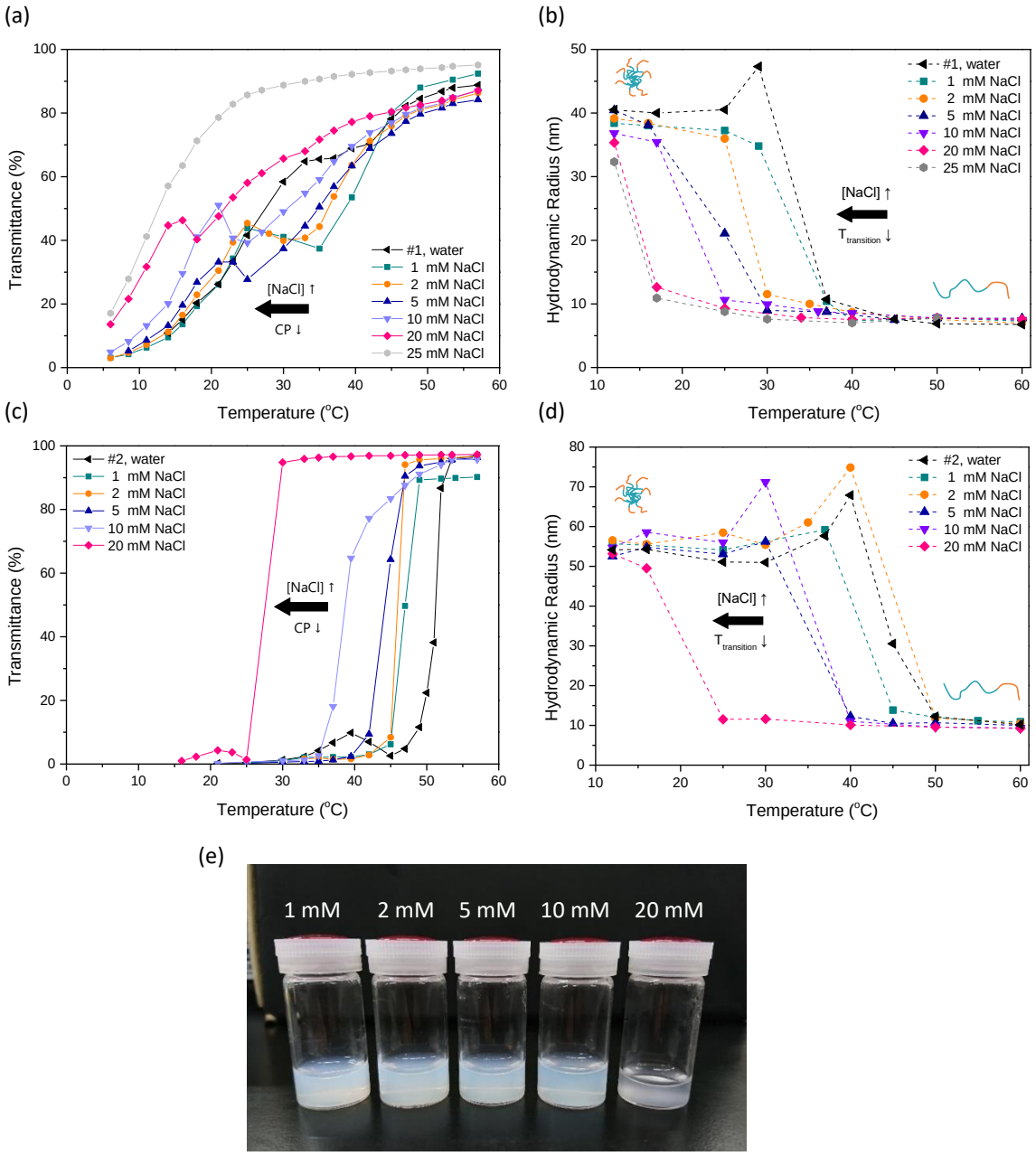

Figure 3.1. (a) Transmittance variations and (b) R_h variations of **#1** aqueous solutions. (c) Transmittance variations and (d) R_h variations of **#2**. (Slow diffusive modes in DLS results were omitted in these plots and separately reported in **Figure 3.9**) (e) Photos of **#2** in several concentrations of $NaCl_{(aq)}$ taken at 25 °C

The R_h distributions at specific temperatures where the turbidity of the solution was highly transparent, around 50%, and low are shown in **Figure 3.2**. In 5 mM $NaCl_{(aq)}$, **#1** showed a single fast or slow decay autocorrelation function (ACF) at the highest or lowest temperature, and two bimodal ACFs at 30 and 25 °C, respectively (**Figure 3.2(a)).** Analysis of this sample (**Figure 3.2(b)**) showed that monodisperse unimers (R_h = 7.7 nm) and micelles

(R_h = 40 nm) at the both ends of temperature, and double diffusive modes in the middle range. Note that the fast diffusive mode (R_h = 9 nm) and the slow mode (R_h = 226 nm) at 30 ºC deviated to R_h = 21 nm/430 nm at 25 ºC while the distribution of the fast mode broadened to over hundreds, which implies a mixed state of unimers, micelles, and aggregates. (The autocorrelation functions and the analysis results of each angle are displayed in **Figure 3.10**) For **#2** in the same NaCl concentration, the ACFs were similarly shown as a single fast/slow mode at the both ends, and slow-fast double diffusive modes at 40 ºC (**Figure 3.2(c)**). The size analysis result (**Figure 3.2(d)**) shows that the unimer-only (R_h = 10 nm) state at 60 ºC altered to the bicomponent state whose R_h = 12.3 nm and 991 nm at 40 ºC, and rapidly turned into the micelle state (R_h = 55 nm) below 30 ºC, respectively. No ACFs having continuous decay were found under the given condition, but the extra salt incorporation changed the state analyzed as triple diffusive modes (**Figure 3.11**), which is similar to the mixed state of **#1** at 25 ºC presumably due to the larger portion of PSPE than the case of **#1**. **Figure 3.2(e)(f)** display alterations of the R_h distribution on increasing NaCl at fixed temperatures. As the change from 2 mM to 5 mM of **#1** and from salt-free sample to 2 mM of **#2**, the polymer micelles started to deform and yield aggregates, and split to unimers and aggregates followed by sole unimers in 20 mM. At the highest concentration, no slow modes emerged.

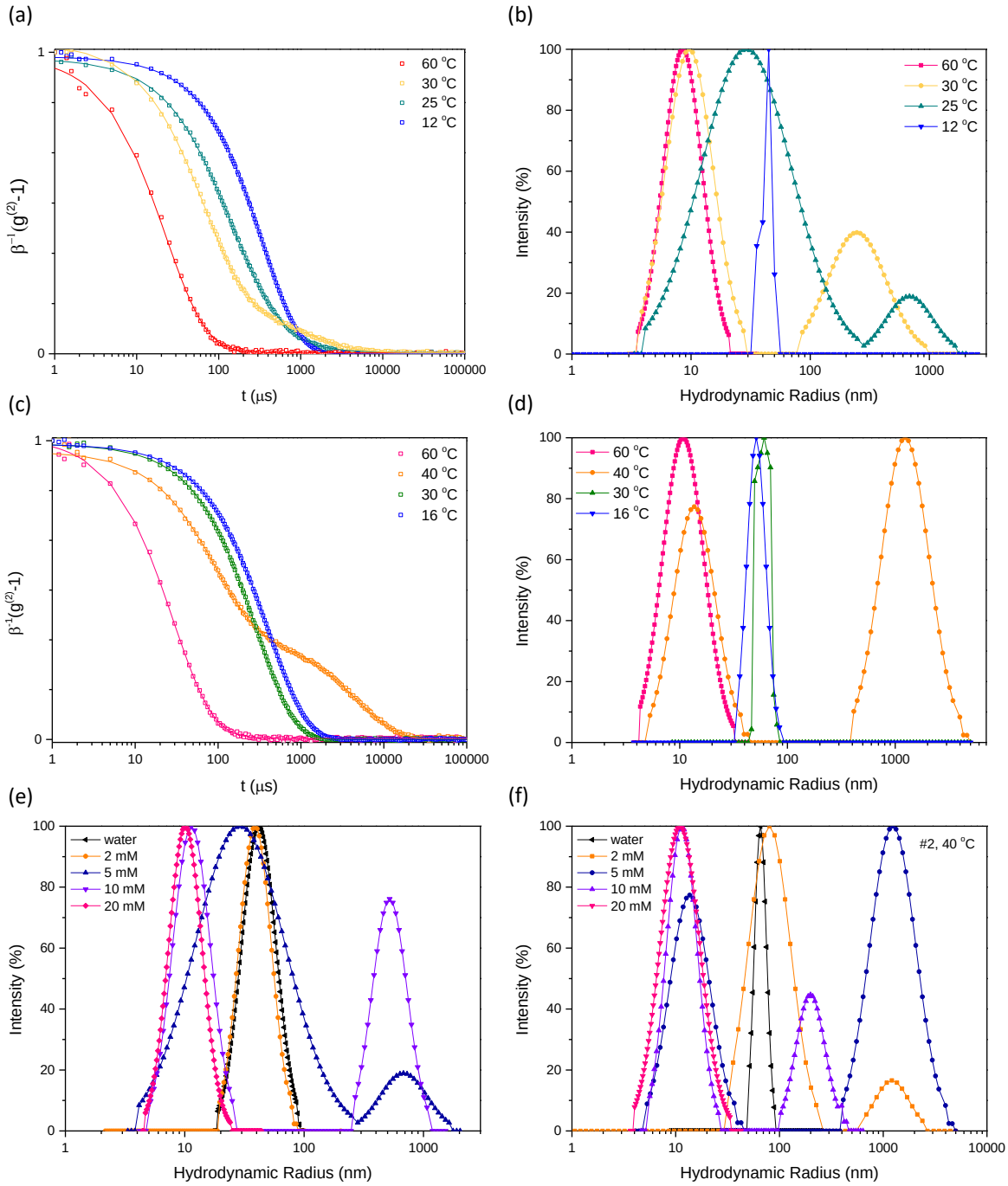

Figure 3.2. (a) ACFs of 5 mM $NaCl_{(aq)}$ **#1** measured at 4 different temperatures (b) Size distributions of 5 mM $NaCl_{(aq)}$ of **#1** (scattering angle = 90°, CONTIN analysis) (c) ACFs of **#2** in 5 mM $NaCl_{(aq)}$ measured at 4 different temperatures (d) Size distributions of 5 mM $NaCl_{(aq)}$ of **#2** (e) Size distributions of **#1** with varying [NaCl] at 25 °C (f) Size distributions of **#2** with varying [NaCl] at 40 °C (scattering angle = 90°, CONTIN analysis)

As listed in **Table 3.2**, the micellar form of **#1** and **#2** showed slight reduction of R_h with increasing salt concentration. Under Na^+ and Cl^- ions, polymer micelles less than 5 nm were generated, while the R_h of the unimers was kept constant. Shrinkage of PGLBT coronas on the PSPE core induced by screened electrostatic forces between chains might be the reason. However, this contradicts with our previous results obtained on

hydrophobic-core micelles (poly(butyl acrylate)-*b*-PGLBT)[24] or brushes formed under the water/air interface (poly(ethylhexyl acrylate)-*b*-PGLBT),[23] which showed chain expansion by added salt known as "anti-polyelectrolyte" effect. Also, no significant chain shrinkage/expansion was found on a homopolymer PGLBT at the same NaCl concentrations. (**Figure 3.13**) Instead, aggregation number reduction by inhibition of electrostatic attraction may contribute to the R_h change. SLS was performed to calculate the aggregation number of micelles, but was not able to determine correctly because the radius of gyration (R_g) varied with the polymer concentration. On a Zimm plot of **#2** in 20 mM $NaCl_{(aq)}$ constructed at 12 ºC (**Figure 3.12**), the R_g increased from 32 nm (conc.: 10 mg/mL) to 50 nm (conc.: 4 mg/mL) while the R_h slightly increased from 53 nm to 59 nm, eventually the $R_{g\ conc.\rightarrow 0}$ was estimated to be 77 nm. Hence, compositions of polymers and salt ions in the solution may attribute to the energetically favoured state of micellar form of PGLBT-*b*-PSPE. Since the hydrophobicity of PSPE blocks is variable, the size reduction of the block copolymer micelles in salt solutions is not appropriate to be understood as the case of ionic[47] and zwitterionic[48] surfactants. In those cases, the size of the micelles increased while the critical micelle concentration was lowered by salt addition because of shielded repulsive interactions among hydrophilic head groups.

Table 3.2. Hydrodynamic radii of unimers and micelles of PGLBT-*b*-PSPEs at a high (60 ºC) and low (12 ºC) temperature in $NaCl_{(aq)}$

#1	Unimers (nm)	Micelles (nm)	#2	Unimers (nm)	Micelles (nm)
Water	7.5	41	Water	10.2	54.1
1 mM NaCl	7.4	38.4	1 mM NaCl	10.9	55.7
2 mM NaCl	8.1	39.2	2 mM NaCl	10.5	56.5
5 mM NaCl	7.7	40.4	5 mM NaCl	10.0	52.5
10 mM NaCl	7.5	36.8	10 mM NaCl	9.4	54.7
20 mM NaCl	7.6	35.3	20 mM NaCl	9.2	53.2

PGLBT-*b*-PSPE in NaBr solutions

To compare the specific ion effect of halide anions upon hydration and the interaction among the polyzwitterion chains, NaBr aqueous solutions were subsequently studied. In the same composition except for replacing chloride with bromide, the polymer chains more tended to remain in the unimer state than the self-assembled state in the same temperature region. As displayed in **Figure 3.3(a)–(e)**, the acquired transmittances and size variations showed that the trend of temperature responsivity was similar to the results of NaCl solutions. Each transition temperature from unimer to intermediate and micelle phase was always lower than those of NaCl solutions having

same concentrations: the transmittance and R_h variations of **#1** in 5 mM $NaBr_{(aq)}$ was similar to that in 20 mM $NaCl_{(aq)}$. Similarly, the behaviour of **#2** in 5 mM $NaBr_{(aq)}$ which showed a sharp change of transmittance and size variation within 30–40 °C was close to that in 10 mM $NaCl_{(aq)}$. **Figure 3.3(e)** apparently shows that smaller amounts of NaBr effectively made the solution clearer compared to the solutions of $NaCl_{(aq)}$. According to the general explanation of Hofmeister series, Br^- is more chaotropic than Cl^-, and they are supposed to exist near polymer chains rather between water molecules.[25, 26, 49] Hence, the attraction among PSPE segments would be further intervened by more closely contacting bromides to the quaternary ammonium groups. It could be assumed that a reduction of the enthalpy of mixing or an increase of the entropy of mixing than when Cl^- is incorporated. Therefore, the unimer state of PGLBT-*b*-PSPE is maintained even at lower temperatures.

In addition, Br^- lowered the R_h of PGLBT-*b*-PSPE micelles more than in $NaCl_{(aq)}$ and salt-free water. As listed in **Table 3.3**, The R_h of **#1** in micellar form (at 12 °C) was reduced to ~33 nm in the 1 mM and 2 mM solutions, which was even smaller than the case of 20 mM $NaCl_{(aq)}$. The R_h of 5 mM solution is thought to an expanded size before reaching equilibrium at lower temperatures as the R_h of salt-free water at 30 °C. The R_h of **#2** also decreased (54 nm to 46 nm) more than in $NaCl_{(aq)}$. Note that no self-assembled objects of **#1** were found in 10 mM $NaBr_{(aq)}$, and this suggests that the smaller amount of Br^- was sufficient to hinder zwitterionic associations effectively and provided a strong hydration force not causing phase separation.

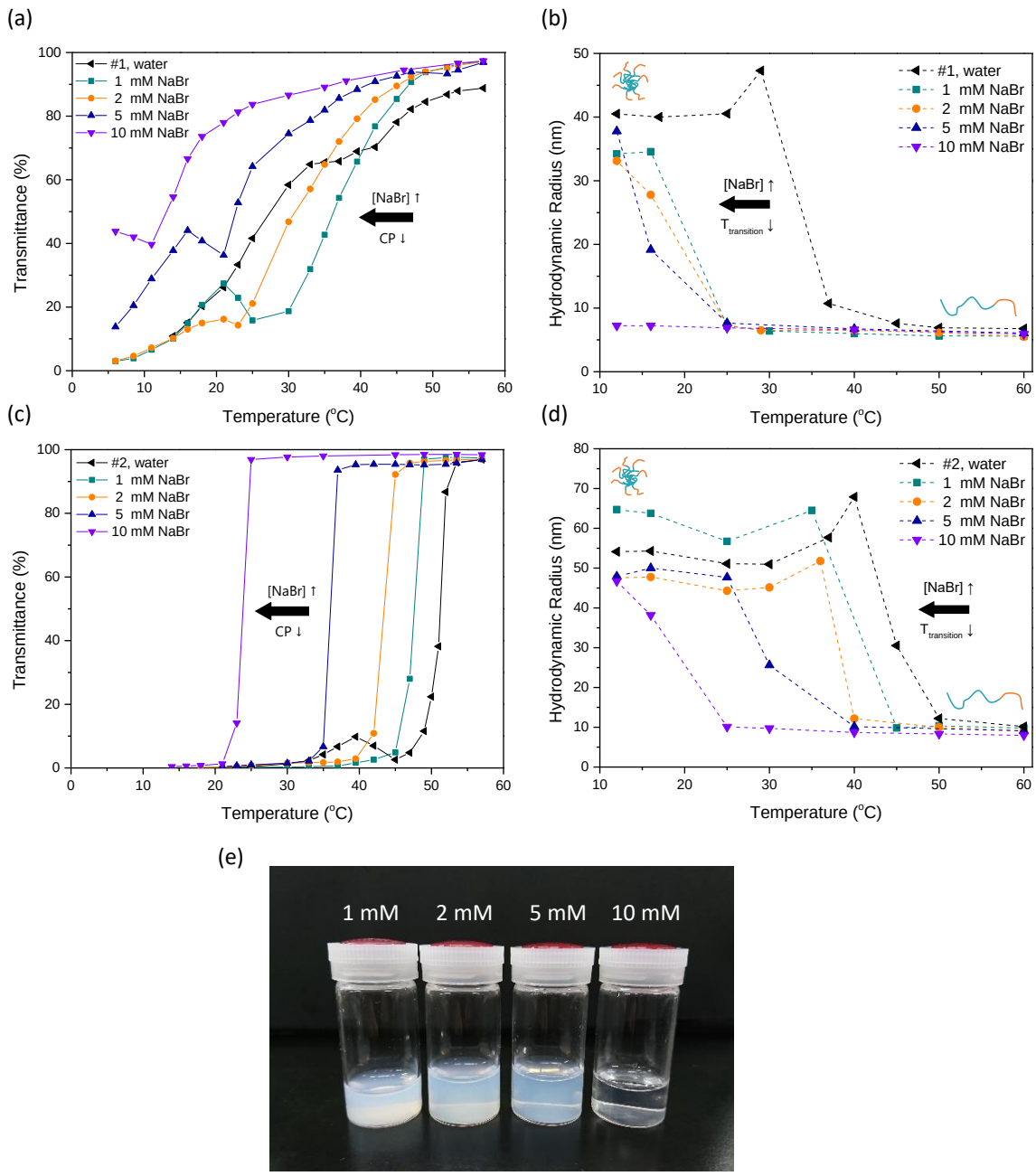

Figure 3.3. (a) Transmittance variations and (b) R_h variations of **#1** in $NaBr_{(aq)}$. (c) Transmittance variations (d) R_h variations of **#2** in $NaBr_{(aq)}$. (slow diffusive modes are shown in **Figure 3.9**) (e) Photos of **#2** in several concentrations of $NaBr_{(aq)}$ taken at 25 °C

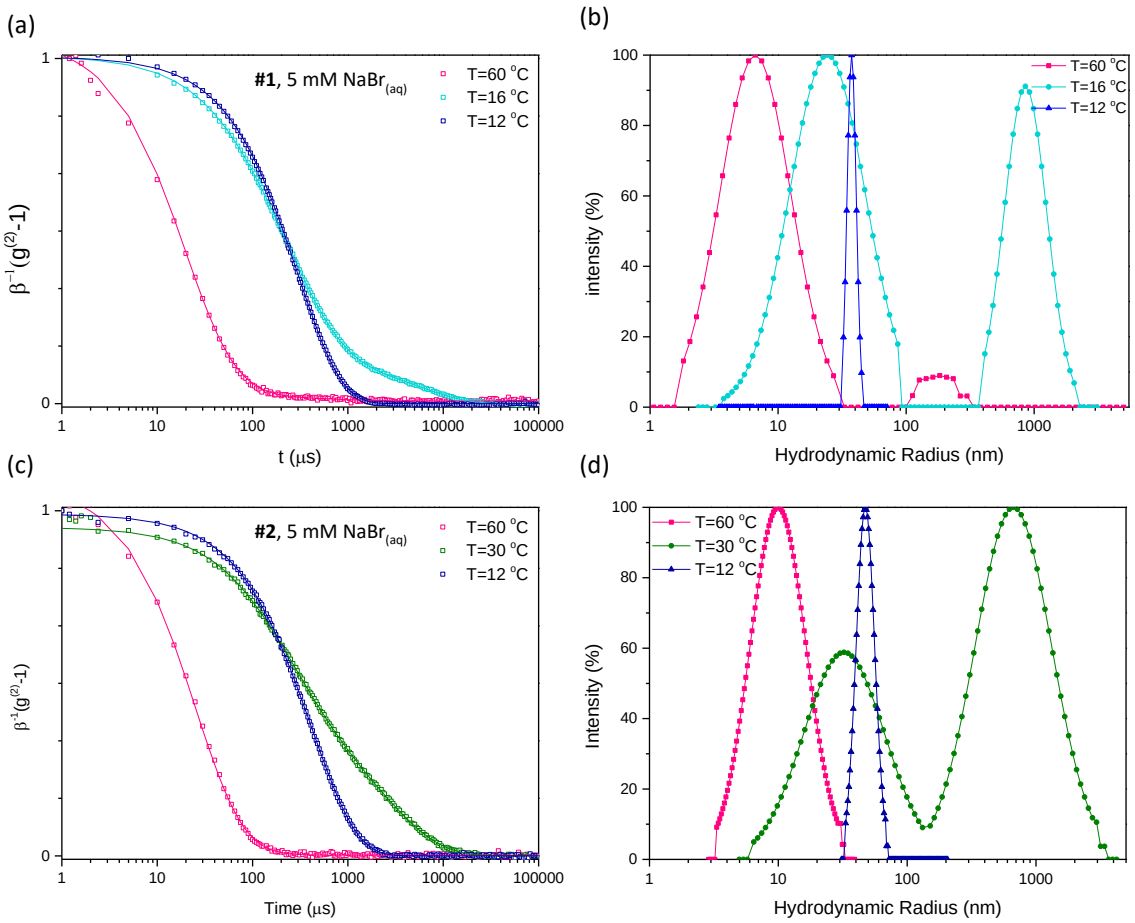

Figure 3.4. (a) ACFs of **#1** in 5 mM $NaBr_{(aq)}$ measured at 3 different temperatures (b) Size distributions of **#1** in 5 mM $NaBr_{(aq)}$ (scattering angle = 90°, CONTIN analysis) (c) ACFs of **#2** in 5 mM $NaBr_{(aq)}$ measured at 3 different temperatures (d) Size distributions of **#2** in 5 mM $NaBr_{(aq)}$ (scattering angle = 90°, CONTIN analysis)

Table 3.3. Hydrodynamic radii of unimers and micelles of PGLBT-*b*-PSPEs at high (60 °C) and low (12 °C) temperature in NaBr solutions in $NaBr_{(aq)}$

#1	Unimers (nm)	Micelles (nm)	#2	Unimers (nm)	Micelles (nm)
Water	7.5	41	Water	10.2	54.1
1 mM NaBr	5.6	34.1	1 mM NaBr	9.8	64.7
2 mM NaBr	5.3	33.1	2 mM NaBr	9.0	47.6
5 mM NaBr	5.4	37.8	5 mM NaBr	9.1	47.9
10 mM NaBr	5.9	-	10 mM NaBr	9.4	46.7

The deviation of polymer objects in $NaBr_{(aq)}$ under varying temperatures appeared similar to that discovered in $NaCl_{(aq)}$. For **#1** in 5 mM $NaBr_{(aq)}$, unimers (R_h = 5.4 nm) dominantly existed at 60 °C in a transparent solution state, then they turned into a broadly distributing fast (R_h = 19 nm) and a slow mode (R_h = 807 nm) at 16 °C where the transmittance change showed reverse-way shift. Further cooling changed the multicomponent intermediate

state to a monodisperse diffusive mode. (**Figure 3.4(a)** and **(b)**) Likewise, **#2** in 5 mM $NaBr_{(aq)}$ existed as unimers (R_h = 9 nm) at 60 °C, a polydisperse state (R_h = 26 nm, 565 nm) at 30 °C then transformed to monodisperse micelles below 25 °C (R_h = 48 nm). (**Figure 3.4(c)** and **(d)**) These results and those obtained in $NaCl_{(aq)}$ imply that the turning points of the transition are under the influence of salt species having different hydration behaviour and degree of interfering zwitterionic attractions. Except the critical temperature, The overall trend of thermoresponsive solution behaviour in $NaBr_{(aq)}$ was similar to that in $NaCl_{(aq)}$ and salt-free water.

PGLBT-*b*-PSPE in NaI and NaF solutions

To get more clues of the specific ion effect, we further investigated the solution behaviour against I^- and F^-. Iodide is considered to be more chaotropic than Br^-, and fluoride is more kosmotropic ion than Cl^-, which prefers to exist in water molecule structure consisting hydrogen bonds in contrast to chaotropes. The transmittance variation of **#1** in $NaI_{(aq)}$ (**Figure 3.5(a)**) showed that the phase transition was obviously suppressed by iodide than chloride and even bromide. The size variation data (**Figure 3.5(b)**) shows that 2 mM of NaI strongly hindered the micelle formation, which was comparable to 5 mM of NaBr or 20 mM of NaCl. The R_h at 12 °C was determined as a size-increased fast mode (R_h = 8 nm) and a slow mode (R_h = 777 nm) (sizes of slow modes are plotted in **Figure 3.9(c)**), respectively. Above 5 mM, the polymer chains were in a fully solvated state and showed no distinctive transmittance and R_h variation.

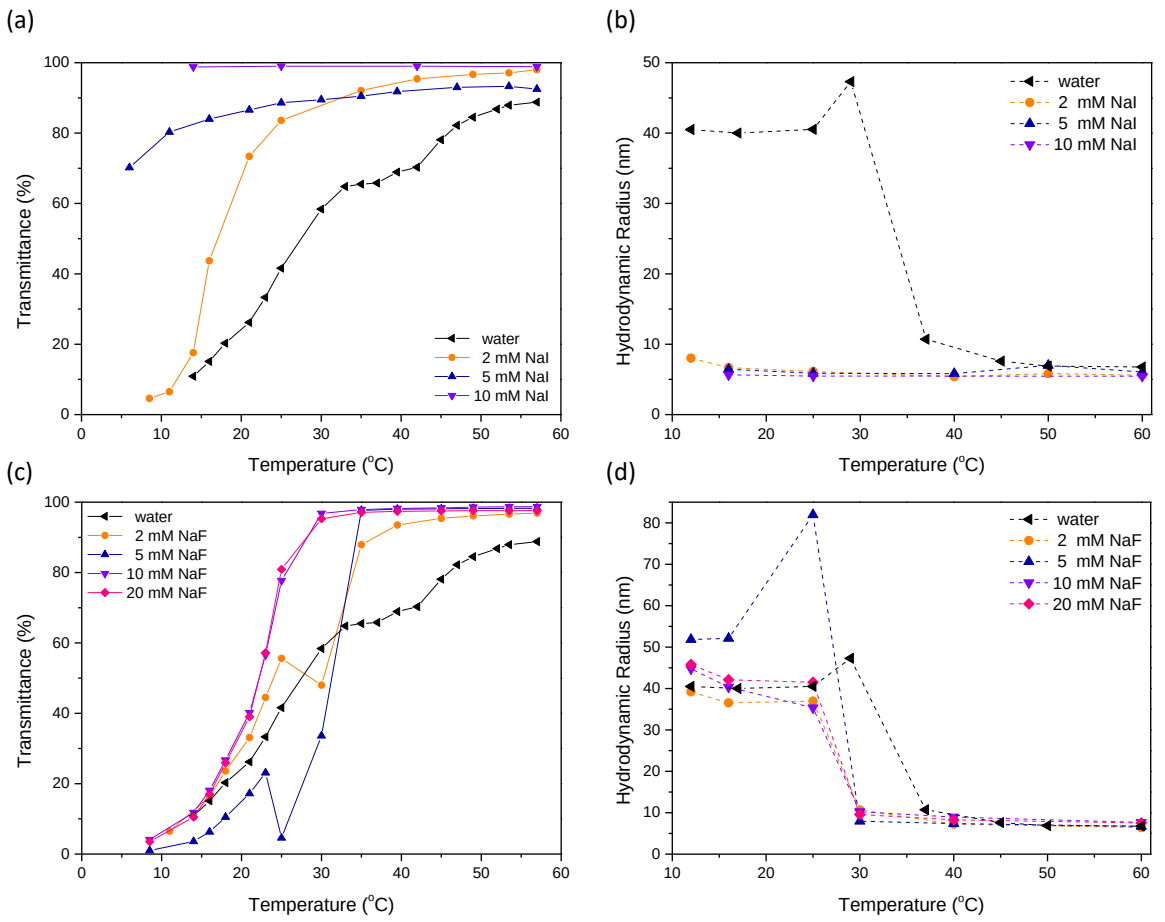

Figure 3.5. (a) Transmittance variations of **#1** in $NaI_{(aq)}$ (b) R_h of **#1** in $NaI_{(aq)}$ at each temperature (c) Transmittance variations of **#1** in $NaF_{(aq)}$ (d) R_h of **#1** in $NaF_{(aq)}$ at each temperature

On the other hand, the effect of a kosmotrope NaF on the temperature-responsive behaviour was opposed to the other anions. As shown in **Figure 3.5(c)**, the transmittance varied more quickly from a transparent to a translucent state within less than ten degree celsius, in contrast to other chaotropes that caused gradual changes. An abrupt decrease from 100 % to below 50 % and subsequent increase appeared on 2 mM and 5 mM solution. The other samples whose concentration was over 10 mM just showed straightforward transmittance alteration. Furthermore, the variation of hydrodynamic radius at each concentration (**Figure 3.5(d)**) showed more subtle differences compared to equivalent NaCl solution. It is notable that unlike other salt solutions, no significant slow diffusive modes emerged when the solution was maintaining a transparent state, but only appeared just prior to the transition. For example, **#1** in 2 mM $NaF_{(aq)}$ existed as only unimers up to 40 °C when the solution was highly transparent, then showed a slow diffusive mode (R_h = 185 nm) at 30 °C on the section of decreasing transmittance.

Additional comparisons of the solution behaviour depending on halides

As covered in the previous section, the temperature-responsive unimer-to-micelle transition of PGLBT-*b*-PSPE in aqueous solutions was significantly influenced by the anion species and this depended on whether the anion is more chaotropic or kosmotropic. The more chaotropic the ion was, the harder was the transition of the block copolymer. This salt-dependent tendency corresponded to several studies of homo-polysulfobetaines[40, 41] as well as thermoresponsive non-ionic polymers[25, 26] showing CP changes with increasing salt concentration. For a PGLBT-*b*-PSPE, **#1**, the degree of CP deviation was in the order of $Cl^- < Br^- < I^-$ amongst chaotropes while a kosmotropic F^- made subtle increase until 5 mM then decreased (**Figure 3.6(a)**). These CP changes with the concentration of halides shared some aspects of salt-dependent behaviour of homo-polysulfobetaines. As the increase of CP of the block copolymers at very low concentrations (1–2 mM) observed in NaCl and NaBr solutions, a similar reverse-way trend of critical temperature (T_c) in salt solutions was reported in PSPE homopolymer studies by Mary et al., which but only appeared starkly on PSPEs of a quite high degree of polymerisation (over 1611).[40] In the article, the critical temperature of PSPE solutions dropped by increasing salt concentration as predicted at sufficiently high salt concentrations (more than 10 mM), while reversely increasing T_c at very low concentrations (less than 2 mM) was observed and the crossover concentration depended on the molecular weight. In addition, NaCl was more prone to increase T_c than other ions NaBr and NaI that promoted the solubility stronger than NaCl without T_c increase. They argued that charge asymmetry which originated from the partial hydrolysis of PSPE repeating unit and selective ion adsorption might result the peculiarity. Meanwhile in our experiment, PGLBT-*b*-PSPEs were synthesised under a lowered temperature (45 ºC) to prevent possible hydrolysis of RAFT agent as well as the ester bond of betaine repeating units, and there was no clear evidence of degradation confirmed through the ^{1}H NMR and zeta potential measurement. The measured zeta potential closed to zero by heating which promotes complete solvation of chains. (**Figure 3.7(a)**)

Besides, the CP increase in $NaCl_{(aq)}$ did not appear from the solutions of **#2,** a higher molecular weight polybetaine having a longer PSPE motif and a higher portion. This difference suggests that both the DP and the block ratio should be taken into account together for evaluating the salt responses. In addition, it should be noted that the CP of PGLBT-*b*-PSPE solutions was not directly equivalent to unimer-to-micelle transition temperature, only to indicate the point where the dipole-dipole attraction among chains becomes dominant. Around the CP, PSPE moieties were just getting close and creating large aggregates which made the solution more turbid, and the unimer-to-micelle transition occurred at much lower temperatures.

The R_h variations of unimers and micelles against salt concentration as shown in **Figure 3.6(b),(c)** show that the size was affected least by NaCl followed by NaF, NaBr and NaI in increasing order. The sizes of polymer micelles slightly reduced with increasing amount of chaotropes while NaF kept their original size or even increased to more than 5 nm. As previously discussed, the R_h shift may be attributed to a change in the aggregation number due to altered thermodynamic equilibrium states rather than stretching of PGLBT segments on PSPE cores. Since several reports[50, 51] and our DLS study on homo-polycarboxybetaine in $NaCl_{(aq)}$ and $NaF_{(aq)}$ (**Figure 3.13**) showed no remarkable size variation of polycarboxybetaine motifs within the salt concentration range, the size changes of the micelles might be the result of the enthalpy and entropy of mixing change driven by attenuated dipole-dipole attractions. The R_h variation of unimers were analogous to the trend of polysulfobetaine homopolymers in salt solutions at moderate concentrations,[41] which ions more chaotropic than Cl^- led to decrease of R_h before full swelling at much higher salt concentrations.

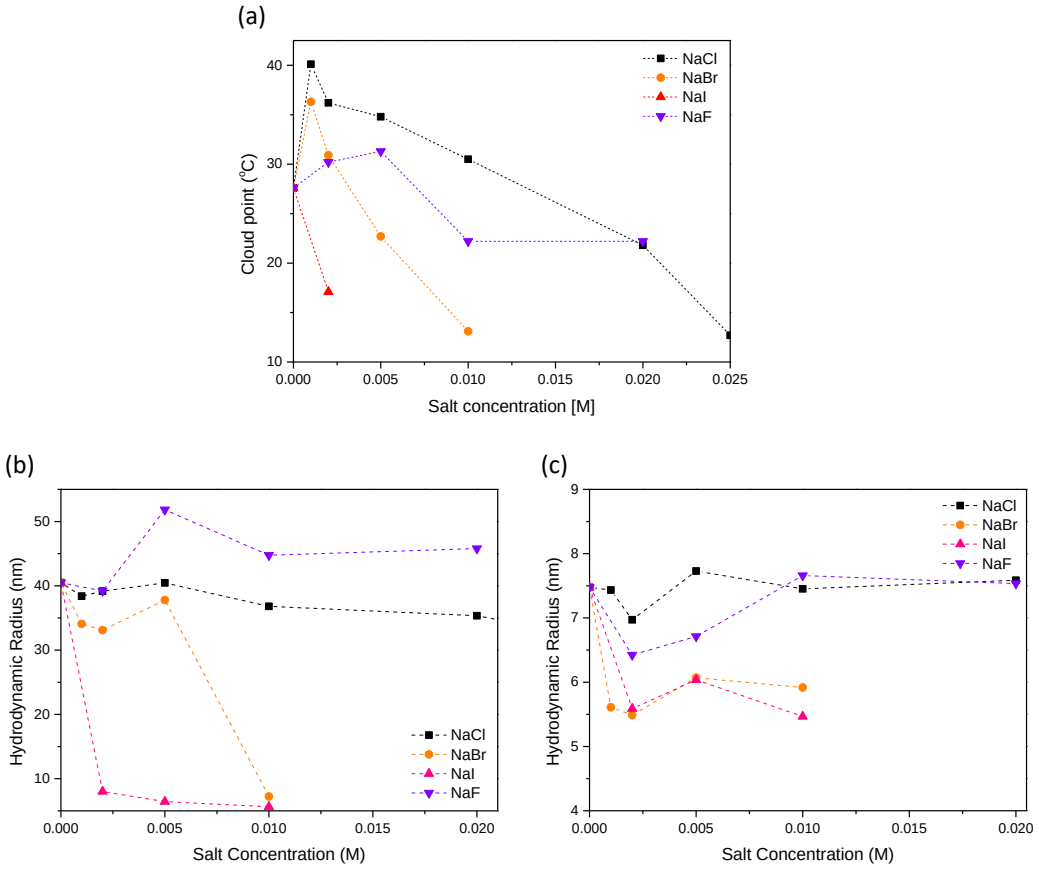

Figure 3.6. (a) Cloud point variations of **#1** by concentrations of salts (NaCl, NaBr, NaI, and NaF) (b) R_h variations of **#1** in the unimer state by salt concentrations (c) R_h variations of **#1** in the micelle state by salt concentrations

The zeta potentials at given conditions (**Figure 3.7(a)**) showed negative values (~ -10 mV) in the micelle regime, and an increase to near zero in the unimer region. This zeta potential variation is attributed to PSPE segments, whose homopolymer showed neutrality in a fully solvated state over the critical temperature and dropped under -10 mV in a collapsed state while PGLBT did not respond to temperature. (**Figure 3.14**) To compare the salt response of zeta potential in two different states (unimers and micelles) in water, the values were obtained at fixed temperatures of 25 ºC and 60 ºC, respectively. (**Figure 3.7(b)**). The zeta potential of **#2** unimers at 60 ºC was almost neutral and showed no response to the increase in NaCl ions, whereas the surface charge at 25 ºC (micelle state) diminished by ion addition that implies screening due to ion pairing. Note that the micelles had a negatively charged slipping plane in spite of zwitterionic PGLBT corona, which may be due to the negative charge of PSPE under the critical temperature. The charge of PSPE in a collapsed state seems contradictory, so it might be proposed that the water molecules are not perfectly segregated from PSPE globules and slightly hydrate the surface as discussed by Doncom et al.[52] The scarcely solvated state could be supported by some extent of visible PSPE signals in the ^{1}H NMR spectrum of PGLBT-*b*-PSPE micelles. (**Figure 3.15**)

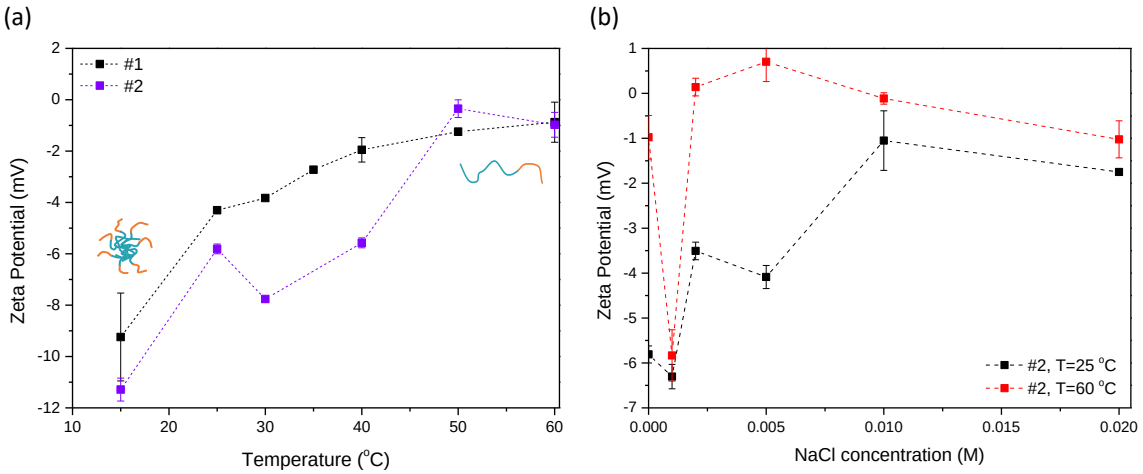

Figure 3.7. (a) Zeta potential variations of PGLBT-*b*-PSPEs against temperature (black: **#1**, violet: **#2**) (b) Zeta potential variations of **#2** against [NaCl] at 25 ºC (micelle state) and 60 ºC (unimer state)

To sum up the solution behaviours of PGLBT-*b*-PSPE in the sodium halide aqueous solutions, the original thermoresponsive self-assembly was disturbed by the halide ions, especially classified as chaotropes. In lower salt concentrations, the ionised sites of the polymer chains are partially shielded by few number of counterions as discussed on homo-polyzwitterions,[41, 43] and that may cause charge imbalance which triggers additional chain associations and higher CP. It is reflected to slow diffusive modes alongside fast-moving unimers and further decreased transmittances before the unimer-to-micelle transition. Above a certain extent of ions, counterions fully

dress the zwitterionic sites thus the micellisation cannot happen no longer. (**Scheme 3.2**) It is assumed that the population of halide ions on the vicinity of the polyzwitterion chains is up to whether the ion is more chaotropic or kosmotropic.

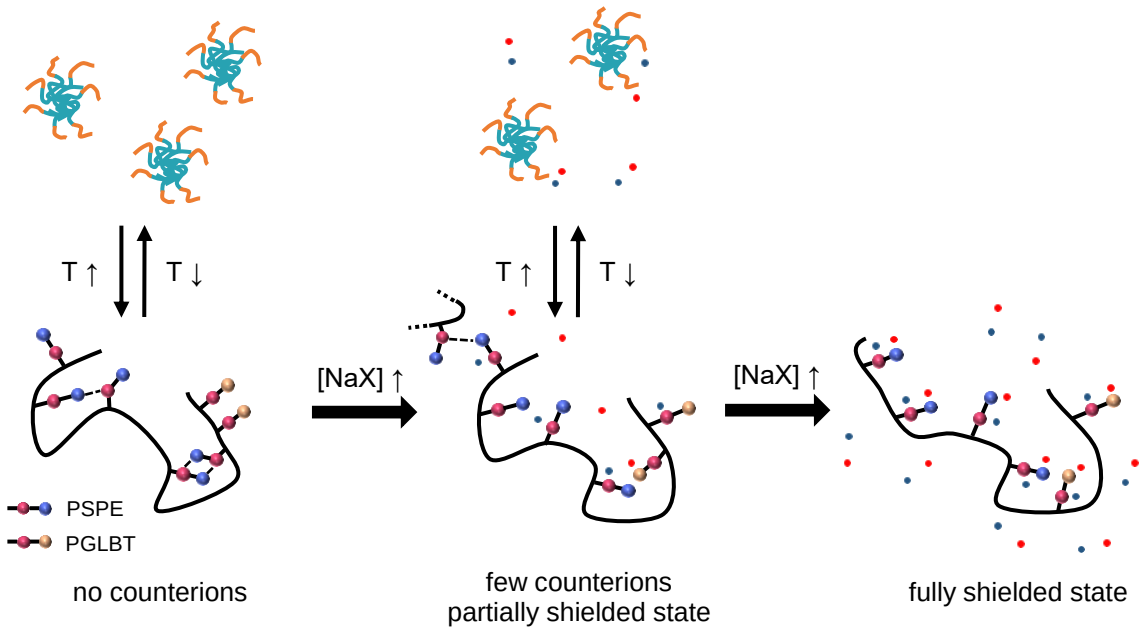

Scheme 3.2. A Proposed model of PGLBT-*b*-PSPE incorporated with salt ions in water. (dashed line: possible zwitterionic attraction, red dot: cations (Na^+), blue dot: halides (X^-: F^-, Cl^-, Br^-, and I^-)

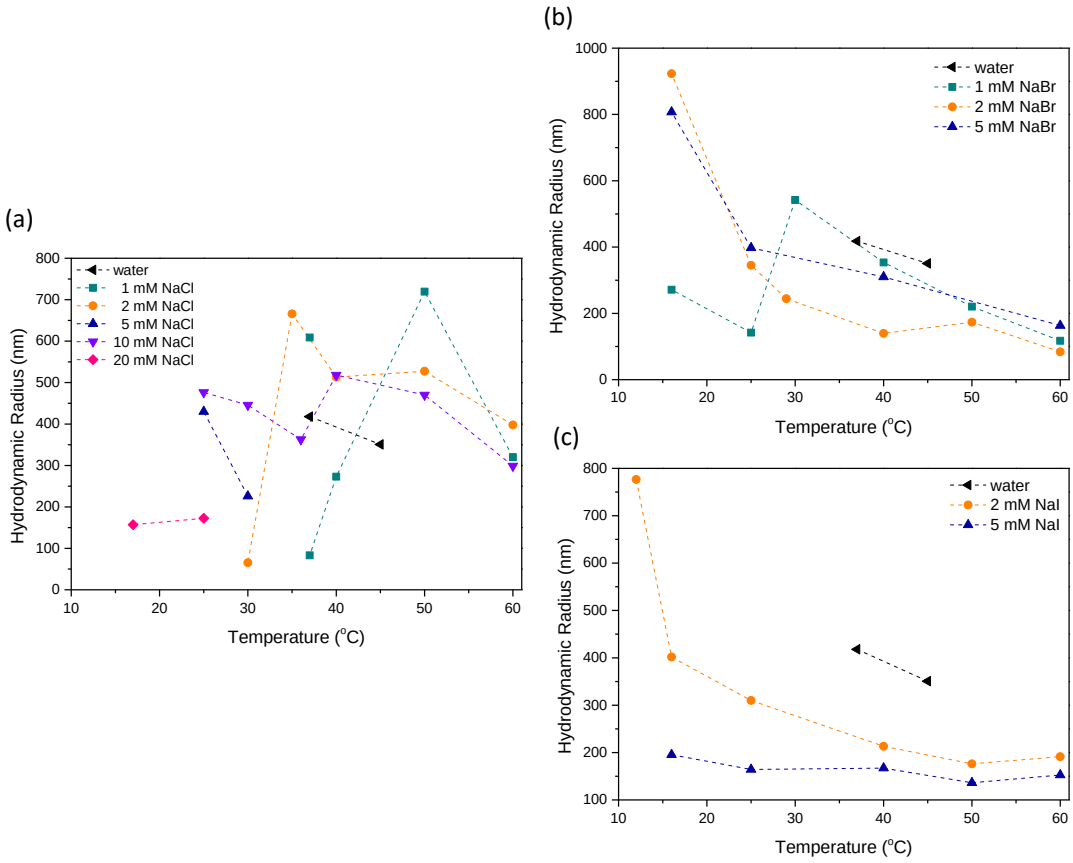

Figure 3.9. Hydrodynamic radii of slow modes of **#1** in (a) $NaCl_{(aq)}$ (b) $NaBr_{(aq)}$ (c) $NaI_{(aq)}$

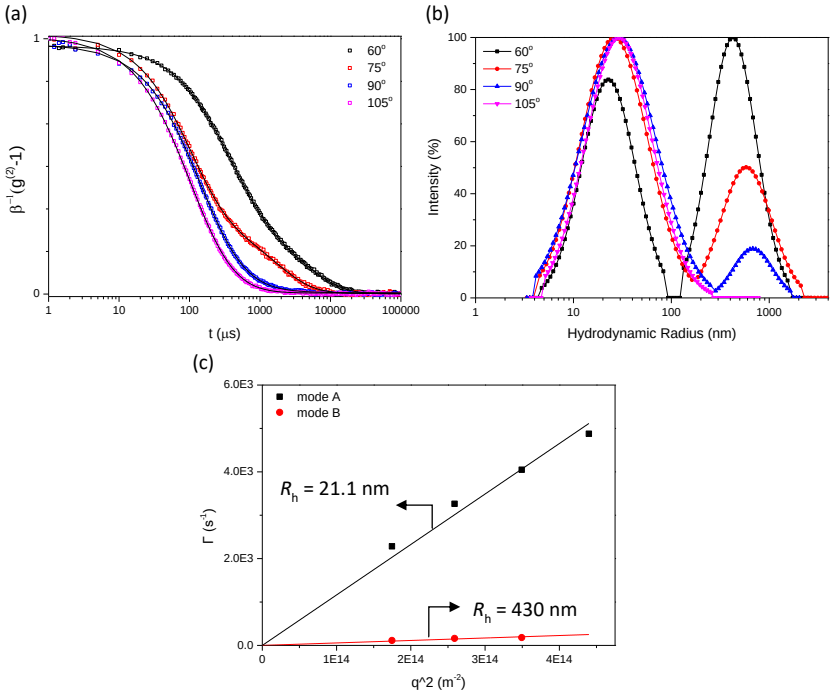

Figure 3.10. (a) DLS autocorrelation functions of **#1** in 5 mM $NaCl_{(aq)}$ at four different angles of 60º, 75º, 90º, and 105º at T = 25 ºC (b) Size distribution of hydrodynamic radii calculated by CONTIN (c) The decay rate Γ versus q^2 of two diffusive modes obtained at multiple scattering angles

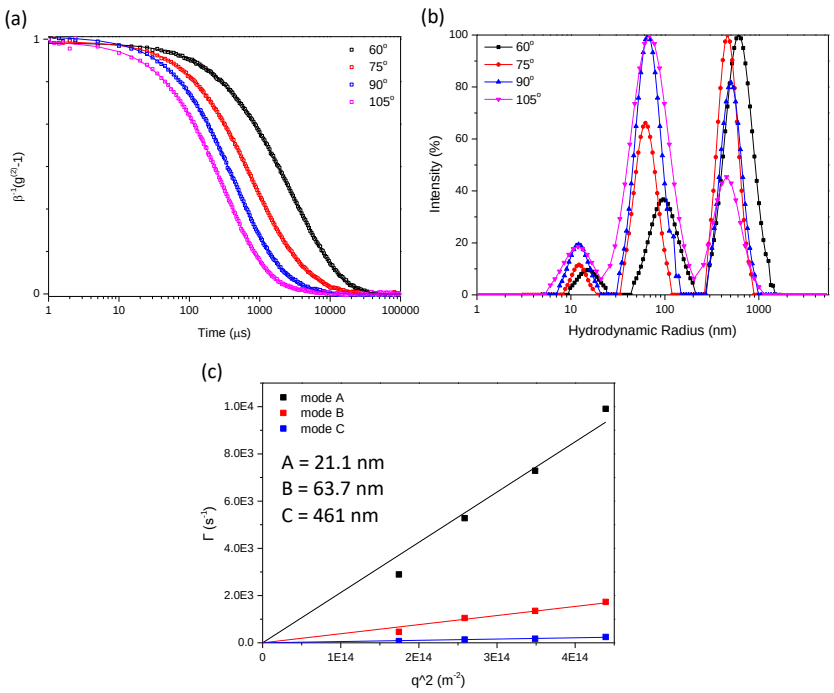

Figure 3.11. (a) DLS autocorrelation functions of **#2** in 20 mM $NaCl_{(aq)}$ at four different angles of 60°, 75°, 90°, and 105° at T = 25 °C (b) Size distribution of hydrodynamic radii calculated by CONTIN (c) The decay rate Γ versus q^2 of three diffusive modes obtained at multiple scattering angles

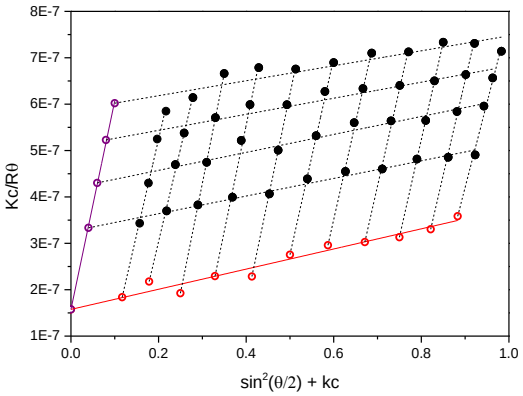

Figure 3.12. Zimm plot obtained by SLS of **#2** in 20 mM $NaCl_{(aq)}$ at 12 °C. $R_{g,c=0}$ = 77 nm, A_2 = 2.25*10^{-5} cm^3mol/g^2 (dn/dc of **#2** = 0.1445 mL/g). The R_g of respective concentrations are as follows: 10 mg/mL: 31.9 nm, 8 mg/mL: 35.9 nm, 6 mg/mL: 40.4 nm, 4 mg/mL: 49.5 nm

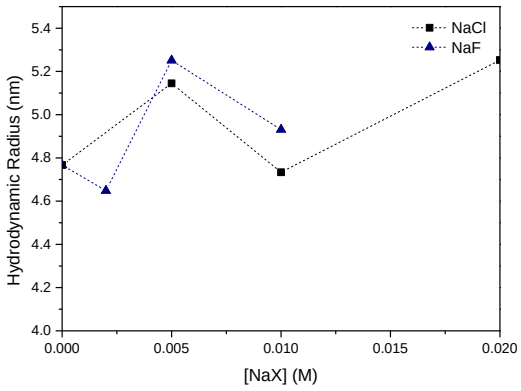

Figure 3.13. Hydrodynamic radii of homopolymer $GLBT_{182}$ in $NaCl_{(aq)}$ and $NaF_{(aq)}$ with several concentrations determined by DLS

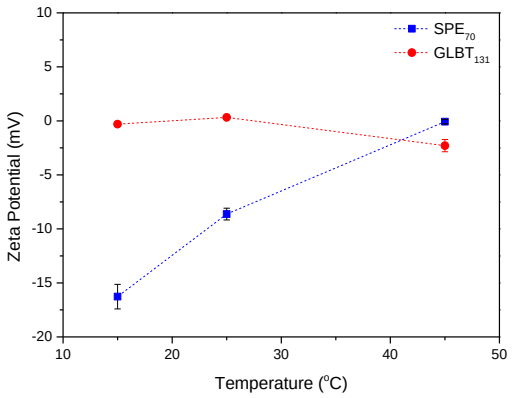

Figure 3.14. Zeta potentials of PSPE (blue) and PGLBT (red) homopolymers at different temperatures

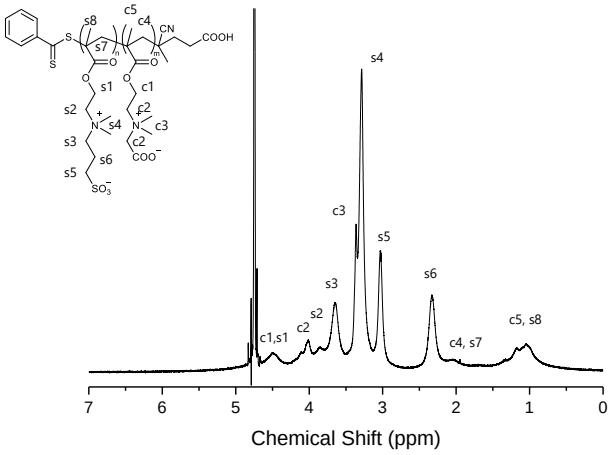

Figure 3.15. ^{1}H NMR spectrum of **#2** in ambient temperature existing as the micelle state

Conclusion

The responses of the double betaine block copolymer PGLBT-*b*-PSPE to changes in salt concentration, salt species, and temperature were studied. Commonly, the added salt ions prevented unimer-to-micelle transition as they were incorporated in the block copolymer. Similar to other data on homo-polysulfobetaines, the dipole-dipole attraction particularly between PSPE segments which drives the hydrophobic collapse was screened by counterion pairing, consequently the self-assembly required a colder environment or even did not occur. Four different halide anions (Cl^-, Br^-, I^-, and F^-) were compared and the strength was in the order of $I^- > Br^- > Cl^-$, which was in agreement with the chaotropic ranking discussed in aqueous solutions of non-ionic polymers and homo-polysulfobetaines. However, a kosmotrope F^- showed quick transition without lag and hardly changed the behaviour at the given concentrations. In the presence of low concentrations of chaotropic anions, the solutions in the unimer state tended to accompany slow diffusive modes at low salt concentrations while the transmittance gradually decreased before the transition. It is thought to emergence of chain clusters induced by counterion adsorption yielding slight charge imbalances at the zwitterion sites, similar to the "ordinary-extraordinary" transition of polyelectrolyte solutions.[53] We expect this study provides key information on the salt sensitivity of diblock copolymer type polybetaines, which would be useful for designing polyzwitterion-based stimuli-responsive materials that are activated in the change of salinities under physiological conditions.

References

1. S. Kudaibergenov, W. Jaeger and A. Laschewsky, *Supramolecular Polymers Polymeric Betains Oligomers*, 2006, **201**, 157-224.
2. A. V. Dobrynin, M. Rubinstein and J. F. Joanny, *Journal of Chemical Physics*, 1998, **109**, 9172-9176.
3. A. B. Lowe, M. Vamvakaki, M. A. Wassall, L. Wong, N. C. Billingham, S. P. Armes and A. W. Lloyd, *Journal of Biomedical Materials Research*, 2000, **52**, 88-94.
4. A. Vaterrodt, B. Thallinger, K. Daumann, D. Koch, G. M. Guebitz and M. Ulbricht, *Langmuir*, 2016, **32**, 1347-1359.
5. M. Kyomoto, T. Shobuike, T. Moro, S. Yamane, Y. Takatori, S. Tanaka, H. Miyamoto and K. Ishihara, *Acta Biomaterialia*, 2015, **24**, 24-34.
6. Y. Chang, S. C. Liao, A. Higuchi, R. C. Ruaan, C. W. Chu and W. Y. Chen, *Langmuir*, 2008, **24**, 5453-5458.
7. Z. Zhang, H. Vaisocherova, G. Cheng, W. Yang, H. Xue and S. Y. Jiang, *Biomacromolecules*, 2008, **9**, 2686-2692.
8. W. Yang, S. F. Chen, G. Cheng, H. Vaisocherova, H. Xue, W. Li, J. L. Zhang and S. Y. Jiang, *Langmuir*, 2008, **24**, 9211-9214.
9. M. Kurowska, A. Eickenscheidt, D. L. Guevara-Solarte, V. T. Widyaya, F. Marx, A. Al-Ahmad and K. Lienkamp, *Biomacromolecules*, 2017, **18**, 1373-1386.
10. J. B. Schlenoff, *Langmuir*, 2014, **30**, 9625-9636.
11. P. S. Liu, Q. Chen, S. S. Wu, J. Shen and S. C. Lin, *Journal of Membrane Science*, 2010, **350**, 387-394.

12. S. L. West, J. P. Salvage, E. J. Lobb, S. P. Armes, N. C. Billingham, A. L. Lewis, G. W. Hanlon and A. W. Lloyd, *Biomaterials*, 2004, **25**, 1195-1204.
13. S. E. Clark and J. N. Weiser, *Infection and Immunity*, 2013, **81**, 392-401.
14. S. Morozova, G. Hu, T. Emrick and M. Muthukumar, *Acs Macro Letters*, 2016, **5**, 118-122.
15. N. Y. Kostina, S. Sharifi, A. D. Pereira, J. Michalek, D. W. Grijpma and C. Rodriguez-Emmenegger, *Journal of Materials Chemistry B*, 2013, **1**, 5644-5650.
16. R. Lalani and L. Y. Liu, *Biomacromolecules*, 2012, **13**, 1853-1863.
17. J. Ladd, Z. Zhang, S. Chen, J. C. Hower and S. Jiang, *Biomacromolecules*, 2008, **9**, 1357-1361.
18. A. Laschewsky, *Polymers*, 2014, **6**, 1544-1601.
19. Y. Zhao, T. Bai, Q. Shao, S. Y. Jiang and A. Q. Shen, *Polymer Chemistry*, 2015, **6**, 1066-1077.
20. M. A. Cooperstein and H. E. Canavan, *Biointerphases*, 2013, **8**.
21. V. M. M. Soto and J. C. Galin, *Polymer*, 1984, **25**, 254-262.
22. M. B. Huglin and M. A. Radwan, *Makromolekulare Chemie-Macromolecular Chemistry and Physics*, 1991, **192**, 2433-2445.
23. H. Matsuoka, Y. Yamakawa, A. Ghosh and Y. Saruwatari, *Langmuir*, 2015, **31**, 4827-4836.
24. S. Murugaboopathy and H. Matsuoka, *Colloid and Polymer Science*, 2015, **293**, 1317-1328.
25. Y. J. Zhang, S. Furyk, D. E. Bergbreiter and P. S. Cremer, *Journal of the American Chemical Society*, 2005, **127**, 14505-14510.
26. Y. J. Zhang and P. S. Cremer, *Annual Review of Physical Chemistry, Vol 61*, 2010, **61**, 63-83.
27. E. Thormann, *Rsc Advances*, 2012, **2**, 8297-8305.
28. H. I. Okur, J. Hladilkova, K. B. Rembert, Y. Cho, J. Heyda, J. Dzubiella, P. S. Cremer and P. Jungwirth, *Journal of Physical Chemistry B*, 2017, **121**, 1997-2014.
29. K. D. Collins, *Biophysical Chemistry*, 2006, **119**, 271-281.
30. K. D. Collins, *Biophysical Chemistry*, 2012, **167**, 43-59.
31. S. Z. Moghaddam and E. Thormann, *Langmuir*, 2017, **33**, 4806-4815.
32. Y. Zhang, S. Furyk, L. B. Sagle, Y. Cho, D. E. Bergbreiter and P. S. Cremer, *Journal of Physical Chemistry C*, 2007, **111**, 8916-8924.
33. L. B. Sagle, Y. J. Zhang, V. A. Litosh, X. Chen, Y. Cho and P. S. Cremer, *Journal of the American Chemical Society*, 2009, **131**, 9304-9310.
34. K. J. Pastoor and C. V. Rice, *Journal of Polymer Science Part a-Polymer Chemistry*, 2012, **50**, 1374-1382.
35. K. J. Pastoor and C. V. Rice, *Macromolecular Chemistry and Physics*, 2015, **216**, 1024-1032.
36. T. Lopez-Leon, A. B. Jodar-Reyes, D. Bastos-Gonzalez and J. L. Ortega-Vinuesa, *Journal of Physical Chemistry B*, 2003, **107**, 5696-5708.
37. A. Salis, F. Cugia, D. F. Parsons, B. W. Ninham and M. Monduzzi, *Physical Chemistry Chemical Physics*, 2012, **14**, 4343-4346.
38. J. M. Peula-Garcia, J. L. Ortega-Vinuesa and D. Bastos-Gonzalez, *Journal of Physical Chemistry C*, 2010, **114**, 11133-11139.
39. N. Schwierz, D. Horinek and R. R. Netz, *Langmuir*, 2010, **26**, 7370-7379.
40. P. Mary, D. D. Bendejacq, M. P. Labeau and P. Dupuis, *Journal of Physical Chemistry B*, 2007, **111**, 7767-7777.
41. J. D. Delgado and J. B. Schlenoff, *Macromolecules*, 2017, **50**, 4454-4464.
42. V. Hildebrand, A. Laschewsky and D. Zehm, *Journal of Biomaterials Science-Polymer Edition*, 2014, **25**, 1602-1618.
43. Z. L. Cao and G. Z. Zhang, *Physical Chemistry Chemical Physics*, 2015, **17**, 27045-27051.
44. M. Kikuchi, Y. Terayama, T. Ishikawa, T. Hoshino, M. Kobayashi, N. Ohta, H. Jinnai and A. Takahara, *Macromolecules*, 2015, **48**, 7194-7204.
45. J. Lim, H. Matsuoka, S. Yusa and Y. Saruwatari, *Langmuir*, 2019, **35**, 1571-1582.
46. Y. Mitsukami, M. S. Donovan, A. B. Lowe and C. L. McCormick, *Macromolecules*, 2001, **34**, 2248-2256.
47. W. Binanalimbele, N. M. Vanos, L. A. M. Rupert and R. Zana, *Journal of Colloid and Interface Science*, 1991, **141**, 157-167.
48. F. H. Florenzano and L. G. Dias, *Langmuir*, 1997, **13**, 5756-5758.
49. P. Lo Nostro and B. W. Ninham, *Chemical Reviews*, 2012, **112**, 2286-2322.
50. A. V. Lezov, P. S. Vlasov, A. A. Lezov, N. S. Domnina and G. E. Polushina, *Polymer Science Series A*, 2011, **53**, 1012-1018.
51. A. Z. Niu, D. J. Liaw, H. C. Sang and C. Wu, *Macromolecules*, 2000, **33**, 3492-3494.
52. K. E. B. Doncom, A. Pitto-Barry, H. Willcock, A. Lu, B. E. McKenzie, N. Kirby and R. K. O'Reilly, *Soft Matter*, 2015, **11**, 3666-3676.

53. M. Muthukumar, *Proceedings of the National Academy of Sciences of the United States of America*, 2016, **113**, 12627-12632.

Chapter 4. Effects of pH on the Stimuli-Responsive Characteristics of Double Hydrophilic Carboxy-Sulfobetaine Block Copolymers

ABSTRACT: We investigated the pH-responsive behaviour of the carboxybetaine-sulfobetaine diblock copolymer, poly(2-((2-(methacryloyloxy)ethyl)dimethylammonio)acetate-*block*-3-((2-(methacryloyloxy)ethyl)-dimethylammonio)propane-1-sulfonate (PGLBT-*b*-PSPE) in aqueous solution under varying temperature. Alongside the temperature-responsive PSPE block which induces self-assembly of polymer micelles under the upper critical solution temperature, the PGLBT motifs having protonation sites caused additional changes in the phase behaviours. In acidic conditions where the pH is lower than the pK_a of PGLBT-*b*-PSPE, the transmittance of polymer solutions more abruptly dropped and became cloudy at higher temperatures compared to the case of salt-free solutions. There were two simultaneous diffusive modes in the turbid solutions equivalent to unimers or micelles, and large aggregates over a few hundred nanometers. Unlike in neutral and basic conditions, those large aggregates did not disappear after the emergence of the polymer micelles. The trend of the temperature-responsive behaviour hardly changed in the alkaline solutions; however, the critical temperature significantly decreased. The surface charge of the unimers and self-assembled objects determined by zeta potential measurement varied from neutral or negative to positive with proton addition, and further positively increased below the micelle formation temperature. This indicates the cationisation of PGLBT moieties and their arrangement in the outer layer of the polymer micelle surface. In spite of the positively charged outer surface, two fast and slow diffusive modes representing micelles and large clusters were repeatedly observed in acidic solutions, and to some extent, size-grown particles eventually precipitated.

Introduction

Polyzwitterions are a class of ionic polymers (polyelectrolytes) which have been gathering attention due to their unique characteristics in aqueous media. Analogous to phospholipids, such as phosphatidylcholine constructing cell bilayers, polyzwitterions have both charges in their repeating unit, and show distinctive characteristics compared to single charged polyelectrolytes or double randomly-charged polyampholytes. Firstly, these equally charged polymers with no net charge have been proved to have good resistance against non-specific protein adsorption, which was comparable to conventional non-ionic hydrophilic polymers[1-4] (e.g., PEG). The antifouling ability of polyzwitterions is attributed to the electrostatically induced strong hydration layer providing repulsive

force on protein[5] and less structured water molecules around zwitterions than bulk water.[6] Upon contact with proteins, perturbation of ordered water molecules around the polysulfobetaine surface was not pronounced while the structural ordering of water around PEG methacrylate was considerably disturbed.[7] Because of this advantage, polyzwitterionic materials have been utilised for designing blood-contacting materials,[8] wound-dressing application,[9] and protein encapsulation,[10] etc.

In addition to the antifouling property, the pairing between negatives and positives in a single chain or with adjacent chains is also a key feature of polyzwitterions. In aqueous media, polyzwitterions including polysulfobetaines, polycarboxybetaines, and polyphosphobetaines exist not only as single chains (unimers) but also chain complexes created by zwitterionic paring, which is typically several orders of magnitude bigger than the unimers.[11-13] For polysulfobetaines, the swollen chains in water are segregated from the water molecule structure under their critical temperatures, which depend on not only the length of the carbon spacer unit separating a positive and a negative site and hydrophobicity of repeating units, but also the concentration of polymers and the molecular weight.[14, 15] This tunable upper critical solution temperature (UCST) behaviour makes polysulfobetaines promising new candidates for developing biocompatible "smart" applications that respond actively to temperature variations, which have been conventionally pursued by non-ionic and lower critical solution temperature (LCST) type stimuli-responsive polymers. For example, hydrogels[16] and nanosized assemblies[17] composed of polysulfobetaine copolymers showed variations of size and swelling behaviour. Self-assembled nanoobjects that consisted of a polysulfobetaine corona and a hydrophobic core were demonstrated by block copolymerisation with a hydrophobic polymer,[18, 19] and "schizophrenic" dual temperature-responsive polymer micelles were made by controlled radical polymerisation with LCST-type polymers.[20-23] In this system, polysulfobetaine motifs became the corona and the LCST-type counterpart formed the core over the LCST and the structure reversed under the UCST.

On the other hand, polycarboxybetaines show no particular phase behaviour and remain inert against temperature. Through molecular dynamics (MD) simulation, it is discussed that the greater charge density difference between cationic and anionic groups of a polycarboxybetaine than that of a polysulfobetaine counterpart leads to less zwitterionic association.[24] In addition, the degree of ionisation of polycarboxybetaines in water must be taken into consideration due to the relatively high pK_a (~3) that originates from the carboxylate group. Unlike polysulfobetaines or polyphosphobetaines consisting of a strong acid and a quaternary ammonium which can exist in a fully ionised state in wide pH range, the end group of polycarboxybetaines can take a protonated form in

acidic condition. Protonated polycarboxybetaines are no longer polyzwitterions but rather polycations and could affect their solution behaviour in a different way. Thus, polycarboxybetaines could be classified as pH-responsive polymers.

Generally, pH-responsive polymers include weak acidic or basic groups in their structure which can release or get protons in response to change of pH. Polymers having carboxyl and tertiary amines or pyridine functional groups show the behaviour because of ionisation or deionisation of the repeating units. For weak polyacids such as polyacrylic acid and its derivatives, coil-to-globule transition, in other words dehydration takes place under their pK_a as a result of protonation of ionised sites on the repeating unit. Over pK_a, the polymer chains tend to be in an ionised state and swelling occurs. This pH-responsive action already has been widely exploited in commercial thickeners and stabilisers for suspensions or emulsions, which are known by their trade name (e.g. carbomers). Weak polybases oppositely lose hydrophilicity over their pK_a and become insoluble by deprotonation. Poly(*N*,*N*-dimethylaminoethyl methacrylate) (PDMAEMA) and their derivatives having more carbons on the branches are in the class, and their pH-responsive behaviour is utilised for obtaining self-assembled micelles[25-28] and pH-responsive gels.[29, 30] Compared to those polymers, the pH responses of polycarboxybetaines have not been frequently exploited, presumably due to their less dramatic change in the solubility. Polycarboxybetaines grafted onto 2D surfaces demonstrated pH-triggered protein adsorption/dissociation[31, 32] or flux change of the membrane.[33]

In the previous study,[34] we systematically revealed the temperature-induced self-assembly of polycarboxybetaine methacrylate-*block*-polysulfobetaine methacrylate (PGLBT-*b*-PSPE) in water. The double betaine block copolymer showed a UCST characteristic which originated from PSPE motifs and existed as PSPE-centred micelles (R_h = 40–60 nm) under the critical temperature, while unimers and larger intermediate objects were found above the point. Thanks to the good biocompatibility of both motifs, this double betaine diblock copolymer is expected to be applied for medical purposes, such as drug carriers holding active materials inside of the self-assembled structure and release at specific temperature or pH conditions. Here, we studied pH-responsive solution behaviours of PGLBT-*b*-PSPE to determine the influence of degree of ionisation of carboxylates in the PGLBT motifs.

Experimental Section

Materials

2-((2-(methacryloyloxy)ethyl)dimethylammonio)acetate (carboxybetaine methacrylate, GLBT) and 3-((2-(methacryloyloxy)ethyl)dimethylammonio)propane-1-sulfonate (sulfobetaine methacrylate, SPE, often referred to SBMA) were kindly donated by Osaka Organic Chemical Industry LTD (Osaka, Japan) and used as received. 4-Cyano-4-(phenylcarbonothioylthio)pentanoic acid was used as a chain transfer agent (CTA) and obtained as reported.[35] A Radical initiator 2,2'-azobis(2-(2-imidazolin-2-yl)propane)dihydrochloride (VA-044) was purchased from Wako Chemicals (Osaka, Japan) and used as received. Deuterated water (D_2O) was purchased from Cambridge Isotope Laboratories. Ultrapure water (minimum resistivity ~18.2 MΩ cm) prepared with a Milli-Q system was used for preparing aqueous solutions and dialysis. Dialysis was performed using regenerated cellulose membranes (MWCO 3500 and 15000) to remove residual monomers and other impurities. 1 M $HCl_{(aq)}$ and $NaOH_{(aq)}$ used for modifying pH of polymer solutions were purchased from Wako Chemicals.

Synthesis of double polybetaine block copolymer PGLBT-*b*-PSPE

Synthesis of PGLBT macroCTA and block copolymer PGLBT-*b*-PSPE The polybetaine homo- and block copolymers were prepared as previously reported.[34] The PGLBT homopolymer was synthesised by reversible addition–fragmentation chain-transfer (RAFT) polymerisation and purified through dialysis prior to the next step. PGLBT-*b*-PSPE was synthesised with PGLBT macroCTA and SPE monomers as previously reported.

Polymer characterisation

The experimental molecular weight (M_n) and the dispersity ($Đ$) of homo- and block copolymers were determined by aqueous size exclusion chromatography (SEC) run with a column (SB-804 HQ, Shodex) and a refractive index detector (RI-830, JASCO, Japan), using a buffer eluent (0.5 M CH_3COOH and 0.3 M of Na_2SO_4) at a flow rate of 0.5 mL/min. The calibration was carried out with a set of poly(2-vinylpyridine) standards (M_n range: 5500 to 142000 g/mol, Sigma-Aldrich). ^{1}H NMR spectra of synthesised PGLBT-*b*-PSPE were acquired using a 400 MHz JEOL JNM-AL400 spectrometer (JEOL, Tokyo, Japan) in deuterated water (D_2O). The degree of polymerisation (DP) of block copolymers was determined by both SEC and ^{1}H NMR results. (The DP of homo-PGLBTs was based on SEC only) The transmittance at 200–600 nm of the aqueous solutions of the block copolymers was recorded with a UV-VIS spectrometer (Hitachi U-3310 spectrophotometer) equipped with a water circulator for temperature control. A quartz cell with a light path of 10 mm was used. Each solution (concentration: 10 mg/mL)

was filtered with a syringe filter unit (pore size: 0.2 μm, mdi) prior to measurement. The transmittance at 400 nm was recorded from 60 to ~5 °C with regular intervals after waiting for 5 min at each temperature. The cloud points (CP) were determined at the point where the transmittance is 50% by interpolation between each point. The pH of each solution was adjusted by adding a few microliters of 1 M $HCl_{(aq)}$ and $NaOH_{(aq)}$.

Dynamic light scattering (DLS) was performed to measure the hydrodynamic radius (R_h) of the polymer chains and self-assembled objects in aqueous solution (concentration = 10 mg/mL). A goniometer (BI-200SM, Brookhaven Instruments, New York, USA) filled with decahydronaphthalene (index matching fluid) was equipped with a 15 mW He-Ne laser (wavelength λ = 632.8 nm) and a water circulator. The scattered light from the sample solutions was detected at 60°, 75°, 90°, and 105° by a BI-DS2 photomultiplier tube. The field autocorrelation functions were obtained by a correlator (TurboCorr, Brookhaven Instruments), and analysed by CONTIN regularization. All the correlation functions are reported as $((g^{(2)}(q,t)-1)/\beta)^{0.5}$. Highly turbid solutions were diluted to 3.33 mg/mL for attenuating multiple scattering. If an autocorrelation function showed multimodal decay, averages of decay rates were determined separately by splitting double or triple bodies and the respective R_h was calculated. The multiple bodies were labeled as "slow" and "fast" diffusive modes depending on their diffusion coefficient. Fast diffusive modes refer to unimers or small-sized micelles, and the slow diffusive modes refer to large aggregates. The more details of light scattering are described in the Supporting Information page. Electrophoretic light scattering was performed with ELSZ-2000 (Otsuka, Japan) using the Smoluchowski approximation to determine the zeta potential.

Results and Discussions

Solution behaviour of PGLBT-*b*-PSPE varied by pH

The pH-responsive characteristics of the double hydrophilic betaine block copolymer PGLBT-*b*-PSPE (the structure and specification are described in **Figure 4.1** and **Table 4.1**) were examined by tracking the alterations of transmittance and hydrodynamic radius. If the acidity of the polymer aqueous solution increases over its pK_a, the net charge of the zwitterionic diblock copolymer would alter from neutral to partly cationic because of protonation of carboxylates on the PGLBT side. The pK_a of carboxybetaines is influenced by the length of spacer unit between ionic sites; given that the distance is longer, pK_a increases from 2 to 5.[36] Polymerised carboxybetaines did not show any significant difference in pK_a with the spacer length.[37] Meanwhile, sulfobetaines typically exist

in deprotonated form over a wide range of pH because the pK_a of sulfuric acid groups is under 1. In our study, the pK_a of $GLBT_{131}$ was determined to be 3.45, and that of the derivative of two block copolymers PCS1 and PCS2 was determined to 3.21 and 3.22 by titration, respectively. (see **Figure 4.9**) Hence, the number of sulfobetaine repeating units did not affect recognisably to the pK_a. Prior to investigating the temperature-responsive behaviour of PGLBT-*b*-PSPE at different pHs, transmittance of the solution at 25 °C was recorded while modifying pH by adding small volumes of 1 M $HCl_{(aq)}$ or $NaOH_{(aq)}$. PCS1, which showed polymer micelles (R_h = 28 nm) below room temperature in a slightly translucent state, became more translucent and eventually turbid below pH ~2.4 as shown in **Figure 4.2**. This turbid state reversibly changed to a slightly translucent state by titration with NaOH then became transparent when excess OH^- was introduced.

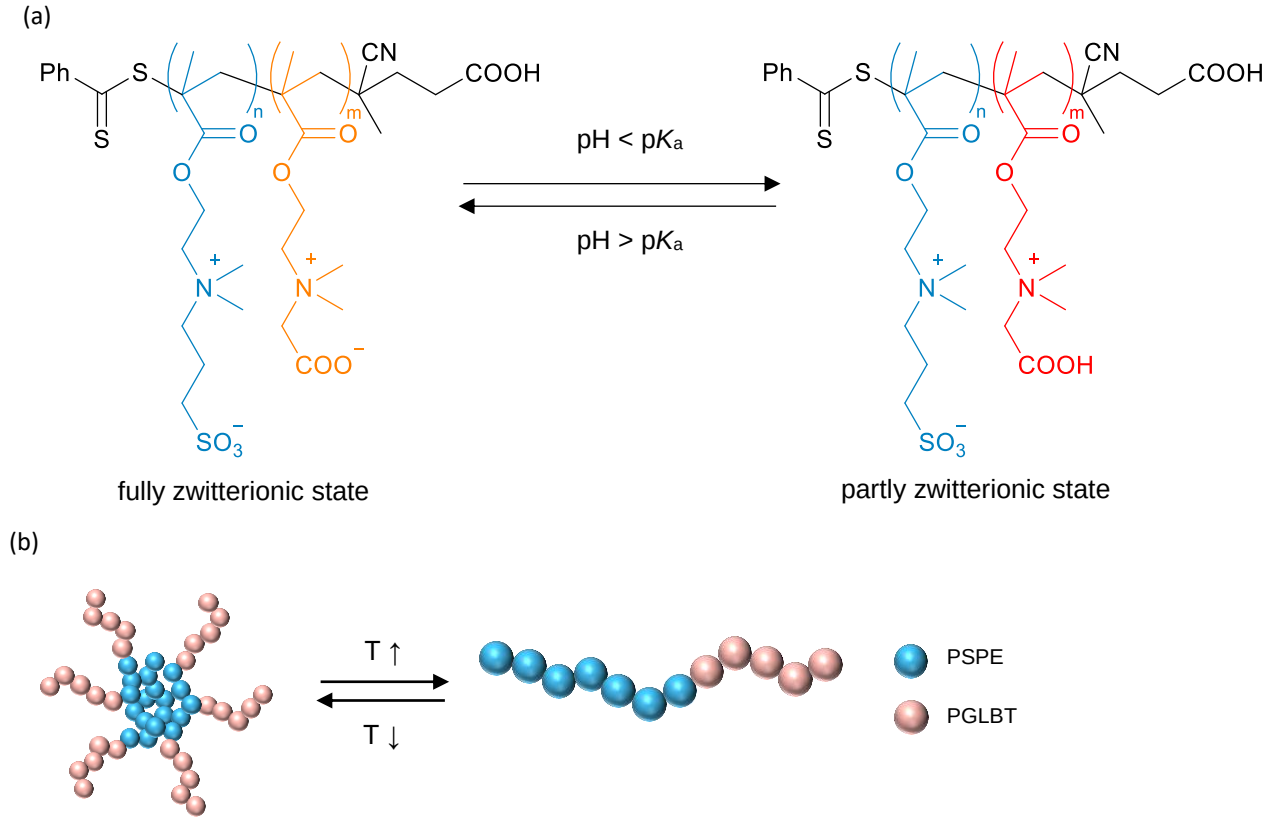

Figure 4.1. (a) Chemical structure of PGLBT-*b*-PSPE and proposed state in acidic condition (b) Cartoons of PGLBT-*b*-PSPE in unimer form and micellar form

Table 4.1. Specifications of PGLBT-*b*-PSPE Samples

Sample name	M_n^{SEC} (g/mol)	DP^{SEC} (GLBT:SPE)	$Đ$ (M_w/M_n)	$*M_n^{1H\ NMR}$ (g/mol)[c]	DP^{NMR} (GLBT:SPE)	Cloud Point (°C)
PCS1	75000	131:167	1.08	93600	131:233	15.8
PCS2	82300	131:193	1.14	240000	131:758	51.2
PCS3	59000	86:144	1.08	99800	86:290	20.0
PCS4	64600	86:164	1.13	143400	86:446	27.6

* the molecular weight was determined from the ^{1}H NMR spectra obtained at 60 °C to analyse the unimer state of the polymers

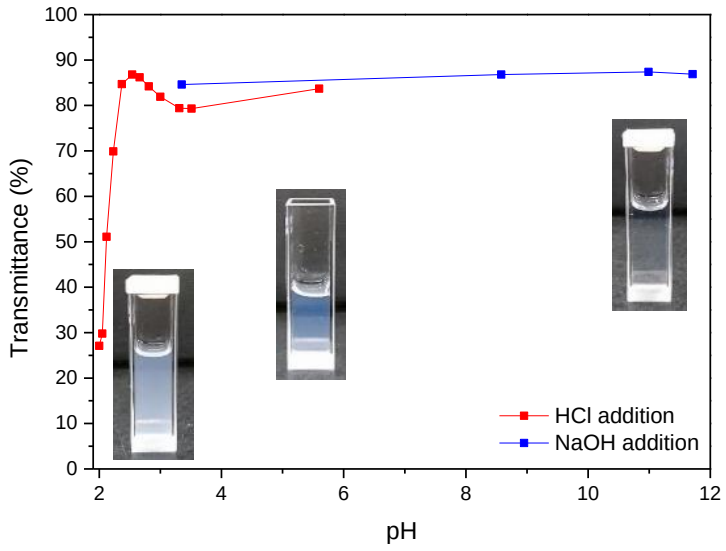

Figure 4.2. Transmittance variations against pH of PCS1. Insets are photos taken at acidic (left), neutral (middle), and basic (right) condition of the solution

It seems contradictory that the partly cationised PGLBT-*b*-PSPE chains exhibited a sudden phase shift represented as a highly fussy state. Recalling the general feature of polyzwitterions, the UCST behaviour of polysulfobetaines originates from Coulombic attractions between the opposite charges of adjacent chains. Applied heat or salt addition promotes solvation of polysulfobetaine chains by breaking this attraction. Consequently, partly cationised PGLBT motifs are thought to provide extra hindrances on PSPE pairing thereby would decrease UCST, however it was not evidently found in the results of the preliminary study. The influence of pH on the temperature-responsive characteristic was examined in more detail. The properties (transmittance and R_h variations) of the block copolymer solutions tuned to be acidic and basic were compared to the previous results acquired in salt-free water. As shown by the black symbols in **Figure 4.3(a)(b)**, the PGLBT-*b*-PSPE chains in salt-free water typically existed as free chains in a transparent state at sufficiently high temperatures, and then large intermediate particles

(over hundreds of nanometers) start to appear with unimers under decreasing temperatures until the emergence of monodisperse spherical micelles (~30 nm). In the acidic solution (pH = 2.7), the transparent sample solution at elevated temperatures (~60 ºC) became quickly hazy than in salt-free water while cooling, then the degree reached to a few % under 25 ºC. (red symbols in **Figure 4.3(a)**) On the other hand, the alkaline solution (pH = 12) showed a delayed transmittance decrease to much lower temperatures, and the solution eventually became bluish translucent at colder temperatures, which is an indication of nanoparticle formation as in the untreated solution. The R_h variation plotted in **Figure 4.3(b)** indicated unimer-to-micelle transition that took place at all three pHs, and the temperatures where a significant size change occurred corresponded to those in the transmittance data. Notably at a low pH, the double diffusive modes persistently remained after a size increase of the fast mode. At 40 ºC, a slow mode whose R_h was over 100 nm was simultaneously detected with another fast mode (R_h = ~7 nm, unimer). The fast mode showed size increase below 25 ºC and reached 27 nm, which was similar to the size of the monodisperse micelles in salt-free water. The slow mode also increased over 400 nm and still dominantly existed even though micellisation occurred, which is unlike the results of the neutral solution where the chains form large aggregates only at the border of the transition temporarily and then disappear. The R_h distributions in acid and alkali medium show the detailed difference against temperature variation. As shown in **Figure 4.3(c)**, the polymers in the acidic condition existed as unimers (60 ºC)/unimers and large aggregates (40 ºC)/large aggregates with micelles (12 ºC), and the slow modes (larger objects) always had higher ratios than the fast modes. On the other hand, the polymers in the pH 12 solution followed the typical size distribution pattern of PGLBT-*b*-PSPE in water but the transition commenced at lower temperatures (**Figure 4.3(d)**). The chains originally able to form micelles at 25 ºC were still in the intermediate state showing bimodal distribution at the temperature, and then formed monodisperse micelles below 16 ºC.

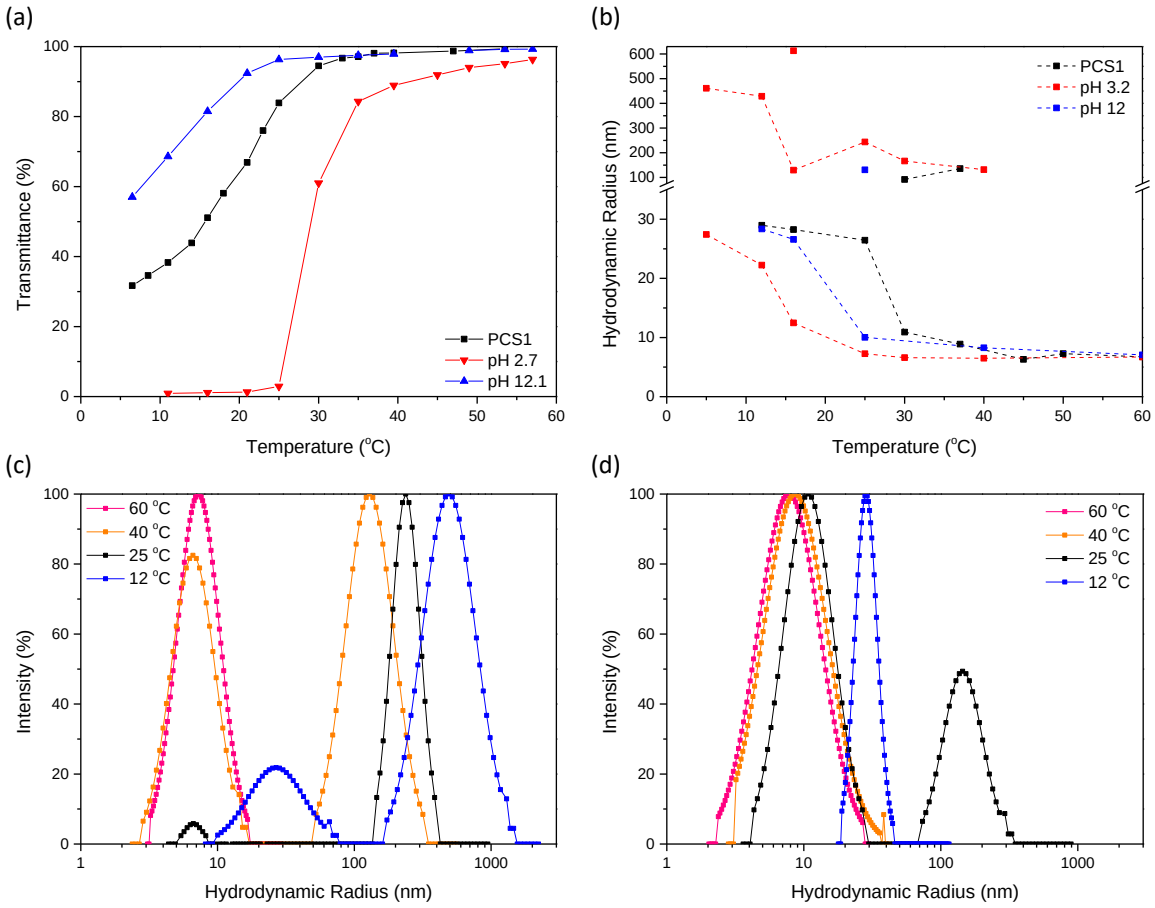

Figure 4.3. Temperature-responsive properties of PCS1 in three different pH: (a) Transmittance variations (b) R_h variations vs temperature (c) R_h distributions in pH 3.2 at selected temperatures (d) R_h distributions in pH 12 at selected temperatures

PCS2, which was synthesised from the same PGLBT was also investigated in the same manner. Due to more SPE units, it showed a higher CP with more abrupt transmittance shift as shown by the black lines in **Figure 4.4(a)**. As revealed on PCS1, addition of HCl or NaOH led to alterations of the original temperature-responsive behaviour. Under cooling, the acidic solution transparent at ~60 ºC quickly became very cloudy than the neutral solution as the red symbols in **Figure 4.4(a)**. Although high fussiness of the solution, the decay rates ($\bar{\Gamma}$) obtained at 4 different angles met in a linear agreement, (The autocorrelation functions and analysis results are shown in **Figure 4.10**) and the determined hydrodynamic radii are plotted in **Figure 4.4(b)**. Similar to the former case, the slow mode continuously appeared above 40 ºC and accompanied by micelles (R_h = 45 nm) below 25 ºC. The size distributions at several temperatures (**Figure 4.4(c)**) show unimers (R_h = 8.7 nm) and chain clusters (R_h = 127 nm) at 60 ºC which are typically visible in homo-polysulfobetaine solutions, and coexisting unimers and aggregates at 40 ºC, and the micelle-aggregate dual state below 25 ºC. The slow mode (R_h ~1000 nm) remained after significant size increase of the fast mode. Meanwhile, the basic solution only showed lowered transition temperatures like PCS1.

Note that the influence of NaOH addition seems to be weighed heavier than the former which had shorter PSPE segments. The cloud point was shifted from 51.2 to 30 °C and the monodisperse micelles emerged below 30 °C, which originally appeared below 40 °C.

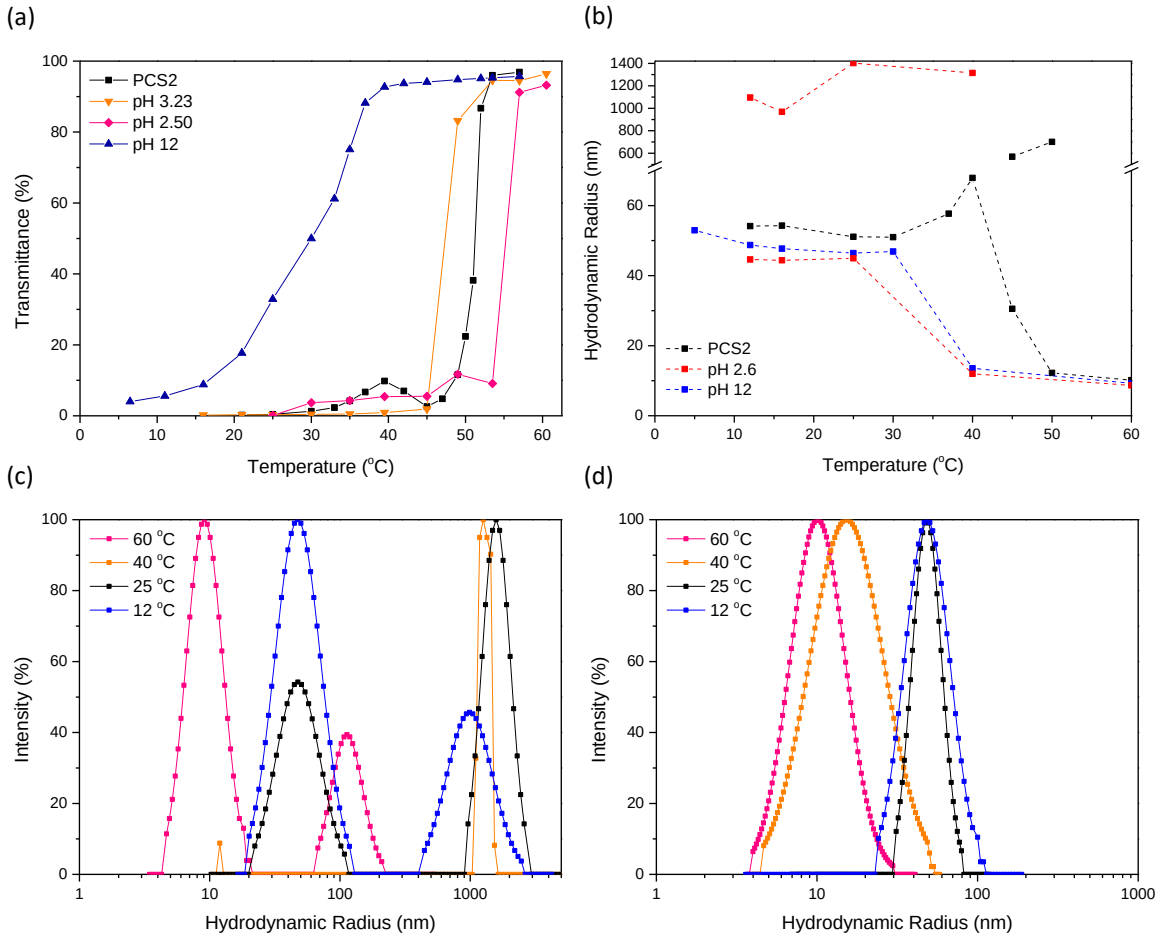

Figure 4.4. Temperature-responsive properties of PCS2 in acidic, neutral, and basic condition (a) Transmittance variations (b) R_h variations vs temperature (c) R_h distributions in pH 2.66 at selected temperatures (d) R_h distributions in pH 12 at selected temperatures (scattering angle = 90°)

The pH-dependent behaviour of two shorter block copolymers that showed transitions at lower temperatures was investigated as well. Both were synthesised using $GLBT_{86}$ as a macroCTA, and the PSPE segments were regulated to have small or large portions in the whole chain. For PCS3, the alteration of the transmittance curve by acid or base was revealed as shown in **Figure 4.5(a)**. Similar to the former two diblock copolymers, high acidity made the CP to be on higher temperatures and alkali suppressed turbidity increase on cooling. The R_h (**Figure 4.5(b)**) indicates formation of polymer micelles (the fast mode varied from 6 to 22 nm) accompanied by persistent slow modes (~100 nm) at pH 3.2 whereas only micelle formation is observed without any slow modes in pH 12. This alteration promoted by proton addition was repeatedly found in PCS4 as displayed in **Figure 4.5(c)** and **(d)**. The

solution became rapidly turbid below ~40 °C with micelle transition accompanied by a larger diffusive mode (~400 nm) (The autocorrelation functions and analysis results at 60 and 25 °C are shown in **Figure 4.11**) Both diblock copolymers lost the sensitivity to temperature at high pHs, and this was more obvious for PCS4 holding more PSPE units as confirmed in the previous sample set. Unlike its counterpart, PCS4 in pH 11.7 solution revealed that there was no transition to micelles but only intermediates at the end of the range (**Figure 4.13**) which suggests that the phase transition temperature may be shifted under 0 °C in this condition. Therefore taking into account of all four cases, PGLBT-*b*-PSPE chains having longer PSPE segment are assumed to be affected more critically by hydroxide ions. Given that the carboxylates of PGLBTs are in a fully ionised state (100% zwitterionic) in high pHs and providing negligible attracting and repelling forces, it would be proposed that the inter/intra-electrostatic attractions among PSPE motifs are hindered by OH^- as well as Na^+. The added ions can adsorb on the ionised sites (quaternary ammonium and sulfonate) in PSPE chain, thereby preventing the phase separation as the diblock copolymers in salt solutions.

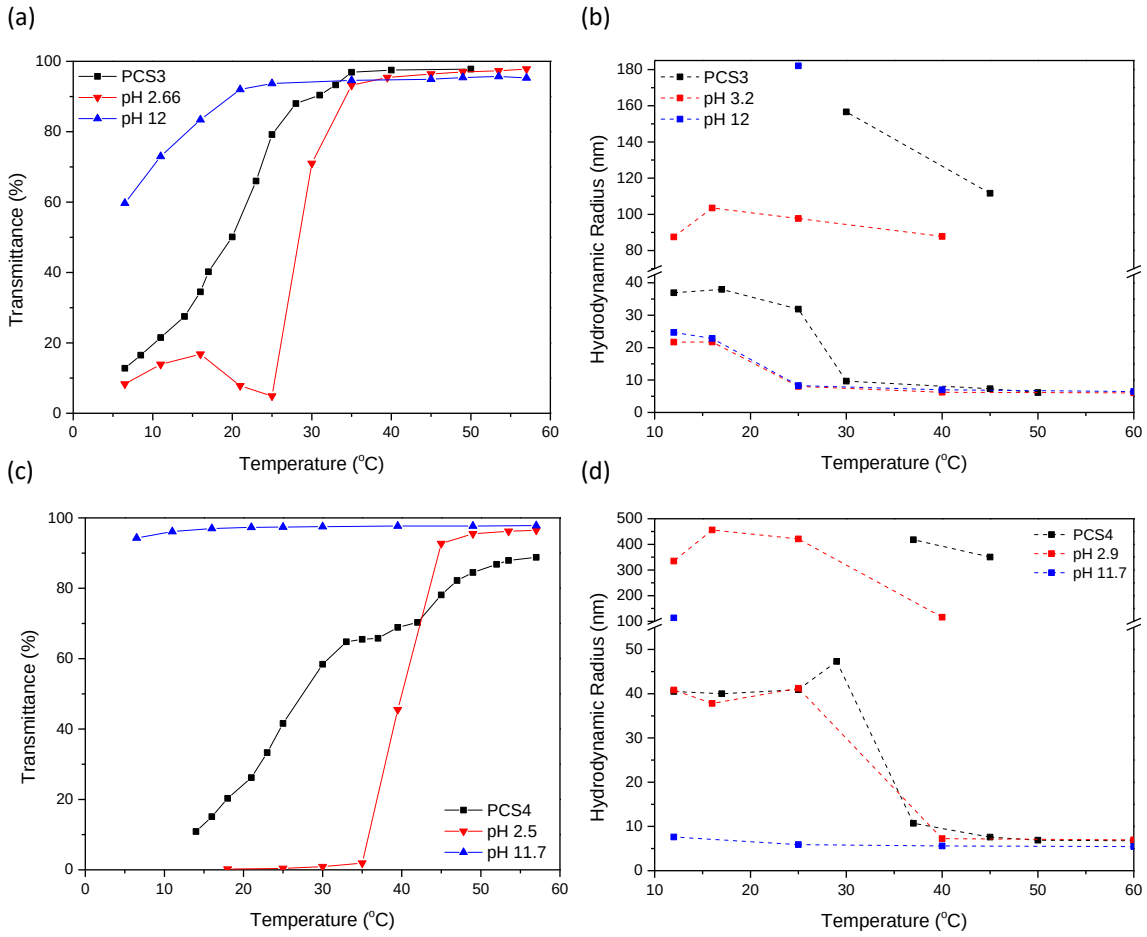

Figure 4.5. (a) Transmittance variations and (b) R_h variations of PCS3 against temperature in pH 3, neutral, and pH 12 (c) Transmittance variations and (d) R_h variations of PCS4 against temperature in pH 3, neutral, and pH 12 (The R_h distributions at several temperatures in acidic/basic condition are shown in **Figure 4.12** and **4.13**)

Surface charge of PGLBT-*b*-PSPE in different pHs

As discussed in the previous section, PGLBT-*b*-PSPE would become a partly cationic polyelectrolyte if H^+ is added to the aqueous solution due to protonation of carboxylates in PGLBT motifs. The charge alteration as well as colloidal stability were confirmed by measuring the zeta potential in each temperature and pH. **Figure 4.6(a)** shows the zeta potential of PCS2 in three different pHs with varying temperature, respectively. For the sample solution in salt-free water, the absolute value decreased to near zero at high temperatures over 50 ºC and negatively increased with a temperature drop. Since the chains in sufficiently high temperatures had no particular interchain/intrachain zwitterionic attractions, the ionised groups in PGLBT and PSPE would equally contribute to the whole surface charge and that led to neutral zeta potential values. On the other hand, the negative charge increase is assumed to be attributed to the PSPE cores of the micelles because a PSPE homopolymer showed ~-10 mV in a turbid state (shrunken chains) and near zero in a transparent state (free chains) (**Figure 4.14**), and this was also verified in the other studies on solution state[38, 39] and sulfobetaine-funtionalised surfaces.[40, 41] In the previous report, we argued that the collapsed PSPE segments consisting the core of PGLBT-*b*-PSPE micelles were not completely segregated from water molecules and might have scarcely hydrated surface as appeared in the ^{1}H NMR spectra.[34] The zeta potential turned positive in acidic condition (red line) at all temperatures, which apparently implies protonated carboxylates in PGLBT moieties in both unimer and micelle forms. Note that the charge increased to ~20 mV in pH 2.5 below 40 ºC, where large aggregates started to emerge with an abrupt transmittance decrease. The positive potential increase would be attributed to the PGLBT corona of the polymer micelles or larger aggregates. This zeta potential variation upon neutral to acidic has also been reported on homo-polycarboxybetaine chains,[13] polycarboxybetaine-coated nanoparticles,[42] and polystyrene-*b*-polycarboxybetaine dispersions.[43] Also, our experiment on each homopolymer (**Figure 4.14**) exhibited this tendency. Meanwhile, PCS2 chains in alkali (blue line) showed almost neutral surfaces followed by a negative increase below 25 ºC where micelles started to emerge. The increased extent of ionised carboxylic groups in PGLBT and hindered UCST behaviour of PSPE by counterions (OH^- and Na^+) may attribute the lesser zeta potential variation than that in pure water.

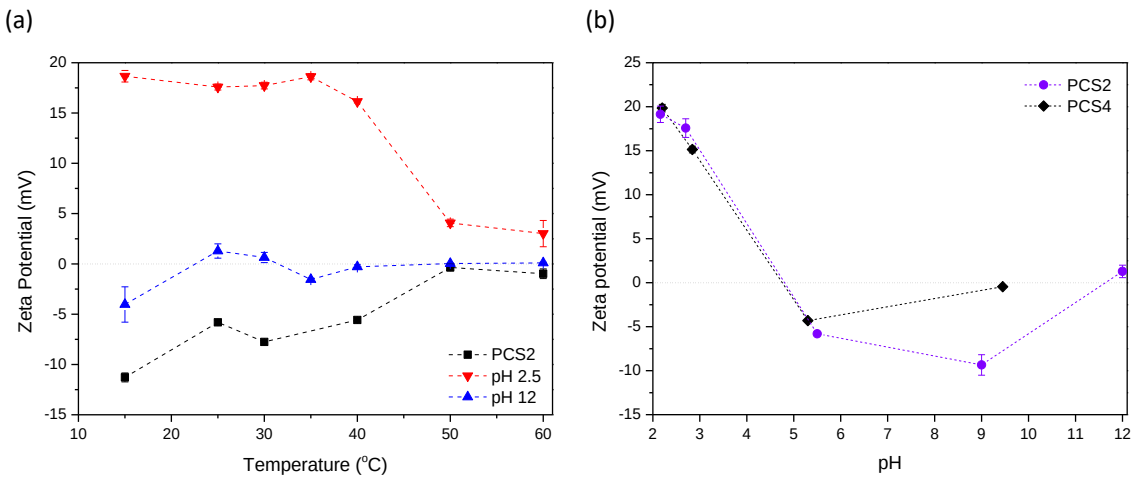

Figure 4.6. (a) Zeta potential of PCS2 vs temperature taken at neutral (■), acidic (▼) and basic (▲) condition (b) Zeta potential of PCS2 and PCS4 vs pH (temperature = 25 °C)

Figure 4.6(b) shows the zeta potentials of two diblock copolymers at 25 °C at several pHs. Both revealed positive values in acidic, slightly negative in neutral, and near zero in alkaline solutions. Two isoelectric points are approximately at pH 4, which is close to the pK_a, and above pH 9. It is thought that the first isoelectric point divides the partially polycationic state and zwitterionic state, and the second isoelectric point relates to the dissociation of micelles to unimers by specific ion effect of Na^+ and OH^-. Recall that the size profiles of the two polymers at 25 °C, the shorter one (PCS4) took micelle and aggregate form in neutral and acidic solution but existed as unimers in a high pH. Consequently, the zeta potentials obtained from acidic to basic are equivalent to the state of cationised PGLBT-covered particles (acidic), zwitterionic PGLBT-covered particles (neutral), and disassembled free chains (basic), respectively. The zeta potential of the longer one (PCS2) corresponded similarly, however the surface charge did not become neutral at pH 9 because the self-assembled particles were maintained under this concentration of NaOH. The zeta potential became neutral at pH 12 while the self-assembled state was still favoured, and it is thought that adsorbed OH^- and Na^+ on the ionised sites of particles screened the potential.

For highly turbid PGLBT-*b*-PSPE aqueous solutions at low pHs, sedimentation occurred since a few hours after preparation of the sample then the turbidity decreased as time passed. The sediments that settled to the bottom were able to be well dispersed by gentle shaking, and the solution became turbid again. After the sedimentation, the supernatant was reexamined by DLS to get the deviated size distribution. The particle size in the supernatant of PCS1 in pH 3.2 was R_h = 27/210 nm, which is showing a size decrease of the larger one compared to the initial R_h (22/429 nm) as shown in **Figure 4.7(a)**. When the fast mode representing polymer micelles did not show

significant size variation, the slow mode significantly got smaller because flocculated larger particles submerged to the glass cell bottom.

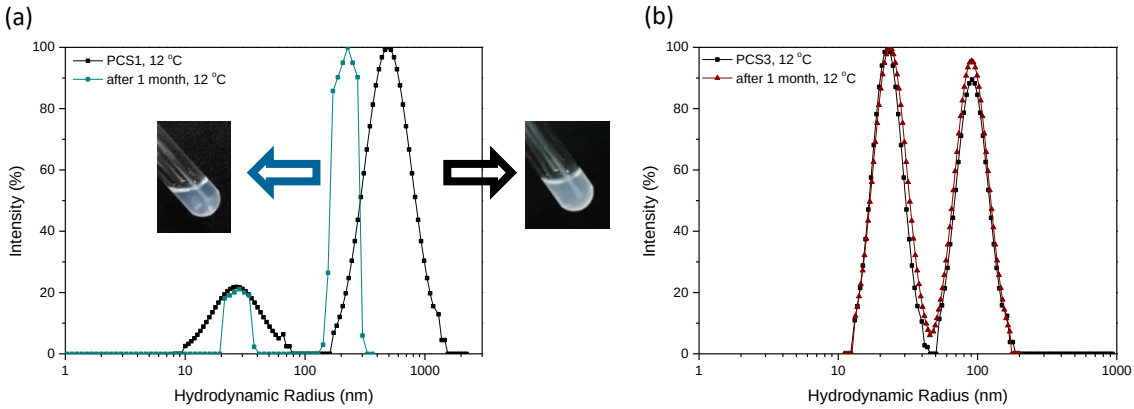

Figure 4.7. R_h distributions of PGLBT-*b*-PSPE aqueous solutions as prepared and after 1 month: (a) PCS1 and (b) PCS3 (temperature = 12 ºC, scattering angle = 90º, and conc. = 3.3 mg/mL)

However, there was no significant size alteration in PCS3 as shown in **Figure 4.7(b)**, where the bimodal distribution representing micelles and large aggregates (R_h = 22/90 nm) was not modified after 1 month passed (R_h = 23/91 nm). It was also easily distinguishable that only few portions of self-assembled polymers precipitated to the bottom of the sample cell. By taking into account these two cases, it is thought that the size growth in acidic solution is not a temporary event as apparent flocculation occurred in spite of the positively charged surface (ζ = +20 mV) of the nanoobjects. In addition, the particles over R_h = 200 nm tended to lose buoyancy.

The solution behaviour of PGLBT-*b*-PSPE against pH and temperature can be summarised as depicted in **Figure 4.8**. The intrinsic unimer-to-micelle transition that originates from zwitterionic pairing among PSPE was maintained in the acidic and basic media, and the critical temperatures of the phase change were altered. The charge shift of PGLBT motifs from neutral to positive occurs by excess protons in solutions and it is reflected by the zeta potential variation. Notably in acidic solutions, the temperature-responsivity was still evident even polycationised PGLBT moieties are present on the other side of the chain, which might potentially hinder zwtterionic pairing. Moreover, the larger aggregates or clusters 10 folds more than polymer micelles coexisted with micelles. Those large objects gradually precipitated as phase separated UCST or LCST type homopolymers, but not all of them participated in the sedimentation.

In the experiment, the only additive for tuning acidity was $HCl_{(aq)}$. Hence, chloride ions could also affect the solution behaviour as revealed in the study examining the specific ion effect of several halides according to

Hofmeister series on polybetaines.[12, 38] Cl^-, which is on the border of kosmotropes and chaotropes,[44] usually promotes solubility of polysulfobetaine by interrupting electrostatic attraction among zwitterionic pairs so that it could not explain the apparent size increase. Eventually, protonation of PGLBT induced by H^+ addition is assumed to be the main factor. Polycationised PGLBT motifs can have attraction with adjacent chains by two paths: electrostatic attraction between sulfonates of PSPE (negative site), or hydrogen bonding between protonated carboxylate ends of PGLBT. Presumably, the former can happen only on free PSPE segments unless the charged groups of PSPE bind to each other, so it is not available to explain the dual-sized particle state which appeared under the transition temperatures resulted by the attractions among PSPE motifs. The positive increase of zeta potential is also hard to explain with this approach. However, taking hydrogen bonding into account, the size-grown particles can be interpreted as clusters of PSPE-cored micelles closely associated with H-bonding between PGLBT chains forming the corona. This approach is not inconsistent with the increased positive surface charge which was accompanied by the phase change. Meanwhile, upon a rough consideration of the average length of hydrogen bond (0.2 nm) and the length of spacer between quaternary ammonium and carboxylate (~0.37 nm), the distance of two quaternary ammoniums when GLBT units make an H-bond with each other is thought be not enough to negate the electrostatic repulsion force. The Debye length ($l_D = [4\pi l_B c_s]^{-0.5}$, where l_B is the Bjerrum length in pure water and c_s is the concentration in inverse cubic meter of added salt) of the solution when pH 2.5 (for PCS2 solution) is approximately 3.3 nm, so the issue of electrostatic repulsion versus H-bonds between PGLBT motifs still has been under elusiveness.

On the other hand, there was no extraordinary solution behaviour on addition of hydroxide and sodium ions. In all cases, the process of unimer-to-micelle transition and the size distribution was identical but each transition point shifted to lower temperatures. Particularly, samples having longer PSPE chains and the same PGLBT lost the transition behaviour more dramatically even for the same amount of $NaOH_{(aq)}$ was added to adjust. Through the results, association of Na^+ and OH^- ions with their counterparts (carboxylate and sulfate/quaternary ammonium) is thought to be the primary reason for the weakened temperature responsivity. Compared to our results about specific ion effect of halides against the same polymer (data not shown), salting-in property of OH^- is approximately equivalent to I^-, which is a strong chaotrope and had strongly hindered the temperature-responsive behaviour with only a small concentration (>2 mM, pH 12). Cleavage of ester groups in PSPE repeating units by a strong base might be another reason. However, the polymer-type SPE is more durable than the monomer and the elimination process of ester groups does not occur quickly as reported by Schönemann et al.[45] ^{1}H NMR spectra

obtained at different pH solutions (**Figure 4.15**) without any residual signals also suggest that the stability against hydrolytic cleavage was guaranteed during the investigation.

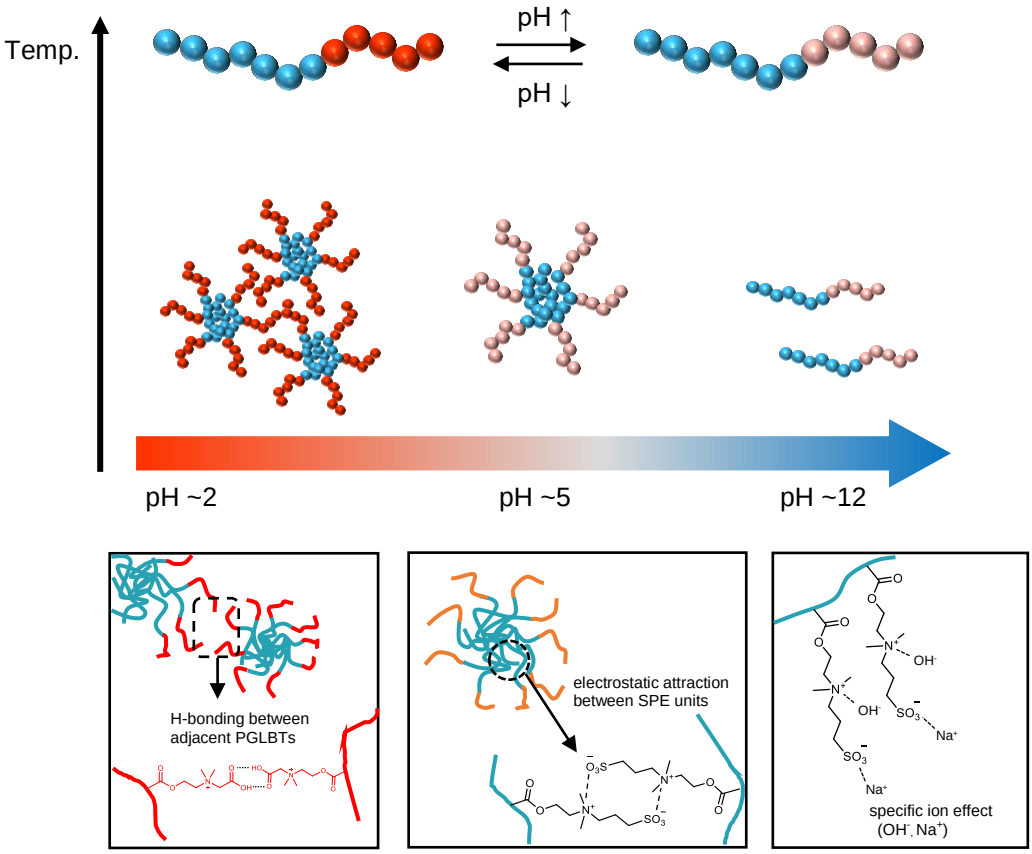

Figure 4.8. Schematics of pH influence on the solution behaviour of PGLBT-*b*-PSPE (blue figures: PSPE, orange: PGLBT, and red: protonated PGLBT)

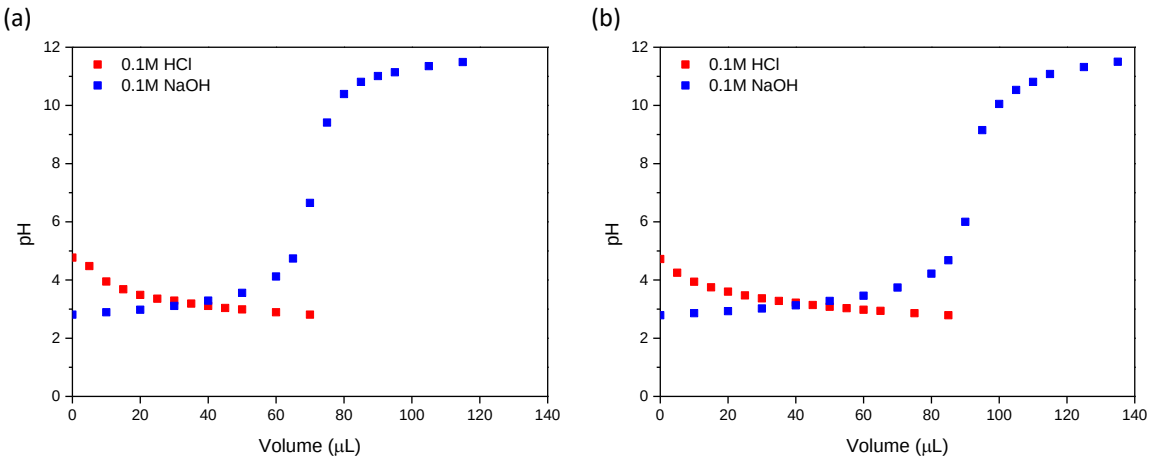

Figure 4.9. Titration of the polymers (a) PCS1 (b) PCS2 by HCl addition (■) and NaOH back titration (■) Potentiometric titration was performed: aliquots of 0.1M $HCl_{(aq)}$ was added to polymer aqueous solution (10 mg/mL). After the pH settled to a constant value, the back titration was performed by addition of aliquots of 0.1 M $NaOH_{(aq)}$. Variations of pH were recorded after each addition.

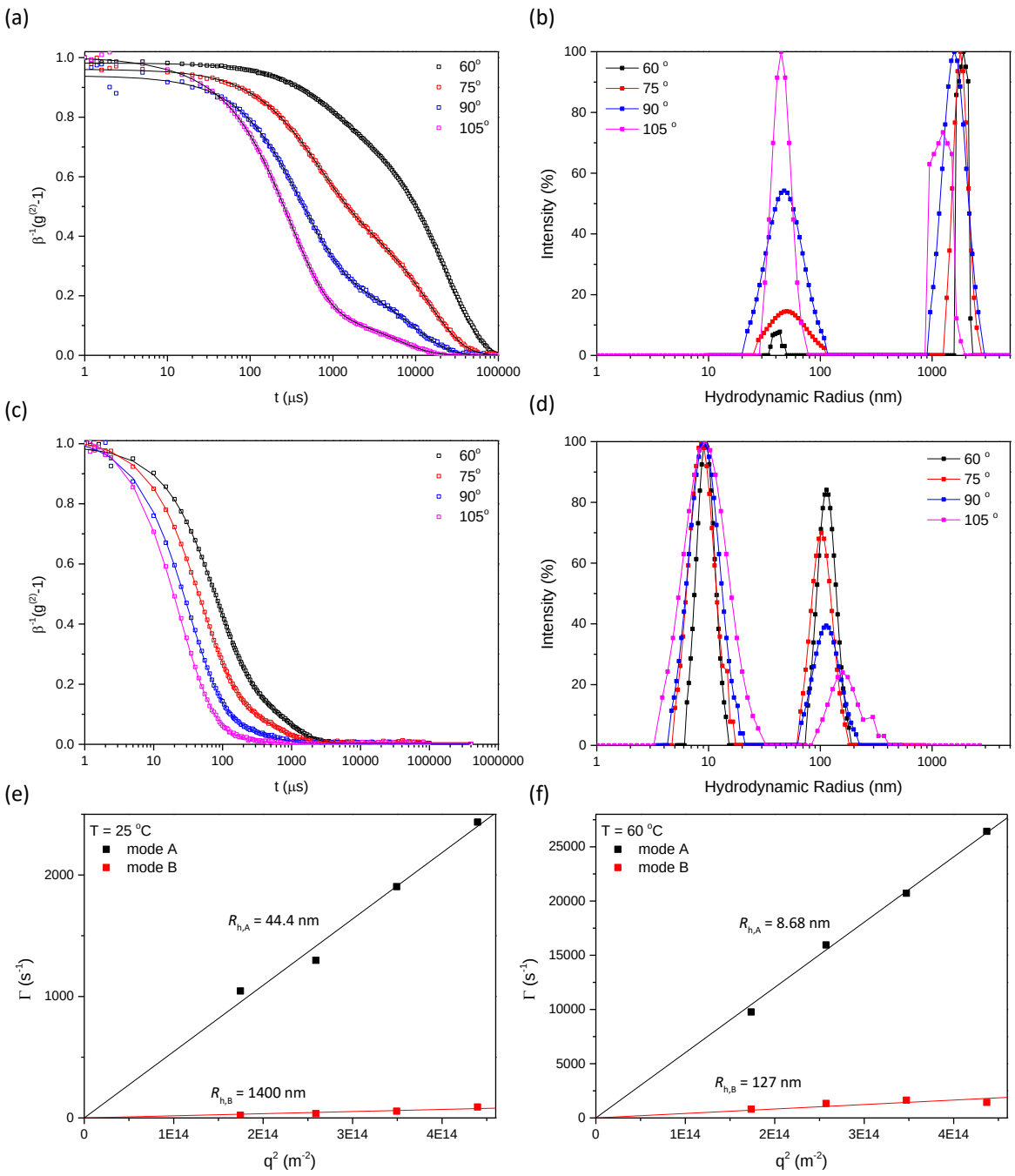

Figure 4.10. (a) autocorrelation functions (ACFs) of PCS2 in pH 2.6 (3.33 mg/mL) obtained at 60º, 75º, 90º, and 105º. Temperature = 25 ºC (b) Size distribution of hydrodynamic radii (R_h) determined by CONTIN fit of 25 ºC at 4 scattering angles (c) ACFs obtained at 60 ºC (d) Size distribution of R_h of 60 ºC (e,f) Plot of the inverse relaxation times Γ vs q^2 of two diffusive modes obtained at 4 scattering angles at 25 ºC (e) and 60 ºC (f)

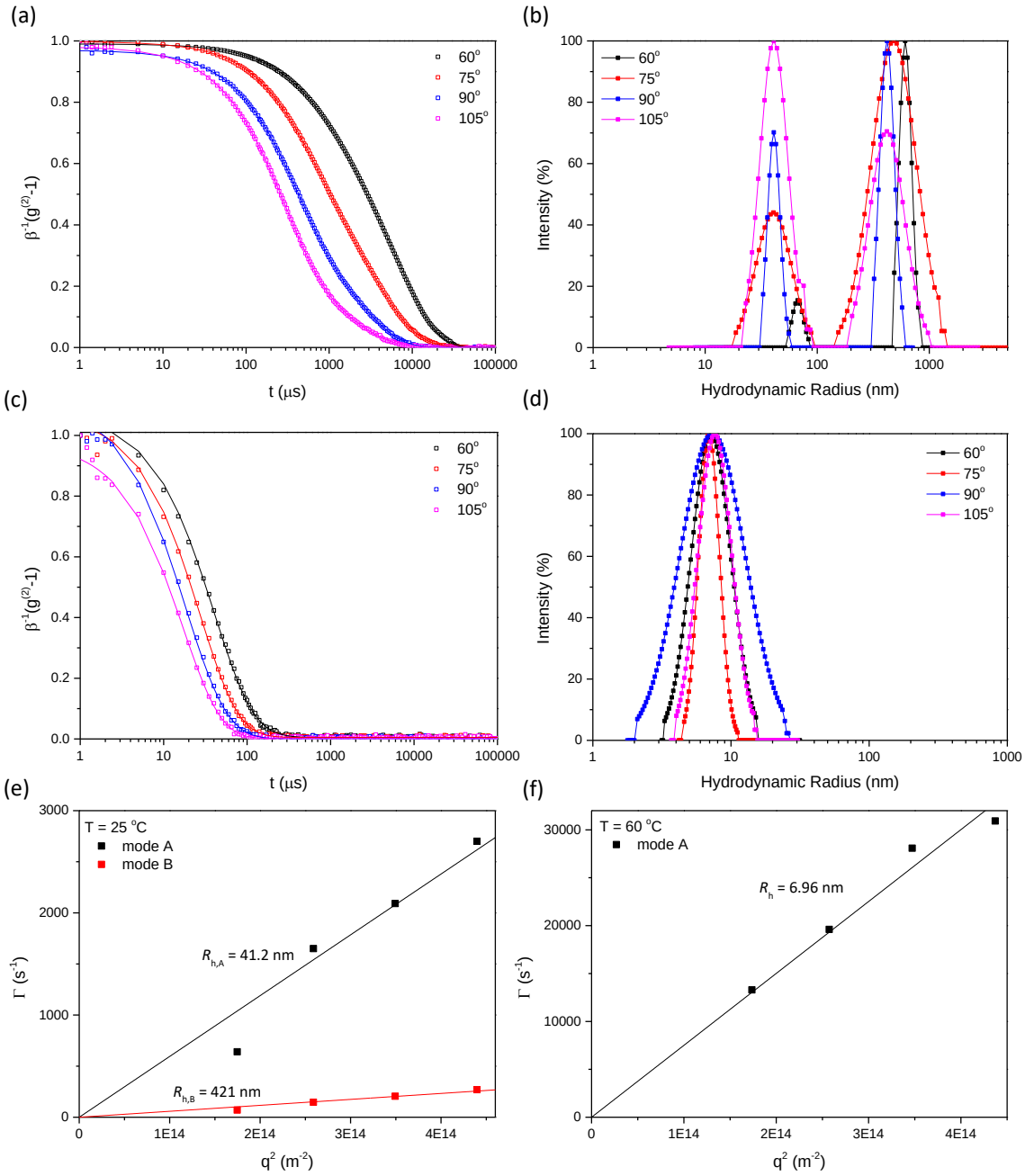

Figure 4.11. (a) DLS autocorrelation functions of PCS4 in pH 2.9 (3.33 mg/mL) obtained at 60º, 75º, 90º, and 105º. Temperature = 25 ºC (b) Size distribution of R_h determined by CONTIN fit (c) ACFs obtained at 60 ºC (d) Size distribution of R_h of 60 ºC (e,f) Plot of the inverse relaxation times Γ vs q^2 of two diffusive modes obtained at 4 scattering angles at 25 ºC (e) and 60 ºC (f).

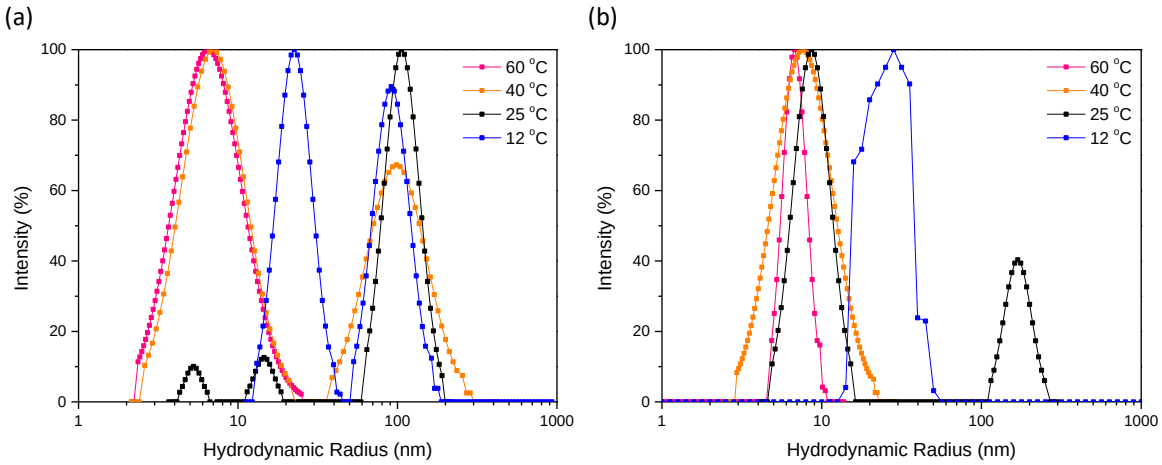

Figure 4.12. (a) R_h distributions of PCS3 in pH = 3.18 at several temperatures (conc. = 3.33 mg/mL) (b) R_h distributions in pH = 12 at several temperatures. (CONTIN fit, intensity-based, scattering angle = 90º)

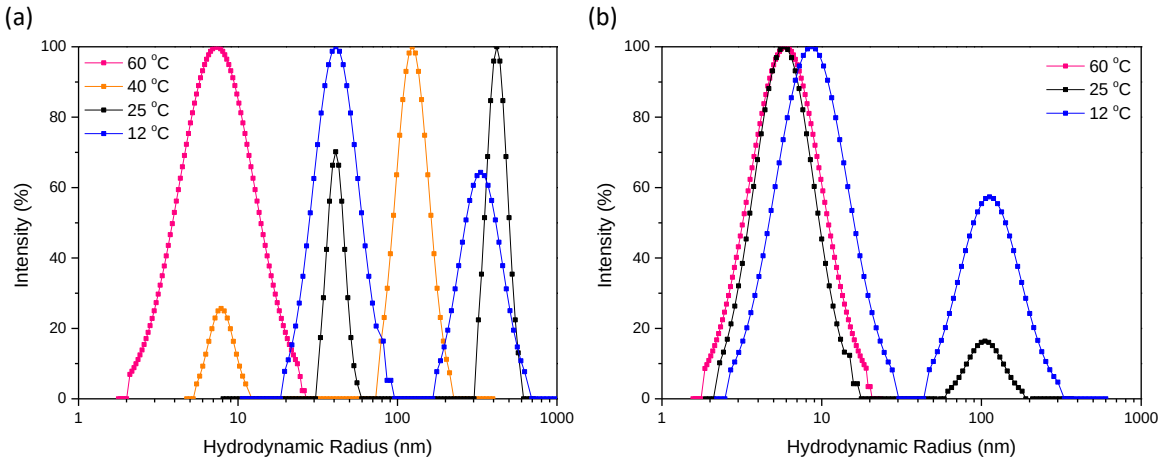

Figure 4.13. (a) R_h distributions of PCS4 in pH 2.9 at several temperatures (conc. = 3.33 mg/mL) (b) R_h distributions in pH = 12 at several temperatures (CONTIN fit, intensity-based, scattering angle = 90º)

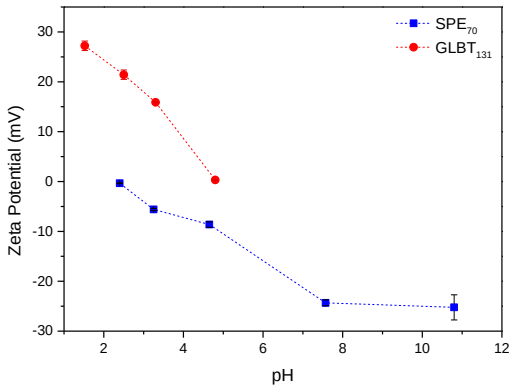

Figure 4.14. Zeta potential of two homo-polybetaines: SPE_{70} and $GLBT_{131}$ under varying pH

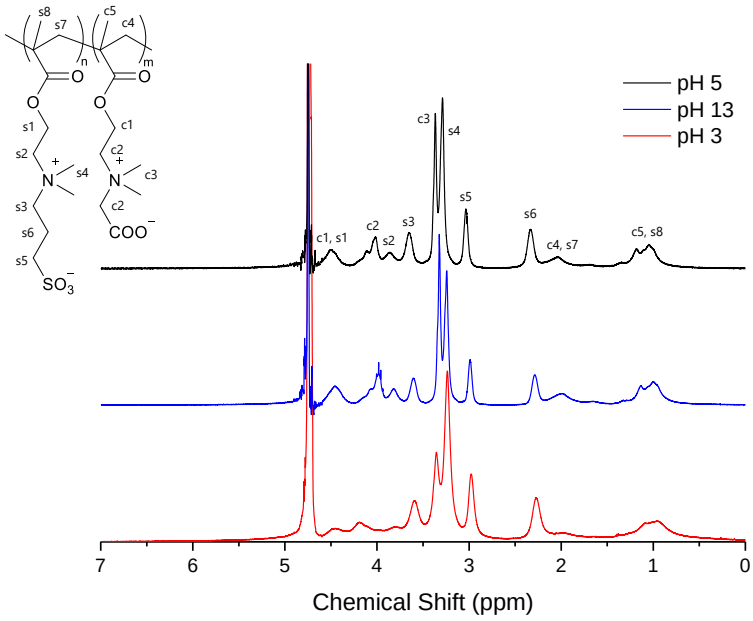

Figure 4.15. ^{1}H NMR spectra of PCS1 at neutral (pH = 5), acidic (pH = 3), and basic (pH = 13) condition obtained at room temperature. The pH was tuned by deuterated hydrochloric acid (DCl) and sodium hydroxide (NaOD) solution.

Conclusion

We elucidated the pH-sensitivity of the double betaine diblock copolymer PGLBT-*b*-PSPE. In acidic condition, all PGLBT-*b*-PSPE samples showed increased CPs and earlier phase transitions while cooling, and lowered CPs and suppressed particle formation in alkaline condition. Notably, slow diffusive modes indicating large aggregations or clusters over dozens of times bigger than micellar forms prevailed in a highly fussy solution and coexisted with fast modes (unimers or micelles) simultaneously at low pHs. However in alkaline condition, the original temperature-responsive behaviour was repeatedly expressed but occurred at lower temperatures. The zeta potential change from zero/negative to positive values by H^{+} addition was attributed to partly cationised PGLBT motifs by protonation of carboxylate ends. Moreover, the zeta potentials substantially increased to ~20 mV below the temperature where the larger particles (over 100 nm) started to emerge. Hence, it suggests a density increase of positively charged PGLBT moieties at the slip plane of the particles, caused by the self-assembly. Even the positively biased surface, the colloidal stability was not maintained and large clusters appeared alongside polymer micelles. Interchain hydrogen bonding between carboxylic acid groups of PGLBT corona could be the main attraction force among positively charged polymeric particles which eventually coagulated with time. On the other hand, the sensitivity to temperature decreased at high pHs although the degree of ionisation of PGLBT would be higher than usual, which may be due to counterion association to the charged sites.

References

1. J. Ladd, Z. Zhang, S. Chen, J. C. Hower and S. Jiang, *Biomacromolecules*, 2008, **9**, 1357-1361.
2. A. J. Keefe and S. Y. Jiang, *Nature Chemistry*, 2012, **4**, 60-64.
3. C. R. Emmenegger, E. Brynda, T. Riedel, Z. Sedlakova, M. Houska and A. B. Alles, *Langmuir*, 2009, **25**, 6328-6333.
4. K. J. Robinson, J. W. Coffey, D. A. Muller, P. R. Young, M. A. F. Kendall, K. J. Thurecht, L. Grondahl and S. R. Corrie, *Biointerphases*, 2015, **10**.
5. Y. He, J. Hower, S. F. Chen, M. T. Bernards, Y. Chang and S. Y. Jiang, *Langmuir*, 2008, **24**, 10358-10364.
6. J. B. Schlenoff, *Langmuir*, 2014, **30**, 9625-9636.
7. C. Leng, H. C. Hung, S. W. Sun, D. Y. Wang, Y. T. Li, S. Y. Jiang and Z. Chen, *Acs Applied Materials & Interfaces*, 2015, **7**, 16881-16888.
8. L. Tauhardt, D. Pretzel, K. Kempe, M. Gottschaldt, D. Pohlers and U. S. Schubert, *Polymer Chemistry*, 2014, **5**, 5751-5764.
9. R. Lalani and L. Y. Liu, *Biomacromolecules*, 2012, **13**, 1853-1863.
10. X. P. Zhang, W. Chen, X. Y. Zhu and Y. F. Lu, *Acs Applied Materials & Interfaces*, 2017, **9**, 7972-7978.
11. S. Morozova, G. Hu, T. Emrick and M. Muthukumar, *Acs Macro Letters*, 2016, **5**, 118-122.
12. J. D. Delgado and J. B. Schlenoff, *Macromolecules*, 2017, **50**, 4454-4464.
13. A. Z. Niu, D. J. Liaw, H. C. Sang and C. Wu, *Macromolecules*, 2000, **33**, 3492-3494.
14. Y. C. Zhu, J. M. Noy, A. B. Lowe and P. J. Roth, *Polymer Chemistry*, 2015, **6**, 5705-5718.
15. V. Hildebrand, A. Laschewsky and E. Wischerhoff, *Polymer Chemistry*, 2016, **7**, 731-740.
16. Y. Chang, W. Yandi, W. Y. Chen, Y. J. Shih, C. C. Yang, Q. D. Ling and A. Higuchi, *Biomacromolecules*, 2010, **11**, 1101-1110.
17. P. Dong, Y. Zhou, W. W. He and D. B. Hua, *Chemical Communications*, 2016, **52**, 896-899.
18. K. E. B. Doncom, N. J. Warren and S. P. Armes, *Polymer Chemistry*, 2015, **6**, 7264-7273.
19. K. E. B. Doncom, H. Willcock and R. K. O'Reilly, *European Polymer Journal*, 2017, **87**, 497-507.
20. N. S. Vishnevetskaya, V. Hildebrand, B. J. Niebuur, I. Grillo, S. K. Filippov, A. Laschewsky, P. Muller-Buschbaum and C. M. Papadakis, *Macromolecules*, 2016, **49**, 6655-6668.
21. N. S. Vishnevetskaya, V. Hildebrand, B. J. Niebuur, I. Grillo, S. K. Filippov, A. Laschewsky, P. Muller-Buschbaum and C. M. Papadakis, *Macromolecules*, 2017, **50**, 3985-3999.
22. N. S. Vishnevetskaya, V. Hildebrand, M. A. Dyakonova, B. J. Niebuur, K. Kyriakos, K. N. Raftopoulos, Z. Y. Di, P. Muller-Buschbaum, A. Laschewsky and C. M. Papadakis, *Macromolecules*, 2018, **51**, 2604-2614.
23. H. Sun, X. L. Chen, X. Han and H. L. Liu, *Langmuir*, 2017, **33**, 2646-2654.
24. Q. Shao, L. Mi, X. Han, T. Bai, S. J. Liu, Y. T. Li and S. Y. Jiang, *Journal of Physical Chemistry B*, 2014, **118**, 6956-6962.
25. A. S. Lee, V. Butun, M. Vamvakaki, S. P. Armes, J. A. Pople and A. P. Gast, *Macromolecules*, 2002, **35**, 8540-8551.
26. X. Andre, M. F. Zhang and A. H. E. Muller, *Macromolecular Rapid Communications*, 2005, **26**, 558-563.
27. A. E. Smith, X. W. Xu, S. E. Kirkland-York, D. A. Savin and C. L. McCormick, *Macromolecules*, 2010, **43**, 1210-1217.
28. E. R. Jones, M. Semsarilar, A. Blanazs and S. P. Armes, *Macromolecules*, 2012, **45**, 5091-5098.
29. T. Boyaci and N. Orakdogen, *Rsc Advances*, 2015, **5**, 77235-77247.
30. L. Lauber, J. Santarelli, O. Boyron, C. Chassenieux, O. Colombani and T. Nicolai, *Macromolecules*, 2017, **50**, 416-423.
31. Z. Zhang, H. Vaisocherova, G. Cheng, W. Yang, H. Xue and S. Y. Jiang, *Biomacromolecules*, 2008, **9**, 2686-2692.
32. Z. Q. Cao, L. Mi, J. Mendiola, J. R. Ella-Menye, L. Zhang, H. Xue and S. Y. Jiang, *Angewandte Chemie-International Edition*, 2012, **51**, 2602-2605.
33. M. Birkner and M. Ulbricht, *Journal of Membrane Science*, 2015, **494**, 57-67.
34. J. Lim, H. Matsuoka, S. Yusa and Y. Saruwatari, *Langmuir*, 2019, **35**, 1571-1582.
35. Y. Mitsukami, M. S. Donovan, A. B. Lowe and C. L. McCormick, *Macromolecules*, 2001, **34**, 2248-2256.
36. J. G. Weers, J. F. Rathman, F. U. Axe, C. A. Crichlow, L. D. Foland, D. R. Scheuing, R. J. Wiersema and A. G. Zielske, *Langmuir*, 1991, **7**, 854-867.

37. V. A. Izumrudov, N. I. Domashenko, M. V. Zhiryakova and O. V. Davydova, *Journal of Physical Chemistry B*, 2005, **109**, 17391-17399.
38. P. Mary, D. D. Bendejacq, M. P. Labeau and P. Dupuis, *Journal of Physical Chemistry B*, 2007, **111**, 7767-7777.
39. M. Du, Y. J. Ma, H. Su, X. Wang and Q. Zheng, *Rsc Advances*, 2015, **5**, 33905-33913.
40. B. R. Knowles, P. Wagner, S. Maclaughlin, M. J. Higgins and P. J. Molino, *Acs Applied Materials & Interfaces*, 2017, **9**, 18584-18594.
41. S. S. Guo, D. Janczewski, X. Y. Zhu, R. Quintana, T. He and K. G. Neoh, *Journal of Colloid and Interface Science*, 2015, **452**, 43-53.
42. S. Abraham, A. So and L. D. Unsworth, *Biomacromolecules*, 2011, **12**, 3567-3580.
43. L. Wu, J. Jasinski and S. Krishnan, *Journal of Applied Polymer Science*, 2012, **124**, 2154-2170.
44. Y. J. Zhang and P. S. Cremer, *Annual Review of Physical Chemistry, Vol 61*, 2010, **61**, 63-83.
45. E. Schonemann, A. Laschewsky and A. Rosenhahn, *Polymers*, 2018, **10**.

Chapter 5. One-Pot Synthesis of Double and Triple Polybetaine Block Copolymers and Their Temperature-Responsive Solution Behaviour

ABSTRACT: Di- and triblock betaine copolymers composed of a sulfobetaine with a carboxy/phosphobetaine were synthesised by one-pot aqueous reversible addition-fragmentation chain transfer (RAFT) polymerisation. The betaine methacrylate monomers were fully converted at each step by tuning the concentrations of the monomers, the chain transfer agent, and the initiator, hence no purification was necessary at the intervals. AB-type diblocks poly(carboxybetaine methacrylate)-*b*-poly(sulfobetaine methacrylate) (PGLBT-*b*-PSPE) and poly(2-(methacryloyloxy)ethyl phosphorylcholine)-*b*-poly(sulfobetaine methacrylate) (PMPC-*b*-PSPE) were prepared to have closely identical block ratios with different total molecular weights. Unlike homo-polysulfobetaine solutions or our previous report on PGLBT-*b*-PSPE, the aqueous solutions of those betaine diblock copolymers showed only weak upper critical solution temperature (UCST) behaviour monitored by transmittance/dynamic light scattering. Even at the lowest temperature, the diblock chains remained in the unimer/aggregate polydisperse state, which is the intermediate stage prior to emergence of monodisperse micelles. The UCST behaviour that originated from electrostatic attraction among PSPE motifs was considered to have been interfered by temperature-inert zwitterionic motifs (PGLBT/PMPC) on the opposite side, having nearly the same composition. The BAB-type triblock copolymer PSPE-PGLBT-PSPE with a 1:1:1 ratio showed a clearer transmittance shift and size variation due to the increased ratio of PSPE placed at both ends. While the transmittance gradually decreased by cooling, larger aggregates (~700 nm) than those of diblocks (~180 nm) emerged with unimers. Then the multiple diffusive modes finally rearranged to monodisperse micelles at much lower temperatures. Flower-like micelles that might consist of PGLBT-loop coronas and tightly packed PSPE motifs at the centre appeared. However, another sample whose ratio was 1:2:1 showed incomplete transition as diblocks having a similar AB ratio.

Introduction

Studies on polyzwitterions and their derivative copolymers have been extensively carried out to utilise their unique characteristics. Having ionic groups with opposite signs on the same repeating unit, the overall charge of polyzwitterions is inherently neutral and exhibits distinguished properties from polyelectrolytes and non-ionic polymers.[1] Ionic polymers usually associate with counterions to keep neutrality and collapse by increasing salt

("salting-out" behaviour), which is attributed to reduced net charge and hydrophilicity. However, polyzwitterions which basically do not contain counterions attract or repel each other between their charged functional groups, and become more soluble and swell in water under increasing salt ("salting-in" behaviour). Dipole–dipole interactions between oppositely charged groups in other chains or the same chain make them globulised and may result in aggregations in salt-free water, and addition of low molecular weight salts hinders those pairings by charge screening.[2] Consequently, polyzwitterions in globular form start to swell in water and increase viscosity.

Among several kinds, polysulfobetaines are particularly known for upper critical solution temperature (UCST) behaviour in aqueous solution because of strong tendency of forming the electrostatic attraction. The critical temperature of polysulfobetaine aqueous solutions is also under influence of salt presence: more amount of salts retard the phase separation to lower temperature by screening.[3, 4] The dipole orientation among polyzwitterion chains is captured as slow diffusive modes simultaneously appearing with fast-diffusing modes representing unimers in dynamic light scattering study,[5-8] which seem to be analogous to "ordinary–extraordinary" transition observed in polyelectrolytes solutions[9-11] but may be brought by different mechanisms.

Besides, polyzwitterions have a distinctive hydration layer as representing an "unperturbed" state according to the studies observing hydrogen bonding around zwitterionic units using Raman[12, 13] or sum frequency generation (SFG) vibrational spectroscopy.[14, 15] Hydrogen bonding (H-bonding) of water molecules at the vicinity of zwitterionic units are not disrupted and the ordering does not have significant differences from that in bulk water, contrary to typical polyelectrolytes causing disruption of H-bonding.[16] Thanks to the unperturbed state of H-bonding and tightly bound water molecules on the chain surface, polyzwitterions show remarkable nonfouling behaviour. Replacement of water molecules around polyzwitterions to other molecules which can adsorb on the surface was more difficult than at non-ionic poly(ethylene glycol) (PEG) or oligo(ethylene glycol) methacrylate (OEGMA) chains.[14] Polyzwitterion-coated 2D surfaces were evaluated to have superior antifouling property than OEGMA or self-assembled monolayers[17] and polyelectrolyte surface[18] on protein adsorption.

The traits have been exploited by copolymerising polyzwitterions with other non-ionic hydrophilic/hydrophobic units to modify and add properties. Statistical copolymers consisting of non-ionic,[19-22] ionic polymers[23] or different kinds of polyzwitterions[24, 25] were tested. Polybetaine-based block copolymers such as amphiphilic,[26-29] double hydrophilic,[30] and dual stimulus-responsive[31-35] types were also developed. Previously, we synthesised a double hydrophilic betaine block copolymer PGLBT-*b*-PSPE (2-((2-(methacryloyloxy)ethyl)dimethylammonio)acetate-*b*-3-((2-(methacryloyloxy)ethyl)dimethylammonio)propane-1-sulfonate) by reversible addition-fragmentation

chain transfer (RAFT) polymerisation and elucidated their responses to temperature, salt, and pH in aqueous media.[36] Technically, both motifs of the block copolymers were strongly hydrophilic and only soluble in high polar solvents among typical organic solvents. PSPE parts became gradually hydrophobic in relative to the opposite side by temperature decrease, then the increased difference of water affinity led polymer chains to create self-assembled structure whose inner side is mostly PSPE to minimise enthalpic penalty under the critical temperature. However, the ratio of PGLBT and PSPE was only roughly controllable because of the low percentage of macroCTA chains (PGLBT homopolymers) properly functioned in the second polymerisation step by indiscernible reasons, presumably related to the stability of the RAFT functional groups. For that reason, the effect of block ratio and total repeating unit numbers on the characteristics of PGLBT-*b*-PSPE was not elucidated in detail.

In this study, we performed one-pot synthesis of betaine methacrylate-based diblock and triblock copolymers by applying the methodology extensively investigated by Perrier's group[37-41] to avoid factors which may destabilise RAFT functionality, and to obtain well-defined block copolymers through a more accessible process within less preparation time.

Experimental Section

Materials

2-((2-(Methacryloyloxy)ethyl)dimethylammonio)acetate (carboxybetaine methacrylate, GLBT) and 3-((2-(methacryloyloxy)ethyl)dimethylammonio)propane-1-sulfonate (sulfobetaine methacrylate, SPE, also referred to SBMA in other reports) were kindly donated from Osaka Organic Chemical Industry LTD (Osaka, Japan) and used as received. 2-Methacryloyloxyethyl phosphorylcholine (MPC) was a kind donation from K. Ishihara's group (Univ. of Tokyo) 4-Cyano-4-(2-phenylethanesulfanylthiocarbonyl)sulfanylpentanoic acid (PETTC) was synthesised according to the literature[42] and used as a chain transfer agent (CTA). The radical initiator 2,2'-azobis[2-(2-imidazolin-2-yl)propane]dihydrochloride (VA-044) was purchased from Wako Chemicals (Osaka, Japan) and used as received. 2,2,2-trifluoroethanol (TFE) was purchased from Nacalai Tesque and used as received. Deuterated water (D_2O) was purchased from Cambridge Isotope Laboratories. Ultrapure water (minimum resistivity ~18.2 MΩ cm) obtained by the Milli-Q system was used for synthesis, dialysis, and aqueous solution

sample preparation. Dialysis was performed using regenerated cellulose membranes (MWCO 3500 and 15000) to remove residues.

Block copolymer synthesis by consecutive RAFT polymerisation

Firstly, CTA (PETTC), monomer, initiator, water and TFE (8:2, v/v) were put into a rubber septum-sealed glass vial with a magnetic stirrer. After vigorous mixing and degassing by 15 minutes of argon bubbling, the vial was placed in an oil bath thermostated at 70 ºC to start RAFT polymerisation. Aliquots were taken during synthesis using a syringe for ^{1}H NMR and SEC analysis. Once full monomer consumption was confirmed, the vial was transferred in an ice bath and cooled to end the reaction. For additional blocks, new monomers were added to the vial with additional initiator and water, and the reactant solution was degassed before the initiation of the next polymerisation. The procedure was repeated until the target block copolymers were obtained. The final products were purified by dialysis against Milli-Q. The reservoir was discarded twice per day, until the electric conductivity of reservoir water was equlibrated then lyophilised to yield yellow powder. The detailed experimental conditions are shown in **Scheme 5.1** and **Table 5.2**–**5.4**

Polymer characterisation

^{1}H nuclear magnetic resonance (NMR) spectra of synthesised polymers were acquired on a 400 MHz JEOL JNM-AL400 spectrometer (JEOL, Tokyo, Japan) in deuterated water (D_2O). Chemical shifts (δ) are reported in ppm relative to H_2O (4.75 ppm). A Minimum of 64 scans were recorded for each sample.

Aqueous size exclusion chromatography (SEC) was peformed with a column (SB-804 HQ, Shodex) and a refractive index detector (RI-830, JASCO, Japan), using a buffer eluent (0.5 M CH_3COOH and 0.3 M of Na_2SO_4) at a flow rate of 0.5 mL/min. The number-average molecular weight (M_n) and dispersity (M_w/M_n, denoted as $Đ$) of each homo- and multiblock copolymers were determined by the calibration performed with a set of poly(2-vinylpyridine) standards. (M_n range: 5500 to 142000 g/mol, Sigma-Aldrich)

The transmittance at 200–600 nm for the aqueous solutions of the block copolymers were recorded from 60 ºC to ~5 ºC at regular intervals after waiting for 5 min at each temperature using a UV-VIS spectrometer (Hitachi U-3310 spectrophotometer) equipped with a temperature-controlling water circulator. A quartz cell with a light path of 10 mm was used. Each solution was filtered by a syringe filter unit (pore size: 0.2 μm, mdi) prior to measurement. The transmittance value at 400 nm was taken for the plot against temperature.

Dynamic light scattering (DLS) was performed to measure the hydrodynamic radius (R_h) of the polymers in aqueous solution. A goniometer (BI-200SM, Brookhaven Instruments, New York, USA) equipped with a 15 mW He-Ne laser (wavelength λ = 632.8 nm) and a water circulator was used. (index matching fluid = decahydronaphtalene) The field autocorrelation functions were obtained by a BI-DS2 photomultiplier tube with a correlator (TurboCorr, Brookhaven Instruments) at four scattering angles (60°, 75°, 90°, and 105°) and analysed by CONTIN regularization. All the autocorrelation functions (ACFs) are reported as $((g^{(2)}(q,t)-1)/\beta)^{0.5}$. The concentration of polymer aqueous solution samples of transmittance and DLS measurement was 10 mg/mL.

Determination of monomer conversions

The monomer conversions were calculated from ^{1}H NMR spectra with following equation as described in the literature[40]:

$$p = \frac{[\mathrm{M}]_0 - [\mathrm{M}]_t}{[\mathrm{M}]_0} = 1 - \frac{[\mathrm{M}]_t}{[\mathrm{M}]_0} = 1 - \frac{\frac{\int I_{5.7-6.2\ ppm}}{\int I_{CTA}}}{\mathrm{DP_{target}}} \quad (5.1)$$

where $[M]_0$ and $[M]_t$ are the monomer concentrations at the initial and passed time t, $\int I_{5.7–6.2\ ppm}/\int I_{CTA}$ is the corrected proton ratio of the unreacted monomer to the CTA at the end of the chain. DP_{target} is the targeted number-average degree of polymerisation. Each conversion was also determined by the following equation:

$$p = \frac{\int I_p}{\int I_p + \int I_m} \quad (5.2)$$

where $\int I_p$ is the corrected integral value of polymer peaks and $\int I_m$ is that for vinyl protons of the monomer.

Determination of number-average theoretical molecular weight ($M_{n,\ theo}$) and theoretical living chain fraction

By the following equation introduced the work of Gody et al,[37] $M_{n,theo}$ can be determined as the following equation:

$$M_{\mathrm{n,theo}} = \frac{[M]_0 \cdot p \cdot M_{\mathrm{M}}}{[\mathrm{CTA}]_0 + 2f[\mathrm{I}]_0(1 - e^{-k_d t})(1 - \frac{f_c}{2})} + M_{\mathrm{CTA}} \approx p \cdot DP_{\mathrm{target}} \cdot M_{\mathrm{M}} + M_{\mathrm{CTA}} \quad (5.3)$$

where $[M]_0$, $[CTA]_0$, $[I]_0$ are the initial concentration of monomer, CTA, and initiator, respectively. M_M and M_{CTA} are the molar mass of the monomer and CTA, respectively. The k_d is the decomposition rate constant of the azoinitiator. ($k_{d(\mathrm{VA-044,70\ °C})} = 4.2995 \times 10^{-4}\ \mathrm{s^{-1}}$, which was an estimated value in the literature[37]) t is the time

of polymerization. The term 2*f* means that one azoinitiator molecule provides two radicals with the efficiency *f*. (*f* was set to 0.5 in the study) The coupling factor f_c represents the ratio of chain termination types. (f_c = 1 is combination of two active chain ends and f_c = 0 is radical disproportionation) In this study, the initiator term could be dismissed as 0 due to the negligible amount of participated initiator, so the equation can be reduced as the form of the right side. Following the same concept,[37] the livingness of chains (% of CTA-ended chains) could be expressed by the equation (5.4):

$$\mathrm{L} = \frac{[\mathrm{CTA}]_0}{[\mathrm{CTA}]_0 + 2f[\mathrm{I}]_0(1 - e^{-k_d t})(1 - \frac{f_c}{2})} \tag{5.4}$$

Results and discussions

In our previous report,[36] the carboxybetaine-sulfobetaine diblock copolymer PGLBT-*b*-PSPE was synthesised by RAFT polymerization following conventional procedures for block copolymerization. PGLBT homopolymers were synthesised using a dithobenzoate type RAFT agent (4-cyanopentanoic acid dithiobenzoate) (CPADB), which is widely used as water-soluble CTA. Unlike synthesis of polybetaine derivative block copolymers that consist of hydrophobic or anionic/cationic units or even a statistical betaine copolymer (PGLBT-*r*-PSPE), the activity of macroCTA (homo-PGLBT) was severely lost in the second polymerization step. Only a few PGLBT homopolymers involved in PSPE growth, and resulted in uncontrollable block ratios. Therefore, the removal of unreacted PGLBT by precipitation into methanol was necessitated. Hydrolytic cleavage of the dithiobenzoate end group was assumed to occur when they were exposed to water molecules[43] although the polymerization was conducted at a lowered temperature (45 °C) by using a faster decomposing azoinitiator (VA-044) to prevent possible hydrolysis. Cyano-hydrolysis on the R group during usage or storage by water contamination[44] also could be the reason. Since trithiocarbonate-type RAFT agents are known for enhanced stability against hydrolysis and less retardation dependent on the concentration of CTA,[45] we selected PETTC, which is a kind of trithiocarbonate RAFT agent having a chemical structure similar to CPADB and successfully conducted polymerization-induced self-assembly of amphiphilic methacrylate copolymers,[42, 46-48] for successive polymerization of betaine methacrylates. Also, purification through dialysis prior to subsequent polymerization steps can be omitted by achieving full conversion of the monomers.

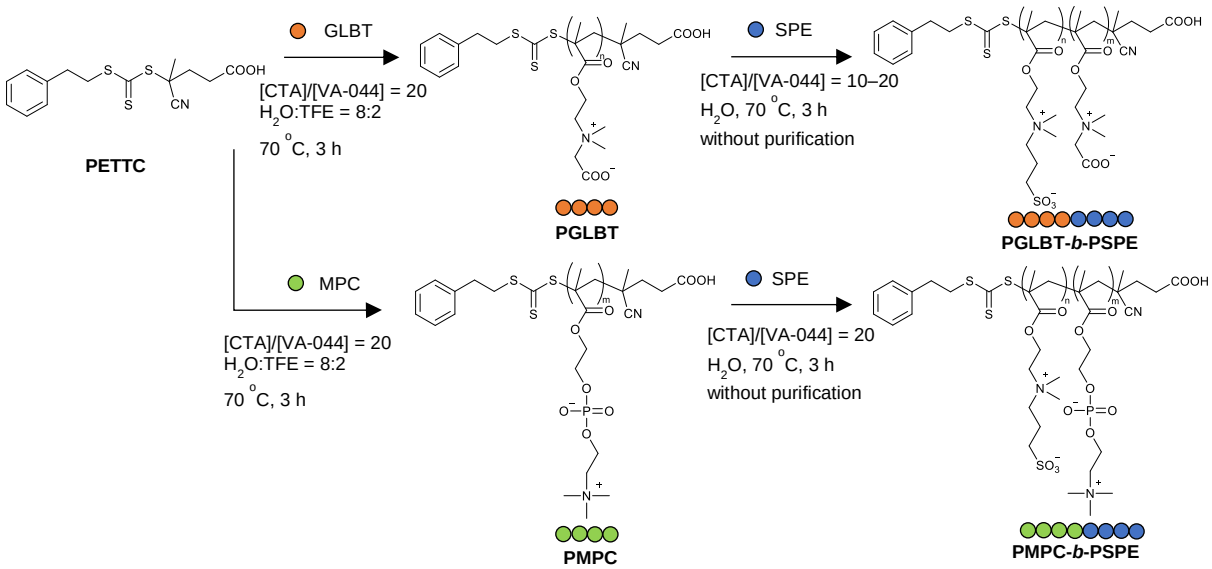

Scheme 5.1. Synthetic routes for the preparation of betaine diblock copolymers by one-pot RAFT polymerisation

One-pot polymerisation of PGLBT-*b*-PSPE and PMPC-*b*-PSPE

We aimed to produce PGLBT-*b*-PSPE having an identical block ratio as a model study. The targeted DP of each block was set to over 50 to make the block copolymers show temperature responsive characters in an easily detectable temperature range. Typically, PSPE homopolymers obtained in our group whose target DP was 50–200 showed cloud points at 10–30 °C. PGLBT was synthesised prior to PSPE in order that purification of residual homopolymers from block copolymer products may become necessary. The reactant solution containing GLBT, PETTC, and VA-044 in water/TFE mixture was placed in an oil bath thermostated at 70 °C. (**Scheme 5.1**) Compared to the previous study, the temperature was increased from 45 to 70 °C to attain full conversion within a short reaction time by increasing the radical decomposition rate. Water was used again as the main solvent because it is one of few good solvents for polybetaines. Moreover, it was reported to induce the highest propagation rate of acrylamide monomers.[49] At the first polymerization step, TFE was required to compensate poor solubility of PETTC in water. Since only fluorinated alcohols (e.g. TFE and 1,1,1,3,3,3-hexafluoroisopropanol (HFIP)) can dissolve polysulfobetaines among organic solvents due to strong polarity, it was assumed to cause no detrimental effect upon the whole step. The conversion of PGLBT calculated by monomer signals (5.7–6.2 ppm, from vinyl ends) with polymer peaks or PETTC peaks (7.4 ppm, from phenyl group) was 90% at 1 h and reached full conversion (~99%) at 3 h. The disappearance of monomer peaks by reaction time is shown in **Figure 5.1(a)**. SPE monomer, additional initiator and water for the second step were subsequently transferred into the quenched PGLBT solution. Only water was added as an additional solvent

because of increased hydrophilicity of the CTA after PGLBT growth. The monomer concentration ([SPE]) was kept lower than [GLBT] at the first step to prevent inhomogeneous mixing by increasing viscosity. On the second block synthesis, an aliquot withdrawn at 2 h showed no clearly visible monomer peaks, and the reaction was terminated at 3 h. The ^{1}H NMR spectra of the crude product as shown in **Figure 5.1(b)** shows additional peaks of SPE repeating units in comparison with the signals of $GLBT_{49}$. The molecular weight distribution (MWD) (**Figure 5.1(c)**) of the diblock copolymers showed a clear shift from a low (homopolymer) to higher molecular weight without residues suggesting that almost every PGLBT macroCTA participated in the SPE polymerization and formed PGLBT-*b*-PSPE. Compared to the previous results of PGLBT-*b*-PSPE synthesis, full conversion of GLBT was not achieved after 24 h; the PGLBT homopolymer had to be purified through excessive dialysis before the next step. Furthermore, most of PGLBT did not act as a macroCTA and yielded only a small portion of the block copolymer. Precipitation into methanol for two times did not thoroughly separate residues from the diblock copolymer products.

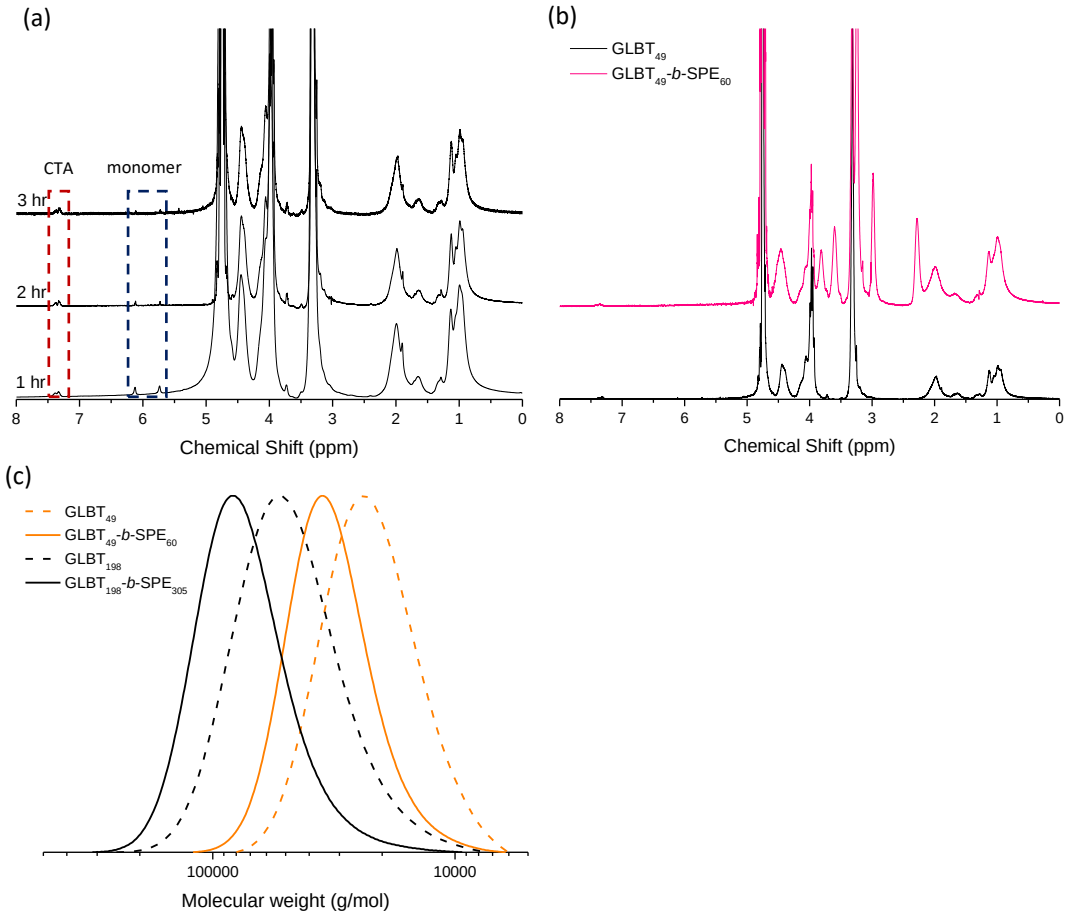

Figure 5.1. (a) ^{1}H NMR spectra of $GLBT_{49}$ taken at 1 h intervals. (b) ^{1}H NMR spectra of $GLBT_{49}$ (black) and $GLBT_{49}$-*b*-SPE_{60} (red) obtained from aliquots withdrawn after 3 h (c) MWDs of $GLBT_{49}$ and $GLBT_{49}$-*b*-SPE_{60}, and $GLBT_{198}$ and $GLBT_{198}$-*b*-SPE_{305} by SEC analysis

To obtain higher molecular weight copolymers, the total DP was doubled or quadrupled with the fixed monomer feed ratio 1:1. The target DP of each segment was set to 100 and 200 with same [CTA]/[I]. For the batch of DP_{target} = 200:200, [I] was increased twice to speed up the polymerization at the second polymerization step because of the reduced monomer concentration for adjusting workable viscosity. Both products resulted in relatively narrowly controlled MWD (~1.3) and monomodal peak shift. However, low molecular weight tailing was observed on the DP_{target} = 200:200 sample, which may be attributed to inhomogeneous mixing. The DP determined by ^{1}H NMR analysis ($GLBT_{198}$-*b*-SPE_{305}) showed excess PSPE, which implies an inhomogeneous solution state during the reaction. The dispersity and number imbalance were improved on the batch of DP_{target} = 100:100, in which the polymerization was carried out keeping the same [CTA]/[I] since less viscosity increase.

Table 5.1. Summary of the betaine block copolymers synthesised in the study

Sample name	$M_{n\ theo}$ (g/mol)	$M_{n\ SEC}$ (g/mol)	$Đ$ (M_w/M_n)	% L_{final}
$GLBT_{49}$-*b*-SPE_{60}	27600	25720	1.14	90.9
$GLBT_{99}$-*b*-SPE_{121}	55500	31200	1.12	90.7
$GLBT_{198}$-*b*-SPE_{305}	128000	68270	1.21	86.6
MPC_{198}-*b*-SPE_{205}	116100	71350	1.29	86.6
SPE_{49}-*b*-$GLBT_{46}$-*b*-SPE_{55}	39300	40100	1.16	82.6
SPE_{99}-*b*-$GLBT_{193}$-*b*-SPE_{135}	107300	71030	1.33	78.8

A different combination of double betaine block copolymer PMPC-*b*-PSPE, which had a phosphobetaine instead of a carboxybetaine, was synthesised by the same method. Basically a methacylate monomer, MPC was rapidly consumed (98% after 1 h) like the other betaine monomers under the same reaction condition, and the reaction was stopped at 3 h when the proton signals of the monomer disappeared. The macroCTA PMPC subsequently reacted with SPE monomers without any purification, and yielded PMPC-*b*-PSPE after 3 h with ~99% conversion. The ^{1}H NMR spectra of both are shown in **Figure 5.2(a)** and the DP was estimated as 198:205. Although the relatively broad MWD (Đ = 1.29) is thought to be attributed to insufficient mechanical strength while mixing the reaction solution, especially at the second step operated under an extremely viscous state, no unreacted homopolymer peak was found in the SEC trace (**Figure 5.2(b)**) and this indicated that most of the homo-PMPC chains conducted SPE growth.

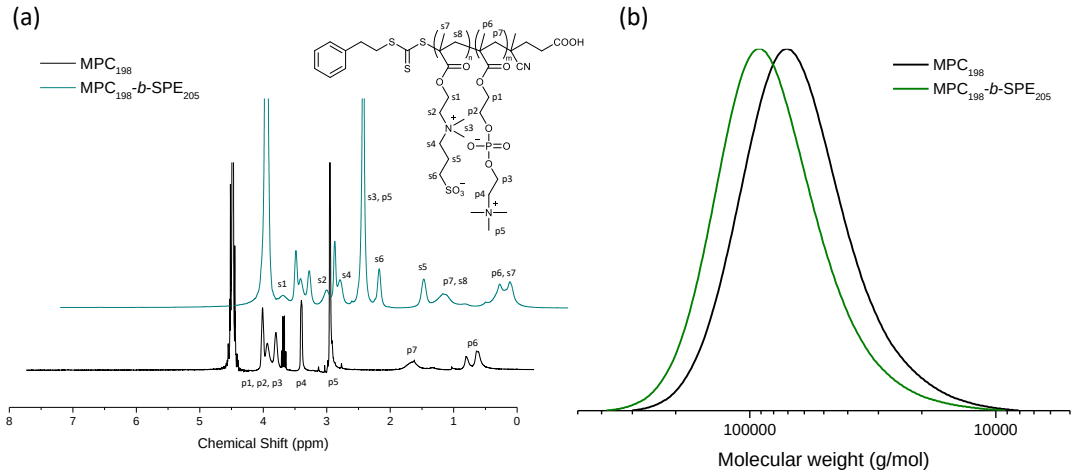

Figure 5.2. (a) ^{1}H NMR spectra of MPC_{198} (black) and MPC_{198}-*b*-SPE_{205} (green) (b) MWDs of MPC_{200} (black) and MPC_{198}-*b*-SPE_{205} (green) by SEC analysis

Temperature-responsive solution behaviour of obtained betaine diblock copolymers

The temperature sensitivity of three PGLBT-*b*-PSPEs targeted to have an identical PGLBT:PSPE ratio with different total DP was characterised. Since PSPE segments could lose hydrophilicity below critical temperatures where intra/interchain electrostatic attractions become prominent, the PSPE moieties merge together and create cores while temperature-independent PGLBT motifs form outer layers. The hydrodynamic radii (R_h) of self-assembled core-shell particle was approximately 40–60 nm with a relatively narrow size distribution,[36] which is a remarkable feature in comparison with similar polysulfobetaine-based block copolymers having a non-ionic counterpart. For example, PEG[50] or PDMAEMA[51] motifs on the opposite side of polysulfobetaine chains led to larger particles over several hundred nanometers. Dual charges of PGLBT may provide adequate repulsive force which could lead to monodisperse and relatively small-sized particle formation and prevent further agglomeration.

In this study, the three obtained PGLBT-*b*-PSPEs showed subtle variations of the transmittance and R_h as compared with our previous study that showed a drastic size and turbidity change around 20–40 °C. As shown in **Figure 5.3(a)**, $GLBT_{49}$-*b*-SPE_{60} existed as individual polymer chains within most of the temperature range while over 90% of the transmittance was maintained. A slow diffusive mode (mode B, the relative weight was 70 % at 90° by intensity-based determination) started to appear with fast-diffusing unimers (mode A) under 10 °C. The presence of the slow diffusive mode related to attractions among dipoles of the pendent groups is not only a common feature of homo-polysulfobetaine aqueous solution[5, 8] but also a prior change before monodispersed particle formation of PGLBT-*b*-PSPE as revealed in our previous study.[36] However, monodisperse particles were

not found at the end of the observation range. In accordance with Gibbs free energy of mixing $\Delta G_m = \Delta H_m - T\Delta S_m$, the enthalpy of mixing of the polymer may be lowered by equally numbered PGLBT to PSPE, and would become sufficient to prevent phase transition. Instead of forming self-assembled structures, the uniformly swollen and hydrated chain state is thought to be thermodynamically preferred at lower temperatures. This weak temperature-responsive solution behaviour reappeared similarly on two other PGLBT-*b*-PSPEs having higher molecular weights. $GLBT_{99}$-*b*-SPE_{121} existed as unimers accompanying a size-increasing slow mode by cooling below 40 °C, and did not create monodisperse micelles (**Figure 5.3(b)**). On the other hand, $GLBT_{198}$-*b*-SPE_{305} showed a significant size increase to 45 nm at the lower temperature (**Figure 5.3(c)**) with more visible transmittance decrease. Only the ACFs of $GLBT_{198}$-*b*-SPE_{305} showed a shift from a fast monomodal decay to a slow monomodal decay while the others were represented by broadly decaying curves at 5 °C. (**Figure 5.6**) It is thought that a higher DP imbalance of the two repeating units drives the polymer chain to create compactly packed PSPE cores below a certain temperature, whereas the nearly identical DP ratio tends to prohibit the transition and keep a polydisperse and intermediate state.

In addition, MPC_{198}-*b*-SPE_{205} showed the same behaviour against temperature as the PGLBT-*b*-PSPEs did (**Figure 5.3(d)**). Having almost same DP of both respective units, the chains existed as homogeneous unimers until 25 °C, then a slow diffusive mode emerged and became dominant at the end. However, alteration to monodisperse micelles did not occur like the previous samples. ($GLBT_{49}$-*b*-SPE_{60} and $GLBT_{99}$-*b*-SPE_{121}) No specific difference from PGLBT-*b*-PSPEs was found. Thus, it is thought that PMPC motifs played the same role as PGLBT in PGLBT-*b*-PSPEs intervening the pairing of polysulfobetaine moieties. It is known that polyphosphobetaines including PMPC are not responsive to temperature like polycarboxybetaines, but multiple diffusive modes in aqueous solution have been reported on double polyphosphobetaine block copolymers consisting of PMPC and inverted phosphobetaine repeating units having slightly high hydrophobicity.[7] Therefore, dipole–dipole attractions between PMPC and PSPE as well as PGLBT with PSPE motifs might occur, but it does not seem to be preferred than the pairing amongst PSPE and not to maintain firmly as PSPE moieties, which create cores of monodisperse micelles.

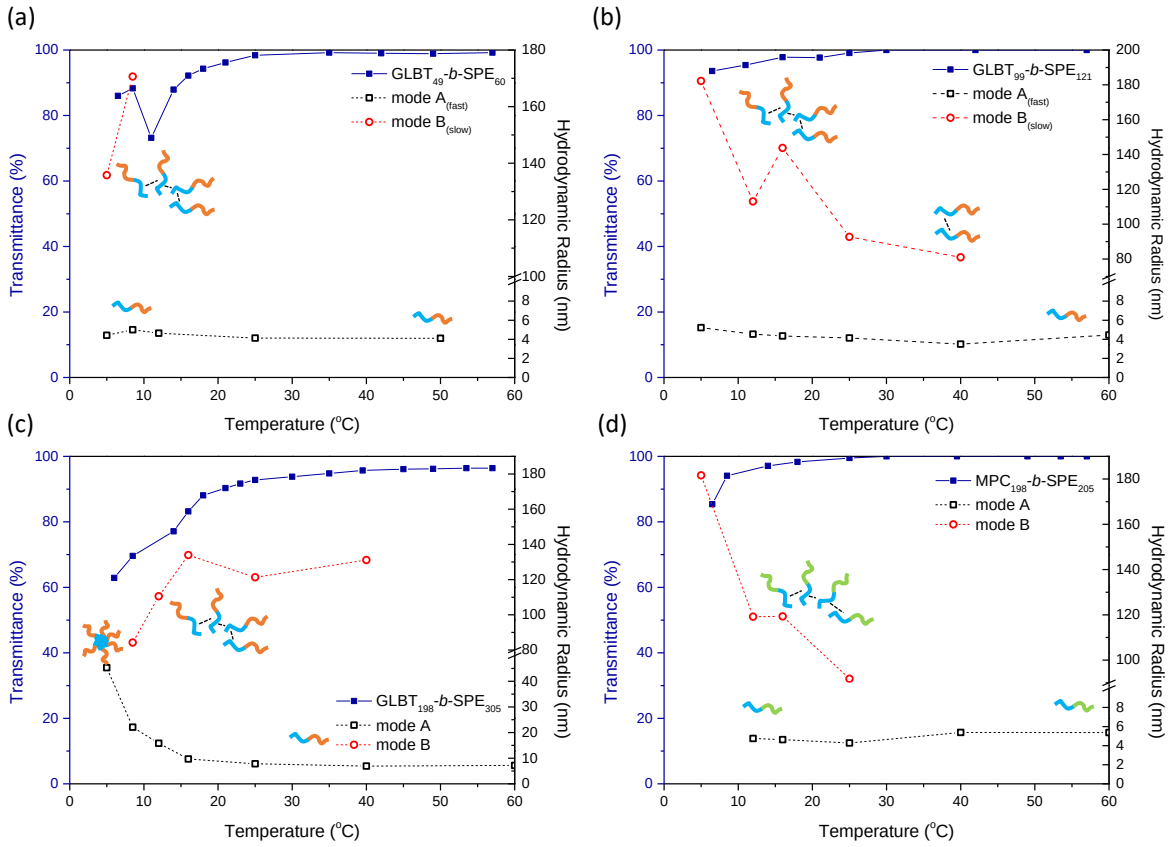

Figure 5.3. Transmittance shift (left y axis, solid symbols) and Hydrodynamic radius variation (right y axis, open symbols) by temperature of double betaine block copolymers (a) $GLBT_{49}$-*b*-SPE_{60} (b) $GLBT_{99}$-*b*-SPE_{121} (c) $GLBT_{198}$-*b*-SPE_{305} (d) MPC_{198}-*b*-SPE_{205}

One-pot polymerisation of triblock betaine copolymers

The arrangement of betaine block copolymers was extended to three consecutive polymerizations through the one-pot approach. In the experiment, PSPE was synthesised prior to PGLBT then thirdly for yielding double PSPE-ended chains, which were expected to show extra possible interaction modes, so that more complex temperature-responsive behaviours than that of diblock copolymers may be envisaged. Each batch was aimed to synthesise 50 units (DP_{target} = 50), and the monomer concentration [M] and [CTA]/[I] was not modified from the condition of the diblock copolymer synthesis except the third step in which [M] was reduced to 1 M to prevent inhomogeneous mixing due to extreme increase in viscosity. A larger amount of initiator (twice the usual) was added to maintain the reaction speed similarly. On the first step, SPE was quickly consumed and the conversion reached ~100 % at 3 h as confirmed from ^{1}H NMR signals of aliquots. The second and third blocks were successively synthesised allowing 3 h for each process with no visible monomer peaks found in ^{1}H NMR spectra. Each block was formed with increasing proton signals of the respective functional groups as shown in **Figure 5.4(a)**, and the DP was determined to be 49:46:55 from the integral ratio. The MWDs (**Figure 5.4(b)**) of aliquots

showed a clear shift to a higher molecular weight region without any shoulders, which revealed full conversion at each step. Since the cumulative chain livingness at the second step was calculated to be 90.8 %, slight tailing of the SEC trace on the final product indicating "dead chain" was inevitable. In spite of the relatively low chain livingness, MWD was kept at about 1.2. Another triblock of the same sequence was aimed to obtain DP as 100:200:100 for SPE/GLBT/SPE, and it was determined as 99:193:135 by the integral ratio.

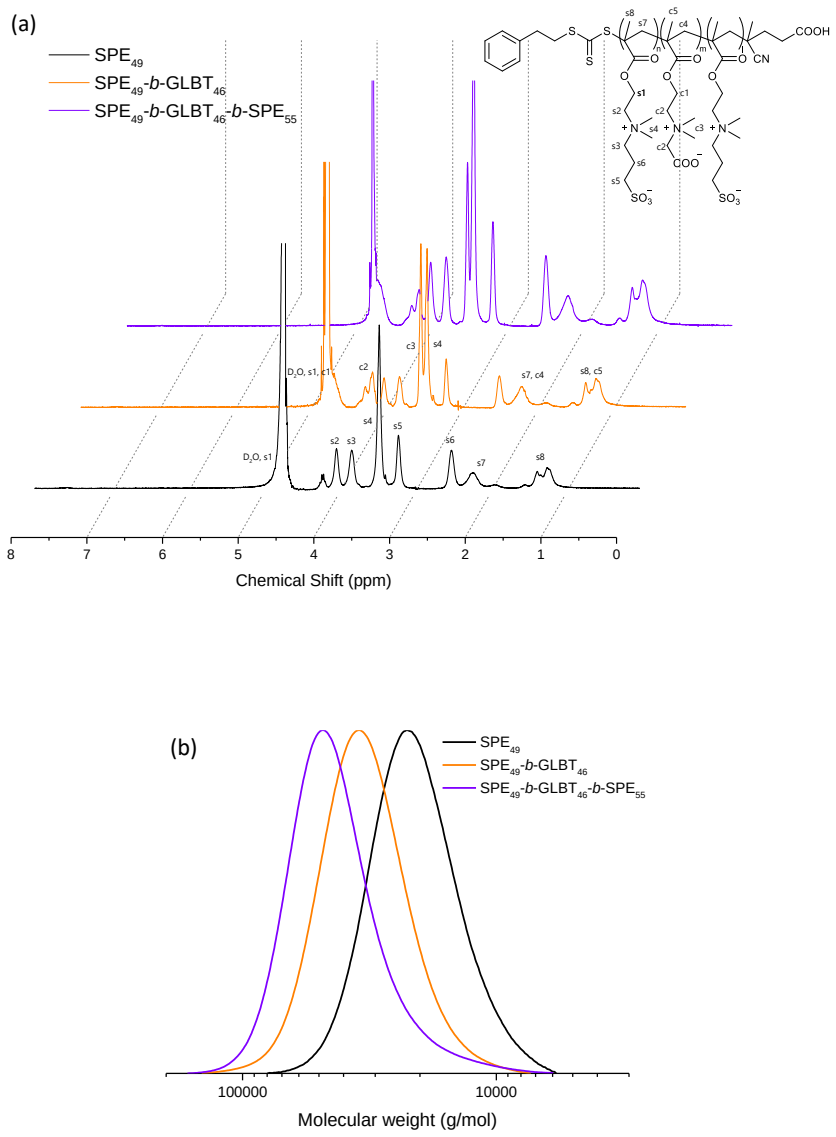

Figure 5.4. (a) ^{1}H NMR spectra (obtained at 60 °C) of SPE_{49}-*b*-$GLBT_{46}$-*b*-SPE_{55} on each synthesis step (b) MWDs by SEC analysis of SPE_{49}-*b*-$GLBT_{46}$-*b*-SPE_{55}

Temperature-responsive solution behaviour of PSPE-PGLBT-PSPE triblock copolymers

The solution behaviour of triblocks PSPE-PGLBT-PSPE was elucidated by turbidimetry and DLS. The first triblock sample (SPE_{49}-$GLBT_{46}$-SPE_{55}) had DPs almost identical with those of the three blocks so that the portion of PSPE was twice that of PGLBT. As a result, the aqueous solution showed more noticeable transmittance and size change (displayed in **Figure 5.5(a)** and **(c)**) than the previously examined diblock copolymer samples that had almost identical DP ratio. Alongside a fast diffusive mode representing freely moving polymer chains, a slow mode emerged below ~40 °C while the transmittance gradually decreased, and persistently appeared until 12 °C where the transmittance started decreasing substantially up to 0%. The slow diffusive mode eventually disappeared after uniformly size-distributed particles emerged as diblock copolymers. The slow diffusive large components were not predominant up to 25 °C (**Figure 5.5(c)**) and the relative weight increased to 57 % at 17 °C and 97 % at 12 °C (intensity-based weight at scattering angle = 90°). The slow mode in the intermediate region is assumed to be aggregated chain clusters originating from dipole–dipole interaction, especially among PSPE segments on both ends of a chain. Its size varied largely from R_h = ~200 nm to 700 nm, and the decay rates of two modes were linear with q^2 for all scattering angles, which represents translational diffusion of objects. (An example at 25 °C is shown in **Figure 5.8**) Since temperature-independent PGLBT motifs were placed between both PSPE sides, the monodisperse particles (R_h = ~30 nm, PDI ($\mu_2/\bar{\Gamma}^2$) = 0.123 by cumulant fit) at 5 °C are assumed as "flower" micelles consisting of PGLBT loops and PSPE cores.

On the other hand, the thermoresponsive behaviour of the SPE_{99}-$GLBT_{193}$-SPE_{135} solution pronounced at lower temperatures, which might be attributed to the lower ratio of PSPE against PGLBT. The transmittance was kept over 90 % with some extent of a slow mode. (R_h = ~130 nm, relative weight = 17 % at 40 °C and 76 % at 25 °C at scattering angle = 90°) Then, a rapid transmittance shift occurred with size variation at around 20 °C and the polydisperse state turned into the fairly monodisperse state around 16 °C. (**Figure 5.8(c)**) Under 16 °C, a single diffusive mode was determined as larger R_h than that of the previous triblock sample, and the size gradually reduced with the decrease in temperature. (R_h = 132 nm, PDI ($\mu_2/\bar{\Gamma}^2$) = 0.22, 5 °C) For reconfirmation of the temperature-responsive behaviour of the triblock whose ratio is PSPE:PGLBT:PSPE = 1:2:1, we synthesised an extra triblock copolymer with same target DP in each block, and it was characterised as SPE_{100}-$GLBT_{198}$-SPE_{104} by ^{1}H NMR analysis. (M_n^{SEC} = 48100 g/mol, $Đ$ = 1.12) However, the triblock copolymer whose ratio was more precisely controlled showed weaker responses to temperature similar to the diblock copolymers having a ratio close to 1:1. (the results are shown in **Figure 5.9**) The dual diffusive mode state continued to 5 °C with over 90%

transmittance, and the transition to a single diffusive mode state did not occur. Accordingly, the difference in total unit number of respective PGLBT and PSPE may affect the chain behaviour crucially, whether it is a AB-type diblock or BAB-type triblock.

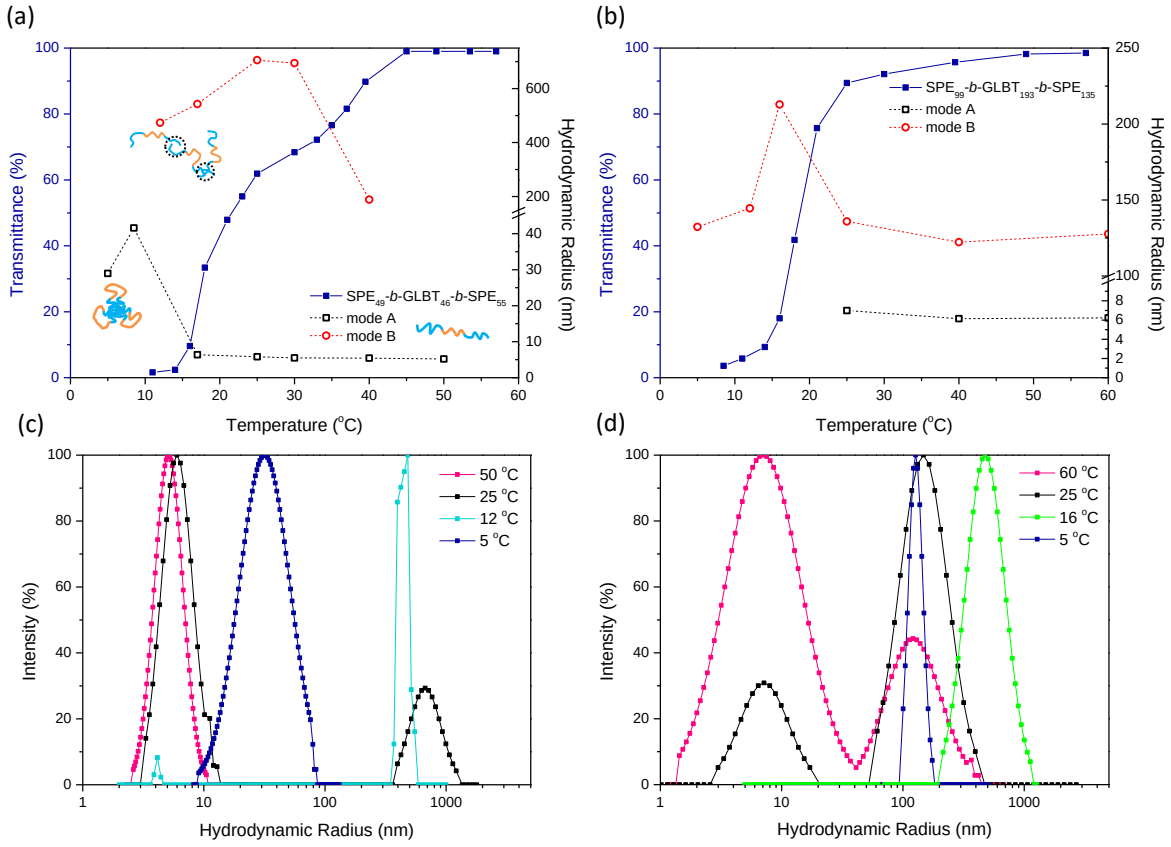

Figure 5.5. Transmittance shift (left y axis, solid symbols) and hydrodynamic radius variation (right y axis, open symbols) of triblock betaine copolymers against temperature (a) SPE_{49}-*b*-$GLBT_{46}$-*b*-SPE_{57} (b) SPE_{99}-*b*-$GLBT_{193}$-*b*-SPE_{135}. (The ACFs collected at each temperature are separately shown in **Figure 5.8**) Intensity-based distribution of hydrodynamic radii at various temperature (c) SPE_{49}-*b*-$GLBT_{46}$-*b*-SPE_{57} (d) SPE_{99}-*b*-$GLBT_{193}$-*b*-SPE_{135}.

Table 5.2. Experimental conditions used in the synthesis of PGLBT-*b*-PSPEs via RAFT polymerisation in water at 70 °C

Steps	**1**	**2**	**1**	**2**	**1**	**2**
Monomer	GLBT	SPE	GLBT	SPE	GLBT	SPE
DP_{target}	50	50	100	100	200	200
$m_{monomer}$ (g)	1.585	2.068	0.951	1.247	1.902	2.497
m_{CTA} (g)	0.05		0.015		0.015	
m_{VA-044} (g)	2.4×10^{-3}	2.4×10^{-3}	0.7×10^{-3}	0.7×10^{-3}	0.7×10^{-3}	1.4×10^{-3}
$V_{solvent}$ (mL)[a]	2.9	3.9	1.5	2	3.5	5.5
$[M]_0$ (mol/L)	2.53	1.89	2.60	2.23	2.52	1.62
$[CTA]_0/[I]_0$	20	20	20	20	20	10
Cumulative L (%)	95.3	91.1	95.3	90.8	95.3	86.6

[a] is the sum of the volume of the solvent added in the first and the subsequent step

Table 5.3. Experimental conditions used in the synthesis of PMPC-*b*-PSPE via RAFT polymerisation in water at 70 °C

Steps	**1**	**2**
Monomer	MPC	SPE
DP_{target}	200	200
$m_{monomer}$ (g)	2.610	2.469
m_{CTA} (g)	0.015	
m_{VA-044} (g)	0.7×10^{-3}	1.4×10^{-3}
$V_{solvent}$ (mL)	3.5	5.5
$[M]_0$ (mol/L)	2.52	1.61
$[CTA]_0/[I]_0$	20	10
Cumulative L (%)	95.3	86.6

Table 5.4. Experimental conditions used in preparation of PSPE-*b*-PGLBT-*b*-PSPEs via RAFT polymerisation in water at 70 °C

Steps	**1**	**2**	**3**	**1**	**2**	**3**
Monomer	SPE	GLBT	SPE	SPE	GLBT	SPE
DP_{target}	50	50	50	100	200	100
$m_{monomer}$ (g)	0.946	0.729	1.035	0.987	1.522	0.993
m_{CTA} (g)	0.023			0.012		
m_{VA-044} (g)	1.1×10^{-3}	1.1×10^{-3}	2.4×10^{-3}	0.6×10^{-3}	1.1×10^{-3}	1.2×10^{-3}
$V_{solvent}$ (mL)[a]	1.35	2.25	3.7	1.4	4.5	4.7
$[M]_0$ (mol/L)	2.51	1.50	1.00	2.60	1.57	0.76
$[CTA]_0/[I]_0$	20	20	10	20	10	10
Cumulative L (%)	95.3	90.8	82.6	95.3	86.6	78.8

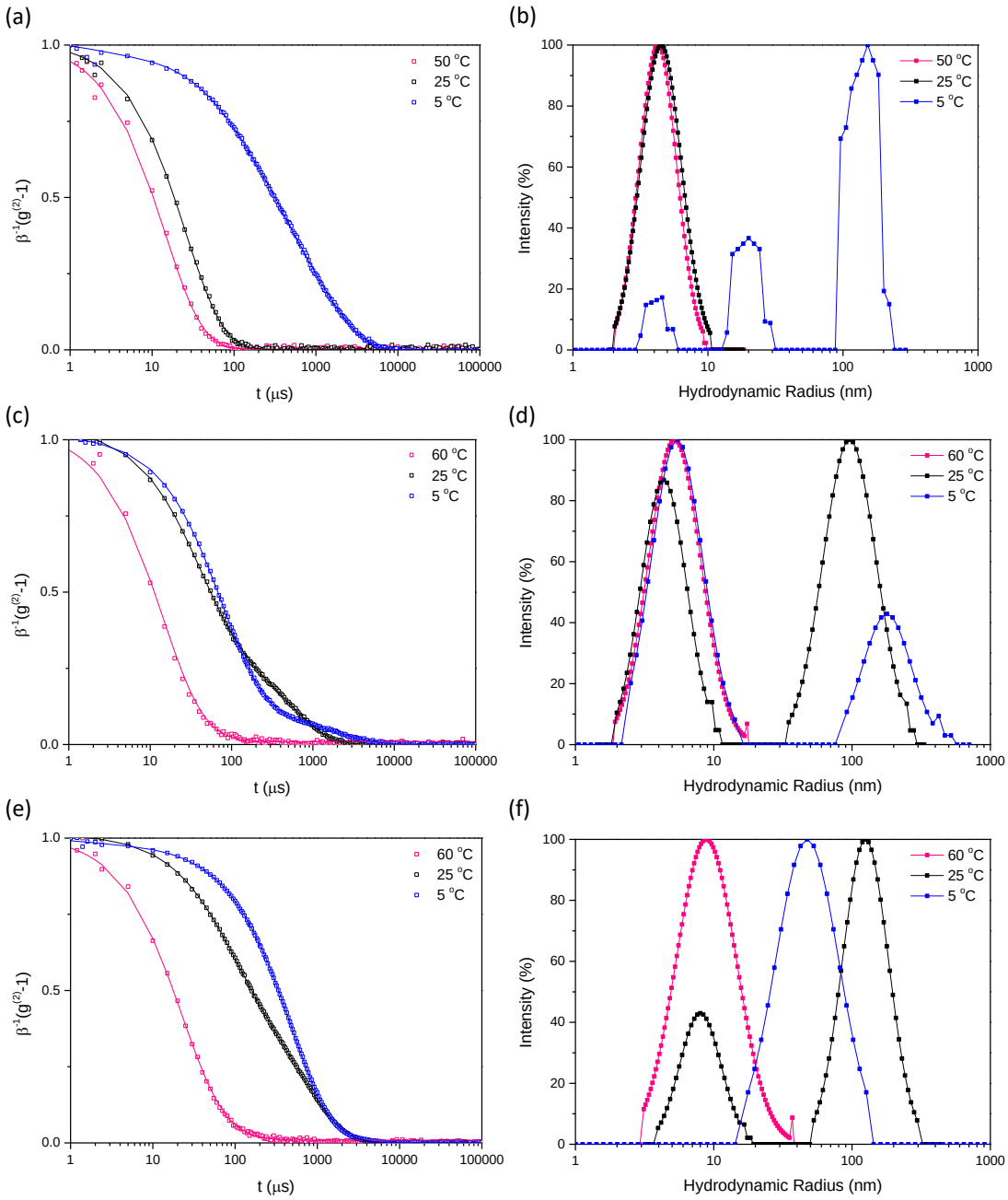

Figure 5.6. (a) ACFs of GLBT$_{49}$-*b*-SPE$_{60}$ in water obtained at 50, 25, and 5 °C (b) R_h distributions of GLBT$_{49}$-*b*-SPE$_{60}$ at 50, 25, and 5 °C (c) ACFs of GLBT$_{99}$-*b*-SPE$_{121}$ aqueous solution at 60, 25, and 5 °C (d) R_h distributions of GLBT$_{99}$-*b*-SPE$_{121}$ at 60, 25, and 5 °C (c) ACFs of GLBT$_{198}$-*b*-SPE$_{305}$ aqueous solution at 60, 25, and 5 °C (d) R_h distributions of GLBT$_{198}$-*b*-SPE$_{305}$ at 50, 25, and 5 °C (scattering angle = 90°, the ACFs were analysed by CONTIN algorithm)

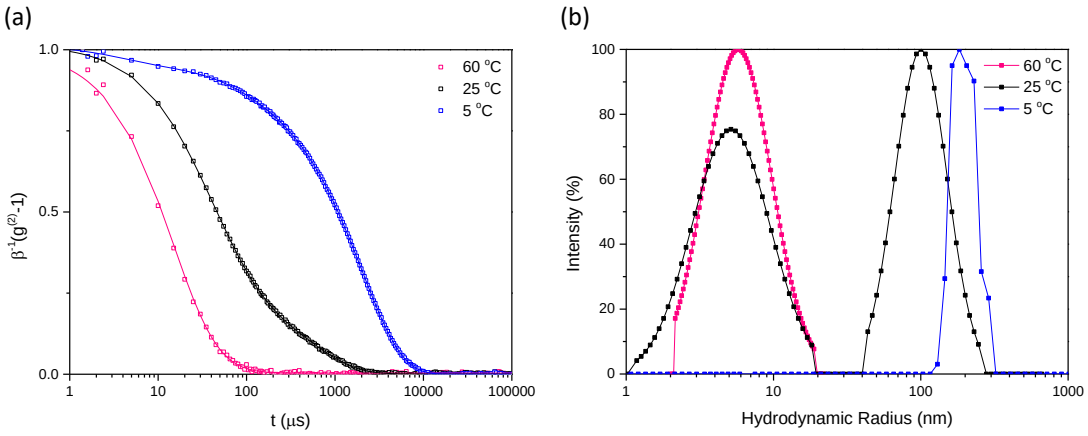

Figure 5.7. (a) ACFs of MPC_{198}-*b*-SPE_{205} in water at 60, 25, and 5 °C. (b) Size distribution of hydrodynamic radii determined by CONTIN fit at 60, 25, and 5 °C (scattering angle = 90°)

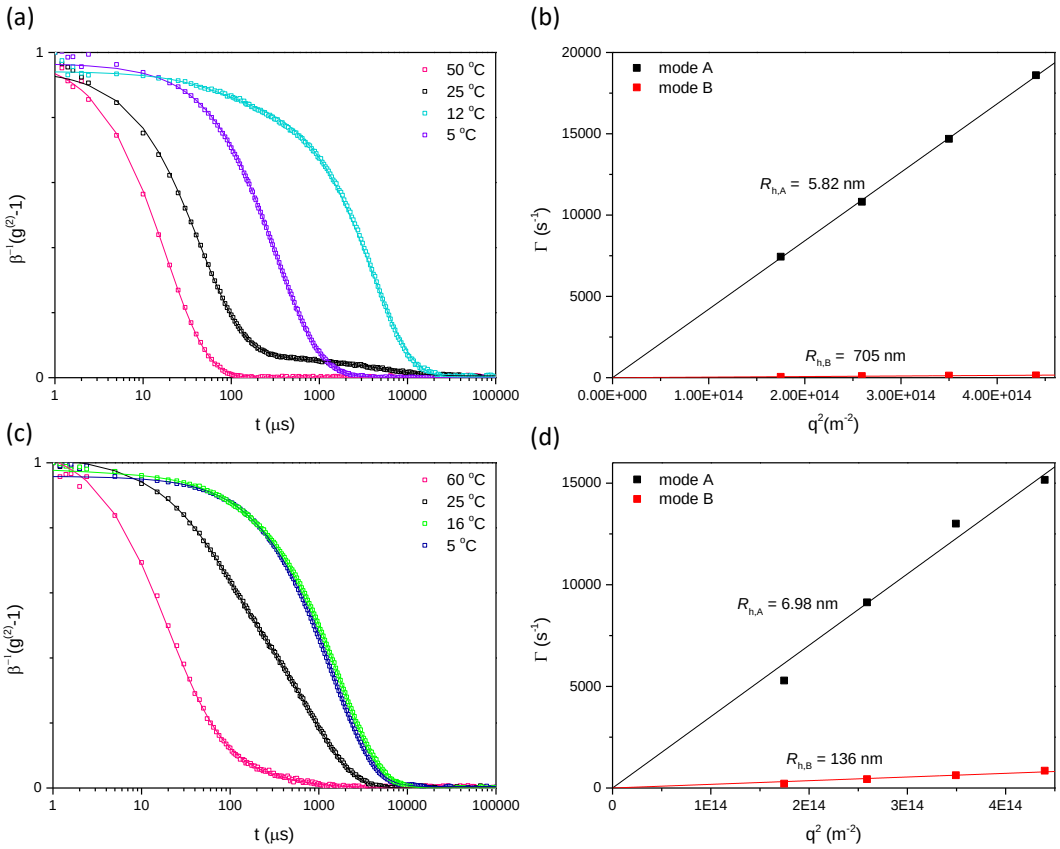

Figure 5.8. (a) ACFs of SPE_{49}-*b*-$GLBT_{46}$-*b*-SPE_{55} aqueous solution (scattering angle = 90°) at four different temperatures (b) Fitting results of Γ vs q^2 on four different angles at 25 °C (c) ACFs of SPE_{99}-*b*-$GLBT_{193}$-*b*-SPE_{135} aqueous solution at four different temperatures (d) Fitting results of Γ vs q^2 on four different angles at 25 °C

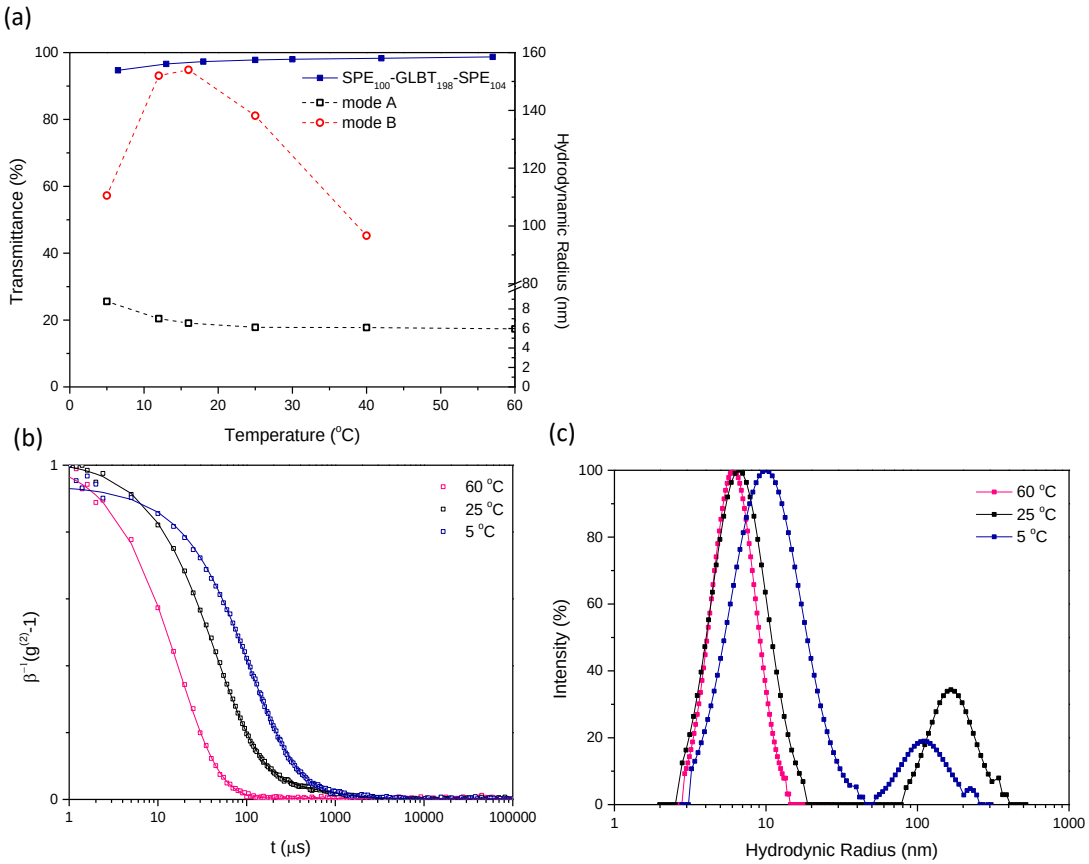

Figure 5.9. (a) Transmittance shift (left y axis, solid symbols) and Hydrodynamic radius variation (right y axis, open symbols) by temperature of SPE_{100}-*b*-$GLBT_{198}$-*b*-SPE_{104} (b) ACFs of SPE_{100}-*b*-$GLBT_{198}$-*b*-SPE_{104} aqueous solution at different temperatures (c) R_h distributions of respective ACFs fitted by CONTIN algorithm (scattering angle = 90°)

Conclusion

We synthesised betaine block copolymers PGLBT-*b*-PSPE and PMPC-*b*-PSPE by one-pot RAFT polymerization and investigated their temperature-responsive properties in aqueous solution. The concentrations of monomers and initiator were carefully optimised to achieve full conversion of betaine methacrylate monomers with DPs of more than 50 within 3 h at 70 °C. By utilizing a trithiocarbonate RAFT agent with minimum usage of radical initiator in water, full consumption of the betaine monomers was achieved and no purification after the first polymerization step was required. The activity of macroCTA corresponded to the theoretically estimated chain livingness in contrast to the previous attempt to synthesise whole betaine block copolymers, in which the macroCTAs had lost the chain livingness significantly. In order to keep accessible viscosity and high DP, a larger amount of initiator was used at a relatively low monomer concentration and this led to relatively low chain livingness values after the second step (~90%) in comparison to the original one-pot RAFT multiblock synthesis method.[39] Nevertheless, betaine diblocks and triblocks could be prepared with narrow MWD (~1.3) and at the

aimed block ratios. The three PGLBT-*b*-PSPE having different total DP but nearly equal block ratio commonly showed little behaviour change with temperature. Unimers with some extent of slow diffusive objects thought to loosely aggregated chain clusters existed over a wide temperature range while the solutions were highly transparent, and the population of aggregates increased with decreasing temperature. However, only a sample holding apparently more SPE units than GLBT assembled polymer micelles as demonstrated on our previous study.[36] Besides, two BAB-type triblocks that consisted of both PSPE ends showed a more noticeable behaviour change, which was also dependent on the entire ratio of PGLBT:PSPE. The triblock with a 1:1:1 ratio showed a more apparent macroscopic change in water while the both ends of PSPE induced larger aggregates under a gradual transmittance decrease. Finally, monodisperse particles emerged below 10 °C which is regarded as "flower" micelle. More detailed studies on the influence of block ratio and chain length on the property of PGLBT-*b*-PSPE are underway.

References

1. A. Laschewsky and A. Rosenhahn, *Langmuir*, 2019, **35**, 1056-1071.
2. G. S. Georgiev, E. B. Karnenska, E. D. Vassileva, I. P. Kamenova, V. T. Georgieva, S. B. Iliev and I. A. Ivanov, *Biomacromolecules*, 2006, **7**, 1329-1334.
3. P. Mary, D. D. Bendejacq, M. P. Labeau and P. Dupuis, *Journal of Physical Chemistry B*, 2007, **111**, 7767-7777.
4. V. Hildebrand, A. Laschewsky, M. Pach, P. Muller-Buschbaum and C. M. Papadakis, *Polymer Chemistry*, 2017, **8**, 310-322.
5. Z. L. Cao and G. Z. Zhang, *Physical Chemistry Chemical Physics*, 2015, **17**, 27045-27051.
6. A. Z. Niu, D. J. Liaw, H. C. Sang and C. Wu, *Macromolecules*, 2000, **33**, 3492-3494.
7. S. Morozova, G. Hu, T. Emrick and M. Muthukumar, *Acs Macro Letters*, 2016, **5**, 118-122.
8. J. D. Delgado and J. B. Schlenoff, *Macromolecules*, 2017, **50**, 4454-4464.
9. S. Forster, M. Schmidt and M. Antonietti, *Polymer*, 1990, **31**, 781-792.
10. M. Schmidt, *Makromolekulare Chemie-Rapid Communications*, 1989, **10**, 89-96.
11. D. Jia and M. Muthukumar, *Journal of the American Chemical Society*, 2019, **141**, 5886-5896.
12. H. Kitano, K. Sudo, K. Ichikawa, M. Ide and K. Ishihara, *Journal of Physical Chemistry B*, 2000, **104**, 11425-11429.
13. H. Kitano, M. Imai, K. Sudo and M. Ide, *Journal of Physical Chemistry B*, 2002, **106**, 11391-11396.
14. C. Leng, H. C. Hung, S. W. Sun, D. Y. Wang, Y. T. Li, S. Y. Jiang and Z. Chen, *Acs Applied Materials & Interfaces*, 2015, **7**, 16881-16888.
15. C. Leng, S. W. Sun, K. X. Zhang, S. Y. Jiang and Z. Chen, *Acta Biomaterialia*, 2016, **40**, 6-15.
16. J. B. Schlenoff, *Langmuir*, 2014, **30**, 9625-9636.
17. J. Ladd, Z. Zhang, S. Chen, J. C. Hower and S. Jiang, *Biomacromolecules*, 2008, **9**, 1357-1361.
18. S. S. Guo, D. Janczewski, X. Y. Zhu, R. Quintana, T. He and K. G. Neoh, *Journal of Colloid and Interface Science*, 2015, **452**, 43-53.
19. P. A. Woodfield, Y. C. Zhu, Y. W. Pei and P. J. Roth, *Macromolecules*, 2014, **47**, 750-762.
20. Y. Chang, S. C. Liao, A. Higuchi, R. C. Ruaan, C. W. Chu and W. Y. Chen, *Langmuir*, 2008, **24**, 5453-5458.
21. M. Das, N. Sanson and E. Kumacheva, *Chemistry of Materials*, 2008, **20**, 7157-7163.
22. Y. Zhao, T. Bai, Q. Shao, S. Y. Jiang and A. Q. Shen, *Polymer Chemistry*, 2015, **6**, 1066-1077.
23. M. J. Fevola, J. K. Bridges, M. G. Kellum, R. D. Hester and C. L. McCormick, *Journal of Applied Polymer Science*, 2004, **94**, 24-39.
24. E. E. L. Kathmann, L. A. White and C. L. McCormick, *Macromolecules*, 1997, **30**, 5297-5304.

25. M. Danko, Z. Kronekova, M. Mrlik, J. Osicka, A. bin Yousaf, A. Mihalova, J. Tkac and P. Kasak, *Langmuir*, 2019, **35**, 1391-1403.
26. H. Matsuoka, Y. Yamakawa, A. Ghosh and Y. Saruwatari, *Langmuir*, 2015, **31**, 4827-4836.
27. S. Murugaboopathy and H. Matsuoka, *Colloid and Polymer Science*, 2015, **293**, 1317-1328.
28. K. E. B. Doncom, N. J. Warren and S. P. Armes, *Polymer Chemistry*, 2015, **6**, 7264-7273.
29. K. E. B. Doncom, H. Willcock and R. K. O'Reilly, *European Polymer Journal*, 2017, **87**, 497-507.
30. T. Mai, S. Boye, J. Yuan, A. Volkel, M. Grawert, C. Gunter, A. Lederer and A. Taubert, *Rsc Advances*, 2015, **5**, 103494-103505.
31. D. Wang, T. Wu, X. J. Wan, X. F. Wang and S. Y. Liu, *Langmuir*, 2007, **23**, 11866-11874.
32. H. Sun, X. L. Chen, X. Han and H. L. Liu, *Langmuir*, 2017, **33**, 2646-2654.
33. N. S. Vishnevetskaya, V. Hildebrand, B. J. Niebuur, I. Grillo, S. K. Filippov, A. Laschewsky, P. Muller-Buschbaum and C. M. Papadakis, *Macromolecules*, 2017, **50**, 3985-3999.
34. N. S. Vishnevetskaya, V. Hildebrand, M. A. Dyakonova, B. J. Niebuur, K. Kyriakos, K. N. Raftopoulos, Z. Y. Di, P. Muller-Buschbaum, A. Laschewsky and C. M. Papadakis, *Macromolecules*, 2018, **51**, 2604-2614.
35. C. Hippius, V. Butun and I. Erel-Goktepe, *Materials Science & Engineering C-Materials for Biological Applications*, 2014, **41**, 354-362.
36. J. Lim, H. Matsuoka, S. Yusa and Y. Saruwatari, *Langmuir*, 2019, **35**, 1571-1582.
37. G. Gody, T. Maschmeyer, P. B. Zetterlund and S. Perrier, *Nature Communications*, 2013, **4**.
38. G. Gody, T. Maschmeyer, P. B. Zetterlund and S. Perrier, *Macromolecules*, 2014, **47**, 639-649.
39. G. Gody, T. Maschmeyer, P. B. Zetterlund and S. Perrier, *Macromolecules*, 2014, **47**, 3451-3460.
40. G. Gody, R. Barbey, M. Danial and S. Perrier, *Polymer Chemistry*, 2015, **6**, 1502-1511.
41. L. Martin, G. Gody and S. Perrier, *Polymer Chemistry*, 2015, **6**, 4875-4886.
42. E. R. Jones, M. Semsarilar, A. Blanazs and S. P. Armes, *Macromolecules*, 2012, **45**, 5091-5098.
43. J. F. Baussard, J. L. Habib-Jiwan, A. Laschewsky, M. Mertoglu and J. Storsberg, *Polymer*, 2004, **45**, 3615-3626.
44. A. V. Fuchs and K. J. Thurecht, *Acs Macro Letters*, 2017, **6**, 287-291.
45. G. Moad, *Macromolecular Chemistry and Physics*, 2014, **215**, 9-26.
46. M. Williams, N. J. W. Penfold, J. R. Lovett, N. J. Warren, C. W. I. Douglas, N. Doroshenko, P. Verstraete, J. Smets and S. P. Armes, *Polymer Chemistry*, 2016, **7**, 3864-3873.
47. J. R. Lovett, N. J. Warren, L. P. D. Ratcliffe, M. K. Kocik and S. P. Armes, *Angewandte Chemie-International Edition*, 2015, **54**, 1279-1283.
48. N. J. W. Penfold, J. R. Lovett, N. J. Warren, P. Verstraete, J. Smets and S. P. Armes, *Polymer Chemistry*, 2016, **7**, 79-88.
49. A. Valdebenito and M. V. Encinas, *Polymer International*, 2010, **59**, 1246-1251.
50. N. M. Nizardo, D. Schanzenbach, E. Schonemann and A. Laschewsky, *Polymers*, 2018, **10**.
51. P. S. Liu, Q. Chen, S. S. Wu, J. Shen and S. C. Lin, *Journal of Membrane Science*, 2010, **350**, 387-394.

Chapter 6. Effect of Block Ratio and Structure on the Thermosensitivity of Double and Triple Betaine Block Copolymers

ABSTRACT: AB-type and BAB-type betaine block copolymers composed of a carboxybetaine methacrylate and a sulfobetaine methacrylate, PGLBT-*b*-PSPE and PSPE-*b*-PGLBT-*b*-PSPE, respectively, were synthesised by one-pot RAFT polymerisation. The block extension with precise ratio control was enabled by optimising the concentration of the monomer, initiator, and chain transfer agent, and full conversion (~99%) of betaine monomers was achieved at each step. Two sets (total degree of polymerisation: ~300 and ~600) of diblock copolymers having four different PGLBT:PSPE ratios were prepared to compare the influence of block ratio and molecular weight upon the temperature-responsive behaviour in aqueous solution. Turbidimetry and dynamic light scattering study revealed that a shift to higher temperatures of the cloud point and micelle formation by increasing the ratio of PSPE, which exhibit upper critical solution temperature (UCST) behaviour. PSPE-dominant diblocks created spherical micelles stabilised by PGLBT motifs, and the transition behaviour diminished by decreasing PSPE ratio. No particular change was found in diblocks that had an identical AB ratio. This trend reappeared in the other set whose entire molecular weight approximately doubled, and each transition point was not recognisably impacted by the total molecular weight. For triblocks, the PSPE double ends provided higher probability of interchain attractions and resulted in a more turbid solution at higher temperatures, compared to the diblocks which had similar block ratios and the molecular weights. The intermediates assumed as network-like soft aggregates eventually rearranged to monodisperse flowerlike micelles.

Introduction

Polyzwitterions, containing a cationic and an anionic group on their repeating unit, belong to a distinctive class of polyelectrolyte. This charge neutrality under the ionised state differentiates them from typical water-soluble polymers. Properties of polyzwitterions in aqueous media are not in common with those of general polyelectrolytes nor non-ionic polymers. Basically, no counterions are incorporated due to their intrinsic charge balance unlike other typical polyelectrolytes. Hence in salt-free water, both charges in their repeating unit allow electrostatic interactions with adjacent motifs. Three interaction modes have been generally discussed: intra-mer, inter-mer, and inter-chain attraction or repulsion. Intra-mer interaction requires bending of the spacer carbons on meeting the inner charged group with the outer charged group.[1] Energy calculation results of molecular mechanics

on zwitterionic surfactants suggested that this pairing does not occur in aqueous media, and more favourable interaction with water molecules rather inner groups, large dipole moment, and steric hindrance could be the reason.[2] Delgado et al. proposed a "soliton-like" model of head-to-tail conformation with nearest neighbours in polysulfobetaines.[3] These intra- or interchain electrostatic interactions are thought to lead to chain collapse of polyzwitterions and low solubility in salt-free water. Consequently, all attraction/repulsion forces can be diminished by additional salts which reduce the Debye length of the solution, representing the range of electrostatic interaction,[4] and chain expansion occurs. This behaviour is opposite to that of ordinary polyelectrolytes which become less soluble in saline solution by charge screening, referred to anti-polyelectrolyte effect[4-7] as determined from the hydrodynamic radii,[3, 8, 9] viscosity,[10] or theoretical analysis.[11]

Amongst polybetaines, polysulfobetaines explicitly show this behaviour. Generally, polysulfobetaine chains are hard to dissolve in pure water and additional salt ions or heat must be applied to promote their solvation. The intra/interchain attraction between polysulfobetaines is so prevalent that the hydrophilic-to-hydrophobic transition occurs below a certain temperature[12] resulting in phase separation in water. Their upper critical solution temperature (UCST) is known to depend on the carbon spacer length which relates to hydrophilic/hydrophobic character as well as molecular weight and the chemical structure.[13-15] Incorporated polysulfobetaine motifs with relatively hydrophobic polymer blocks,[16-18] crosslinked hydrogels,[19, 20] or on the surface of inorganic nanoparticles[21, 22] provided a thermoresponsive character in the systems. In addition, the block copolymers with lower critical solution temperature (LCST)-type nonionic polymers[23-27] revealed "schizophrenic" micelle formation beyond their UCST and LCST.

On the other hand, the stimuli-responsive character of polycarboxybetaines is triggered by pH instead of temperature. Composed of a weak acid (carboxylate) and a dimethylammonium, the charge neutrality of polycarboxybetaines turns into positive under acidic condition (pK_a ~3) due to protonated carboxylate ends. In this state, the chains are no longer polyzwitterions and the solution behaviour would be much closer to that of polycations. The charge-switching ability could be used to build active surfaces which can protect them from protein adhesion and kill and release bacteria.[28-30] Flux change upon elution of aqueous solutions having various salt and pH conditions was demonstrated by pH- and salt-responsive swelling behaviour of polycarboxybetaine chains coated on the membranes.[31]

Another important feature of polyzwitterions is their antifouling ability. On a bare, non-coated surface, protein adsorption is promoted by an electrical double layer of the liquid-substrate surface in the case of charged proteins[32]

and hydrophobic interactions.[33] Additional adhesion of microbes or subsequent cell growth by consuming nutrients follows on the protein layer.[34] To prevent the initial biofilm formation, a surface is usually coated with hydrophilic polymers (e.g. polyethylene glycol (PEG), polyethylene glycol methacrylate (PEGMA)) which provide a hydration layer to ban initial adsorption. Compared to the non-ionic hydrophilic polymers which showed a disrupted hydration layer upon contact with proteins, both free chains and coatings of polyzwitterions showed superior antifouling properties because of unperturbed water molecule ordering.[35-37] The anti-fouling property of polyzwitterions is regarded to be advantageous for stimuli-responsive application against temperature, pH or salt (e.g. drug carrier) which is required for high stability in the living body.

We have investigated a new combination of double hydrophilic betaine diblock copolymers composed of a carboxy- and a sulfobetaine methacrylate (PGLBT-*b*-PSPE), which is a stimuli-responsive double hydrophilic block copolymer (DHBC). Having temperature-responsive PSPE at the one side and pH-responsive PGLBT at the other side, the diblock copolymer could change their state in water from free chains to PSPE-centred micelles reversibly.[38] However, the copolymerisation of these two betaine monomers was poorly performed by conventional step-by-step RAFT polymerisation and always left a large extent of unreacted first block (PGLBT, used as macroCTA). Although the product treated by precipitation yielded relatively pure diblock copolymers with narrow dispersity, accurate prediction of the block ratio was not possible in this synthetic route. Detailed study of block ratio on the thermoresponsive characters was also impossible by the result. The main reason was assumed to be the poor stability of the dithioester end group in water during synthesis and dialysis. By carefully modifying the type of CTA, ratio of CTA to initiator, and concentration of monomers under the consideration of theoretical chain livingness,[39] PGLBT-*b*-PSPE but also PMPC-*b*-PSPE (incorporated with a phosphobetaine) and PSPE-PGLBT-PSPE triblocks were successfully synthesised by iterative polymerisations. Each polymerisation step resulted in high conversion (~99%), which enabled chain extension without a purification step. In this study, the betaine block copolymers with different block ratios and similar total degree of polymerisation were obtained by the one-pot procedure to elucidate the influence of the PGLBT/PSPE ratio and the molecular weight on the temperature-responsive solution behaviour.

Experimental Section

Materials

2-((2-(Methacryloyloxy)ethyl)dimethylammonio)acetate (carboxybetaine methacrylate, GLBT) and 3-((2-(methacryloyloxy)ethyl)dimethylammonio)propane-1-sulfonate (sulfobetaine methacrylate, SPE, which is often described as SBMA in other reports) were kindly donated by Osaka Organic Chemical Industry LTD (Osaka, Japan) and used as received. 4-Cyano-4-(2-phenylethanesulfanylthiocarbonyl)sulfanylpentanoic acid (PETTC) was synthesised according to the literature[40] and used as a chain transfer agent (CTA). A radical initiator 2,2'-azobis[2-(2-imidazolin-2-yl)propane]dihydrochloride (VA-044) was purchased from Wako Chemicals (Osaka, Japan) and used as received. Ultrapure water (minimum resistivity ~18.2 MΩ cm) obtained by Milli-Q system was used for synthesis, dialysis, and preparation of polymer solutions. 2,2,2-trifluroethanol (TFE) was purchased from Nacalai Tesque and used as received. Dialysis was performed through regenerated cellulose membranes (MWCO 3500 and 15000) to remove residues.

Synthesis of PGLBT-*b*-PSPE by one-pot RAFT polymerisation

GLBT, PETTC, and initiator were transferred into a rubber septum-sealed glass vial with a magnetic stirrer and dissolved into the mixture of water and TFE (8:2, v/v). The homogeneous solution was degassed by 15 minutes of argon bubbling, then immersed in an oil bath thermostated to 70 ºC. The reaction was quenched in an ice bath after full consummation of GLBT monomers was identified through ^{1}H nuclear magnetic resonance (NMR) analysis of aliquots. For the second polymerisation, SPE, additional initiator and water were put into the vial and homogeneously dissolved. The required amount of SPE and initiator were determined based on the theoretical number-based molecular weight of PGLBTs. The reaction was started after 15 min of argon purging in the same manner, and terminated after full conversion of SPE monomers, then the final product was purified by excess dialysis against Milli-Q water. The lyophilised product yielded as yellow powder. Generally, the reaction time was 3 h and extended to 6 h for the batches of DP_{target} = 600. Detailed reaction conditions are shown in **Table 6.5**, **6.6**, and **6.7**.

Polymer characterisation

^{1}H NMR spectroscopy The spectra of synthesised polymers that dissolved in deuterated water (D_2O) were acquired on a 400 MHz JEOL JNM-AL400 spectrometer (JEOL, Tokyo, Japan). A minimum of 64 scans were recorded for each sample.

Size exclusion chromatography (SEC) The molecular weight distribution was determined through a column (SB-804 HQ, Shodex) and a refractive index detector (RI-830, JASCO, Japan) operating in aqueous condition. A buffer solution (0.5 M CH_3COOH and 0.3 M of Na_2SO_4) was eluted with a flow rate of 0.5 mL/min as the mobile phase. The number-average molecular weight (M_n) and dispersity (M_w/M_n, denoted as $Đ$) were determined by the calibration curve obtained through a set of poly(2-vinylpyridine) standards. (M_n range: 5500 to 142000 g/mol, Sigma-Aldrich)

Turbidimetry The transmittance variation of the block copolymer aqueous solutions (10 mg/mL) was recorded along a temperature range (from 60 ºC to ~5 ºC) by a UV-VIS spectrometer (Hitachi U-3310 spectrophotometer). A quartz cell with a light path of 10 mm was used, and the temperature was controlled by a water circulator appended on the cell holder. Transmittance of 200–600 nm was scanned at each temperature after 5 min of stabilisation and values at 400 nm was taken for reporting. Each solution was filtered through a syringe filter unit (pore size: 0.2 μm, mdi) prior to measurement.

Light scattering Dynamic light scattering (DLS) was carried out to determine the hydrodynamic radii of the polymer objects in aqueous solution (10 mg/mL). Sample cells were immersed in a temperature-controlled goniometer (BI-200SM, Brookhaven Instruments, New York, USA) equipped with a 15 mW He-Ne laser. (wavelength λ = 632.8 nm, index matching fluid = decahydronaphtalene) The field autocorrelation functions of four scattering angles (60º, 75º, 90º, and 105º) were obtained by a BI-DS2 photomultiplier tube with a correlator (TurboCorr, Brookhaven Instruments). Static light scattering (SLS) was carried out in a single concentration (10 mg/mL or 5 mg/mL) to measure R_g of micellar objects.

The normalised intensity autocorrelation function $g^{(2)}(q,t)$ is measured through

$$g^{(2)}(q,t) = \frac{\langle I^*(q,0)I(q,t)\rangle}{\langle I(q,0)^2\rangle} \tag{6.1}$$

$g^{(2)}(q,t)$ is related to the normalised electric field autocorrelation function $g^{(1)}(q,t)$ by the Siegert relation (S1),

$$g^{(2)}(q,t) = 1 + \beta\left|g^{(1)}(q,t)\right|^2 \tag{6.2}$$

where β is a coherence factor depending on the experimental conditions, and $g^{(1)}(q,t)$ is to be evaluated. For a polydisperse particle system, the $g^{(1)}(q,t)$s can be written as:

$$g^{(1)}(q,t) = \int_0^\infty G(\Gamma)\exp(-\Gamma t)d\Gamma \tag{6.3}$$

where G(Γ) is the intensity-based normalised distribution of decay rates $\int G(\Gamma)d\Gamma = 1$ and able to be calculated through inverse Laplace transform. (CONTIN regularization was applied by a software, BIC Particle Explorer, Brookhaven Instruments) The translational diffusion coefficient $D_t = \Gamma/q^2$ was obtained from the slope of the decay rate $\bar{\Gamma}$ versus q^2. The scattering vector q is

$$q = \frac{4\pi n}{\lambda}\sin\left(\frac{\theta}{2}\right) \tag{6.4}$$

where n is the refractive index of the water, λ is the wavelength of the incident laser (632.8 nm), and θ is the scattering angle. The hydrodynamic radius R_h was determined by the Stokes-Einstein equation:

$$R_h = \frac{k_B T}{6\pi\eta D_t} \tag{6.5}$$

Where k_B is the Boltzmann constant, T is the absolute temperature, and η is the viscosity of solvent (water), respectively.

In the static light scattering (SLS) measurements, the scattering intensity were recorded over an angular range between 40° and 150° at 10° intervals. A partial Zimm equation (6.6) of the inverse scattering intensity ($1/I_{ex}$) versus the square of the scattering vector q^2 at a single concentration was used to determine the radius of gyration (R_g), as follows

$$\frac{1}{I_{ex}(q)} = C(1 + \frac{R_g^2 q^2}{3}) \tag{6.6}$$

where C is the arbitrary constant, and I_{ex}(q) is the intensity of scattered light. Several points that were apparently discrepant from the overall results were exempted from the linear fitting.

Transmission electron microscopy (TEM) TEM observations were performed using a JEOL (Tokyo, Japan) JEM-2100 with an accelerating voltage of 160 KV. All samples for TEM observation were prepared by placing one drop of the aqueous solution on a copper grid coated with thin films of Formvar and carbon. Excess water was blotted using filter paper. The samples were stained by sodium phosphotungstate and dried under vacuum. TEM samples which should be prepared with cooling were prepared in a cooling device, Funakoshi (Tokyo, Japa) Cryoporter CS-80C.

Atomic force microscopy (AFM) AFM measurements were carried out under the following condition: A Seiko SPI3800 probe station an SPI300 unit system in dynamic force mode (non-contact mode) were operated with microcantilevers. (OMCL-AC240TS-C3, Olympus, typical resonance frequency: 70 kHz and typical spring constant: 1.7 N/m) For sample preparation, aqueous suspensions of colloidal PGLBT-*b*-PSPE particles was dropcast onto a microscope slide glass (IWAKI, Japan) and dried at room temperature for three days.

Determination of monomer conversion and theoretical molecular weight

The monomer conversion was calculated from ^{1}H NMR spectra using the following equation as described in the literature[41]:

$$p = \frac{[\mathrm{M}]_0 - [\mathrm{M}]_\mathrm{t}}{[\mathrm{M}]_0} = 1 - \frac{[\mathrm{M}]_\mathrm{t}}{[\mathrm{M}]_0} = 1 - \frac{\frac{\int I_{5.7-6.2\ ppm}}{\int I_{CTA}}}{\mathrm{DP_{target}}} \tag{6.7}$$

where $[\mathrm{M}]_0$ and $[\mathrm{M}]_\mathrm{t}$ are the monomer concentrations at the initial and elapsed time t, $\int \mathrm{I}_{5.7–6.2\ ppm}/\int \mathrm{I}_{CTA}$ is the corrected proton ratio of the unreacted monomer to the CTA at the end of the chain. $\mathrm{DP_{target}}$ is the targeted number-average degree of polymerisation. Each conversion was also determined by the following equation:

$$p = \frac{\int I_p}{\int I_p + \int I_m} \tag{6.8}$$

where $\int \mathrm{I_p}$ is the corrected integral value of polymer peaks and $\int \mathrm{I_m}$ is for vinyl protons of the monomer (at 5.7–6.2 ppm). The theoretically predicted molecular weight ($M_\mathrm{n}^\mathrm{theo}$) was determined by the conversion values:

$$M_\mathrm{n}^\mathrm{theo} = p \cdot \mathrm{DP_{target}} \cdot \mathrm{M_M} + \mathrm{M_{CTA}}, \qquad \mathrm{DP_{target}} = \frac{[\mathrm{M}]}{[\mathrm{CTA}]} \tag{6.9}$$

Results and Discussions

Preparation of PGLBT-*b*-PSPE having controlled block ratios

The AB-type diblock betaine copolymer PGLBT-*b*-PSPEs having various block ratios and total DP were prepared through one-pot synthesis approach as described in **Chapter 4**. The total target DP ($\mathrm{DP_{target}}$) was set to 300 and 600, and the aimed ratio of PGLBT:PSPE was varied from 1:1 to 1:5. The procedure of the synthesis and reaction conditions is described in **Scheme 6.1**, and the information of obtained block copolymers is listed in **Table 6.1**.

According to the fundamentals of RAFT polymerisation, the activation–deactivation process does not affect the overall number of radicals, and radical sources (e.g. azoinitiator, redox initiator or photoinitiator) must be incorporated to conduct polymerisation. In the azoinitiator system, once a radical fragment provides radicals to monomers, chain propagation continues through the Z group and R group of RAFT agent. The Z group determines the reactivity of C=S against radicals on the addition of propagating radical and fragmentation step[42] while the R group reinitiates other monomers by acting as homolytic leaving group.[43] As a result, two types of polymer chains are produced under a rough consideration: initiator-end chians without the Z group, and Z group ended chains. Therefore, the number of chains without the Z group, in other words "dead" chains, is governed by the initial amount of azoinitiator.[44] Perrier group discussed the theoretical chain livingness calculated by comparing Z-group ended chains to entire chains with consideration of decomposition rate of azoinitiator, and successfully demonstrated multiblock copolymerisation while keeping high chain livingness.[39, 41, 44, 45] Consequently, initiators must be introduced as less as possible for suppressing initiator-end chain generation rather than CTA-end chains commencing further polymerisation. The usage of less initiator which necessarily lowers the polymerisation rate is compensated by increasing concentrations of monomers,[39] increasing reaction temperature,[41] (boosting decomposition rate of initiators) using more reactive radical sources,[39] and choosing good solvents inducing polymerisation acceleration.[46]

In this study, VA-044 was used instead of other typical radical sources because of higher decomposition rate (estimated to k_d = 4.2995 × 10^{-4} s^{-1} at 70 ºC in the literature[39]) at the ratio of 0.05:1 = [VA-044]:[CTA], and monomer concentration [M] of 2.5–3 mol/L. Water is reported to increase the rate of propagation (k_p) of vinyl monomers among other solvents,[46] and is one of few solvents which can dissolve betaine monomers and polymers. Under the reaction condition, the theoretical chain livingness (percentage of CTA-end chain) was lower than that of the ideal examples[39, 45] because of the increased dosage of initiator ([CTA]:[I] was modified from 400 to 20) and lowered monomer concentration. This modification was inevitable in our experiments especially for obtaining high molecular weight betaine methacrylate polymers mediated by a different trithiocarbonate RAFT agent (PETTC), particularly for synthesising sufficiently long PSPE blocks pronouncing temperature-responsivity near room temperature. By regulating the concentration of monomers and initiators to keep the chain fidelity (low percentage of dead chain end) within the practical reaction time, full conversion (~99%) of betaine monomers at each step of polymerisation was successfully achieved at about 3 h, and this enabled consecutive betaine block extension without pause regardless of AB block ratio. TFE was used as a co-solvent with water only in the first

polymerisation step due to enhancement of insufficient solubility of PETTC in water, and it did not affect the polymerisation rate.

In the DP_{total} ~300 series, the obtained block copolymers had well-controlled ratios of PGLBT:PSPE as aimed with no residual PGLBT macroCTAs. The ratio and number-average molecular weight were calculated from ^{1}H NMR spectra by comparing the signals of PSPE to those of PGLBT, measured at 60 °C to exclude zwitterionic attractions which reduce the intensity of PSPE signals. (**Figure 6.1**) Results of SEC analysis (**Figure 6.2(a)**) show clear curve shifts from lower molecular weight representing homo-PGLBT to higher molecular weight indicating PGLBT-*b*-PSPE with narrow dispersities (< ~1.2). In the case of DP_{total} = 600, some of batches resulted in incomplete chain extension in spite of undetectable trace of SPE monomers in aliquots withdrawn even after 6 h of the reaction seen in ^{1}H NMR spectra. A subtle extent of residual homo-PGLBT was found on SEC chromatograms and removed by precipitation into MeOH (the SEC analysis results of before and after precipitation are displayed in **Figure 6.10**). Eventually, the ratios of polymers whose target ratio of PGLBT:PSPE = 1:2, 1:3 and 1:5 were estimated to be 1:4, 1:5 and 1:6. Nevertheless, the molecular weight distributions (MWDs) of copolymerised moieties were kept within the accepted range of well-performed RAFT polymerisation ($Đ$ < 1.3) as displayed in **Table 6.1** and **Figure 6.2(b)**.

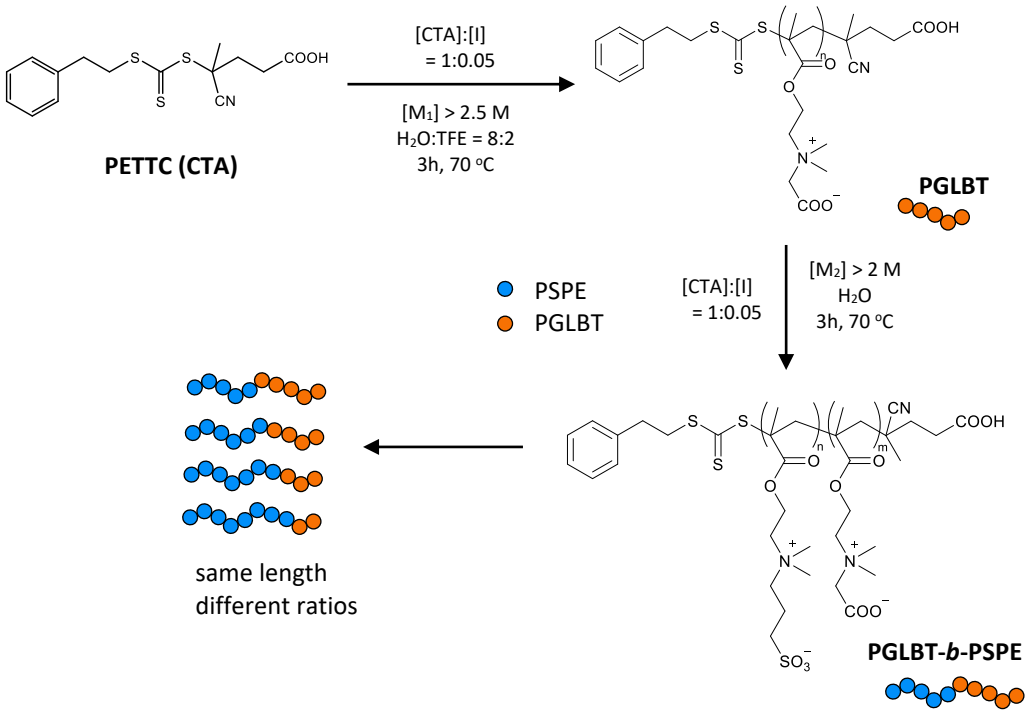

Scheme 6.1. The synthetic route of PGLBT-*b*-PSPE by one-pot RAFT polymerisation

Table 6.1. Summary of the double betaine block copolymers synthesised in the study

	M_n^{theo} (g/mol)	M_n^{SEC} (g/mol)	$Đ$ (M_w/M_n)
GLBT$_{149}$-*b*-SPE$_{161}$	77400	36400	1.12
GLBT$_{100}$-*b*-SPE$_{245}$	90300	43800	1.17
GLBT$_{74}$-*b*-SPE$_{277}$	93600	45100	1.14
GLBT$_{49}$-*b*-SPE$_{229}$	74900	41700	1.15
GLBT$_{297}$-*b*-SPE$_{330}$	156400	71300	1.20
GLBT$_{198}$-*b*-SPE$_{811}$	269500	89100	1.18
GLBT$_{149}$-*b*-SPE$_{742}$	239700	88300	1.21
GLBT$_{99}$-*b*-SPE$_{630}$	197640	66500	1.16

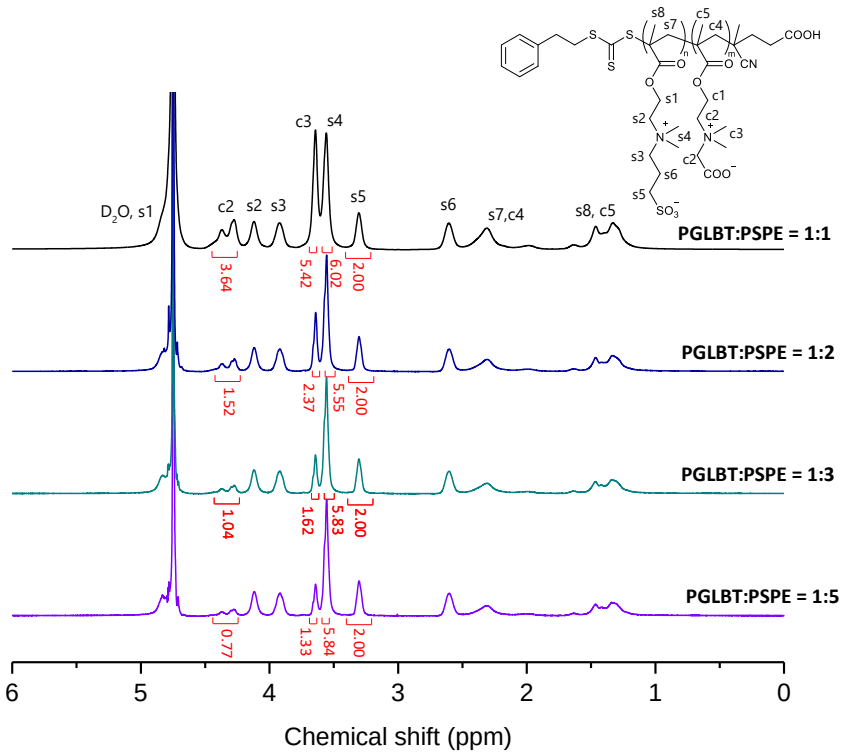

Figure 6.1. ^{1}H NMR spectra of 4 PGLBT-*b*-PSPEs having several ratios acquired in D_2O at 60 °C (DP_{total} = ~300)

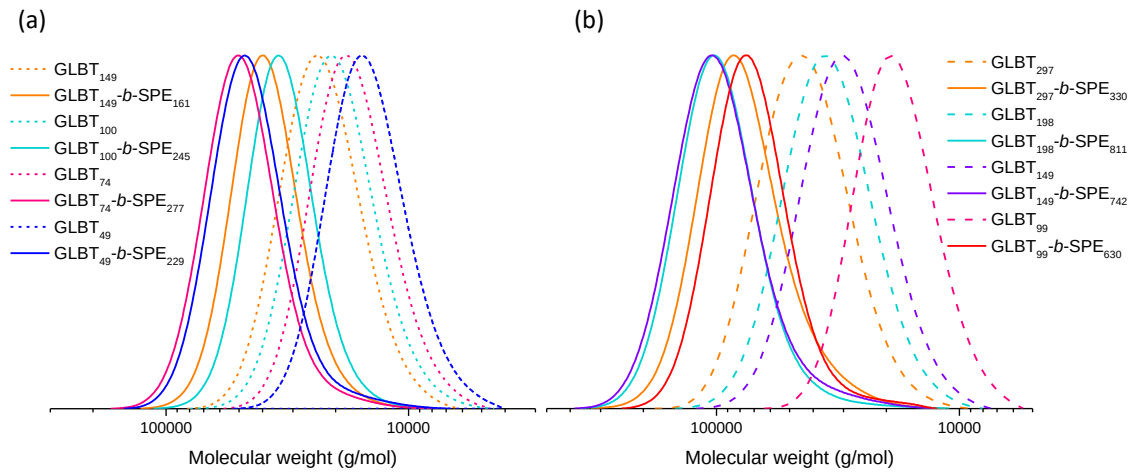

Figure 6.2. Molecular weight distributions of homo-PGLBTs (dashed lines) and PGLBT-*b*-PSPEs extended from the homo-PGLBTs. The total target DP was (a) 300 and (b) 600

Since the residues did not occur on the DP_{target} = 300 batches, it is thought to be attributed to the extremely increased viscosity which caused an inhomogeneous mixed state. Only $GLBT_{297}$-*b*-SPE_{330} was not under this problem presumably due to the identical target ratio per block that may ease the viscosity issue. The formation of residues was not thoroughly prevented by reducing the monomer concentration and increasing the amount of initiator at the second polymerisation, which inevitably led to low chain livingness. However, it should be noted that the residual homo-PGLBT chains of DP_{target} = 600 series was just a minor issue in comparison with the attempt to synthesise PGLBT-*b*-PSPE through conventional step-by-step RAFT block copolymerisation. More than half of the macroCTA (homo-PGLBT) did not participate in SPE polymerisation and the precise block ratio control was unachievable.

For the synthesis of BAB-type triblock, PSPE-PGLBT-PSPE, the chain extension was performed through the same one-pot procedure. Since we previously confirmed that the BAB triblock having the same overall AB composition (1:2:1) did not show significant temperature-responsive solution behaviour, PSPE-dominant two copolymers were synthesised at the ratio of 2.5:1:2.5 and 1:1:1 to get the whole ratio of 5:1 and 2:1. Two consecutive chain growth steps were performed for 3 h, considered adequate to get full conversion (~99%) of the monomers, and any retardation or residues were not found on the SEC analysis results as shown in **Figure 6.3**. Each DP was estimated by ^{1}H NMR spectra shown in **Figure 6.11** and the results are in **Table 6.2**. The MWD curve at each step monomodally shifted to higher molecular weights on both cases. Note that the final product of the 2:5:1:2.5 batch showed gradual tailing of MWD and this widened the dispersity. In the second step of the experiment, an additional initiator ([CTA]:[I] was modified from 20:1 to 12.5:1) was used to compensate the

polymerisation rate against decreased monomer concentration (2.5–3 mol/L to 1 mol/L) adjusted for workable viscosity. The theoretically estimated chain livingness was 88% at the second step and 84% on the final step, meanwhile the chain livingness of the 1:1:1 batch was 91% at the second step and 85% at the final step. (**Table 6.7**) Hence, the tailing of SPE_{248}-$GLBT_{99}$-SPE_{277} is thought to originate from the increased portion of dead chains that are not able to reinitiate further polymerisation.

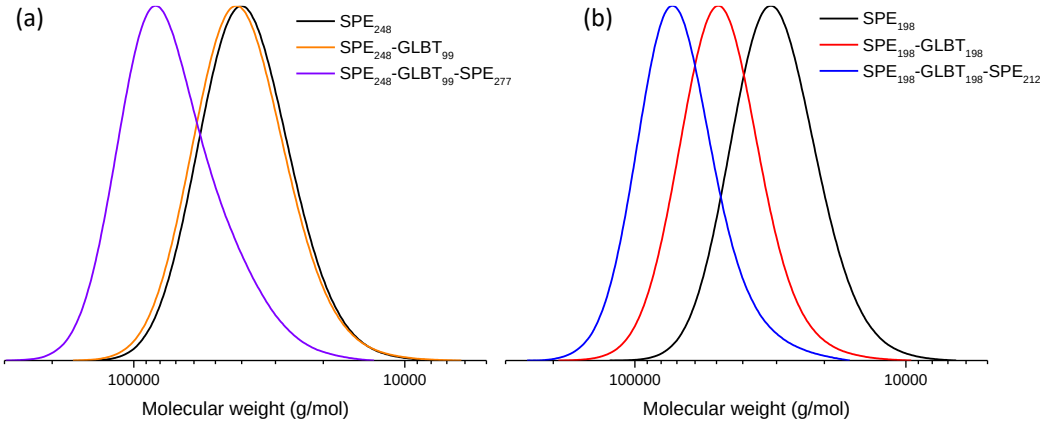

Figure 6.3. Molecular weight distributions for each 3 polymerisation steps of betaine triblock copolymer PSPE-*b*-PGLBT-*b*-PSPE (total DP ~600) (a) SPE_{248}-$GLBT_{99}$-SPE_{277} (target ratio = 2.5:1:2.5) (b) SPE_{248}-$GLBT_{99}$-SPE_{277} (target ratio = 1:1:1)

Table 6.2. Summary of the BAB-type betaine triblock copolymers synthesised in the study

	M_n^{theo} (g/mol)	M_n^{SEC} (g/mol)	$Đ$ (M_w/M_n)
SPE_{248}-$GLBT_{99}$-SPE_{277}	168300	66300	1.20
SPE_{198}-$GLBT_{198}$-SPE_{212}	157500	64500	1.13

Influence of block ratio on the solution behaviour of PGLBT-*b*-PSPE

Now the block ratio effect on the solution behaviour of PGLBT-*b*-PSPE can be evaluated systematically by comparing the polymer samples having four different ratios and two different total target DPs. Firstly, transmittance and size variation of the aqueous solutions of DP_{total} ~300 series was investigated. Our hitherto studies revealed that sufficiently high portions of PSPE to PGLBT is required to render the UCST behaviour in aqueous solutions above 0 °C, particularly for PSPE-centred micelle formation. **Figure 6.4** shows the transmittance increase/decrease and hydrodynamic radius change referring unimers (R_h < 10 nm), monodisperse micelles (R_h = 30–40 nm) or inter-chain assemblies (as intermediates, R_h > 100 nm) of respective sample solutions

against temperature. As reported previously, no particular alteration of either transmittance or R_h happened on $GLBT_{149}$-*b*-SPE_{161} solution because of nearly identical unit number of both substances. It is thought that the temperature-independent PGLBT motifs intervened association among PSPE segments and the hydrophilicity of entire chain was scarcely altered. Accordingly, the solution behaviour did not show any clear differences even at the lowest end of the temperature range. Few extent of the larger objects (R_h > 100 nm, intensity-based relative weight = 10–50%), which are common in PGLBT-*b*-PSPEs that originate from the interchain attraction between PSPE pairs prior to phase separation, accompanied with unimers at 5 °C.

More apparent thermoresponsivity appeared on the other polymer samples whose PSPE motif more than doubled against PGLBT. $GLBT_{100}$-*b*-SPE_{245} solution showed a slight transmittance shift to ~70% while the unimers transformed to polymer micelles at 5 °C. $GLBT_{74}$-*b*-SPE_{277} synthesised at the target ratio of 1:3 showed a more recognisable change as expected. The transmittance dropped to ~50% at the end of the range, and the polymers in micellar form appeared below 12 °C. The clearest temperature-responsive behaviour was found in the $GLBT_{49}$-*b*-SPE_{229} solution sample among the four due to the sufficiently large portion of PSPE segment. The transmittance abruptly decreased to 0% as PSPE homopolymers under 20 °C, but intriguingly, micellar objects did not emerge unlike other typical PGLBT-*b*-PSPEs. The autocorrelation functions and analysed R_h of four polymers at 12 °C in **Figure 6.6(a)(b)** displayed different sensitivity against temperature—unimers and chain clusters (PGLBT:PSPE = 1:1), unimers and micelles (1:2), micelles (1:3), and size-grown aggregates (1:5). Among them, the $GLBT_{49}$-*b*-SPE_{229} solution did not turn into a bluish translucent state attributed to Rayleigh scatterers, which are generally shown in micelle solutions, but rather a very turbid state in which white sediments settled to the bottom with passage of time. (see insets of **Figure 6.4(a)**) The hydrodynamic radius of this state was analysed to be over 1000 nm with inhomogeneity by DLS (**Figure 6.6(a)(b)**), nevertheless the high turbidity causing multiple scattering of light source and angle-dependent scattering intensities made the precise analysis more complicated. In spite of $GLBT_{49}$ segments providing hydrophilicity and repulsive forces against the opposite side of a chain, this phase separation repeatedly occurred under several heating and cooling cycles.

Recalling our previous study, PGLBT-*b*-PSPE chains are in an intermediate state before rearranging monodisperse micelles in the cooling cycle. In the state, freely moving individual chains start to close together due to zwitterionic attractions among PSPE but not tightly bind together yet. These clustering objects are reflected as slow diffusive modes with fast diffusing unimers in DLS with subtle or gradual decreases of transmittance, but sedimentation does not occur. Both of the diffusive modes disappear and a new single-decaying ACF emerges which means

reformation of monodisperse micelles. On the other hand, PSPE homopolymer chains cannot create polymer micelles owing to lack of a permanent hydrophilic segment; thus chain collapse and phase separation is inevitable. Besides, increasing concentration (10 mg/mL to 40 mg/mL) of GLBT$_{49}$-*b*-SPE$_{229}$ triggered micellisation at 25 °C (**Figure 6.12**), attributed to shortened average distances of adjacent chains, but that culminated in phase separation with additional cooling. Consequently, the distinctive phase behaviour of GLBT$_{49}$-*b*-SPE$_{229}$ could be interpreted that the GLBT$_{49}$ part is deficient in maintaining the stable layer covering the PSPE core, even if the micellar form once emerged. However, it needs more consideration because the previously obtained PGLBT-*b*-PSPEs had not bespoken the phase separation even though having more than 5 times of PSPE against PGLBT. The phenomenon will be discussed further in the other samples of the DP$_{total}$ ~600 series.

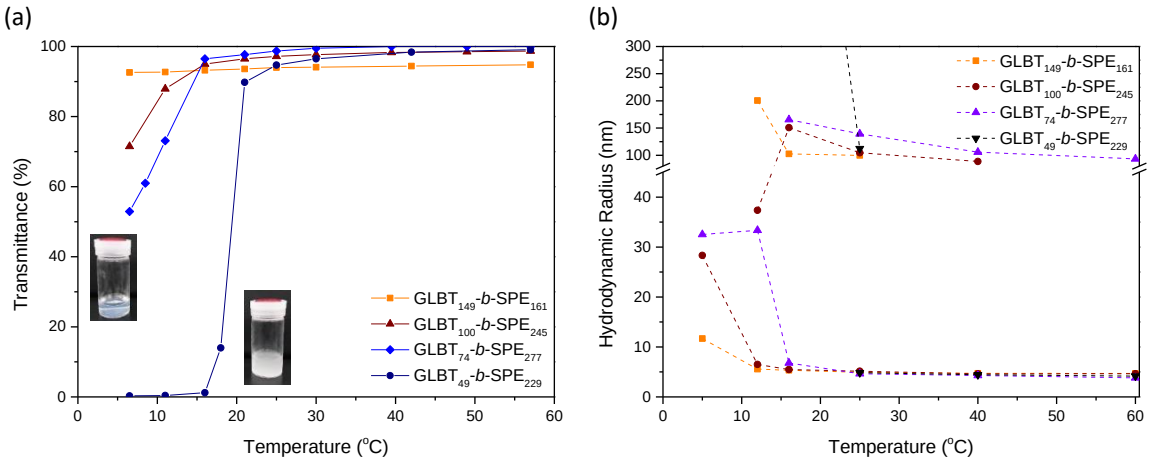

Figure 6.4. (a) Transmittance variations and (b) size variations against temperature in a series of PGLBT-*b*-PSPEs whose total target DP was 300. Insets of (a) are photos of GLBT$_{74}$-*b*-SPE$_{277}$ (left) and GLBT$_{49}$-*b*-SPE$_{229}$ (right) taken below 10 °C.

The temperature-responsive solution behaviour of PGLBT-*b*-PSPEs having twice longer chain length and same target block ratios was revealed as shown in **Figure 6.5**. Although their molecular weight approximately doubled, the polymer solutions did not show drastic differences in the trend and the transition points. Apparent thermoresponsive alterations did not occur in GLBT$_{297}$-*b*-SPE$_{330}$ (DP$_{target}$ = 1:1) solution as in GLBT$_{149}$-*b*-SPE$_{161}$, but the chains took a micellar form (R_h = from 6 nm to 31 nm) at the lowest of the temperature range with a slight transmittance decrease because of slightly increased imbalance of both blocks. The other three polybetaine solutions showed clearer temperature-responsive behaviour compared to their counterparts in the DP ~300 series; The unimer-to-micelle transition took place at higher temperatures (e.g. GLBT$_{149}$-*b*-SPE$_{742}$ turned into micelles under 20 °C meanwhile under 15 °C for GLBT$_{74}$-*b*-SPE$_{277}$) with the increase in cloud point to higher temperature. As shown in **Figure 6.6(c)(d)**, three diblocks bearing more PSPE than PGLBT existed as monodisperse micelles

at 12 °C whereas GLBT$_{297}$-*b*-SPE$_{330}$ was still in the intermediate state, represented as a bimodal ACF. However, it should be noted that the actual block ratios of these block copolymers were higher than the target ratios and the actual block ratios of the DP$_{total}$ ~300 series as well, so the transition shift to higher temperatures could be due to the increased portion of PSPE to PGLBT rather than the increase of total molecular weight.

Note that GLBT$_{99}$-*b*-SPE$_{630}$, which is a counterpart of GLBT$_{49}$-*b*-SPE$_{229}$, did not go under phase separation even holding higher PSPE to PGLBT ratio. Showing an abrupt transmittance shift around 20 °C as GLBT$_{49}$-*b*-SPE$_{229}$, GLBT$_{99}$-*b*-SPE$_{630}$ chains transformed to micelles (R_h = 60 nm) rather than immensely grown sediments, and the size of the micelles was maintained under additional cooling. In other words, no coalescence occurred after micellisation. The intriguing difference between the two polymers suggests that there is a minimum DP of PGLBT for protection from coalescence of adjacent PSPE cores and stabilisation of the core-shell type polymer micelles.

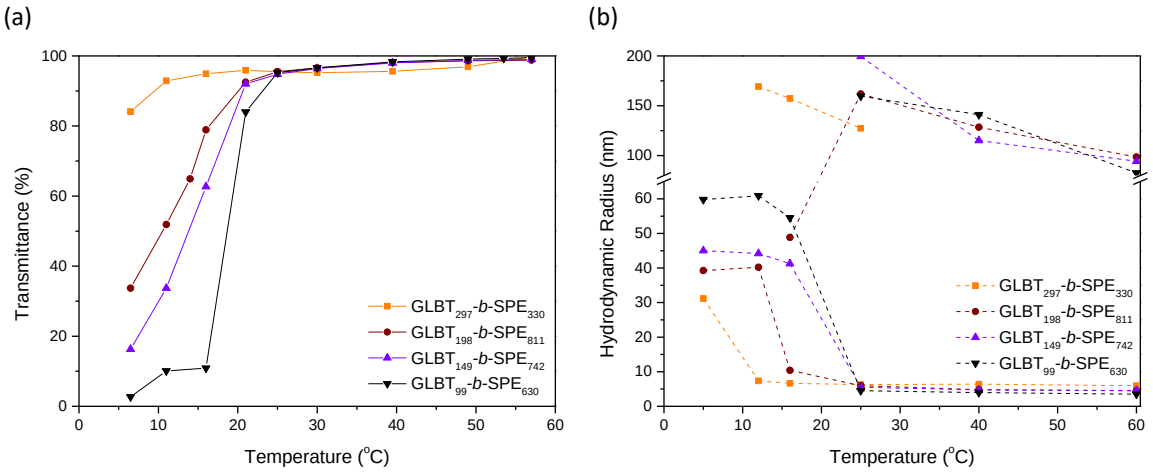

Figure 6.5. (a) Transmittance variations and (b) size variations against temperature in a series of PGLBT-*b*-PSPEs whose total target DP was 600

Table 6.3. Cloud points and R_h, R_g of PGLBT-*b*-PSPE in water (DP_{total} = ~300 and ~600, conc. = 10 mg/mL)

	Cloud Point (°C)	R_h (unimer) (nm)	R_h (micelles) (nm)	PDI[b] (micelles) $(\mu_2/\bar{\Gamma}^2)$	R_g (micelles) (nm)	R_g/R_h
$GLBT_{149}$-*b*-SPE_{161}	-	4.71	-	-	-	-
$GLBT_{100}$-*b*-SPE_{245}	-	4.63	28.3	0.12	41.7	1.47
$GLBT_{74}$-*b*-SPE_{277}	~5	3.82	33.4	0.13	28.1	0.84
$GLBT_{49}$-*b*-SPE_{229}	19.4	4.18	(phase separation)	-	-	-
$GLBT_{297}$-*b*-SPE_{330}	-	5.95	31.2	0.26	53.4	1.45
$GLBT_{198}$-*b*-SPE_{811}	8.4	4.47	40.2	0.15	33.9[a]	0.71[a]
$GLBT_{149}$-*b*-SPE_{742}	14.7	4.58	44.2	0.11	40.2[a]	0.78[a]
$GLBT_{99}$-*b*-SPE_{630}	18.7	3.51	60.9	0.16	60.4	0.99

[a] the concentration was diluted to 5 mg/mL
[b] obtained by cumulant analysis

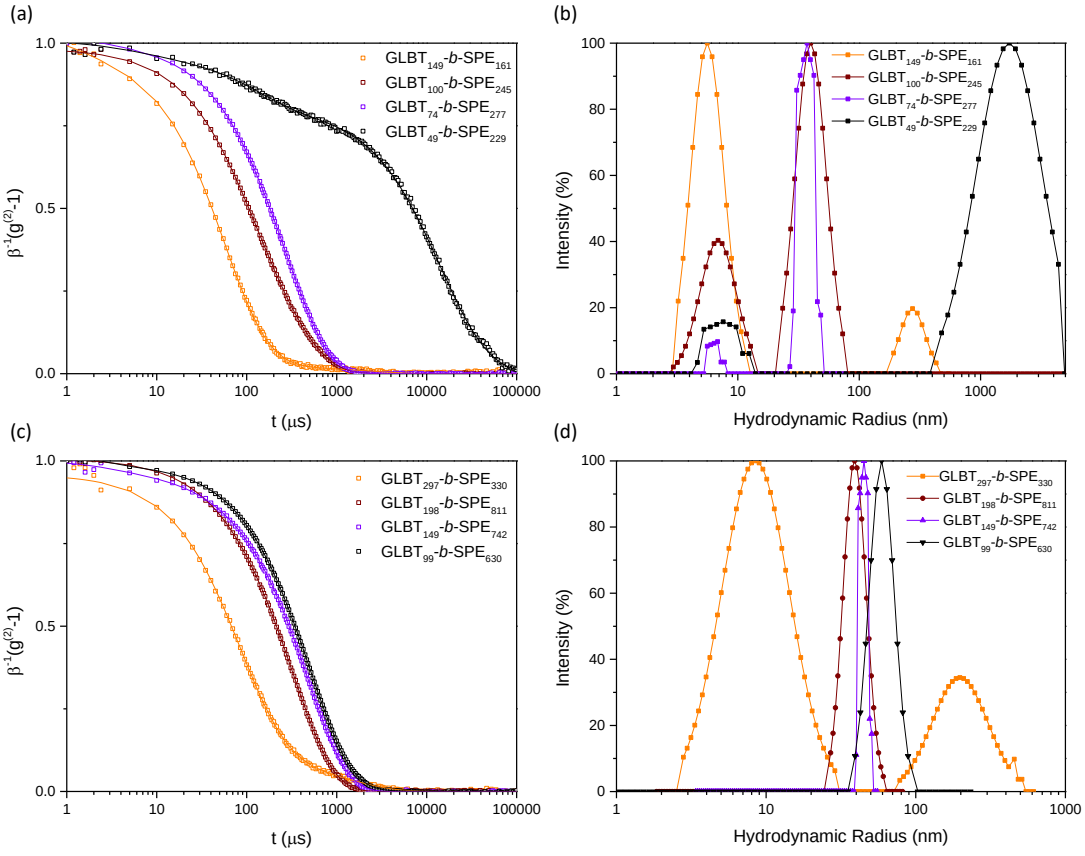

Figure 6.6. ACFs ((a) and (c)) and CONTIN analysis results ((b) and (d)) of PGLBT-*b*-PSPE aqueous solutions having different block ratios and total chain length. (a) and (b): DP_{total} = ~300, (c) and (d): DP_{total} = ~600. The ACFs and size distributions are obtained at 90°, 12 °C.

TEM images of $GLBT_{99}$-*b*-SPE_{630} solution revealed that the shape of the self-assembled polymer nanoparticles is spherical as shown in **Figure 6.7(a)**, and it corresponded to the R_g/R_h (**Figure 6.13**). However, some extent of anisotropic objects like strings or thin sheets were also found (**Figure 6.7(b))**. It should be noted that the solution cooled under the transition temperature was dropcast on a TEM grid, then it was dried under ambient temperature at which $GLBT_{99}$-*b*-SPE_{630} existed in the intermediate state. Indeed, additional merging/disassociation could not be ruled out. The shape factor R_g/R_h values were mainly 0.7–1.0 for the diblocks whose block ratio [PGLBT]:[PSPE] was over 1:2, and this indicates that the structure of the particles at low temperatures is spherical (R_g/R_h = 0.775).[47, 48] The shape was also confirmed by AFM measurement of a polymer solution-coated surface prepared at room temperature (**Figure 6.15**). Besides, in the additional measurement of the $GLBT_{99}$-*b*-SPE_{630} sample whose concentration was diluted by half (5 mg/mL), strings and thin sheets were predominant (**Figure 6.16**) and the R_h of the polymer objects extraordinarily increased over 100 nm under 12 °C. The angle-dependent scattering intensity corroborates the anisotropically self-assembled state of the diluted sample. Since any extraordinary self-assembly was not found from the other PGLBT-*b*-PSPE samples diluted to 5 mg/mL, this block ratio might yield the unexpected transformation when the distance between chains increased.

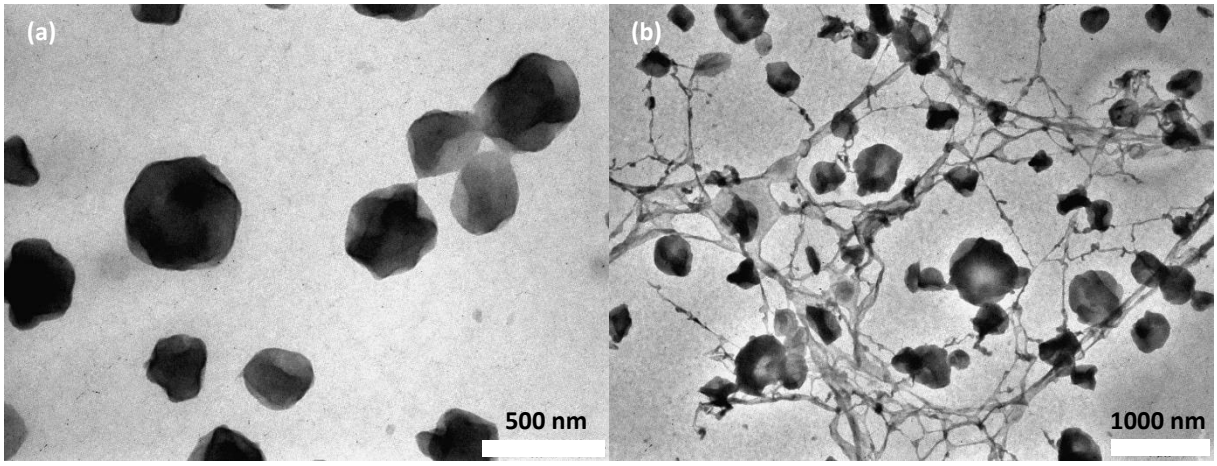

Figure 6.7. TEM images of $GLBT_{99}$-*b*-SPE_{630} obtained from the solution in the micelle state (a) spherical particles (b) spherical objects with stringlike objects (conc. = 10 mg/mL)

Solution behaviour of BAB triblock PSPE-*b*-PGLBT-*b*-PSPE

The two BAB-type triblock copolymers SPE_{248}-$GLBT_{99}$-SPE_{277} and SPE_{198}-$GLBT_{198}$-SPE_{212} in aqueous solution were investigated to determine the influences of the polymer structure on the thermoresponsive characters. BAB-type triblocks in which B blocks are able to associate with each other and A blocks are inert and provide unchanging water affinity may have B-centred particles (closed association) or network formation connected by

B blocks (bridging, open associations).[49] For PSPE-PGLBT-PSPE, thermoresponsive zwitterionic attractions among PSPE would induce PSPE-centred particles having PGLBT outer loops (flower micelles) or loosely formed clusters consisting of associated PSPE nodes. The variations of transmittance and hydrodynamic radius against temperature are shown in **Figure 6.8**. The transmittance of SPE_{248}-$GLBT_{99}$-SPE_{277} aqueous solution rapidly dropped to a few % around 40 °C while triple diffusive modes existed, then became a highly fuzzy state until 25 °C. The turbid solution turned into a translucent state at 25 °C where a monomodal ACF representing monodisperse micelles (R_h = 43 nm) started to emerge, and the state was fixed at lower temperatures as shown in **Figure 6.9(a)(b)** that displays ACFs and size distributions at several temperatures. The starkest contrast to the diblock of a similar block composition ($GLBT_{99}$-*b*-SPE_{630}) is extreme fuzziness below the cloud point which might be related to predominant slow modes about 700 nm (at 40 °C) and over ~1900 nm (at 30 °C). These slow diffusive objects in the middle range of temperature are thought to floppy networks in which PSPE motifs bound to other PSPEs of adjacent chains by bridging. However, similar to diblocks, the state was not maintained under 25 °C as depicted in **Figure 6.9(a)(b)** showing a clear transition from a bimodal fast-slow decaying ACF to an unimodal decaying ACF. Once monodisperse particles (micelles) emerged, they continued to be present below the temperature. Therefore, the network-like objects are assumed not to be in a thermodynamically favoured state under a certain temperature. To reduce the enthalpic penalty caused by decreasing temperature, close associations of zwitterionic pairing are thought to be preferred to reduce surface tension. Hence, the pairings rearrange to flowerlike micellar form, which may be the more stable formation at much lower temperatures. The shape factor of the monodisperse particles (R_g/R_h = 0.87) (**Figure 6.14**) suggests that the structure of self-assembled PSPE-PGLBT-PSPE is spherical.

This behaviour was expected to be repeated in the SPE_{198}-$GLBT_{198}$-SPE_{212} solution, however the thermoresponsive features appeared weaker and the chains did not reach the micelle state due to reduced ratio of PSPE to PGLBT. Compared to the AB-type diblock $GLBT_{198}$-*b*-SPE_{811}, the cloud point of the BAB-type was higher even at the lower PSPE balance (2:1 to 4:1), and the R_h of slow mode in the intermediate region was larger than that of the AB-type. While the transmittance gradually decreased until 15 °C, a slow diffusive mode (network-like assemblies) emerged alongside unimers then the relative percent of the slow mode exceeded that of unimers at 25 °C. (**Figure 6.9(c)(d)**)

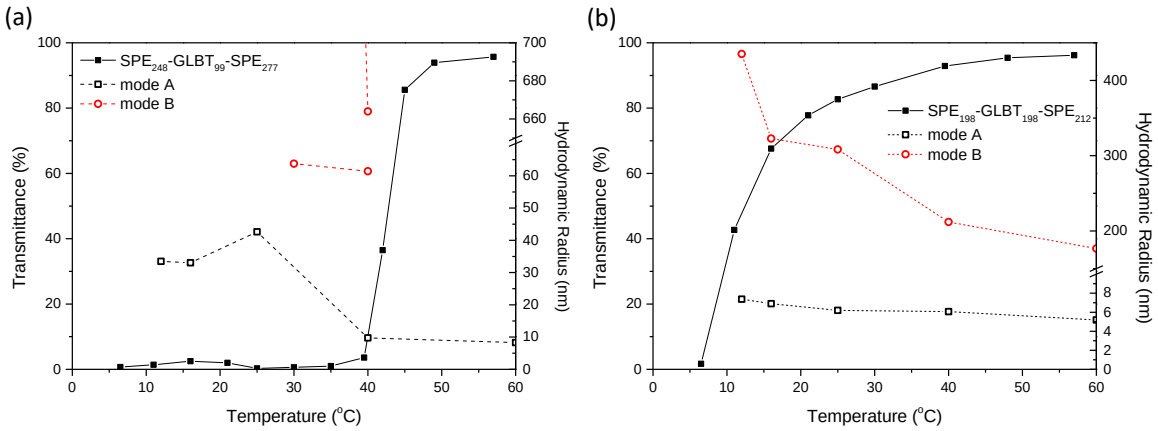

Figure 6.8. Variations of transmittance (■) and R_h (open symbols) against temperature of triblock betaine copolymers (a) SPE_{248}-$GLBT_{99}$-SPE_{277} (b) SPE_{198}-$GLBT_{198}$-SPE_{212}

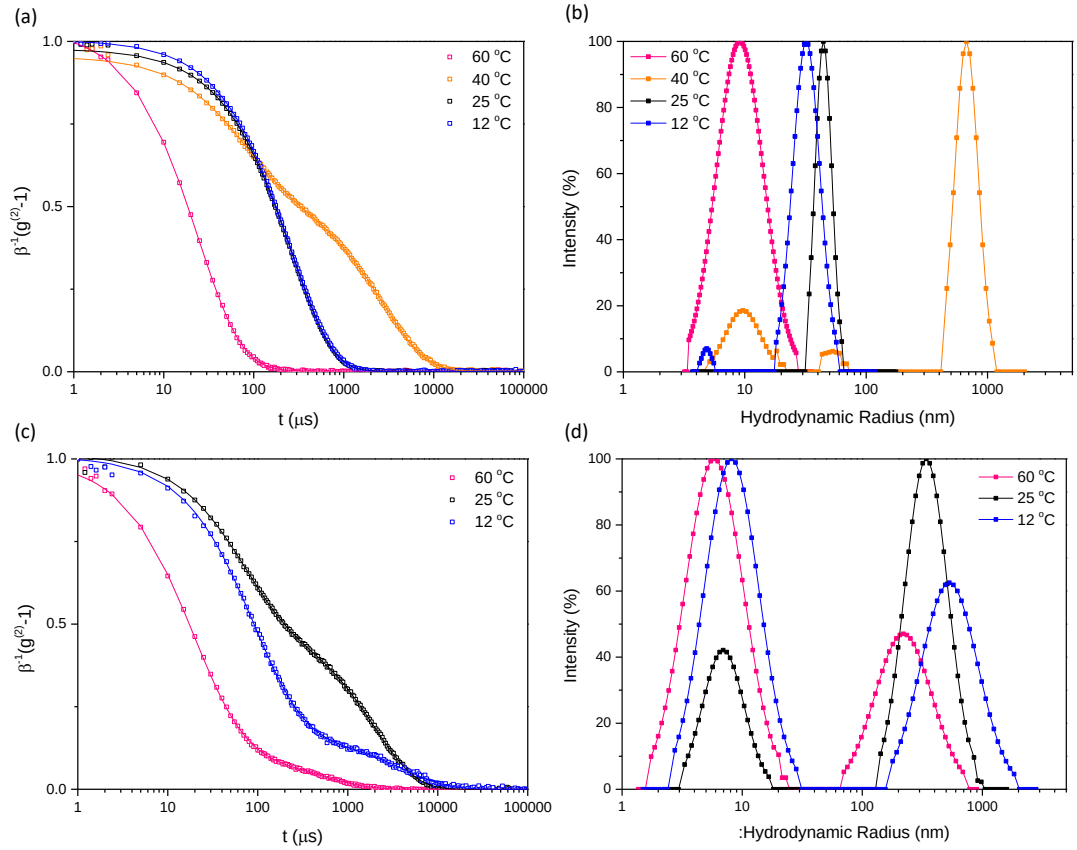

Figure 6.9. ACFs ((a) and (c)) and analysis results by CONTIN ((b) and (d)) of two triblock PSPE-PGLBT-PSPE aqueous solutions. (a) and (b): SPE_{248}-$GLBT_{99}$-SPE_{277} (c) and (d): SPE_{198}-$GLBT_{198}$-SPE_{212}. The ACFs and size distributions are obtained at 90°, 12 °C.

Table 6.4. Cloud points and R_h, R_g of PSPE-*b*-PGLBT-*b*-PSPE in water (conc. = 10 mg/mL)

	Cloud Point (°C)	R_h (unimer) (nm)	R_h (micelles) (nm)	PDI[b] (micelles) ($\mu_2/\bar{\Gamma}^2$)	R_g (micelles) (nm)	R_g/R_h
SPE_{248}-$GLBT_{99}$-SPE_{277}	42.8	8.31	43	0.14	57.6[a]	0.87[a]
SPE_{198}-$GLBT_{198}$-SPE_{212}	12.5	5.20	-	-	-	-

a: the sample was diluted to conc. = 2.5 mg/mL

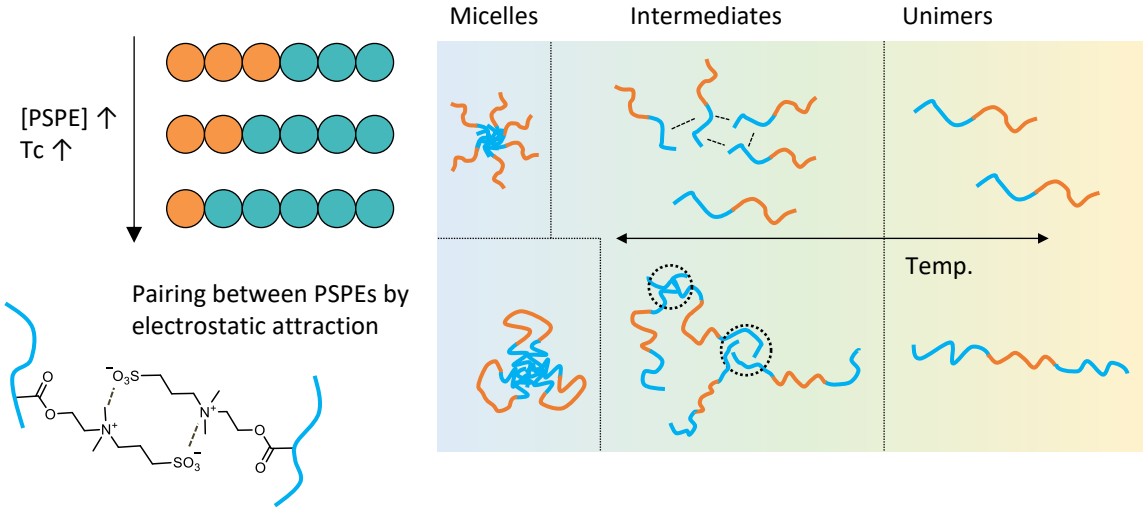

Scheme 6.2. Proposed model of unimer-to-micelle transition processes for PGLBT-*b*-PSPE and PSPE-*b*-PGLBT-*b*-PSPE in this study

Table 6.5. Experimental conditions for the synthesis of PGLBT-*b*-PSPEs via RAFT polymerisation in water at 70 °C (sum of DP_{target}: 300)

Sample	$GLBT_{149}$-*b*-SPE_{161}		$GLBT_{100}$-*b*-SPE_{245}		$GLBT_{74}$-*b*-SPE_{277}		$GLBT_{49}$-*b*-SPE_{229}	
Steps	**1**	**2**	**1**	**2**	**1**	**2**	**1**	**2**
Monomer	GLBT	SPE	GLBT	SPE	GLBT	SPE	GLBT	SPE
DP_{target}	150	150	100	200	75	225	50	250
$m_{monomer}$ (g)	1.427	1.851	0.951	2.469	0.713	2.814	0.476	3.086
m_{CTA} (g)	0.015		0.015		0.015		0.015	
m_{VA-044} (g)	0.7×10^{-3}	0.7×10^{-3}	0.7×10^{-3}	0.7×10^{-3}	0.7×10^{-3}	0.7×10^{-3}	0.7×10^{-3}	0.7×10^{-3}
$V_{solvent}$ (mL)[a]	2.2	2.7	1.7	4.2	1.3	4	0.75	4.25
$[M]_0$ (mol/L)	3.01	2.45	2.60	2.10	2.55	2.52	2.95	2.60
$[CTA]_0/[I]_0$	20	20	20	20	20	20	20	20
Cumulative L (%)	95.3	90.8	95.3	90.8	95.3	90.8	95.3	90.8

[a] is the sum of the volume of the solvent added in the first and the next step

Table 6.6. Experimental conditions for the synthesis of PGLBT-*b*-PSPEs via RAFT polymerisation in water at 70 ºC (sum of DP_{target}: 600)

Sample	**$GLBT_{297}$-*b*-SPE_{330}**		**$GLBT_{198}$-*b*-SPE_{811}**		**$GLBT_{149}$-*b*-SPE_{742}**		**$GLBT_{99}$-*b*-SPE_{630}**	
Steps	**1**	**2**	**1**	**2**	**1**	**2**	**1**	**2**
Monomer	GLBT	SPE	GLBT	SPE	GLBT	SPE	GLBT	SPE
DP_{target}	300	300	200	400	150	450	100	500
$m_{monomer}$ (g)	1.902	2.493	1.268	3.292	0.951	3.703	0.634	3.086
m_{CTA} (g)	0.01		0.01		0.01		0.01	
$m_{VA\text{-}044}$ (g)	0.5×10^{-3}	0.7×10^{-3}	0.5×10^{-3}	1.0×10^{-3}	0.5×10^{-3}	1.0×10^{-3}	0.5×10^{-3}	1.0×10^{-3}
$V_{solvent}$ (mL)	2.80	3.50	1.70	4.60	1.20	4.50	1.00	7.00
$[M]_0$ (mol/L)	3.16	2.55	3.46	2.56	3.68	2.95	2.95	2.12
$[CTA]_0/[I]_0$	20	14	20	10	20	10	20	10
Cumulative L (%)	95.3	90.8	95.3	86.6	95.3	86.6	95.3	86.7

Table 6.7. Experimental conditions for preparation of BAB-type PSPE-PGLBT-PSPEs via RAFT polymerisation in water at 70 ºC (sum of DP_{target}: 600)

Sample	**SPE_{198}-$GLBT_{198}$-SPE_{212}**			**SPE_{248}-$GLBT_{99}$-SPE_{277}**		
Steps	**1**	**2**	**3**	**1**	**2**	**3**
Monomer	SPE	GLBT	SPE	SPE	GLBT	SPE
DP_{target}	200	200	200	250	100	250
$m_{monomer}$ (g)	2.304	1.793	2.337	3.086	0.959	3.118
m_{CTA} (g)	0.014			0.015		
$m_{VA\text{-}044}$ (g)	0.7×10^{-3}	0.7×10^{-3}	0.9×10^{-3}	0.7×10^{-3}	1.2×10^{-3}	0.7×10^{-3}
$V_{solvent}$ (mL)	2.70	3.20	4.20	3.60	4.10	5.60
$[M]_0$ (mol/L)	3.05	2.60	2.00	3.07	1.09	1.99
$[CTA]_0/[I]_0$	20	20	14	20	12.5	20
Cumulative L (%)	95.3	90.8	84.9	95.3	88.3	84.1

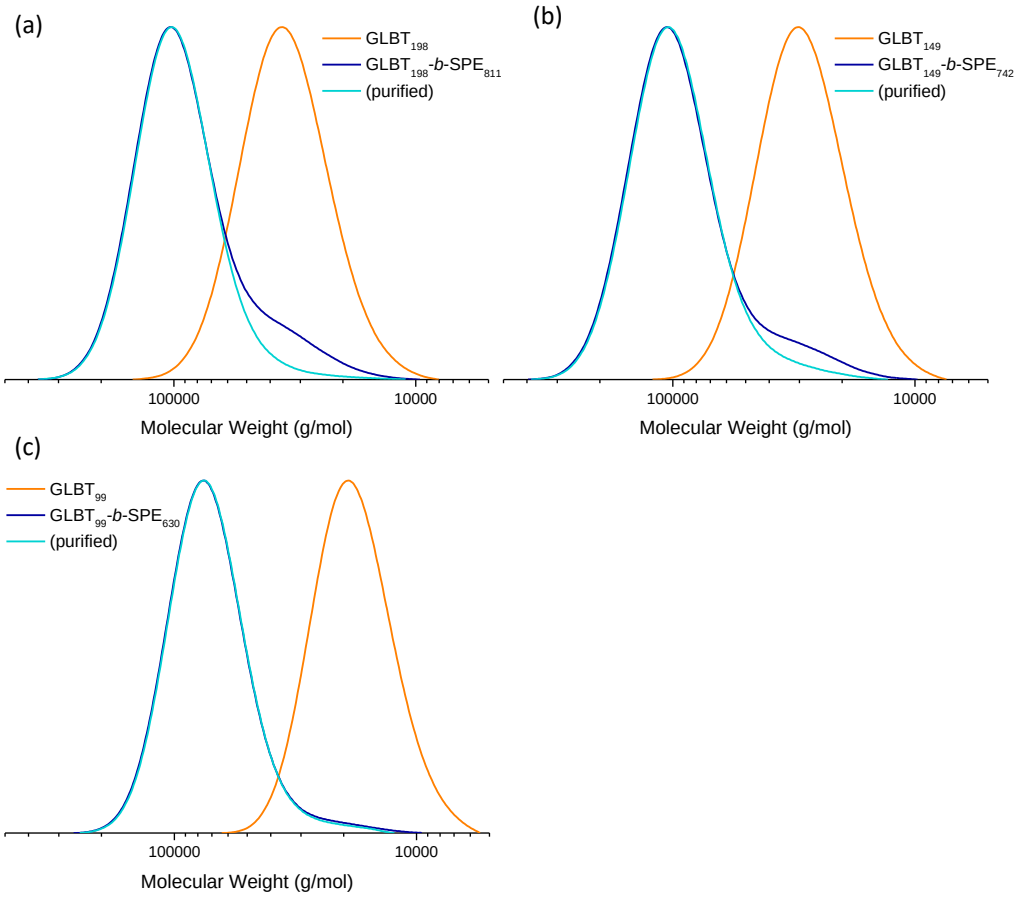

Figure 6.10. Molecular weight distributions of crude and purified PGLBT-*b*-PSPEs and PGLBTs as their macroCTAs (total DP_{target}: 600) (a) $GLBT_{198}$-*b*-SPE_{811} (b) $GLBT_{149}$-*b*-SPE_{742} (c) $GLBT_{99}$-*b*-SPE_{630}

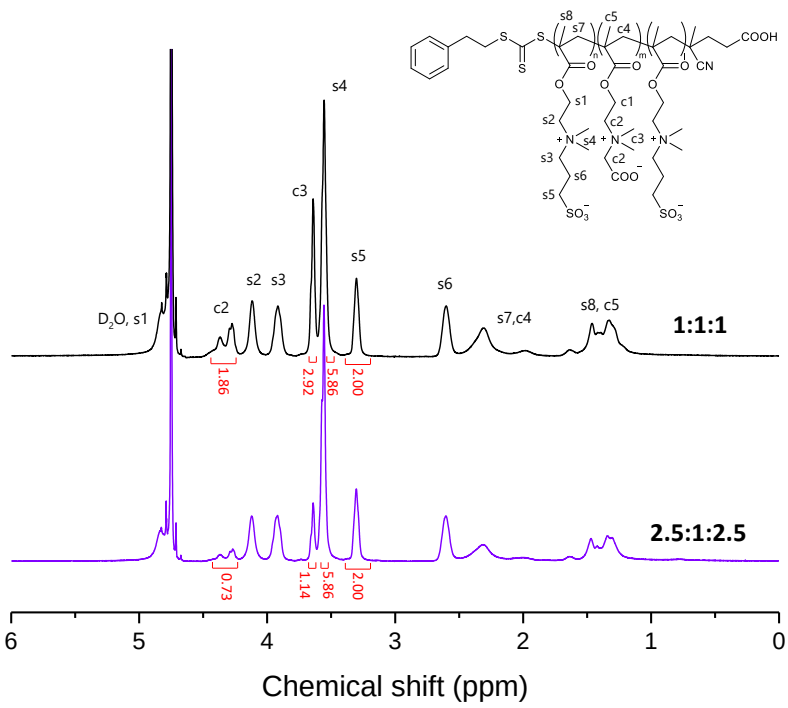

Figure 6.11. ^{1}H NMR spectra of two triblocks in D_2O at 60 °C. SPE_{198}-$GLBT_{198}$-SPE_{212} (target ratio = 1:1:1, black line) and SPE_{248}-$GLBT_{99}$-SPE_{277} (target ratio = 2.5:1:2.5, blue line)

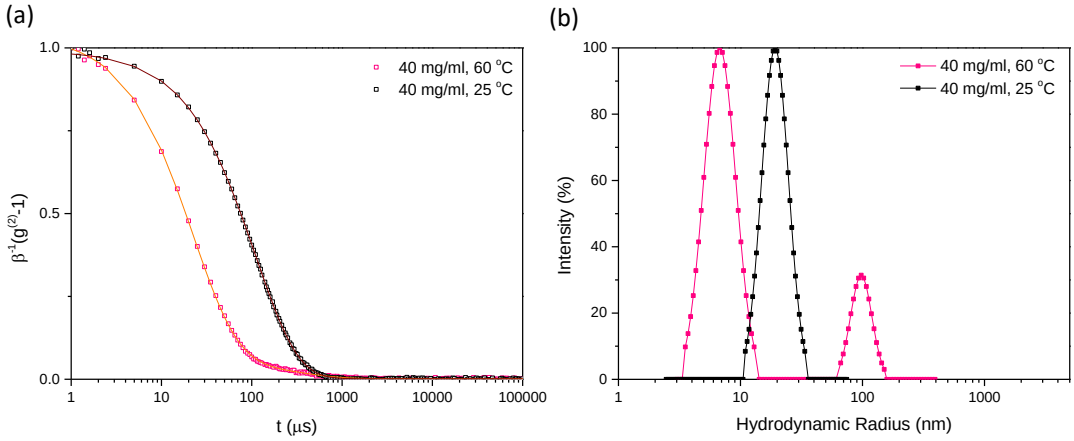

Figure 6.12. (a) ACFs and (b) the CONTIN analysis result of $GLBT_{49}$-*b*-SPE_{229} solution (conc. = 40 mg/mL) measured at 25 and 60 °C, respectively.

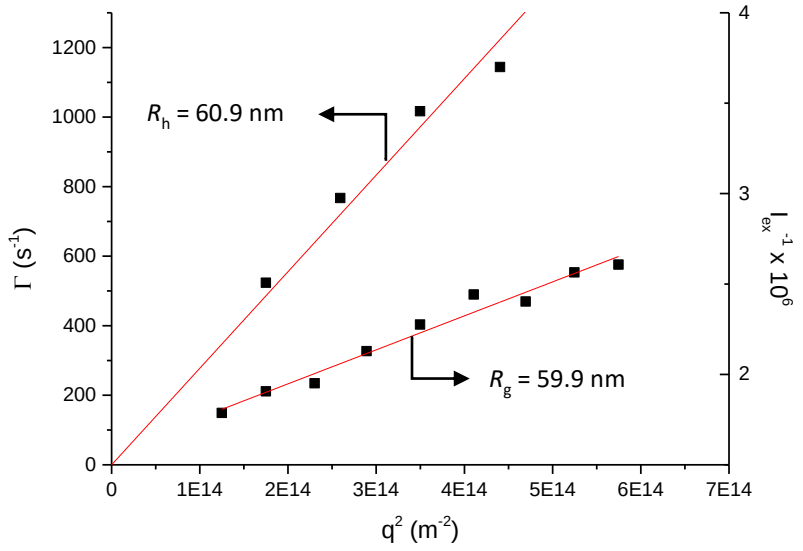

Figure 6.13. Angular dependent DLS and SLS measurements of (a) GLBT$_{99}$-*b*-SPE$_{630}$ at 12 ºC (conc. = 10 mg/mL)

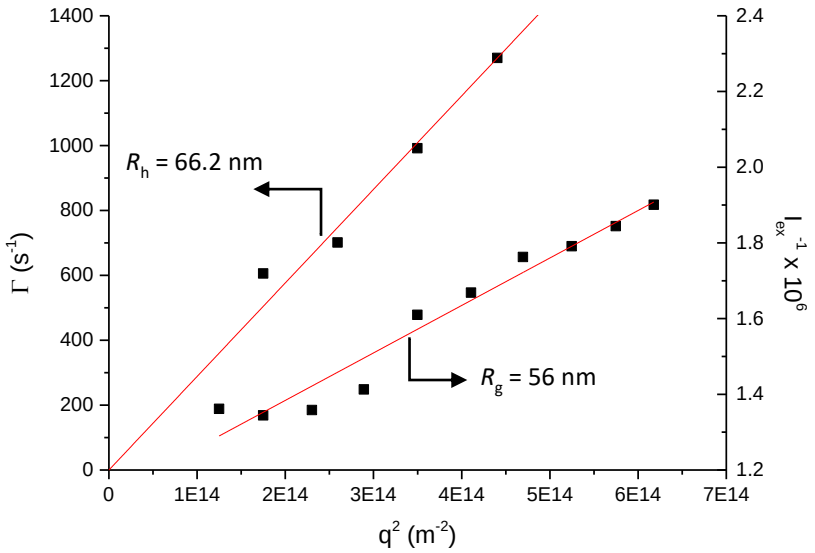

Figure 6.14. Angular dependent DLS and SLS measurements of (a) SPE$_{248}$-GLBT$_{99}$-SPE$_{277}$ at 16 ºC (conc. 2.5 mg/mL)

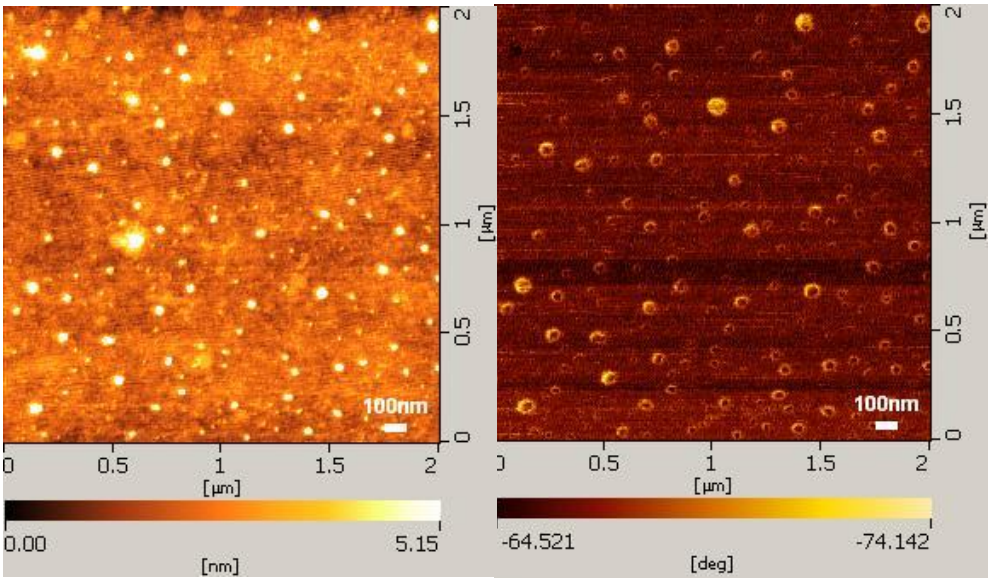

Figure 6.15. AFM image of GLBT$_{198}$-*b*-SPE$_{811}$ (50 mg/mL) on a glass substrate (left: height mode, flattened, right: phase mode).

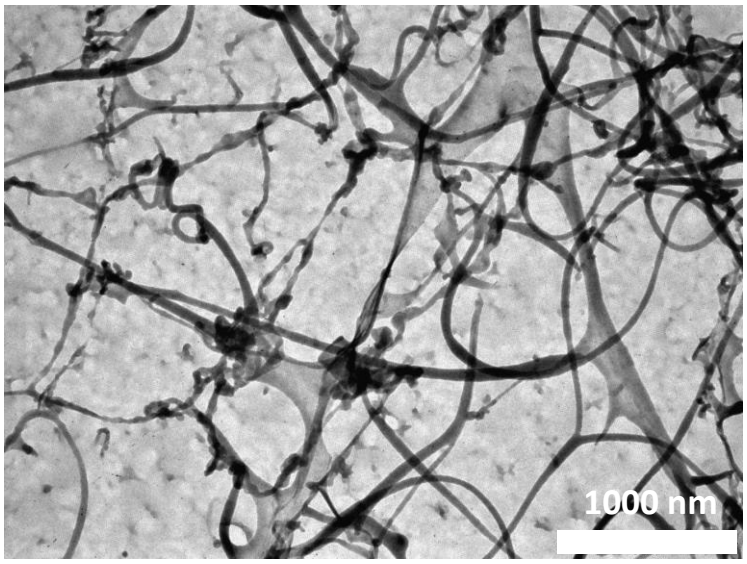

Figure 6.16. TEM image of GLBT$_{99}$-*b*-SPE$_{630}$ obtained from the solution in the self-assembled state (conc. = 5 mg/mL)

Conclusion

AB-type and BAB-type of carboxybetaine-*block*-sulfobetaine methacrylate block copolymers were obtained by one-pot aqueous RAFT polymerisation with good control of the block ratio. For AB-type PGLBT-*b*-PSPEs aimed to have AB ratios of 1:1 to 1:5, the cloud point of unimer-to-micelle transition rose directly by the increasing portion of PSPE. However, there was no meaningful change in the solution behaviour depending on total DP as found in the other series prepared with the same AB ratios. Thus, it is proposed that the effect of the entire chain

length is not as significant as the block ratio on the temperature-responsive characteristics. For BAB triblock PSPE-PGLBT-PSPEs, the responses against temperature were more sensitive in comparison with diblocks having similar block ratios and chain lengths. The solutions became turbid at higher temperatures while the chains existed as unimers and slow diffusive objects a few-fold larger than equivalents of diblocks, which is assumed as a network-like structure by paring between adjacent PSPE segments. The triblocks in this state eventually reformed monodisperse particles at much lower temperatures, hence it is thought to flowerlike micelles of which PGLBT loops are in the outside and PSPE motifs are in the inside. We envision the elucidation of whole betaine block copolymers might be useful for developing temperature-responsive soft materials which require high antifouling property, such as nanocarriers for drug-delivery systems or stimuli-responsive active surfaces.

References

1. J. B. Schlenoff, *Langmuir*, 2014, **30**, 9625-9636.
2. J. G. Weers, J. F. Rathman, F. U. Axe, C. A. Crichlow, L. D. Foland, D. R. Scheuing, R. J. Wiersema and A. G. Zielske, *Langmuir*, 1991, **7**, 854-867.
3. J. D. Delgado and J. B. Schlenoff, *Macromolecules*, 2017, **50**, 4454-4464.
4. P. Mary, D. D. Bendejacq, M. P. Labeau and P. Dupuis, *Journal of Physical Chemistry B*, 2007, **111**, 7767-7777.
5. A. B. Lowe and C. L. McCormick, *Chemical Reviews*, 2002, **102**, 4177-4189.
6. F. Wang, J. F. Yang and J. Zhao, *Polymer International*, 2015, **64**, 999-1005.
7. H. Matsuoka, Y. Yamakawa, A. Ghosh and Y. Saruwatari, *Langmuir*, 2015, **31**, 4827-4836.
8. Z. L. Cao and G. Z. Zhang, *Physical Chemistry Chemical Physics*, 2015, **17**, 27045-27051.
9. A. Z. Niu, D. J. Liaw, H. C. Sang and C. Wu, *Macromolecules*, 2000, **33**, 3492-3494.
10. E. E. L. Kathmann, L. A. White and C. L. McCormick, *Macromolecules*, 1997, **30**, 5297-5304.
11. R. Kumar and G. H. Fredrickson, *Journal of Chemical Physics*, 2009, **131**.
12. O. Azzaroni, A. A. Brown and W. T. S. Huck, *Angewandte Chemie-International Edition*, 2006, **45**, 1770-1774.
13. Y. C. Zhu, J. M. Noy, A. B. Lowe and P. J. Roth, *Polymer Chemistry*, 2015, **6**, 5705-5718.
14. V. Hildebrand, A. Laschewsky, M. Pach, P. Muller-Buschbaum and C. M. Papadakis, *Polymer Chemistry*, 2017, **8**, 310-322.
15. A. Laschewsky and A. Rosenhahn, *Langmuir*, 2019, **35**, 1056-1071.
16. K. E. B. Doncom, N. J. Warren and S. P. Armes, *Polymer Chemistry*, 2015, **6**, 7264-7273.
17. K. E. B. Doncom, H. Willcock and R. K. O'Reilly, *European Polymer Journal*, 2017, **87**, 497-507.
18. K. E. B. Doncom, A. Pitto-Barry, H. Willcock, A. Lu, B. E. McKenzie, N. Kirby and R. K. O'Reilly, *Soft Matter*, 2015, **11**, 3666-3676.
19. Y. Chang, W. Yandi, W. Y. Chen, Y. J. Shih, C. C. Yang, Q. D. Ling and A. Higuchi, *Biomacromolecules*, 2010, **11**, 1101-1110.
20. B. G. Yang, C. Y. Wang, Y. B. Zhang, L. Ye, Y. F. Qian, Y. Shu, J. M. Wang, J. J. Li and F. L. Yao, *Polymer Chemistry*, 2015, **6**, 3431-3442.
21. Z. X. Dong, J. Mao, M. Q. Yang, D. P. Wang, S. Q. Bo and X. L. Ji, *Langmuir*, 2011, **27**, 15282-15291.
22. C. Durand-Gasselin, R. Koerin, J. Rieger, N. Lequeux and N. Sanson, *Journal of Colloid and Interface Science*, 2014, **434**, 188-194.
23. J. Virtanen, M. Arotcarena, B. Heise, S. Ishaya, A. Laschewsky and H. Tenhu, *Langmuir*, 2002, **18**, 5360-5365.
24. N. S. Vishnevetskaya, V. Hildebrand, B. J. Niebuur, I. Grillo, S. K. Filippov, A. Laschewsky, P. Muller-Buschbaum and C. M. Papadakis, *Macromolecules*, 2016, **49**, 6655-6668.

25. N. S. Vishnevetskaya, V. Hildebrand, B. J. Niebuur, I. Grillo, S. K. Filippov, A. Laschewsky, P. Muller-Buschbaum and C. M. Papadakis, *Macromolecules*, 2017, **50**, 3985-3999.
26. M. Ranka, H. Katepalli, D. Blankschtein and T. A. Hatton, *Langmuir*, 2017, **33**, 13326-13331.
27. Y. Zhao, T. Bai, Q. Shao, S. Y. Jiang and A. Q. Shen, *Polymer Chemistry*, 2015, **6**, 1066-1077.
28. Z. Zhang, H. Vaisocherova, G. Cheng, W. Yang, H. Xue and S. Y. Jiang, *Biomacromolecules*, 2008, **9**, 2686-2692.
29. L. Mi, M. T. Bernards, G. Cheng, Q. M. Yu and S. Y. Jiang, *Biomaterials*, 2010, **31**, 2919-2925.
30. L. Mi and S. Y. Jiang, *Angewandte Chemie-International Edition*, 2014, **53**, 1746-1754.
31. M. Birkner and M. Ulbricht, *Journal of Membrane Science*, 2015, **494**, 57-67.
32. L. D. Blackman, P. A. Gunatillake, P. Cass and K. E. S. Locock, *Chemical Society Reviews*, 2019, **48**, 757-770.
33. B. Bendinger, H. H. M. Rijnaarts, K. Altendorf and A. J. B. Zehnder, *Applied and Environmental Microbiology*, 1993, **59**, 3973-3977.
34. J. W. Costerton, Z. Lewandowski, D. E. Caldwell, D. R. Korber and H. M. Lappinscott, *Annual Review of Microbiology*, 1995, **49**, 711-745.
35. C. Leng, H. C. Hung, S. W. Sun, D. Y. Wang, Y. T. Li, S. Y. Jiang and Z. Chen, *Acs Applied Materials & Interfaces*, 2015, **7**, 16881-16888.
36. C. Leng, S. W. Sun, K. X. Zhang, S. Y. Jiang and Z. Chen, *Acta Biomaterialia*, 2016, **40**, 6-15.
37. P. S. Liu, Q. Chen, S. S. Wu, J. Shen and S. C. Lin, *Journal of Membrane Science*, 2010, **350**, 387-394.
38. J. Lim, H. Matsuoka, S. Yusa and Y. Saruwatari, *Langmuir*, 2019, **35**, 1571-1582.
39. G. Gody, T. Maschmeyer, P. B. Zetterlund and S. Perrier, *Nature Communications*, 2013, **4**.
40. E. R. Jones, M. Semsarilar, A. Blanazs and S. P. Armes, *Macromolecules*, 2012, **45**, 5091-5098.
41. G. Gody, R. Barbey, M. Danial and S. Perrier, *Polymer Chemistry*, 2015, **6**, 1502-1511.
42. D. J. Keddie, G. Moad, E. Rizzardo and S. H. Thang, *Macromolecules*, 2012, **45**, 5321-5342.
43. M. R. Hill, R. N. Carmean and B. S. Sumerlin, *Macromolecules*, 2015, **48**, 5459-5469.
44. G. Gody, T. Maschmeyer, P. B. Zetterlund and S. Perrier, *Macromolecules*, 2014, **47**, 639-649.
45. G. Gody, T. Maschmeyer, P. B. Zetterlund and S. Perrier, *Macromolecules*, 2014, **47**, 3451-3460.
46. A. Valdebenito and M. V. Encinas, *Polymer International*, 2010, **59**, 1246-1251.
47. J. P. Patterson, M. P. Robin, C. Chassenieux, O. Colombani and R. K. O'Reilly, *Chemical Society Reviews*, 2014, **43**, 2412-2425.
48. W. M. Wan, X. L. Sun and C. Y. Pan, *Macromolecules*, 2009, **42**, 4950-4952.
49. M. S. Donovan, A. B. Lowe, T. A. Sanford and C. L. McCormick, *Journal of Polymer Science Part a-Polymer Chemistry*, 2003, **41**, 1262-1281.

List of Publications

Chapter 2. Temperature-Responsive Behaviour of Double Hydrophilic Carboxy-Sulfobetaine Block Copolymers and Their Self-Assemblies in Water

Jongmin Lim, Hideki Matsuoka, Shin-ichi Yusa, and Yoshiyuki Saruwatari

Langmuir, 2019, 35, 1571−1582

Chapter 3. Effects of Halide Anions on the Solution Behaviour of Double Betaine Hydrophilic Block Copolymer PGLBT-*b*-PSPE

Jongmin Lim, Hideki Matsuoka, and Yoshiyuki Saruwatari

Submitted to *Langmuir*

Chapter 4. Effects of pH on the Stimuli-Responsive Characteristics of Double Betaine Hydrophilic Block Copolymer PGLBT-*b*-PSPE

Jongmin Lim, Hideki Matsuoka, and Yoshiyuki Saruwatari

Langmuir, 2020, 36, 1727−1736

Chapter 5. One-Pot Synthesis of Double and Triple Polybetaine Block Copolymers and Their Temperature-Responsive Solution Behaviour

Jongmin Lim, Hideki Matsuoka, and Yoshiyuki Saruwatari

To be submitted

Chapter 6. Effect of Block Ratio and Structure on the Thermosensitivity of Double and Triple Betaine Block Copolymers

Jongmin Lim, Hideki Matsuoka, Yusuke Kinoshita, Shin-ichi Yusa, and Yoshiyuki Saruwatari

To be submitted

Other Publications

Facile Synthesis of Thermally Stable Core-Shell Gold Nanoparticles via Photo-Cross-Linkable Polymeric Ligands

Misang Yoo, Seyong Kim, Jongmin Lim, Edward J. Kramer, Craig J. Hawker, Bumjoon J. Kim, and Joona Bang

Macromolecules, 2010, 43, 3570–3575

"Click" Synthesis of Thermally Stable Au Nanoparticles with Highly Grafted Polymer Shell and Control of Their Behavior in Polymer Matrix

Jongmin Lim, Hyunseung Yang, Kwanyeol Paek, Chul-Hee Cho, Seyong Kim, Joona Bang, and Bumjoon J. Kim

Journal of Polymer Science Part A: Polymer Chemistry, 2011, 49, 3464–3474

Acknowledgements

Firstly, I deeply appreciate to my supervisor Professor Hideki Matsuoka for giving me the opportunity to study in his research group in the last four years. I am thankful for his supervision of my work, especially when I got lost the path of my research and concentrated on trivial things. His generous support and patience made me pursue my own work to the end.

I am grateful to Professor Shin-ichi Yusa and his workgroup (Univ. of Hyogo) for the fruitful cooperation.

Much appreciation must be given to Professor André Laschewsky (Univ. of Potsdam) for many useful comments and sharing insights of polyzwitterions. Without his help, I could have not treated the reaction product properly and drawn meaningful data.

Also, I am sincerely grateful to Professor Remco Tuinier and his group (Eindhoven Univ. of Technology) for giving me a chance of a short visit. It was delightful to share my research interests to your group members, and to get useful hints and inspirations of my research field from you and your colleagues.

I am indebted to Dr Yuanming Zhang and Ted Costa (Brookhaven Instruments), and Jun Nakayama and Hidenori Omukai for critical advices about setup of light scattering instruments and data analysis. It was nearly impossible to accomplish my work without your precious help.

To all friends outside of my field, thank you for letting me take a short rest from my study during the tumultuous years. Sharing many anecdotes covering a wide range allowed me to maintain much flexibility in my thought and kept from total exhaustion.

Finally, great thanks should go to my family, who always encouraged me and supported everything during the long journey.